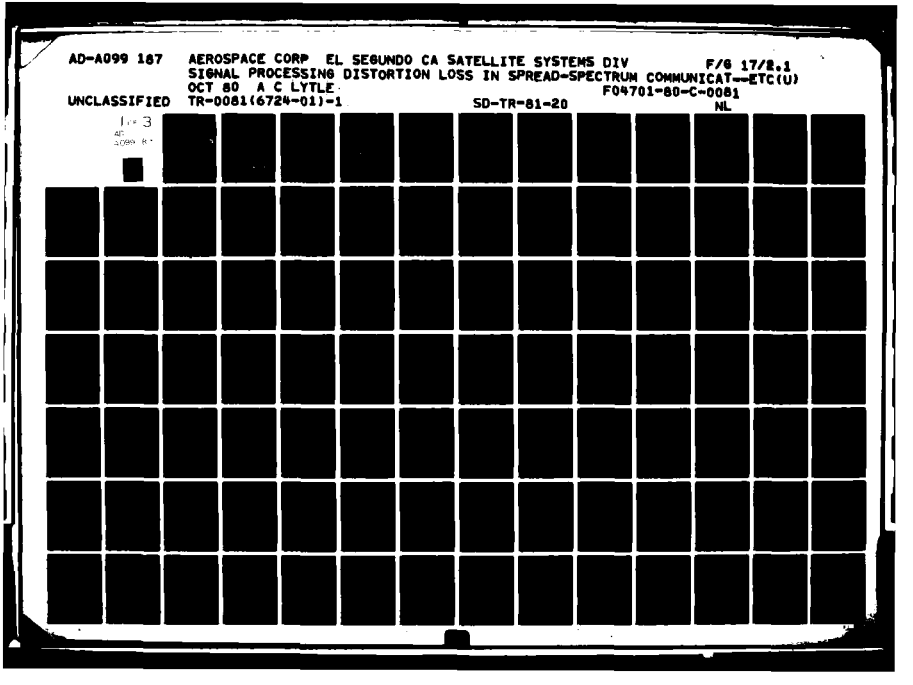
AD-A099 187 AEROSPACE CORP EL SEGUNDO CA SATELLITE SYSTEMS DIV F/G 17/2.1
SIGNAL PROCESSING DISTORTION LOSS IN SPREAD-SPECTRUM COMMUNICAT--ETC(U)
OCT 80 A C LYTLE F04701-80-C-0081
UNCLASSIFIED TR-0081(6724-01)-1 SD-TR-81-20 NL
1 of 3
AD A099 187

REPORT NO. SD-TR-81-20

LEVEL II

12

Signal Processing Distortion Loss in Spread-Spectrum Communication, Command, Control, and Navigation Systems

A. C. LYTLE, JR.
Satellite Systems Division
Program Group
The Aerospace Corporation
El Segundo, Calif. 90245

1 October 1980

Prepared for

SPACE DIVISION
AIR FORCE SYSTEMS COMMAND
Los Angeles Air Force Station
P.O. Box 92960, Worldway Postal Center
Los Angeles, Calif. 90009

This final report was submitted by The Aerospace Corporation, El Segundo, CA 90245, under contract F04701-80-C-0081 with the Space Division, Air Force Systems Command, P.O. Box 92960, Worldway Postal Center, Los Angeles, CA 90009. It was reviewed and approved for The Aerospace Corporation by H. E. McDonnell, Principal Director, Communications Satellite Systems Directorate, Satellite Systems Division.

This report has been reviewed by the Public Affairs Office (PAS) and is releasable to the National Technical Information Service (NTIS). At NTIS, it will be available to the general public, including foreign nationals.

This technical report has been reviewed and is approved for publication.

APPROVED

Michael E. McDonald

Michael E. McDonald, Lt Col, USAF
Chief, Engineering and Test
FLTSATCOM System Program Office

Publication of this report does not constitute Air Force approval of the report's findings or conclusions. It is published only for the exchange and stimulation of ideas.

FOR THE COMMANDER

George E. Breton

George E. Breton, Col, USAF
System Program Director
FLTSATCOM System Program Office

UNCLASSIFIED

SECURITY CLASSIFICATION OF THIS PAGE (When Data Entered)

19 REPORT DOCUMENTATION PAGE		READ INSTRUCTIONS BEFORE COMPLETING FORM
1. REPORT NUMBER 12 SD-TR-81-20	2. GOVT ACCESSION NO. AD-A099 787	3. RECIPIENT'S CATALOG NUMBER
4. TITLE (and Subtitle) 6 SIGNAL PROCESSING DISTORTION LOSS IN SPREAD-SPECTRUM COMMUNICATION, COMMAND, CONTROL, AND NAVIGATION SYSTEMS		5. TYPE OF REPORT & PERIOD COVERED 9 Final Repts
		6. PERFORMING ORG. REPORT NUMBER 14 TR-0081(6724-01)-1
7. AUTHOR(s) 10 A. C. Lytle, Jr.		8. CONTRACT OR GRANT NUMBER(s) 15 F04701-80-C-0081
9. PERFORMING ORGANIZATION NAME AND ADDRESS The Aerospace Corporation El Segundo, California 90245		10. PROGRAM ELEMENT, PROJECT, TASK AREA & WORK UNIT NUMBERS
11. CONTROLLING OFFICE NAME AND ADDRESS 11		12. REPORT DATE 1 October 1980 13. NUMBER OF PAGES (12) 213
14. MONITORING AGENCY NAME & ADDRESS (if different from Controlling Office) Space Division Air Force Systems Command Los Angeles Air Force Station P.O. Box 92960, Worldway Postal Center Los Angeles, Calif. 90009		15. SECURITY CLASS. (of this report) Unclassified 15a. DECLASSIFICATION/DOWNGRADING SCHEDULE

16. DISTRIBUTION STATEMENT (of this Report)

Approved for public release; distribution unlimited

17. DISTRIBUTION STATEMENT (of the abstract entered in Block 20, if different from Report)

18. SUPPLEMENTARY NOTES

19. KEY WORDS (Continue on reverse side if necessary and identify by block number)

Amplitude distortion	Delay distortion	Distortion Loss
Bandpass filters	Differential delay distortion	Equalization
Communication Networks	Differential Phase Distortion	Group Delay
Communication system	Digital Data Transmission	Intersymbol interference
Data transmission	Distortion	Group delay distortion

20. ABSTRACT (Continue on reverse side if necessary and identify by block number)

An integral equation for calculating exact signal processing loss in direct-sequence PSK-modulated, pseudonoise, spread spectrum digital transmission, caused by passband amplitude and/or phase distortion is derived in closed form. Methods for computer-assisted or manual means of evaluating the integral are worked out in several examples taken from operational satellite systems hardware. Procedures, design tables, and computer programs are provided for combinations of passband distortion and signal spectrum-weighting characteristics. Passband

DD FORM 1473

UNCLASSIFIED

SECURITY CLASSIFICATION OF THIS PAGE (When Data Entered)

19. KEY WORDS (Continued)

Networks	Signal distortion
Network Theory	Signals Processing
Phase distortion	Signal Processing Loss
Phase shift keying	Spectral energy distribution
Protection ratio loss	Spread spectrum
Pseudonoise transmission	Wideband transmission

20. ABSTRACT (Continued)

distortion specification and allocation is considered, analyzed, and discussed.

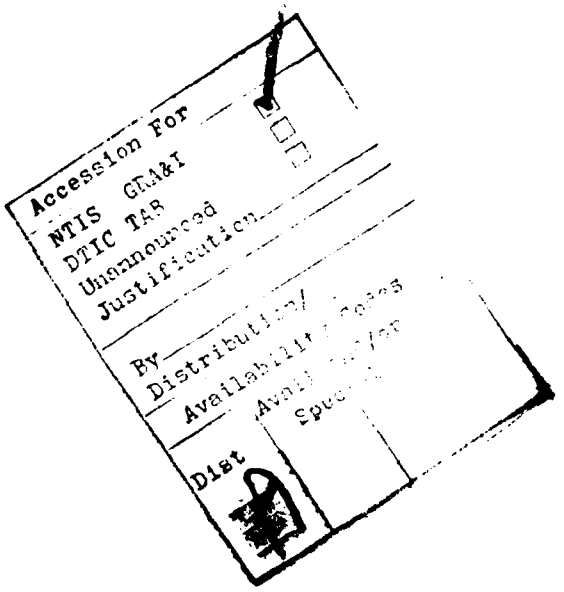

FOREWORD

Communications at gigabit speeds, whether for restricting user accesses, enhancing signal-to-noise ratios, for low probability of intercept, or for code division multiple access service require correspondingly wider signalling spectra. That places a premium on tighter control of amplitude and differential group delay distortion characteristics of the associated channel hardware. It also calls for more rapid and accurate means for measuring and evaluating quantitatively the effects of signal passband distortion in terms of loss in processing gain versus specific passband characteristics. This study demonstrates a technique which was developed for that purpose and which has been proved in evaluation of contemporary orbiting wideband satellite systems.

An innovative, exact method of analysis has been discovered and its application perfected. It significantly simplifies and therefore greatly speeds channel distortion loss analysis and calculation in PN signal processing systems.

Signal processing performance degradation in direct-sequence, digital phase-shift keying, pseudonoise communication, command and control, radar and navigation systems, using correlation demodulation, is related via a generalized closed-form integral equation to general passband distortion characteristics. Manual-only, as well as computer-aided analysis and design methods have been developed and are shown applied step-by-step to measured or a wide range of postulated distortion characteristics.

Differential group delay distortion loss measurement theory is derived. Distortion allocation tradeoff and specification models are discussed. Signal loss due to the presence of both phase and amplitude distortion is studied via formulas and tables for application to linear, soft-limiting, or hard-limiting cases. The possibility of noise enhancement effects due to passband amplitude ripple is shown and examined.

The above material, plus useful tables and figures of previously unpublished design data provided herein qualifies this study as a handbook of

theory, measurement, design, and analysis of primary significance in general PN-PSK communications-related system analysis, performance evaluation, and design. This handbook is complete in itself.

To enable this publication to be useful as a tool to technicians and to engineers, certain slight liberties may have been taken with mathematical symbolism, but enough derivation and descriptive material has been included so that it should satisfy readers who are interested in either theory or application.

ACKNOWLEDGMENTS

Acknowledgment is gratefully extended to former colleagues P. M. Hooten and W. E. Leavitt who defined the problem and the scope of the original investigation as it applied to performance evaluation of advanced wideband communications and navigational satellite systems and hardware. C. F. White, A. Ziffer, and L. S. Bearce provided welcome computer programming expertise. Recognition is accorded the MARISAT/Gapfiller and FLTSATCOM programs, from which some typical test results were utilized. Appreciation is further extended to the AFSC Space Division's Satellite Engineering Office (YK) at the Los Angeles Air Force Station and to The Aerospace Corporation FLTSATCOM Program Office for sponsorship of this publication. Gratitude is openly accorded the Publications Section of The Aerospace Corporation, El Segundo, California, for the preparation of this report in its published form.

APOLOGIA

Controversy has surrounded the preparation of this text almost from its inception. Members of the mathematically elite corps tended to be annoyed by some of the departures from the use of classically rigorous symbolism, whereas communications engineers, to whom this treatise is addressed primarily, sometimes felt uncomfortable with the remnant use of mathematics included as is. The engineering technologist who has the task of setting up for and making the actual measurements needs a pragmatic approach. Therefore, only if each class of reader is unable to use this report to understand what differential group delay distortion is, how to measure and to interpret the findings, and/or how to specify or to modify those characteristics, will the author feel he has failed.

An initial survey which sampled all three classes of potential user shows that a satisfactory compromise has been reached, balancing sophistication with hands-on ability to accomplish each intended purpose. That purpose was initially, and still is, to fill a void the author found in the literature as to the origin, the method of measurement, quantification and interpretation of the presence of differential group delay distortion characteristics.

Utilization of this treatise allows its users to obtain accurate numbers on real-life hardware, as well as on postulated characteristics. Therefore, we believe the original purpose has been accomplished.

May the reader and the user live happily ever after!

CONTENTS

CONTENTS (Continued)

CONTENTS (Continued)

FIGURES

FIGURES (Continued)

FIGURES (Continued)

FIGURES (Continued)

TABLES

TABLES (Continued)

TABLES (Continued)

SECTION 1. BACKGROUND

1.1 INTRODUCTION

Some method of signal processing for signal enhancement, recovery, or signal protection is ordinarily necessary in single and multiple-access communication services subject to high levels of interference. Figure 1.1 diagrams one of several methods of coding and spectrum spreading which has been found to have applicability for these purposes. Application of such techniques to baseband data transfer results in increased spectral occupancy, often in a rather large time-bandwidth product. Recovery of the original baseband data from direct-sequence modulation through utilization of a correlation detection process can yield theoretical signal gain equal to the above time-bandwidth product (Ref. 16). Unless the system end-to-end passband amplitude and/or phase response characteristics are free of distortion, i.e., unless the transfer function is linear in both amplitude and phase with frequency, the total theoretical gain will not be realized. Use is made of the fact that an entire communication system, or a channel thereof, may be treated as a band-limited circuit whose amplitude response and/or differential group delay data may be measured and characterized accurately. Study and handling of a large number of group delay plots during network and hardware evaluation led to invention of a very useful analytical convenience identified herein as "departure functions." After careful generation of the departure functions describing a channel under investigation, the distortion losses may be determined directly, using either manual/graphical or analytical means. Whether the departure functions are derived from measured data or are postulated and apportioned as in a design specification makes little difference in the system degradation computation process.

To a limited extent, amplitude and phase characteristics of a typical communications channel can be specified and adjusted almost independently. By skillful manipulation of amplitude and phase departure function

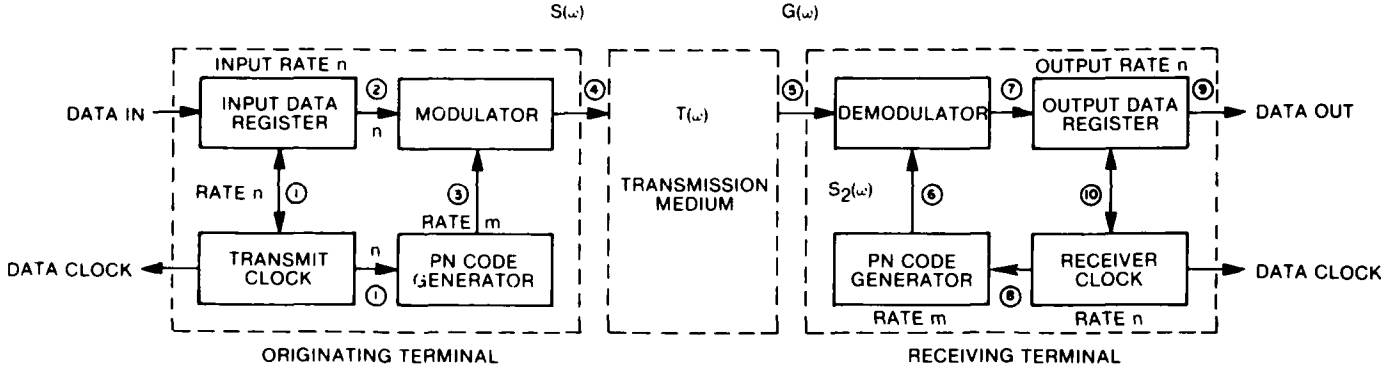

Fig. 1-1. A Basic PN Data Transmission System

characteristics, and their appropriate allocations within systems, or at subsystem levels, it may be possible to avoid use of independent equalization devices.

If wideband PSK data is to be transmitted through extended networks of non-uniform hardware characteristics, equalization devices may be placed at certain convenient locations so that subsystem inter-operability or inter-changeability is practical. This enables coding gain degradation to be minimized in large or/and multi-terminal networks. As signalling spectra become wider, the requirements for dispersed equalization to minimize distortion loss usually becomes increasingly stringent. Methods for allocating characteristics to various points in a communication network, or to individual black boxes in a system, are discussed. Although the subject of equalization is not treated in this publication since it is a field in its own right, several of the better known references are cited for convenience (Refs. 21-26).

Previously, the difficulty in formulation and manipulation of the equations involved in determining signalling distortion losses was countered by using "rules of thumb." This procedure usually leads to over-specification of differential group delay or phase characteristics "just to be on the safe side." The usual consequence of this approach is equipment over-design with its inherent excessive cost, size, and/or weight. Over-specification is now no longer necessary, utilizing the methods set forth in this document.

Complete computer programs, tables of necessary functions, and typical worked-out examples are provided.

This study is based upon use of digital binary waveforms having pseudo-noise time distribution statistics for application in direct sequence, spread-spectrum communications. Most texts on communication theory establish the relationships between simple periodic binary waveforms and their corresponding frequency spectrum components via the Fourier series or transform (Refs. 19, 25, 27, 32, 33, 44, 46). Fewer extend the processes into the aperiodic and random waveforms, where statistical and probabilistic representations of the Fourier Transforms are required (Refs. 32, 39, 40, 49). It is

not the purpose of this text to duplicate or re-derive those references, but to employ their results. Therefore, the author borrows liberally therefrom.

The most fundamental and important relationship, with which the reader would do well to become familiar, is the transform pair

$$F(t) = \frac{1}{2\pi} \int_{-\infty}^{+\infty} f(\omega)\, e^{+j\omega t}\, d\omega$$

$$F(\omega) = \int_{-\infty}^{+\infty} f(t)\, e^{-j\omega t}\, dt$$

These relationships allow direct determination of the frequency component amplitudes and phases generated by communication signals and vice versa. As mentioned already, simple digital binary time varying waveforms are assumed in this approach.

One very important result established by the above transform pair is that a "simple bit" has a continuous $(\sin x/x)^2$ power spectrum whose envelope is partially represented in Figure 1-2a. A single bit which is repeated periodicaly will have spectral lines somewhat as shown in Figure 1-2b, where the ratio of bit width to bit repetition is as indicated (Refs. 32 and 33). Wave trains having random bit widths will generate the $(\sin x/x)^2$ power spectral envelope whose null frequencies are multiples of the clock keying rate.

All other required relationships will be derived in the body of the text.

1.2 APPLICATIONS

Using only the approaches and the materials provided in this report, network, system, or device passband distortion loss effects can be studied and determined to arbitrary accuracy. The designer, referring to the tables and curves of Appendices A through F, can predetermine the effects of modifying

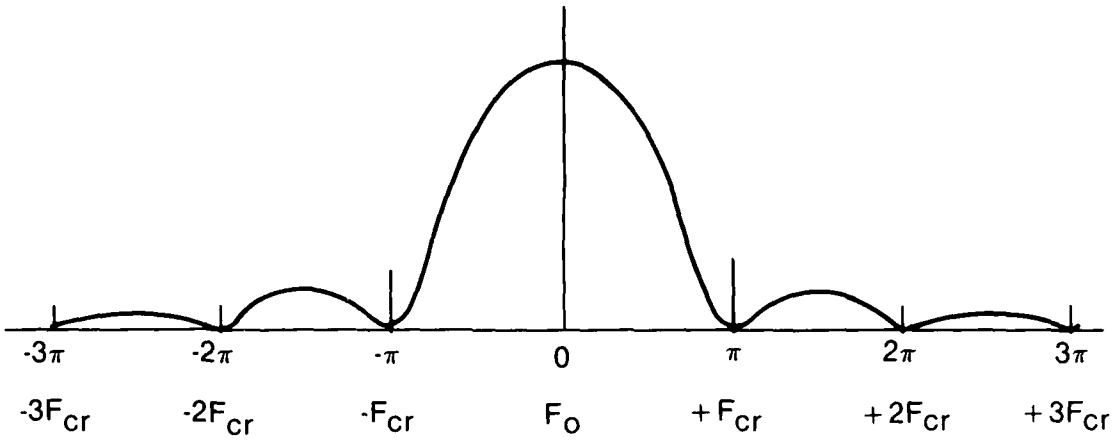

WHERE F_o = IF OR CARRIER FREQUENCY

AND Fcr = CODE CLOCK OR CHIP RATE = $1/\tau$

AND τ = BIT OR CHIP WIDTH

Fig. 1-2a. Spectral Energy Distribution for PN Signal

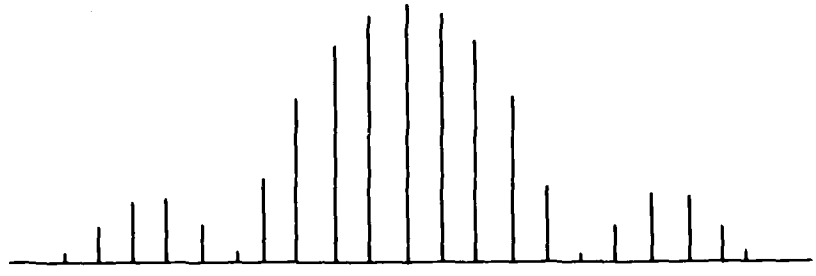

(CHIP OF WIDTH τ SENT EVERY FIFTH INTERVAL OF τ)

Fig. 1-2b. Line Spectrum for Non-Symmetry Ratio of 5 to 1

the phase and/or the amplitude characteristics. With some expertise in FORTRAN, the designer will be able to adapt the computer programs of Appendix E to suit his own specific application.

Typical questions which may be addressed relative to transmission of direct-sequence, pseudonoise-modulated carriers through distorted media by application of the techniques developed in this report include the following:

a. How much distortion degradation will this particular network or device produce due to its particular differential group delay characteristic? (Determination of the amount of distortion loss which can be accepted is usually an operational consideration, and hence is not within the intended scope of this presentation.)

b. How much signal energy distortion loss is produced by linear, parabolic, cubic, and higher-order terms, and by ripple of various magnitudes and frequencies of occurrence, whether occurring in the phase or the amplitude characteristic, either singly or in combinations?

c. How can these effects be measured and expressed analytically, and how can they be evaluated?

d. How much equalization need be applied to reduce the distortion loss to desired levels, or, if possible, to eliminate it?

e. How can the effects of imperfect and variable levels of limiting be treated?

f. What is the specific relationship between spectral truncation and signal loss?

g. How can one determine analytically the transmission distortion loss caused by non-symmetrical passband characteristics?

h. How can one specify or allocate distortion characteristics which will result in a pre-determined signal loss?

1.3 A BASIC PN COMMUNICATON SYSTEM DEGRADATION MODEL

The process of recovering data from a pseudonoise modulated carrier involves multiplying that carrier by a replica PN carrier properly phased in time. The related mathematical process is known as the convolution of two

functions, maximizing the correlation coefficient of the two functions. The device in which this is accomplished is herein called a correlation detector or demodulator. Gold (Ref. 36) and Golomb (Ref. 38) have shown that the properties of the PN sequence, and hence their spectra, are monotonic and are expressible analytically. This PN characteristic, plus network transfer-function measurement equipment and increased computing capability, has brought the signal examination process to practice.

Figure 1-1 is a diagram of the basic elements of a PN-coded digital communication system. It shows simplified originating and receiving terminals, and contains a propagation medium which is shown as a band-limited channel. The steady-state parameters of interest between the input and output ports in the transmission medium usually can be measured conveniently with sufficient accuracy, in terms of amplitude and phase shift characteristics, for any subsequent analysis.

Non-stationary and random contributions due to most propagation paths between antennas will not be separable from other transient phenomena when attempting to measure open-loop system performance. The effects of ionospheric scintillation may appear as instrumentation instability superimposed on signal fades.

Spurious products can be generated during the correlation-detection process, originating due to passband nonlinearities. These may be sufficiently large to increase the already present noise floor, reducing the processing gain otherwise available.

1.4 DISCUSSION OF TERMINOLOGY

This section briefly introduces several terms and phrases in the context in which they are used throughout this document. These include coding gain, implementation loss, spectral energy distribution, phase, truncation loss, correlation of two power spectral distributions, and transmission impairment. References are suggested where appropriate.

1.4.1 Implementation Loss

Implementation loss is present when performance of the PN communication system falls short of theory. Several forms of implementation loss are addressed. These include losses resulting from use of finite signal spectra, transmission impairment loss due to amplitude and phase distortion in physically realizable signal passbands, and loss due to imperfection in code tracking. Implementation loss is the sum of these losses.

1.4.2 Coding Gain

The theoretical gain available from pseudonoise coding may be expressed and determined in the following manner:

$$\text{Gain} = 10 \log_{10} R \qquad \text{in dB} \tag{1.1}$$

where

$$R = \frac{\text{PN Clock Rate}}{\text{Data Clock Rate}} \tag{1.2}$$

Assuming isochronal code bits or chips, the concomitant spectral occupancy can be determined via the associated Fourier transform pair previously introduced (see also Ref. 32, Chapter 6). It can be demonstrated via the transform that the coding gain is also expressible as the ratio

$$R = \frac{\text{Data Bit Width}}{\text{PN Bit Width}} \tag{1.3}$$

1.4.3 Spectral Energy Distribution

Figures 1-2a and 1-2b indicate the envelope and discrete spectrum of a portion of the theoretical energy distribution for a random PN waveform, where τ is the chip width. For reasons of practical hardware implementation

and spectral conservation, the transmitted sideband spectrum usually is restricted so as to lie between the first nulls of the theoretical distribution. The energy loss due to such truncation can be determined by calculating the energy present in the truncated portion and dividing it by the energy contained in the total, or untruncated spectrum, mathematically described as lying between plus and minus infinity.

Taking advantage of spectral symmetry and using single-sided integration, one obtains the necessary values:

$$\int_0^{\infty} \left(\frac{\sin x}{x}\right)^2 dx = \frac{\pi}{2} = 1.57079623 \qquad (1.4)$$

$$\int_0^{\pi} \left(\frac{\sin x}{x}\right)^2 dx \cong 1.41815157 \pm 2 \times 10^{-9} \qquad (1.5)$$

The energy loss which wouldxbe experienced at the output of an ideal correlation demodulator, given such a truncated spectrum convoluted (cross-correlated) with a pure spectrum, is found from the following equation:

$$\text{Loss} = 20 \log_{10} \frac{1.41815157}{\pi/2} = -0.888 \text{ dB} \qquad (1.6)$$

This loss is tolerated as a necessary hardware implementation tradeoff. If the spectrum were not truncated, most of the received energy outside the first nulls would be received at a level below receiver front-end thermal noise. Therefore, the spectral utilization in this document has been limited to that portion of a $(\sin x/x)^2$ spectrum lying between the first nulls.

1.4.4 Truncated Spectral Energy Loss

Figure 1-3 shows the spectral power distribution versus percent of the total band-centered bandwidth utilized when the comparison spectrum is limited to the energy which lies between the first lower and first upper nulls of a $(\sin x/x)^2$ signal spectrum. It should be recognized that the upper 25%

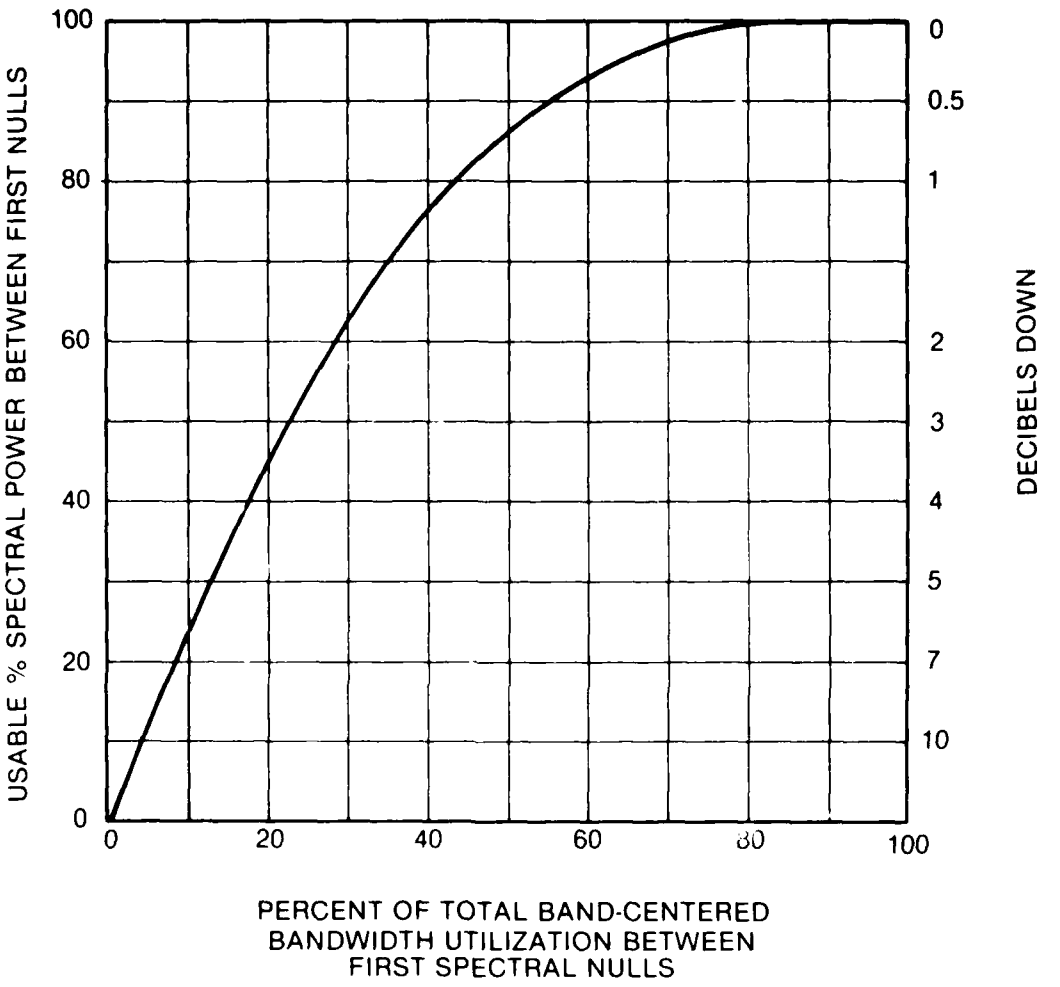

Fig. 1-3. Spectral Energy Distribution vs Bandwidth Utilization

of the spectrum remaining after truncation contributes very little to system performance, permitting relaxation in that portion of the passband phase and amplitude characteristic. A further investigation of truncation may be found in Ref. 34.

1.4.5 Convolution, or the Correlation of Two Power Spectrum Distributions

The ability to multiply two finite-energy signals in the frequency domain, and to convolute their Fourier transforms in the time domain is one direct result of application of Parseval's theorem (sometimes also known as the Parseval-Rayleigh theorem) (Ref. 27, Section number 2.5, or Ref. 32). The correlator-demodulator output voltage $E_o(x)$, available from taking the cross-correlation product or convolving one signal voltage spectrum $S_1(x)$ with another similar signal voltage spectrum $S_2(x)$, can be found from amplification of the following definition of correlation detection.[a]

$$E_o(\mu) = \int_{-\infty}^{+\infty} S_1(x)\, S_2(x - \mu)\, dx \text{ volts} \qquad (1.7)$$

where $E_o(\mu)$ reaches its maximum when $S_1(x) = S_2(x)$ and the frequency offset $\mu = 0$.

Now, let $S_1(x)$ be a perfect spectrum, and let $S_2(x)$ be a distorted version of the same spectrum, where T(x) describes and represents the distortion function. Then

[a]There is a well-established bank of worked-out Fourier transforms relating the usual communication signalling waveforms to their respective spectral distributions. However, if the waveform has pseudonoise characteristics, it is possible to employ statistical and probabalistic means. It turns out under the latter conditions that auto-correlation functions and spectral density functions are Fourier transform pairs. However, proof that such is the case is well beyond the intended scope of this treatise (see Refs. 32, 49).

$$S_2(x) = T(x)\, S_1(x) \tag{1.8}$$

To obtain the available power from E(x), one could substitute (1.8) in (1.7) and square E(x). Assuming unit load-resistance, the expression for maximum available power P_a then becomes

$$P_a = E_o^2(x) = \left[\int_{-\infty}^{+\infty} S_1^2(x)\, T(x)\, dx\right]^2 \tag{1.9}$$

1.4.6 Transmission Impairment

T(x) is useful to represent analytically the distortion characteristics of a transmission circuit, both in amplitude and in phase, A(x) and $\phi(x)$, respectively. These expressions are later further broken down to represent departure from ideal characteristics of their respective kinds.

1.4.7 Differential Group Delay Distortion

A portion of a PN signal spectrum representing signalling components generated by a perfect isochronous waveform as in Fig. 1-4a, is shown in Fig. 1-4b and 1-5a. When the signal spectrum is passed through a wide rectangular filter having a linear phase characteristic, as in Fig. 1-4c, the recovered signal waveform (Fig. 1-4d) is changed only by a time delay or shift of "t" seconds. The expression

$$t(\omega) = d\phi(\omega)/d\omega \tag{1.10}$$

defines the passband phase slope (see Ref. 25, Section 3.14). The whole spectral group has thus been delayed, and hence the term "group delay" is applied, while adding "differential" refers delay to midband.

In typical band-limited devices, the measured phase characteristic will depart from perfect linearity: some of the output spectral

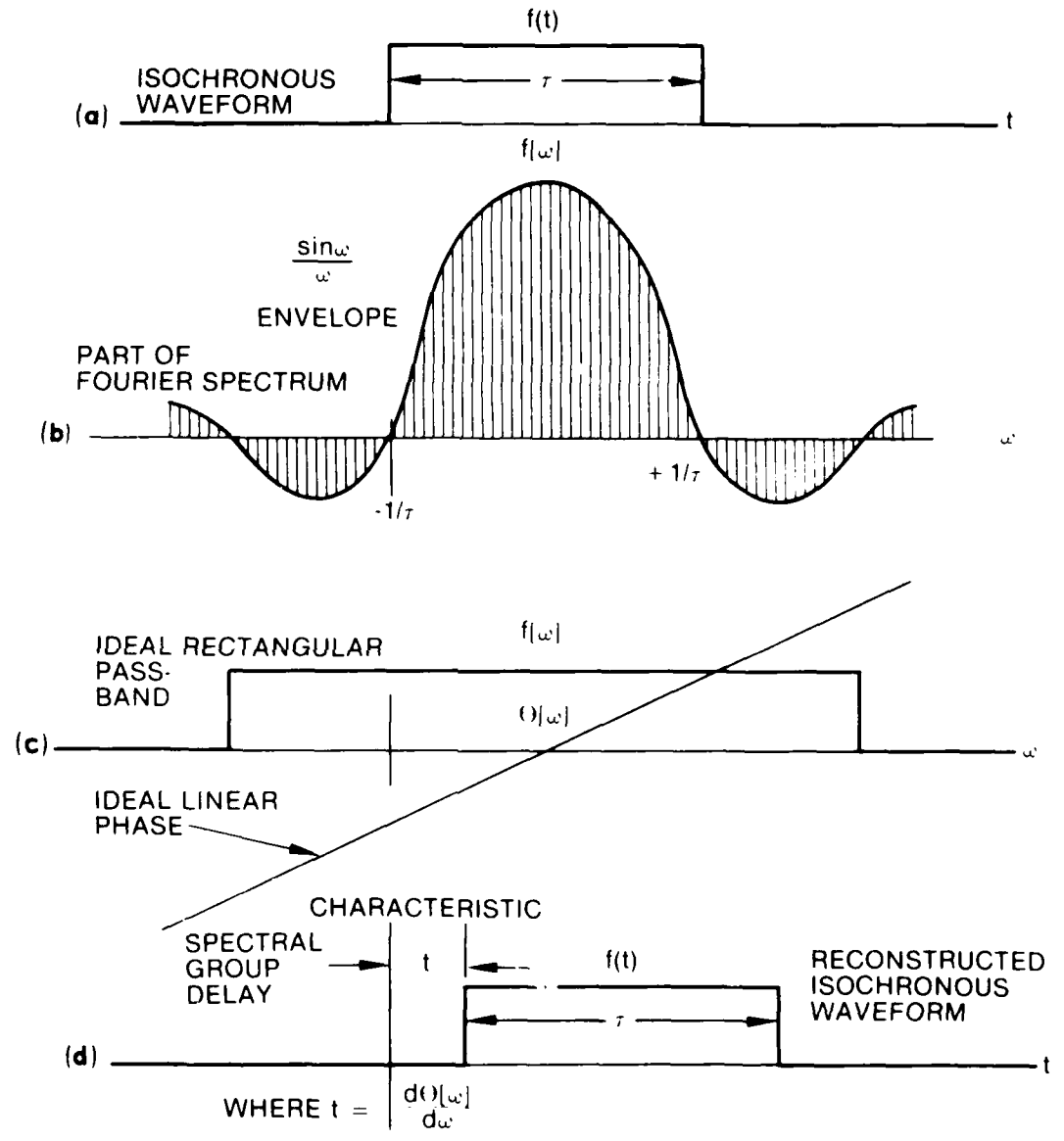

Fig. 1-4. Developing the Concept of Group Delay

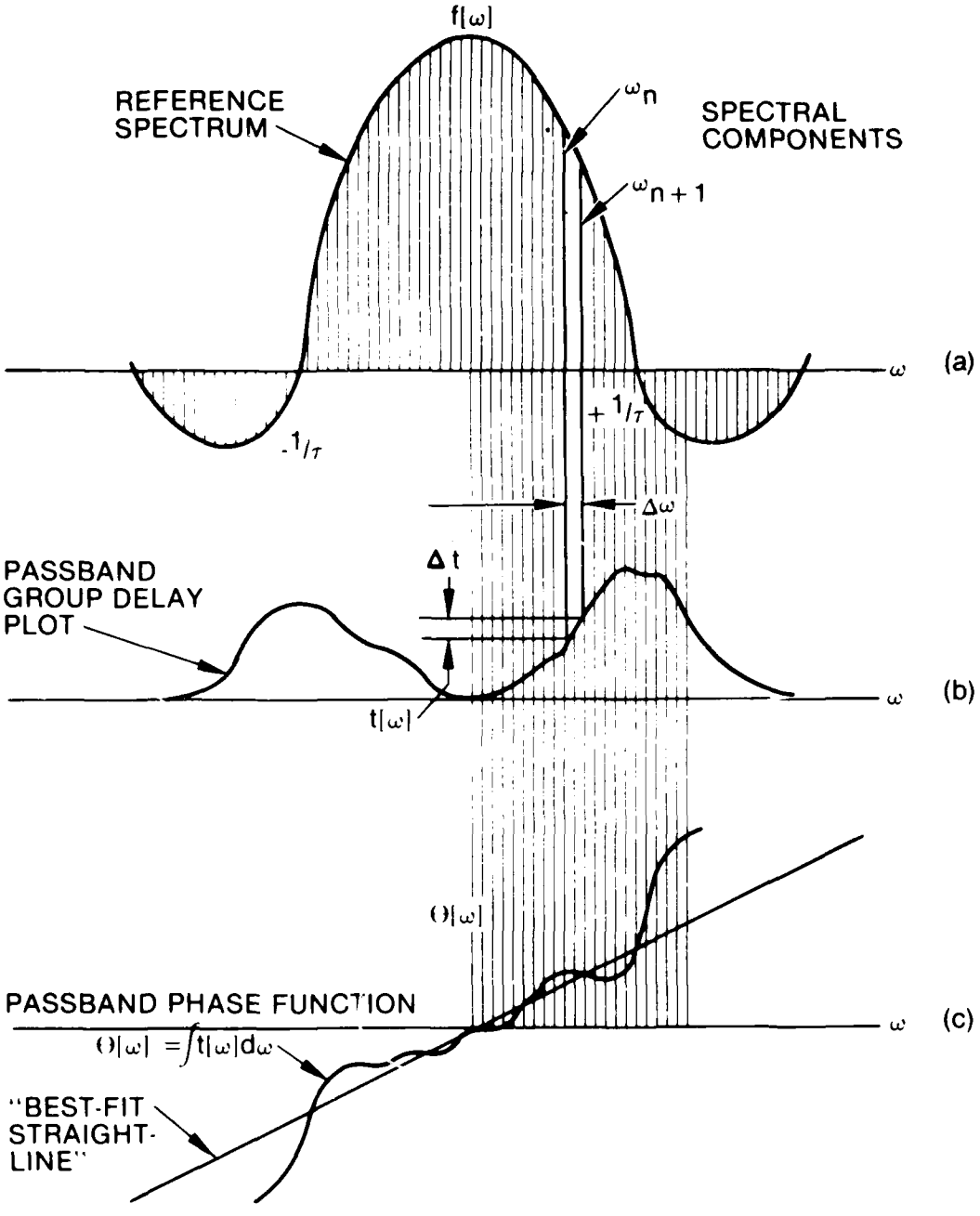

Fig. 1-5. Developing the Concept of Differential Group Delay Distortion

components of Fig. 1-5a will arrive early or late relative to the carrier, causing distortion of the reconstructed time waveform. A typical band-limited group-delay plot with its corresponding phase characteristic is shown in Fig. 1-5b and c. Zero group delay, by definition, occurs at band center. Delay peaks occur in the vicinity of the passband half-power skirt points.

The group delay plot of Fig. 1-5b shows adjacent frequency spectral components ω_n and ω_{n+1} to be delayed from the spectral linear differential-phase line by non-proportional and unequal amounts. Therefore, spectral component recombination at the device output produces a distorted waveform. The extent of differential time-delay distortion between adjacent spectral components may be determined directly from a differential group delay (DGD) plot similar to Fig. 1-5c, from which corresponding DGD distortion functions may be generated. Integrating $t(\omega)$ across the passband of the device under consideration generates the passband phase function. Departures from the best straight-line fit to the phase function generate the values of a phase distortion function, labeled "phase departure function."

1.4.8 Phase Departure Function

The best straight-line fit to an integrated group delay curve is identified as and often found to be closely approximated by the linear term in a power series representation of the phase function. It is not necessary to find a power series, since a linear least squares computer program will usually yield an accurate approximation quickly and of sufficient accuracy for subsequent calculation of the distortion loss value. An accuracy of about 5 percent is believed generally available without special precautions beyond those given in the body of this treatise.

1.4.9 Phase

The usual interpretation of the term "phase" should be expanded to include the concept of "differential phase." The two concepts are often used interchangably herein intending to represent relative phase of spectral sideband components rather than absolute sideband or carrier phase. Relative phase distortion results in time-domain waveform distortion, since associated

spectral sideband components then depart from a linear relationship, also resulting in decreased available signal power.

Another useful consideration to gain insight into the physical aspect of performing the Fourier Transform manipulation is to consider that phase interchanges with time-difference. For example, when performing a convolution of one spectrum over another, as by shifting the frequency axis of one spectrum relative to the frequency axis of the other spectrum, the frequency shift may be viewed as a rather rapid radian-phase shift, which corresponds in the time domain to moving one PN code over the second PN code. This is in essence what happens during the code search process. When code lock has occurred, the code separation in time is within a fraction of a code bit. While in the frequency domain, the integration product of the convolution (or cross correlation) process becomes positive real, or non-orthogonal, yielding a correlation "spike."

The phase departure function affords a rigorous method for analytical examination of PN signal losses because distortion loss has been made a direct function of passband-induced spectral distortion.

Methods of obtaining the DGD plot, deriving the corresponding phase distortion function, and calculating signal distortion loss by manual means on an HP-34, HP-97 or more elegant machine, are described later.

It will also be shown that amplitude distortion functions also contribute to signal energy loss in the absence of ideal passband limiting.

1.5 THE FUNDAMENTAL LOSS-DEGRADATION EQUATION

This study is based upon a normalized expansion of Eq. (1.9). Let the transmission distortion function T(x) be written in the form

$$T(x) = A(x)\ \phi(x) \tag{1.11}$$

where A(x) represents the passband amplitude function and $\Phi(x)$ represents its phase function.

Let a correlator-demodulator output voltage due to a signal received over a distorted channel be divided by the output voltage due to a signal received over a perfect channel. The resulting normalized loss degradation equation is thus defined:

$$L_d = \frac{\int_{-\ell}^{+\ell} [S(x)]^2 A(x)\, \phi(x)\, dx}{\int_{-\ell}^{+\ell} [S(x)]^2\, dx} \qquad (1.12)$$

The loss is given by the expression

$$\text{Loss} = 20 \log_{10} L_d \quad \text{dB} \qquad (1.13)$$

When integration is carried out over the arbitrary limits of $\pm\ell$, both symmetrical and non-symmetrical passbands may be treated. It is intended that distortionless passbands are represented when $A(x) = \phi(x) = 1$, causing the energy ratio to be unity and the loss to be zero. The denominator represents the output of an ideal local PN reference generator, while the numerator represents distorted incoming PN signal power.

Spectral weighting is implied in the function S(x) and is defined identically for both the numerator and denominator, so that the approach via the above is perfectly general. While this study was conducted for the more-or-less special case in which

$$S(x) = \frac{\sin(x)}{x} \qquad (1.14)$$

the keying waveform need only be assumed to be isochronous PN-PSK of arbitrary shaping. Slight departures therefrom have not been found to invalidate this analysis nor the test results gained therefrom.

The numerical coefficient "20" rather than "10" precedes the logarithmic symbol in Eq. (1.13) because the code-correlator demodulator output is a voltage level proportional to the product of its two input signals levels, so that L_d is a voltage ratio. Because most contemporary systems are designed so that the radiated spectrum is truncated at $\pm 1/\tau$, the limits of integration ℓ are scaled to equal π, for computational convenience, at the first nulls.

In computing the design curves presented in Appendices A, B, and C, perfect passband symmetry and spectral symmetry were assumed. Also, spectral center and passband center frequencies are assumed coincident. These assumptions make it convenient to integrate over the passband characteristics from band center to the upper first null. Scale factors may be introduced for investigation of other truncations such as using bandwidths greater or lesser than represented by the first null frequencies, or other products of chip-width and filter width.

Non-symmetrical passbands are treated by methods given in Sections 4 and Appendix C.

1.6 DEPARTURE FUNCTIONS INTRODUCED

A class of functions is described which permits convenient manipulation of analytical expressions for passband distortion characteristics. Superfluous terms in the passband expression are deleted, retaining only those which relate significantly to energy loss production. Passband symmetry is not requisite to the use of departure-function analysis.

Distortion is expressed analytically in terms of deviations from ideal characteristics between defined passband frequency limits. Thus, an amplitude departure function describes analytically the deviation from a rectangular passband. Such amplitude effects which may be described include "round shoulders," ripple, skewed shapes, or combinations thereof, and are normalized relative to band center. Similarly, a phase departure function defines any deviation from a straight-line of phase versus frequency throughout its passband, and also may be normalized to zero at midband, i.e., at

spectral center. Hence, the previously introduced functions A(x) and $\phi(x)$ become departure functions when defined so that they have the value of unity in the absence of distortion. The amplitude function A(x) may be greater or less than unity as some point in the passband. For reasons to be discussed later, the phase function $\theta(x)$ has a magnitude equal to or less than one at all points in and out of the passband. Both amplitude and phase departure functions may be contributing simultaneously to signal loss as in the case of imperfect amplitude limiting, and especially in the situation where input signal level variation is a cause of variable limiting. As will be shown, that situation poses no problem to loss determination or analysis.

The phase departure function $\phi(x)$ is usually the most important of the two functions when treating digital phase-shift communications It is used to describe the extent and manner, as a function of frequency offset relative to band center, by which the incoming spectral components differ in phase from their corresponding locally generated PN components. A linear departure between the incoming and the local reference spectral components relative to the carrier frequency represents a time delay and normally is removed by the bit-clock synchronizing circuitry. If such effects are not completely removed, a phase-departure function will still exist, resulting in definite calculable signal energy loss. Higher-order terms in the departure function are not removed by the synchronizing circuitry.

When considering phase departure functions, it will be seen that the magnitude of the departure function at any point in the passband is set by the magnitude of the phase angle in what is essentially a vector dot-product situation that exists between corresponding elements of two similar signal spectra. A correlator-demodulator performs a dot-product and summation function to accumulate and produce its output signal. Stated in another way, corresponding spectral components at particular frequencies across the passband are squared and then multiplied by the cosine of the departure function angle at each of those corresponding points. When the energy content in each pair of spectral components at any instant is integrated across the passband of interest in the post-correlation filter, the desired output signal is reconstructed.

As will be shown in Section 2, phase distortion losses and amplitude distortion losses may be calculated separately, expressed in decibels, and added. If ideal hard-limiting exists prior to the input of the correlator-demodulator, the amplitude transfer function reduces to unity, so that only the phase departure function need be considered. Several such examples are calculated and presented in Section 4.

When the appended departure function loss tables were being computed for the various coefficient magnitudes given in Appendices A, B, and C, integration was accomplished in intervals of 0.01 radian from band center to band edge. Even-order symmetry was assumed of the amplitude departure function. Either even or odd-order symmetry may be assumed for the phase departure function. In the case of skewed spectral energy distributions, non-symmetrical passband characteristics, or incoming signal spectrum not centered in the passband, the expressions will require appropriate modification. The expressions are still valid for non-symmetries if integration is carried out over the entire passband, usually from the lower first null to the first upper null.

Another necessary assumption in mechanizing the presented form of the loss equations was that constant transmitted caloric signal power be maintained in both the distorted and the undistorted cases, providing a common power reference across the spectrum of interest. The necessity for that assumption may be realized if a distortionless transmitter is sending signals to two identical receivers, one of which also has no internal distortion, while there is known passband distortion in the other. The differences in receiver correlator-demodulator outputs will then be predictable by the analytical method presented herein. Conversely, if a distortionless receiver "listens" to a transmitter whose output can be made either distortion-free or may be equipped with known amounts of distortion, it will be seen that the caloric power output remains the same, but the received correlator-demodulator output is reduced predictably due to introduction of the injected known amount and type of departure function.

SECTION 2. DERIVATIONS

2.1 EXAMINING THE DEPARTURE FUNCTION

This publication is intended to be the equivalent of a reference text for use by communication systems engineers. Most of the rigorous mathematics is included in the references, but for convenience, enough of the mathematical background is included to enhance understanding of the processes presented herein. Many excellent references are available, but those likely to be useful are numbered 4 through 11, 14, 16, 19, 25, 28, 33, 38, and 39. The more engineering-oriented references are 1, 2, 20, 27, 31, 32, 34, and 37. The remaining references provide deeper insights into special cases which are noted throughout the text.

Classical network theory (Ref. 4 through 10) shows that electric wave-filter amplitude and phase characteristics are interrelated in the frequency domain by the Hilbert Transform. Therefore, attempts to design filters with independently predetermined amplitude and phase response characteristics do not always meet with total success. The search for filters having special passband characteristics has led to development of various complex polynomials, of which the Butterworth and the Tchebyshev (Ref. 45, Chap. 14) types are probably the most likely to be encountered.

It is well known that a carrier modulated by a digitial data stream and then passed through a bandpass filter will appear at the output bearing the appropriate transfer characteristics of the filter. When a designer is unable to obtain exactly the output amplitude and phase characteristic he desires, he often makes use of all-pass filters as equalizers at the carrier or some intermediate frequency (Refs. 20 through 26) and thus obtains the amplitude, the group delay, or/and the phase response required.

Let D(t) represent a random binary data stream in the time domain. Its frequency spectrum can be found from its Fourier transform pair (Refs. 27 and 32) or it may be derived analytically from

$$S(\omega) = \int D(t)\varepsilon^{-j\omega t}\, dt \qquad (2.1)$$

When the signal is passed through a band-limiting electrical circuit, or through an entire electrical system viewed as a bandpass filter, the output spectrum may be expressed conveniently in such a way that the distortion effects are present in the signal's analytical expression via $T(\omega)$. Bringing forth Eq. (1.10) with a change in variable

$$T(\omega) = A(\omega)\, \phi(\omega) \qquad (2.2)$$

where $T(\omega)$ may now be considered to be a complex variable in which $A(\omega)$ is the real term and $\phi(\omega)$ is the imaginary term (see Ref. 43). In linear devices, the output signal spectrum $G(\omega)$ will be represented by the product of the input signal spectrum $S(\omega)$ with the complex variable $T(\omega)$ as per the following:

$$G(\omega) = S(\omega)\, T(\omega) \qquad (2.3)$$

The exact transfer function can sometimes be calculated, but is usually measured and approximated analytically, permitting calculation of the output signal spectral characteristics.

Subsequent analysis may now make use of the previously introduced departure function, expressing the differences between the ideal characteristics and the actual characteristics, by expanding the transfer function $T(\omega)$ using the following departure-function format:

$$A(\omega) = 1 - \alpha(\omega) \qquad (2.4)$$

and

$$\phi(\omega) = 1 - \beta(\omega) \tag{2.5}$$

where $\alpha(\omega)$ and $\beta(\omega)$ are, respectively, the normalized Fourier series or the Maclaurin or Taylor power series expansions (see Refs. 33 and 37) of the differences (i.e., the distortion) between their measured characteristics and their ideal rectangular passband amplitude and linear phase passband responses, respectively. Note that $\alpha(\omega)$ and $\beta(\omega)$ are both zero in the absence of passband distortion. When they are non-zero, they are responsible for conversion of signal energy into noise energy via their higher-order product terms. Some of those products will fall in the signal passband and may significantly reduce the available signal-to-noise ratio.

If $A(\omega)$ is expressed exponentially, then Eq. (2.4) may be rewritten

$$A(\omega) = \varepsilon^{-\alpha(\omega)} \tag{2.6}$$

so that at zero departure from the ideal response there is zero attenuation. Similarly, Eq. (2.5) may be rewritten

$$\phi(\omega) = \varepsilon^{-j\beta(\omega)} \tag{2.7}$$

so that with no phase non-linearity distortion, there will be no signal output distortion loss caused by the phase characteristic. In the distortionless case $\Gamma(\omega)$ will still equal unity, so that in exponential form the equation for the transfer function $T(\omega)$ will be written

$$T(\omega) = \varepsilon^{-[\alpha(\omega) + j\beta(\omega)]} = \varepsilon^{0} = 1$$

2.2 TIME-DOMAIN APPLICATION OF THE DEPARTURE FUNCTION

Because of its applicability in signal analysis, the versatility of the frequency-domain departure function, as it applies to distortion in the time domain will be demonstrated.

Since passband distortion characteristics are easily measurable in the frequency domain, along with the signal spectra which they modify, it is feasible to find the resulting waveforms G(t) in the time domain by converting the frequency characteristics by use of the inverse Fourier transform.

To apply the inverse transform directly, consider the following equation by use of Eq. (2.3):

$$G(t) = \frac{1}{2\pi} \int_{-\infty}^{+\infty} S(\omega)\ T(\omega)\epsilon^{+j\omega t}\ d\omega \tag{2.8}$$

Now, entering Eqs. (2.3) and (2.5) into Eq. (2.8) and expanding enables G(t) to be broken up into four convenient expressions:

$$G(t) = G_{\alpha}(t) + G_{\beta}(t) + G_{\alpha\beta}(t) + G_{o}(t) \tag{2.9}$$

where

$G_{\alpha}(t)$ represents the amplitude distortion terms

$G_{\beta}(t)$ represents the phase distortion terms

$G_{\alpha\beta}(t)$ represents the second-order or cross-product terms

$G_{o}(t)$ represents the output waveform recreated from an undistorted signal spectrum, and should accurately describe the original signal.

Expanding and examining each of these terms enables the complexity of the subsequent mathematical manipulation required.

$$G_{\alpha}(t) = -\frac{1}{2\pi} \int_{-\infty}^{+\infty} S(\omega)\, \varepsilon^{[\alpha(\omega) + j\omega t]}\, d\omega \qquad (2.10)$$

$$G_{\beta}(t) = -\frac{1}{2\pi} \int_{-\infty}^{+\infty} S(\omega)\, \varepsilon^{[j\beta(\omega) + j\omega t]}\, d\omega \qquad (2.11)$$

$$G_{\alpha\beta}(t) = \frac{1}{2\pi} \int_{-\infty}^{+\infty} S(\omega)\, \varepsilon^{[\alpha(\omega) + j\beta(\omega) + j\omega t]}\, d\omega \qquad (2.12)$$

$$G_{0}(t) = \frac{1}{2\pi} \int_{-\infty}^{+\infty} S(\omega)\, \varepsilon^{j\omega t}\, d\omega \qquad (2.13)$$

When the indicated operations are performed, these expressions provide a convenient means for determining and for isolating the time-domain distortion contributions, characteristic for characteristic, directly from the frequency-domain departure functions.

Application of the above four equations is also important to digital receiving systems having "memory": when the energy from one data bit overlaps the energy received from a preceding (or following) data bit, biasing the "one-or-zero" decision process, the receiver is said to have "memory." PN systems, to which this study is principally addressed, do not rely upon memory, i.e., do not rely upon absolute synchronization, but the present analysis of distortion for the PN case still can be applied directly to the memory or synchronous case.

It is suggested that the reader consult Refs. 25 and 26 if there is interest in gaining further insight into simultaneous use of time convolution. However, such joint incorporation with convolution requires evaluation of double integrals, tends to be laborious, and gains little except the personal conviction of the validity of the process.

2.3 EXAMINING THE SIGNAL MODEL

Up to this point several necessary concepts have been presented. The material in these next few paragraphs extends and examines in more detail the relationships between the signal and the loss computation process.

Assuming quasi-perfect passband symmetry, the normalized loss function introduced by Eq. (1.11) may be rewritten in the frequency domain as follows:

$$L_d = \frac{\int_0^{\pi} T(\omega) \cdot S^2(\omega)\, d\omega}{\int_0^{\pi} S^2(\omega)} \tag{2.14}$$

where L_d is identified as the distortion loss. The "dot-product" appearing in the numerator will be discussed later. The denominator represents the theoretical undistorted signal power available.

Let Fig. 2-1 represent an incoming line spectrum at a particular instant of time, with arbitrary phases for each spectral component, entering the correlator at the left. Another incoming replica signal spectrum, at the same instant of time, is shown coming from the local code generator. The local spectrum is assumed to be ideal (see Ref. 32, Sections 8 and 9, and Ref. 33, Section 7.2). The correlator output signal in Fig. 2-2 is intended to represent the sum of the products of corresponding spectral line pairs, each at a different phase angle relative to the adjacent distortion-generated phase angle. The phase of each side-band element is thus advanced or retarded relative to its straight-line place in a perfect spectrum. Figure 2-2 attempts to show that the reconstructed correlator output signal acts like and may be treated as the sum of a number of paired-vector products, strictly in accordance with the real power each related pair contributes to the total output.

Because the frequency translation process is linear, translation of the correlator-demodulator processes to some other intermediate frequency, or to zero-frequency, for analytical convenience loses nothing. Where an ideal

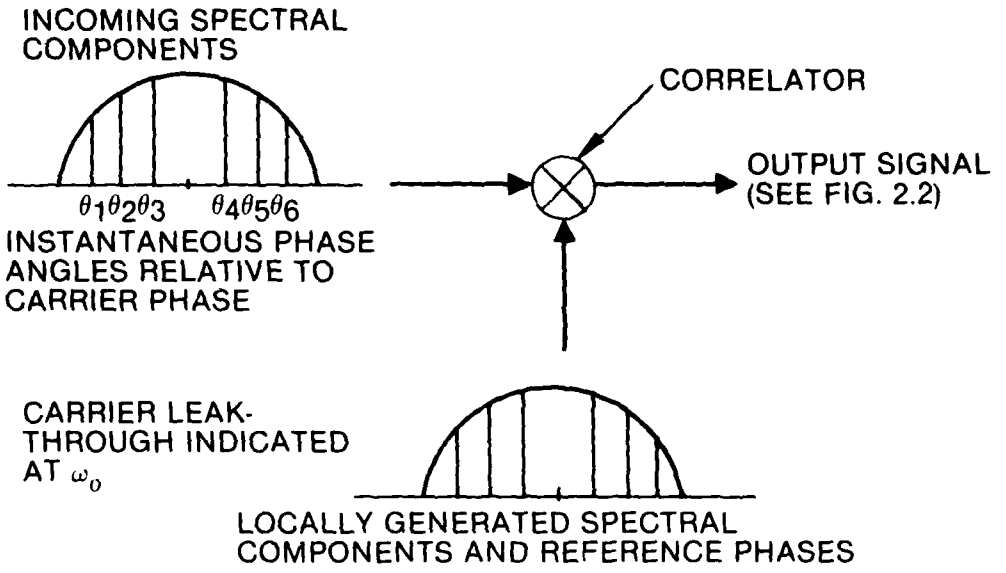

Fig. 2-1. Multiplication of Two Spectra in the Frequency Domain

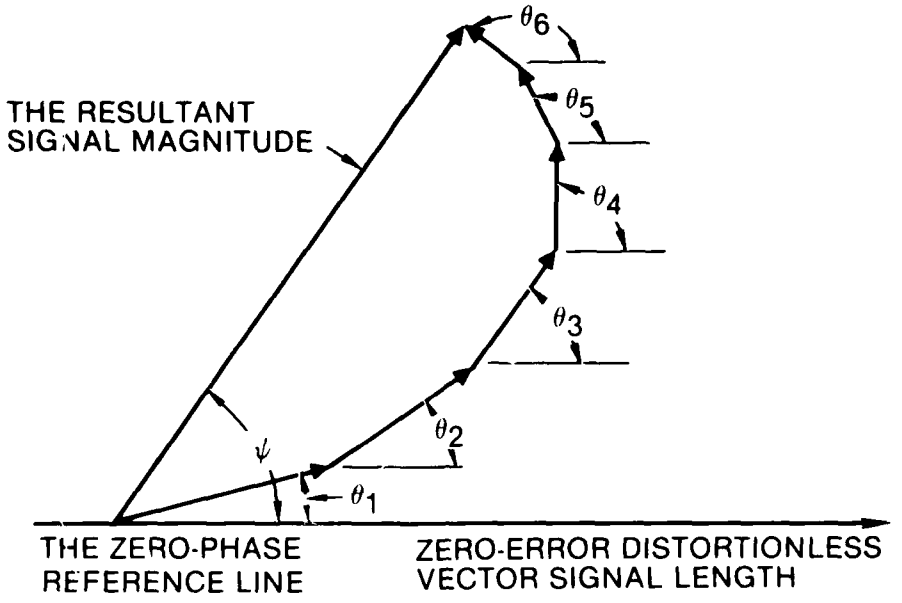

Fig. 2-2. Output Signal Resultant from Phase-Distorted Input Components

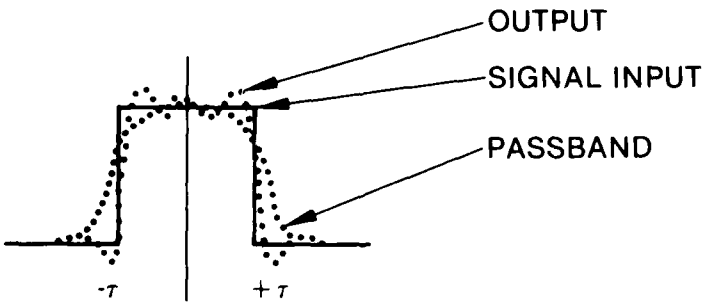

Fig. 2-3. A Typical Waveform Resulting from Passing a Perfect Rectangular Isochronous Signal Through an Ideal Band-Limited Circuit

hard-limiter precedes the demodulator, the amplitude variations are removed, so that the dot-product of Eq. 2.14 implies the self-products, or squares, of corresponding spectral pair components at a mutual frequency, multiplied by the cosine of the distortion angle at that same frequency. The single-sided loss degradation integral then becomes

$$L_d = \frac{\int_o^{\pi} \left(\frac{\sin x}{x}\right)^2 \cos f(x)\, dx}{\int_o^{\pi} \left(\frac{\sin x}{x}\right)^2 dx} \qquad (2.15)$$

where $x = \omega$. The limits of integration are now given from band center to band edge, shown as zero to π, to be interpreted by the computer as the first $(\sin (x)/x)^2$ null, and where $f(x)$ is the phase departure function. The denominator integral has a fixed one-sided value of approximately 1.41815157 but usually during computation its reciprocal is used, as $K = 0.705143$. Hence Eq. (2.11) becomes

$$L_d = K \int_o^{\pi} (\sin x/x)^2 \cos f(x)\, dx \qquad (2.16)$$

If the integration were done across the two-sided passband, from $-\pi$ to $+\pi$, the value of the lower integral would exactly double, and K would halve. When a departure function is not symmetrical about the carrier frequency, two-sided integration is necessitated, and is treated further in Section 4.

The fact that the phase departure function appears under the cosine operator enables further manipulation during formulation of the departure function because it is an "even" function.

Departure of the keying waveform from a perfect rectangular shape outlined in Fig. 2-3, for whatever cause, results in a correlator output magnitude below the unit correlation peak. However, such is considered to be

a part of the price of implementation in reasonably priced hardware, has little effect on the method of calculation or its accuracy, and has only a minimal effect on system performance. Other system losses usually tend to obscure losses incurred by use of finite bandwidths.

In Fig. 2-2 component vector numbers correspond to spectral locations represented in Fig. 2-1 rather than to term numbers in the departure functions.

Usually each pair's phase relative to the best straight-line fit deviates increasingly with frequency offset from band center. As indicated in Fig. 2-2, the smallest components are seen actually to subtract energy from the output signal magnitude. The angle ψ corresponds to a spectrally weighted or average departure function angle, and approximates a meaningful average distortion angle, which will be considered further in Sections 4 and 5.

2.4 EXAMINING THE CORRELATOR-DEMODULATOR OUTPUT

A theoretically perfect output from an ideal pseudonoise code correlator will appear as a triangular waveform in the time domain, about as shown in Fig. 2-4, where "n" is the code length and τ is the chip duration. The output A(t) is given by the following expression:

$$A(t) = 1 \text{ for } -\tau \leq t \leq \tau$$

and

$$= \pm 1/n \text{ elsewhere} \qquad (2.17)$$

During a code search the correlator is in effect performing continuous cross-correlation, since an ideal or desired code is usually orthogonal to anything but to itself. This accounts for the small values of A(t) outside the correlation interval of $\pm\tau$. When the proper code segment enters the correlation aperture, the correlator output voltage pulse climbs to its peak and then recedes as the code segment moves out of the aperture. Usually some method is employed to recognize correlation and to cause the two codes to remain time-synchronized at or very near the correlation peak. Since most codes are not ideal, subsidiary peaks of lower magnitude are apt to occur periodically. To avoid "lock-up" on the wrong epoch of the codes, proper attention is given this possibility in design of the synchronization tracking circuits (Refs. 16 and 42).

During the presence of high levels of interference, it is possible that the correlation spike may be difficult to detect, so it is important that all hardware-related sources of signal degradation be minimized. If the input signal to the correlator is band-limited to the first null pair, and the local code-generator is not, the loss will be only about one dB, as was found from Eq. (1.6). Attempting preservation of an infinite bandwidth to avoid the loss of that one dB is usually not an economic possibility, even within a local code generator. If either of the two spectral signal distributions is

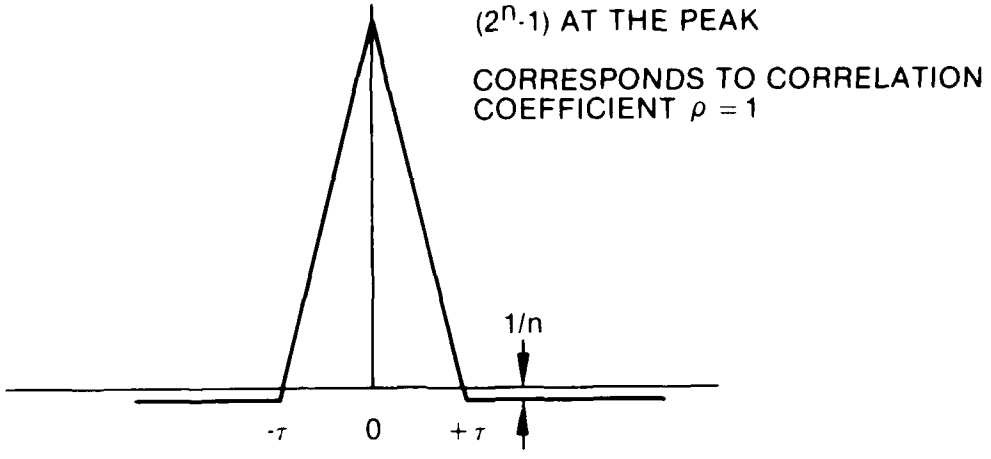

Fig. 2.4(a). Correlator Output Waveform for Maximal or Perfect Code

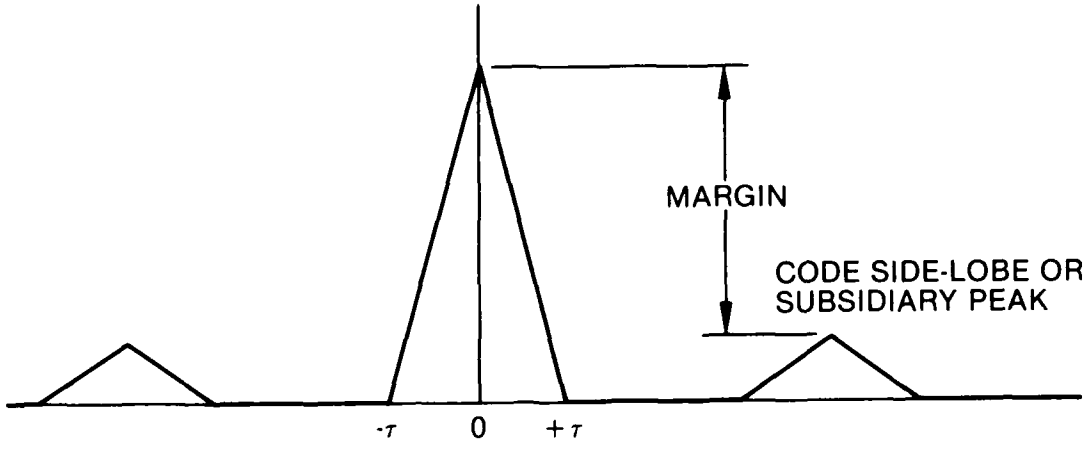

Fig.2.4(b). Typical Correlator Output Waveform for Non-Maximal Code

frequency-translated to make easier the correlation-demodulation process, it is important that meticulous care be taken to maintain phase linearity, avoiding generation of spectral phase distortion. If possible, the originating and the receiving station should use similarly optimized hardware implementations for the encoder-modulator and for the replica generator to minimize distortion losses. Frequency translation per se need not introduce phase distortion, as shown later in Section 2.8.

In summary, a brief introduction has been offered to use of the convolution integral in the frequency domain as the basis for analysis of correlation signal loss in the time domain. While it is not within the intended scope of this study to expand and expound on that process, very interesting implications abound.

The reader is invited to study Ref. 28, page 145 on, if another engineering-oriented treatise on correlation detection is desired. In that reference, Lange enables attainment of the same result from expansion of a time series, again by calculating from the power spectrum $S(\omega)$, which is yet another way for calculation of the joint probability distribution function $P(x,y)$ and the case correlation maximum.

In Ref. 29, R. M. Fano addressed the problem another way, making a similar analysis of the problem, and yielding a similar result.

Other related references are numbers 26, 32, 33, and 34.

2.5 THE BASIC GROUP DELAY MEASUREMENT EQUATIONS

When measuring group delay, a modulated carrier is swept through the passband of the device under test (DUT) per Fig. 3-1. If amplitude-modulated, the output of the DUT is square-law rectified to recover the throughput modulation signal, which along with a sample of the original modulation, is fed into a vector voltmeter (VVM). One output of the VVM is a DC voltage proportional to the phase difference in the two signal modulations. That voltage is fed into the Y axis input of an X-Y plotter. A sweep voltage from the signal generator is fed into the X axis of that same plotter. Together they

produce a plot of the differential group delay characteristic of the DUT, the band-center frequency reading usually being selected as the delay reference point. That plot is later integrated and further processed to obtain the passband differential phase response, or distortion characteristic, from which the departure function is obtained.

Assume that the amplitude-modulated input signal to the DUT has the form

$$A_i(\omega,t) = A\{1 + m\cos\omega_m t\}\{\cos\omega_o t\} \tag{2.18}$$

and that the output signal, before rectification, has the form

$$A_o(\omega,\theta,t) = A(\omega)\{1 + m\cos_m t\}[\cos\{\omega_o t + \theta(\omega)\}] \tag{2.19}$$

where

m = the amplitude modulation coefficient

ω = the carrier frequency relative to band-center

ω_m = the fixed modulation frequency on the carrier

ω_o = the swept carrier frequency at any time t

$A(\omega)$ = the passband amplitude response

$\theta(\omega)$ = the passband phase characteristic

where A_i, A_o, and A represent the amplitudes of the input, the output, and the carrier oscillator. To facilitate the subsequent analysis, a ratio of output to input is defined as

$$f(\omega,\theta) = A_o(\omega,\theta)/A_i(\omega) \tag{2.20}$$

where the input carrier generator amplitude $A_i(\omega)$ is set equal to unity.

Multiplying through and combining terms yields carrier "in-phase" and "quadrature" (I and Q) terms, plus upper and lower sideband terms which carry the effects of the passband differential phase characteristic, as shown following:

$$f(\omega,\theta) = \{\cos \omega_o t\} \cos \theta(\omega) - \{\sin \omega_o t\} \sin \theta(\omega)$$

$$+ \frac{m}{2} \cos \{\omega_m t + \omega_o t + \theta(+\omega)\} + \frac{m}{2} \cos \{\omega_m t - \omega_o t - \theta(-\omega)\}$$

(2.21)

where the term $\theta(-\omega)$ describes the phase offset at $(\omega_o - \omega_m)$ and where the term $\theta(+\omega)$ describes the phase offset at $(\omega_o + \omega_m)$. Since $\theta(\omega)$ may be defined as zero at band center ω_o, the expression simplifies somewhat to the following three terms:

$$f(\omega,\theta) = \cos \omega_o t \qquad \text{carrier}$$

$$+ \frac{m}{2} \cos \{\omega_o t + \omega_m t + \theta(\omega)\} \qquad \text{upper sideband}$$

$$+ \frac{m}{2} \cos \{\omega_o t - \omega_m t - \theta(-\omega)\} \qquad \text{lower sideband}$$

(2.22)

When this signal is ideally square-law detected, the carrier term reduces to DC, and new sidebands and harmonic products are generated. To identify those products and evaluate their contributions, Eq. (2.21) will be squared to correspond with square-law rectification.

To simplify the arithmetic "bookkeeping" involved, the coefficient m/2 is replaced by letter "a," the argument of the upper sideband is replaced by "U," and the argument for the lower sideband is replaced by "L." This leaves Eq. (2.21), when squared, in the following form:

$$\{\cos \omega_o t + a \cos U + a \cos L\}^2 \tag{2.23}$$

Six new terms are created. It is possible to simplify the expression resulting from expanding Eq. (2.22) because of the internal signal-sampling design in the vector voltmeter. That leaves the following expression:

$$[f(\theta,\omega)]^2 = m \{\cos \omega_o t\} \{\cos U\} + \frac{m}{2} \{\cos (\omega_o t)\} \cos L + \frac{m^2}{2} \{\cos U\} \cos L \tag{2.24}$$

When Eq. (2.24) is expanded, six more terms are generated, including a signal at double the carrier frequency, complete with upper and lower sidebands.

The only term useful to the VVM phase-measurement circuitry is the sum of the two components at frequency ω_m, which is fed to Probe B of the VVM via band-restrictive filters.

$$E_B = \frac{m}{2} \cos \{\omega_m t + \theta(+\omega)\}$$

$$+ \frac{m}{2} \cos \{\omega_m t + \theta(-\omega)\} \qquad (2.25)$$

Probe A of the VVM is fed a sample A_s of the pre-modulation signal for use as a phrase reference.

$$E_{ref} = E_A = A_s \cos \{\omega_m t\} \qquad (2.26)$$

The VVM Input A circuitry phase-locks to Signal A. Inside the VVM a 20 kHz sampler converts each input to a 20 kHz replica of Inputs A and B, faithfully preserving the original amplitude and phase characteristics of the input signals. Amplitude characteristics are measured by the voltmeter circuitry. The phase difference between Inputs A and B is measured by feeding the 20 kHz signal replicas through amplifiers, clippers, and 1-kHz passband filters. Filter outputs are used to trigger a flip-flop, thereby controlling the symmetry of the square-wave output in accordance with the phase-difference of the two input signal fundamental frequencies. The phase-meter current is therefore controlled by the square-wave symmetry, and so is the VVM phase signal output to the XY plotter.

Phase differences between the two input channel signals may be read at scale ranges of ±180°, ±60°, ±18°, and ±6°, the latter enabling a resolution of 0.1 deg. The VVM sensitivity at any scale range may be expanded by appropriate settings of the X-Y plotter Y-axis gain control. When sweeping near and outside passband edges, the DUT phase characteristic changes radically, causing the phase meter needle to move off-scale wildly, especially when the scale factors have been selected to provide high in-band resolution. One way to avoid or reduce plotter damage and annoyance is to turn ON the modulation as the passband edge is entered, and OFF as the passband is exited.

Another method is to tie the frequency limit switch of the sweeping generator to the X-axis limit switch or pen-lift of the plotter.

Because of the amplifier-clipper property of the VVM phase metering circuits, modulation factor "m" loses its meaning after a large-enough demodulated input signal (100 μvolts or better) is received at the VVM input jack. A good signal-to-noise ratio is required at the VVM input ports to assure noise and jitter-free traces on the X-Y plotter paper. Under actual test conditions, the amplitude-modulation index (factor) has been varied over the range $0.05 < m < 4.0$, causing only slight DC level-shift or offset between otherwise identical curves for successive DUT group delay passes, using the same sheet of plotter paper.

2.6 OBTAINING THE DIFFERENTIAL PHASE FUNCTION VIA GROUP DELAY

2.6.1 Differential Group Delay Measurement

Probably the first published article on group delay measurement appeared in Ref. 50 in the year 1930, using instrumentation available at that time. Measurement of differential group delay using contemporary instrumentation is introduced in this section, and is further elaborated upon in Section 3.

A sufficiently stable sweepable carrier is first modulated, amplitude leveled, and then passed through the device under test (DUT). The DUT signal is demodulated, so that the modulation waveform is recovered. The difference between the zero-crossings of the original and the recovered modulati ompared in a phase meter. They are then automatically plotted in units of lead or lag. As the modulated carrier is swept through the passband, the quantity plotted is the average slope of the passband differential phase characteristic at each point. The frequency increment over which the slope is averaged is twice the modulating frequency, since the phase-meter sums the dot products of the demodulated lower and upper sidebands. A description of a laboratory bench installation found useful in making these measurements in the UHF and microwave regions is contained later in Section 3.

Whether differential group delay characteristics are measured using an automated sweeper and plotter combination, or manually operated with data taken point by point makes little difference other than the convenience of having a continuously smooth curve with which to do subsequent analysis. A smoothed automated stepped-frequency plot is presented as the parabolic curve of Fig. 4-1. A continuously swept, gain-phase-meter plot usually resembles Fig. 4-3. In either case, the Y-axis is usually calibrated directly in time, typically in the range of milliseconds to nanoseconds per inch of signal delay or advance relative to band center. Delay curves are then integrated, the new phase shift of the curve becoming the area under the delay curve, becoming in turn the differential phase characteristic in degrees.

Per Figs. 4-1 and 4-2, a passband differential-phase plot is typically a distortion function superimposed upon a positive-increasing function of frequency (Ref. 43, Chapter 2). Therefore, timing delays to the lower-frequency side of band center represent "negative" or phase lag relative to band center, while the upper side of the group delay curve becomes, upon integration, phase lead. These are important considerations, and are treated further in the next section, and introduced in Figs. 2-5 and 2-6.

Inspection of Figs 2-5 and 2-6 will show two lines, each labeled "line of equal areas" about halfway up each plot. Consider now the shaded areas between the lower and the upper band edges, and lying above and below the horizontal line. Each "line of equal areas" is drawn at that ordinate at which the shaded areas above and below that line are equal. That value of time delay is the slope of the linear least-squares, or "best straight-line fit," after the group delay plot has been integrated to obtain the passband differential phase function plot. If the t = 0 coordinate is moved up coincident with the "line of equal areas," a relative time departure function is obtained. Integrating the new time departure function directly produces the desired phase departure function.

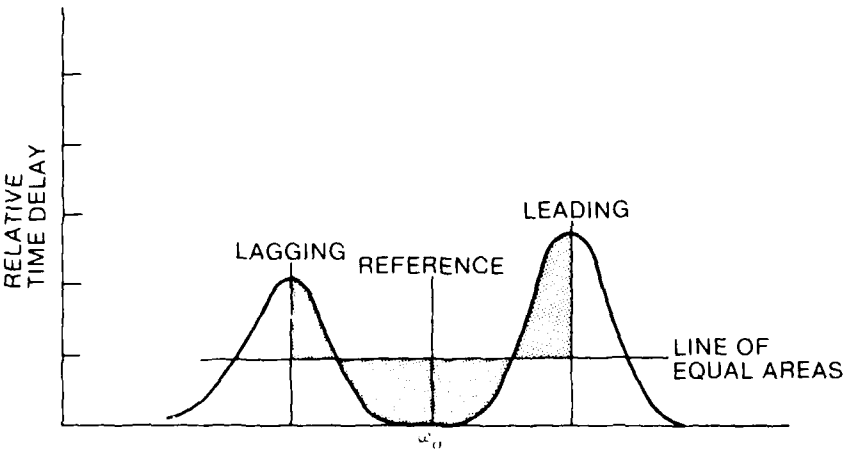

Fig. 2-5. Differential Group Delay Plot - Automa t

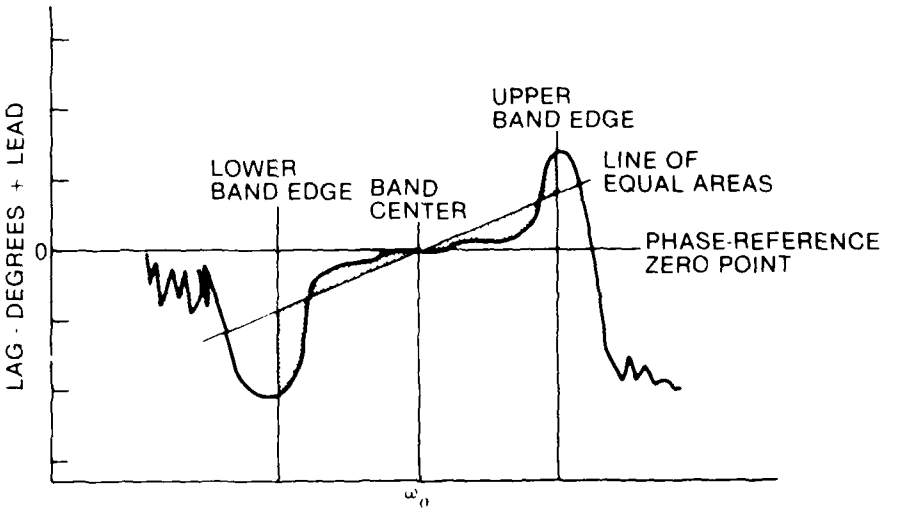

Fig. 2-6. Vector Voltmeter Plot of Differential Group Delay

Before attempting to take advantage of the apparent simplicity of the "line of equal areas" approach, it is recommended that the reader become familiar with the numerical techniques presented and used in the remainder of this study.

The subject material is novel and innovative, not having appeared elsewhere in the literature on group delay distortion analysis. Therefore, care is being taken to ensure maximal comprehension on the part of future users.

The typical program for finding the linear least squares, or regression equation results in the form $Y = mX + b$ where the constant of integration (b) represents system phase delay and may therefore be set to zero so the best-fit line passes through zero at midband. Assuming perfect action in the PN synch circuits, term "b" is subtracted, leaving direct visibility of sideband-pair phase differences, enabling loss calculation directly therefrom.

"Goodness-of-fit" is also provided as part of the curve-fitting process, the coefficient being given as r^2 which is equal to unity when the fit of the equation is perfectly matched to the data. Values of 0.75 and above are commonly acceptable but higher values are of course preferred.

2.6.2 Integrating a Differential Group Delay Plot

The fundamental equation being solved comes from rewriting Eq. (1.10) to yield

$$\theta(\omega) = \int t(\omega)\, d\omega$$

$$= \psi(\omega) + \psi_o$$

where the ψ_o, as the constant of integration, represents absolute phase shift, and $\psi(\omega)$ is the desired function. Usually ψ_o is arbitrarily equated to zero, further simplifying calculation and plotting without loss in accuracy.

Figure 2-7 provides a view of some relationships between time delay and phase characteristics of a portion of a bandpass circuit. For every particular frequency in the passband there exists only one corresponding phase-response characteristic. Absolute phase at any point is unimportant to this study, but the tangent at each point of the curve is important. As shown in Fig. 2-7, the slope at any frequency has the dimensions of time. Usually the point of reference is taken as band center, since the information of interest in PN spread-spectrum communication is the relative time of arrival of each output sideband pair, with respect to the corresponding components of the input modulating signal.

Since vector voltmeter and/or gain-phase meter outputs represent time delay, or phase slope rather than passband phase, a method is needed to convert delay plots into phase plots. The usual conversion process involves numerical or graphical integration since many delay plots do not lend themselves conveniently to analytical description in a reasonable number of terms.

Graphical integration, or "square-counting" begins by selection of convenient units of frequency as required by the desired passband resolution $\Delta\omega$, then dividing the X-axis into these units. The frequency axis also must be divided into enough sectors "2n" to assure the required time-phase resolution in the finished product. The average Y-axis ordinate, corresponding to frequency interval $\Delta\omega$, is multiplied by that common frequency increment. These products are summed between the limits where the passband of interest is $2n\Delta\omega$, as expressed analytically below:

$$\psi(\omega) = K \sum_{i=-n}^{+n} t(\omega)\Delta\omega = K\Delta\omega \sum_{i=-n}^{+n} t(\omega) \qquad (2.27)$$

In actual practice, the summation is taken in two steps, from band center outward to each of the lower and the upper band edges, so that band-center phase-shift will automatically be zero. The constant K and the incremental frequency $\Delta\omega$ include modulation sensitivity, phase meter, and plotter scale factors, as will be demonstated later via examples in Section 4.

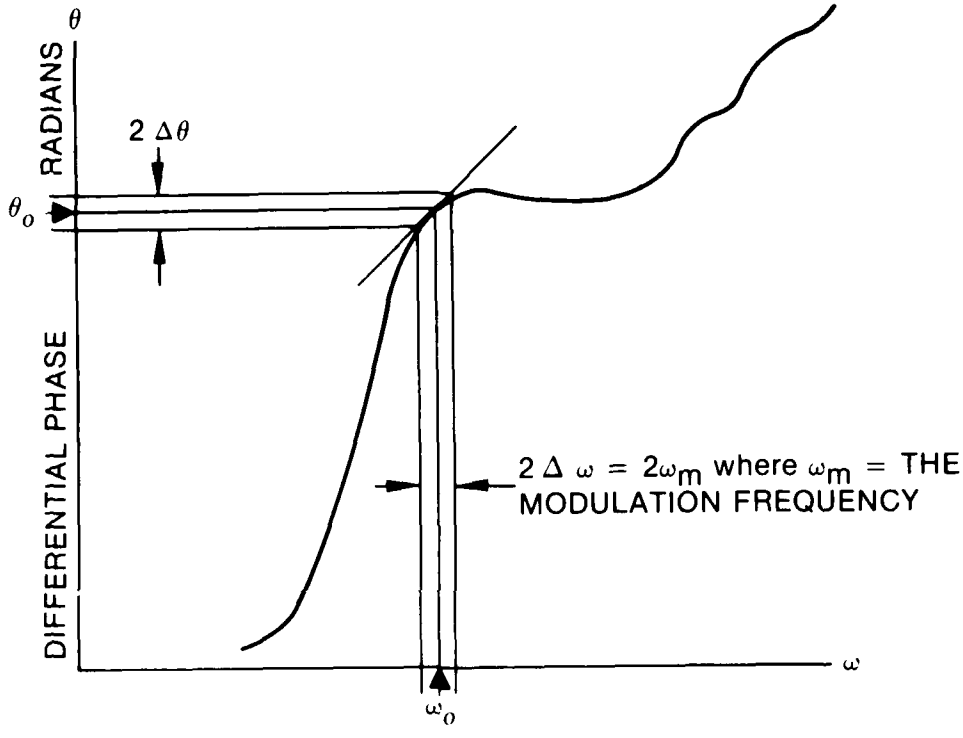

$$\text{SLOPE} = \frac{2\Delta\theta}{2\Delta\omega} = \text{GROUP DELAY}, \text{ OR, } \frac{d\theta}{d\omega} = \text{DIFFERENTIAL GROUP DELAY}$$

$$= \text{RADIANS / RADIANS PER SECOND} = \text{SECONDS}$$

Fig. 2-7. Time-Delay Relationships

2.7 DEVELOPING THE DEPARTURE FUNCTION

2.7.1 Series Representations of the Passband Functions

In a system with a well-behaved passband, it may be feasible to use a dedicated, although perhaps complicated, computer routine to describe the transfer function. Series expansions in ω, or in $\Delta\omega$ about some frequency ω_n in the passband may be obtained for differential group delay plots as well as for amplitude plots. When an analytical representation has been achieved for the group delay characteristics, it can be integrated to obtain the desired phase function. When undertaking curve-fitting from an X-Y plot, it is well to have pre-scaled the frequency and the time-delay axes very carefully, to avoid establishing outlandish coefficients and/or unwieldy analytical expressions. When an X-Y plot has been integrated and its corresponding phase function has been established, no difficulty should be encountered in converting the result into a departure function.

However, when attempting to define a phase function or a departure function near to or outside the passband edges, the relative rate-of-change of phase versus frequency may cause the phase function to fluctuate widely and rapidly due to phase cycle-slipping. Curve-fitted equations under such circumstances would be found to be unreliable between the points at which their data was entered, as few curve-fitting algorithms will handle discontinuities well. It is sometimes difficult to obtain a satisfactory curve-fit that is uniformly accurate over all parts of a passband having even moderately high rates of change near band edges. High rates of change represent high signal distortion in those same parts of the passband and spectrum. It is fortunate when most of a signal spectrum lies within the smooth central two-thirds of a passband.

Use of Taylor, Maclaurin, or Fourier series expansions (Ref. 46) has been found most convenient when the frequency axis is normalized with zero radians at band-center and $\pm\pi$ radians at band edge spectral nulls. The simplest series expressions usually result from adjusting the frequency plot slightly to result in zero-phase at band center.

Equation (2.28) presents the generic term for the Taylor-series expansion of the passband phase function about an arbitrary frequency ω_o (see Ref. 46, Sections 10 through 13, and Ref. 14, Sections 42.7 and 44.25). Both the Taylor and the Fourier series are most tractable when $\omega_o = 0$ with ω scaled so that the limits of the function are defined as $\pm \pi$ radians at spectral null or passband "edges."

$$\theta(\omega) = \sum_{n=0}^{k} \frac{1}{n!} \frac{\partial^n}{\partial \omega^n} (\omega_o) (\omega - \omega_o)^n + R_n \qquad (2.28)$$

where $\partial^n/\partial\omega^n$ is the value of the n^{th} derivative of $\theta(\omega)$ evaluated at ω_o. The summation is taken to k terms until remainder R_n is arbitrarily small. When the value of $\omega_o = 0$, the Taylor expansion reduces to a Maclaurin power series in ω. The physical significance of each coefficient of the resulting expansion is treated later on in Section 4.3.

Equations (2.29) present the generic form for a Fourier series expansion (see Ref. 14, Section 42-9):

$$\theta(\omega) = \frac{A_o}{2} + \sum_{n=1}^{\infty} [A_n \cos n\omega + B_n \sin n\omega] \qquad (2.29)$$

where

$$A_n = \frac{1}{\pi} \int_{-\pi}^{\pi} \theta(\omega) \cos n\omega d\omega$$

and

$$B_n = \frac{1}{\pi} \int_{-\pi}^{\pi} \theta(\omega) \sin n\omega d\omega$$

If the function to be analyzed or synthesized is not simple enough to describe analytically, it may be approximated by numerical integration methods. Computer routines are available for converting such functions within required functional limits.

2.7.2 Examining a Parabolic Departure Function

An example of a second-order Maclaurin-series term, i.e., a parabolic differential group delay function, is provided to show how the coefficients of a power series expansion may be used. Reference is made to Fig. 2-8 in which $\theta_2(\omega) = b_2\omega^2$, where the coefficient b_2 is the parabolic distortion in radians at band edge, i.e., at the point $|\pm\omega_{be}| = 1/\tau$, thus defining band edge at the first spectral null pair. Reference is now made to Eq. (2.28) while calculating the coefficient b_2. Then,

$$\theta(\omega) = \theta_2\left(\pm\frac{1}{\tau}\right)^2 = b_2\omega_{be}^2 \qquad \text{at band edge} \tag{2.30}$$

so that

$$b_2 = \theta_2/\omega_{be}^2 = \theta_2/(2\pi f_{be})^2 = \theta_2\left(\frac{1}{2\pi\tau}\right)^2 \tag{2.31}$$

where τ is the chip width. Usually the process of computation is simplified somewhat by normalizing the band-edge variable, thus giving the following relationship:

$$\theta(\omega) = b_2\left(\frac{\omega}{\omega_{be}}\right)^2 = b_2 d^2(x) \tag{2.32}$$

for $\omega \leq \omega_{be}$ and $0 < x < 1$, so that the computer variable

$$d(x) = \frac{\omega}{\omega_{be}} \leq 1$$

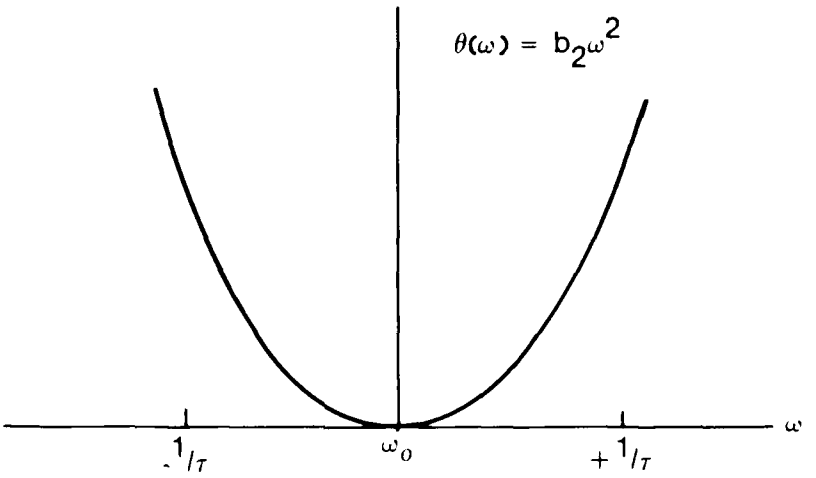

Fig. 2-8. Parabolic Differential Phase Distortion

For convenience in computer mechanization of these and other related equations, use is made of x as the independent variable corresponding to the usual use of frequency as the independent variable, so quantity 'x' is the more easily tied to DO-Loop counters. It is found convenient to express passband frequency normalized in terms such that $x = \pi$ at the spectral nulls, to fit most computer subroutines useful in this type of analysis.

Therefore, from above, 'x' replaces ω/ω_{be}, and appears at band edge as x/π. Therefore, the general series term becomes written as

$$\theta_n(x) = b_n \left(\frac{x}{\pi}\right)^n \tag{2.33}$$

Therefore, at band edge, the full phase value of each b_n is achieved rather conveniently as x varies from zero to π.

The departure function for the above parabolic distortion function is thus calculated as a single term, correctly yielding the band-edge value of parabolic delay. This approach simplifies power-series evaluation on a computer. For example, to evaluate a cubic component, merely substitute 3 for n and proceed.

Then, for this case, the general loss integral Eq. (2.15) becomes

$$L = 20 \log_{10} \left[K \int_{-\pi}^{+\pi} (\sin x/x)^2 \cos \left(b_3 \left(\frac{x}{\pi}\right)^3 \right) dx \right] \tag{2.35}$$

where K is the reciprocal value of the constant denominator term and equals approximately 0.352571623, considering two-sided passband width.

2.7.3 Handling Higher-Order Terms

While it is true that perhaps the greatest contributors to phase distortion loss are the parabolic and cubic terms, often there will be significant ripple terms, particularly when Butterworth or Tchebychev design

polynomial functions have been used. It may then become attractive to consider using a Fourier-series representation. Which form to use depends upon the relative ease of implementation of the distortion function. A combination of terms from both power and Fourier series may find application to minimize length of the functional expression, consisting of those applicable or appropriate parts of the following equation (see Figs. A-16 through A-23):

$$\theta(\omega) = \theta_0 + \theta_1\omega + \theta_2\omega^2 + \theta_3\omega^3 + \ldots. \theta_n\omega^n$$

$$+ b_1 \cos \beta_1\omega + b_2 \cos \beta_2\omega + \ldots. b_n \cos \beta_n\omega$$

$$+ c_1 \sin \zeta_1\omega + c_2 \sin \zeta_2\omega + \ldots. c_n \sin \zeta_n\omega \ldots \quad (2.36)$$

The opportunity will be taken here to remind the reader that the differential group delay loss is dependent upon the overall throughput distortion characteristic. End-to-end loss cannot be determined on the basis of the separate distortion curves for each element of a system because the throughput phase distortion characteristic of each element is additive-cumulative. The accumulated departure function must be obtained. However, certain benefits result from that fact, annoying though it may be to the designer who would allocate losses to individual "boxes." A distortion term arising in one box is sometimes mitigated by an opposing distortion in another box in some part of their mutual passband. Skillful manipulation of interface matching may sometimes permit that possibility but sometimes it is still advisable to employ equalization somewhere in the system. It may sometimes be necessary to equalize a particular box because of difficulty in obtaining more or less identical end-to-end phase characteristics during the manufacturing process. Proper equalization of individual boxes may enable participating in a large network of dissimilar boxes.

2.7.4 A Test Case

An interesting validation of the approach used herein is provided, permitting comparison of the results of a simple isochronous square-wave convolution exercise with the results derived analytically from full-scale spectral correlation/convolution.

By definition, convolution involves "sliding" one function over another, and summing their product over a range of small increments consistently with the use of the classical summation or integral symbols seen elsewhere (Refs. 25 and 37). The convolutional process produces correlation when exercise of the incrementation process has brought coincidence of the two functions. Then their product is evaluated to determine the magnitude of their correlation coefficient.

In the following example, the result of applying a graphical/manual correlation process is compared to application of Eq. (2.15). This is a [illegible] case of degradation-loss calculation equivalent to a 90° band-edge [illegible] (first-order) differential phase error, which is comparable to the case [illegible] a 9[illegible] timing error exists.

[illegible] hard-limiting is assumed, producing a flat-topped distortion-[illegible] amplitude characteristic. As shown by the first-order curve of Appendix [illegible], the calculated loss should be 1.[illegible] db.

The example of Fig. 2-9 represents the case in which, after multiplicative correlation closely resembling squaring or frequency-doubling, the product of the two isochronous voltage waveforms is now separated by 90° in [illegible]-time, or by one-quarter of a bit cycle. Using the selected "one-zero-one" combinations, output energy is produced during three-fourths of the [illegible]-time by the correlated functions. During the other quarter-cycle, the [illegible] product is zero, indicating no produced energy.

[illegible] case, the maximum available correlation coefficient is [illegible] of the maximum possible of 1.0, or,

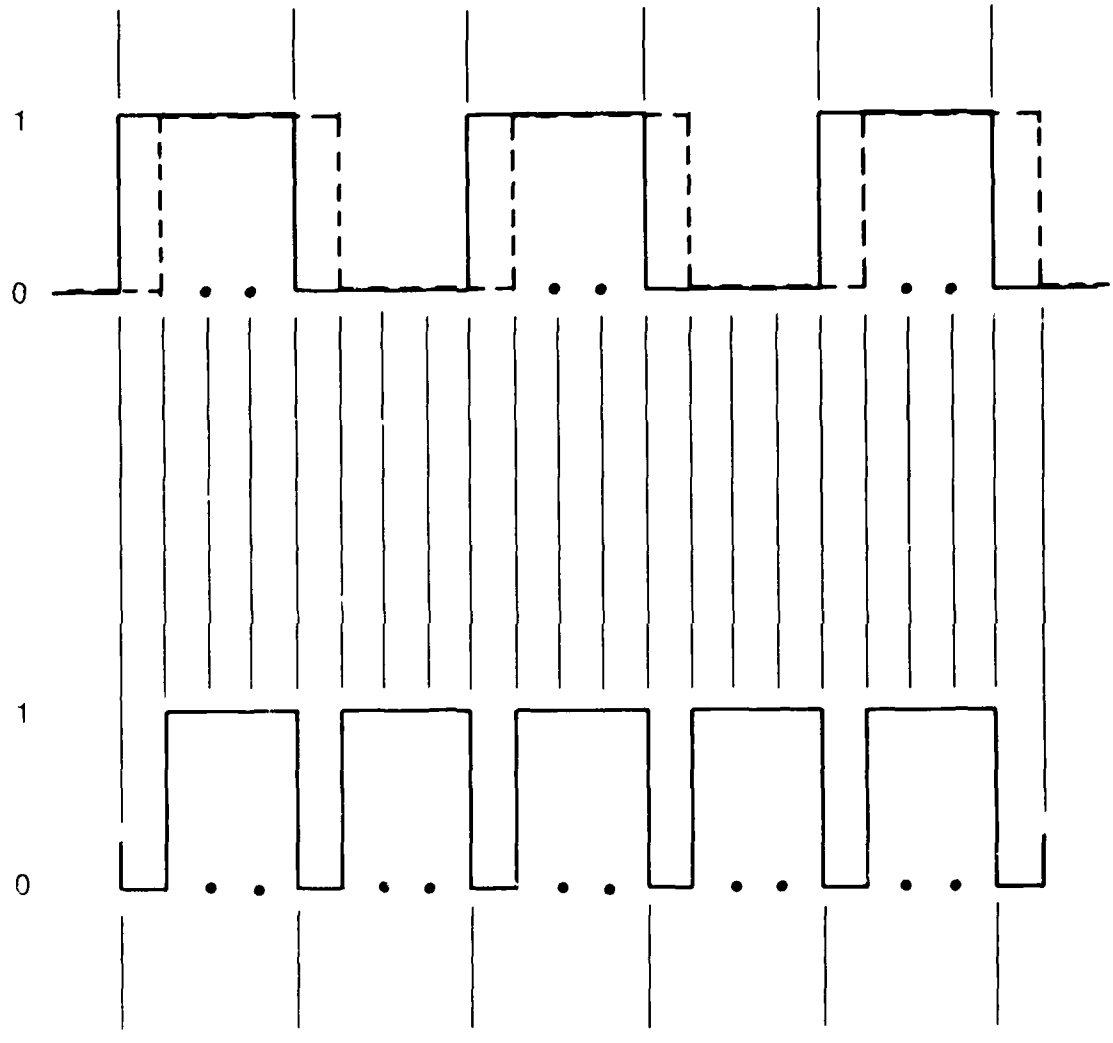

Fig. 2-9. Correlating Two Offset Square Waves

$$\rho = \frac{\text{Energy Recovered}}{\text{Energy Available}}$$

$$= 0.75/1.00$$

$$= 0.75 \qquad (2.37)$$

For the stated conditions the equivalent loss defined by (2.15) becomes

$$\text{Degradation Loss} = 10 \log_{10} (0.75) = 1.249 \text{ dB} \qquad (2.38)$$

This loss is slightly greater, about 0.03 dB, than the loss calculated by the $(\sin x/x)^2$ model of spectral energy distribution because the model uses spectral truncation at $\pm \pi$ rather than at $\pm \infty$. The "one-zero-one" example assumes presence of all the frequency-domain components, so represents a slightly greater loss, since the higher components are unavailable.

This example is an interesting validation of the Parseval-Rayleigh theorem (Ref. 26) by demonstrating the equivalence of time-domain and frequency-domain energy computation.

It also nicely validates the computer model of Eq. (2.15) by showing exactly what to expect in an unsynchronized phase-keyed digital link band-limited at $\pm 1/\tau$. (This test case was suggested by W. E. Leavitt.)

2.8 A USEFUL RULE-OF-THUMB APPROXIMATION

An approximation method sometimes useful in obtaining a quick estimate of differential group delay (DGD) distortion loss may be developed by several methods, some of which are introduced in these paragraphs.

Two spectral distributions are multiplied to determine the output signal when one carrier is modulated and the other is a continuous-wave carrier free from the effects of phase noise. For simplification, each signal spectral distribution is assigned unity amplitude.

Let the continuous-wave carrier be defined as

$$\varepsilon^{j\omega_o t} \tag{2.39}$$

Let the second carrier be phase-modulated, as represented by the expression

$$\varepsilon^{j\{\omega_\mu t + \mu(t)\}} \tag{2.40}$$

where $\omega_\mu t$ and $\mu(t)$ are respectively the second carrier and its modulation function.

Furthermore, let a passband be defined to possess distortion departure $\psi(\omega)$ in the exponential form

$$\varepsilon^{j\psi(\omega)} \tag{2.41}$$

The voltage developed across a unit resistance carrying the product of the above terms is given by

$$E_{out} = \left\{\varepsilon^{j\omega_o t}\right\}\left\{\varepsilon^{j(\omega_\mu t + \mu(t))}\right\}\left\{\varepsilon^{j\psi(\omega)}\right\} \tag{2.42}$$

By de Moivre's theorem (Refs. 37 and 46), the real part of the output voltage, representing the loss function, is given by

$$Re(E) = \cos\{\omega_o t + \omega_\mu t + \psi(\omega) + \mu(t)\} \tag{2.43}$$

This can be simplified for interpretation by defining the angular modulation factor as follows:

$$\mu(t) = \frac{\pi}{2} \quad [1 + d(t)] \tag{2.44}$$

where $d(t) = \pm 1$, representing binary logic states. Frequency translation to baseband will be accomplished by homodyne (direct heterodyne) such that $\omega_\mu = \omega_o$, enabling (2.43) to be rewritten as follows:

$$R_e(E) = \cos \{\psi(\omega)\} + \frac{\pi}{2} [1 + d(t)]\} \tag{2.45}$$

When expanded, this expression becomes merely

$$R_e(E) = \cos \{\psi(\omega)\} \leq 1 \tag{2.46}$$

It may be indeed inferred that phase-noise ψ_n on the continuous-wave carrier also would add directly to the phase departure function as $\psi(\omega) + \psi_n$. To avoid problems in making distortion degradation measurements, it is therefore highly desirable to maintain both a high signal-to-noise ratio and a high carrier generator output-to-noise ratio. While most correlator-demodulator local oscillators will be sufficiently free of phase noise to cause insignificant trouble via Eq. (2.46), a study of Fig. 2-4 can disclose how phase-jitter amplitudes may reduce the size of the signal correlation peak.

Equation (2.46) is consistent with Eq. (1.11) in showing that the magnitude of the demodulator output will be unity, or less, depending upon the characteristics of the departure function. For example, typical "clean" digital keying signals will shift signal phase in integer-multiples of $\pi/2$ or $\pi/4$ radians. However, the very sharpness of the keying transitions, as availble for study via Eq. (2.45), will be degraded by the distortion function $\psi(\omega)$. As the argument of the departure function approaches zero, Eq. (2.46) becomes an increasingly-accurate indicator of degradation loss.

Consider now a second approach.

Let there be a signal correlation process involving the passband departure function $\psi(\omega)$. The convolution function "sliding" process will be limited to the interval $-\pi = \alpha = +\pi$ such that the correlator output $E(\psi)$, under distortion conditions is expressed as

$$E(\psi) = \int_{-\pi}^{\pi} (\sin \alpha)\ (\sin \{\alpha + \psi(\omega)\})\ d\omega \tag{2.47}$$

where α is the relative phase of adjacent sideband components and $\psi(\omega)$ is the passband phase departure function, which disturbs the sideband relative phase relationships, and where the incrementing variable $d\omega$ is at least an order of magnitude smaller than the departure function variable α. Expanding and evaluating Eq. (2.47) between spectral nulls

$$E(\psi) = \int_{-\pi}^{\pi} [\sin \alpha]\ [\sin \alpha \cos \psi(\omega) + \cos \alpha \sin \psi(\omega)]\ d\alpha$$

$$= \int_{-\pi}^{\pi} \sin^2 \alpha \cos \psi(\omega)\ d\alpha + \int_{-\pi}^{\pi} \sin \alpha \cos \alpha \sin \psi(\omega)\ d\alpha$$

$$= \cos \psi(\omega) \int_{-\pi}^{\pi} \sin^2 \alpha\, d\alpha \qquad + 0$$

$$= \pi \cos [\psi(\omega)] \tag{2.48}$$

When this result is applied to Eq. (2.15) and integrated to infinity to represent the general case, an interesting simplification results in the following useful rule of thumb:

$$L_d = \frac{\int_0^\infty [\sin \alpha]^2 \, [\cos \psi(\omega)] \, d\alpha}{\int_0^\infty [\sin \alpha] \, [\sin \alpha] \, [d\alpha]} = \frac{\pi/2 \cos \psi(\omega)}{\pi/2}$$

$$= \cos \psi(\omega) \tag{2.49}$$

When an average or unweighted departure function value ψ is calculated for a particular passband, then the group delay signal-energy distortion loss-function may be expressed as

$$\text{dB Loss} = 20 \log_{10} \cos \psi(\omega) \tag{2.50}$$

or

$$= 20 \log \cos \psi \tag{2.51}$$

Due to the heavy influence of the spectral weighting function, appearing in the loss function to the fourth power [see Eq. (2.57)], it may not be desirable to base a finished design on the basis of the above approximations, since exact computation is within the reach of the designer, and many distortion functions have already been computed and are plotted in the appendices of this treatise.

Yet another approach to derivation of the approximation function is provided by R. A. Le Fande in Ref. 18.

2.9 AMPLITUDE DEPARTURE FUNCTIONS

Situations requiring calculating the effects of amplitude distortion also may be treated by use of departure functions. If a passband amplitude characteristic X-Y plot has been obtained and has been expressed in a power series, the resulting series should be normalized to yield the following format:

$$A(\omega) = 1 - \left[a_o + a_1\omega + a_2\omega + a_2\omega^2 + ... a_n\omega^n\right] \quad (2.52)$$

In this function, the "1" represents the rectangular value atop the undistorted passband, and therefore the bracketed terms are the distortion terms, representing the departure function $\alpha(\omega)$ of Eq. (2.4) The term a_o accumulates offsets caused by power-series approximation in a finite number of terms. Ideally a_o would be normalized to unity at the band center reference point. Analysis then proceeds as below.

In the absence of ideal hard-limiting, it is necessary to consider both the phase and the amplitude expressions when calculating loss. Recalling Eq. (2.2), putting it in polar coordinates, and expanding it about some frequency ω_o

$$T(\omega) = A(\omega) \cdot \phi(\omega) \quad (2.53)$$

$$= A(\omega - \omega_o)\, \varepsilon^{j\phi(\omega - \omega_o)} \quad (2.54)$$

where

$$A(\omega - \omega_o) = \sum_{n=0}^{\infty} A_n(\omega - \omega_o)^n \quad (2.55)$$

and

$$\phi(\omega - \omega_o) = \sum_{n=0}^{\infty} \phi_n(\omega - \omega_o)^n \quad (2.56)$$

Reference may be made to Section 2.7.1 for calculation of A_n and ϕ_n. Engineering judgement is required to resolve the tradeoffs between accuracy

and convenience in calculating the limits of summation in (2.55) and (2.56) above.

By making use of the identity

$$\varepsilon^{u} = 1 + u + \frac{u^2}{2!} + \frac{u^3}{3!} + \ldots . \frac{u^n}{n!} \ldots$$

where $u = j(\omega - \omega_o)$ (see Ref. 14), it may be seen that both real and imaginary or quadrature terms will be present in $T(\omega)$, as will be found when substituting Eqs. (2.56) and (2.55) into (2.54) and expanding. It is therefore readily found that cross-coupling exists between the amplitude and the phase departure functions. The relative magnitude of the cross-coupling terms determines whether they need to be considered in the loss computation simultaneously, or separately, or if at all.

2.10 A GENERALIZED TRADEOFF LOSS MODEL

In typical designs, the first nulls of the $(\sin x/x)^2$ distribution occur close to the edges of a rectangular passband of width $2/\tau$. However, passbands may be narrower or wider than that value. The spectral distribution may also be skewed, some part of the spectrum lying in a highly distorted area, as on a passband edge location. If it is desired to study such spectral distributions, the integral-form loss Eq. (1.11) may be written in a generalized form as follows:

$$L_d = 20 \log_{10} \left[\frac{\int_{-\ell}^{+\ell} (\sin x/x)^2 A(x) \cos \psi(x) \, dx}{\int_{-\lambda}^{+\lambda} (\sin x/x)^2 \alpha(x) \cos \phi(x) \, dx} \right] \text{dB} \qquad (2.57)$$

where

$$\ell = T\pi/\tau = \gamma\pi \qquad \text{for } 0 < |\gamma| < \infty$$

$$\lambda = \Omega\pi \qquad \text{for } 0 < |\Omega| < \infty$$

and

$$x = \xi\omega \qquad \text{for } 0 < |\xi| < \infty$$

where the limiting values of ℓ, λ, and ξ become evident by assessment of the problem at hand.

The conditions represented by the numerator show signal energy gain or loss relative to the spectral energy conditions referenced in the denominator. Setting $\lambda, \ell < 1$ corresponds to reducing the spectral energy which enters a given fixed passband, possibly reducing the correlator input signal-to-noise ratio (S/N). If the normal signal input strength is sufficiently great so that the output S/N is not impaired significantly, it is possible to state that any bandwidth $> 2\ell$ provides no useful signal enhancement.

The effects of spectrum and bandwidth reduction or expansion may thus be studied relative to any given set of conditions via the quantity ℓ, relative to another referenced system set forth in the denominator.

Other weighting functions may also be treated by replacing the above $(\sin x/x)^2$ terms with any other appropriate spectral distribution.

SECTION 3. MEASUREMENTS

3.1 OBTAINING PASSBAND DISTORTION CHARACTERISTICS

A treatise on calculating delay distortion loss would not be complete if it did not discuss in detail a method for measurement of differential group delay distortion characteristics, plus a description of how to use them to determine the corresponding loss.

Figure 3-1 depicts a block diagram of a typical measurement setup which will measure both passband amplitude and differential group delay distortion, and will plot them on an X-Y recorder or plotter. The hardware functions represented are required at any signal or carrier throughput frequency, although the physical form of some of the hardware components may vary considerably over a wide range of frequency bands.

In the following discussion, the device under test (DUT) was a low-level-input 700 MHz up-converter feeding a klystron power amplifier, delivering approximately two kilowatts at a carrier frequency of 8350 MHz. The differential group delay distortion (DGDD) loss characteristic is required, considering a PN signal occupying ± 20 MHz centered about its carrier frequency. Figure 3-2 depicts the test equipment used. The distortion loss caused by the DGD characteristic under the above-stated conditions is calculated in a worked-out example, using departure functions, in Section 4.

The radio-frequency output of a swept signal generator is amplitude-modulated by a 2.777 MHz signal and is amplitude-leveled to provide constant output as the generator sweeps [illegible]igh the passband of the DUT. Percentage modulation and signal level [illegible]en to obtain proper DUT input level, and enough vector voltmeter (VVM) demodulated signal input to assure a high-quality, noise-free trace. The block diagram indicates that the VVM is fed by a sample of the modulating signal prior to the signal modulating process. The VVM samples these two input signals at a 20 KHz rate and displays the zero-crossing difference in nanoseconds of signal-phase lead or lag relative to the reference input. A voltage proportional to the full-scale phase display VVM

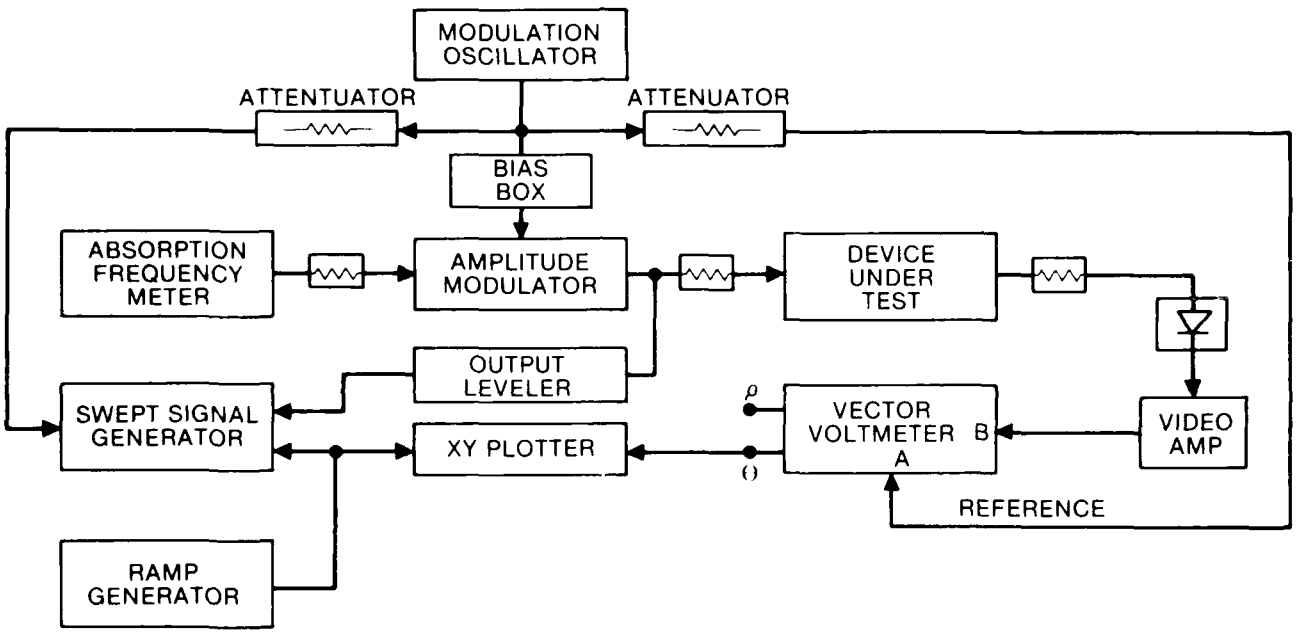

Fig. 3-1. Block Diagram of a Typical Differential Group Delay Distortion Measurement Set-Up

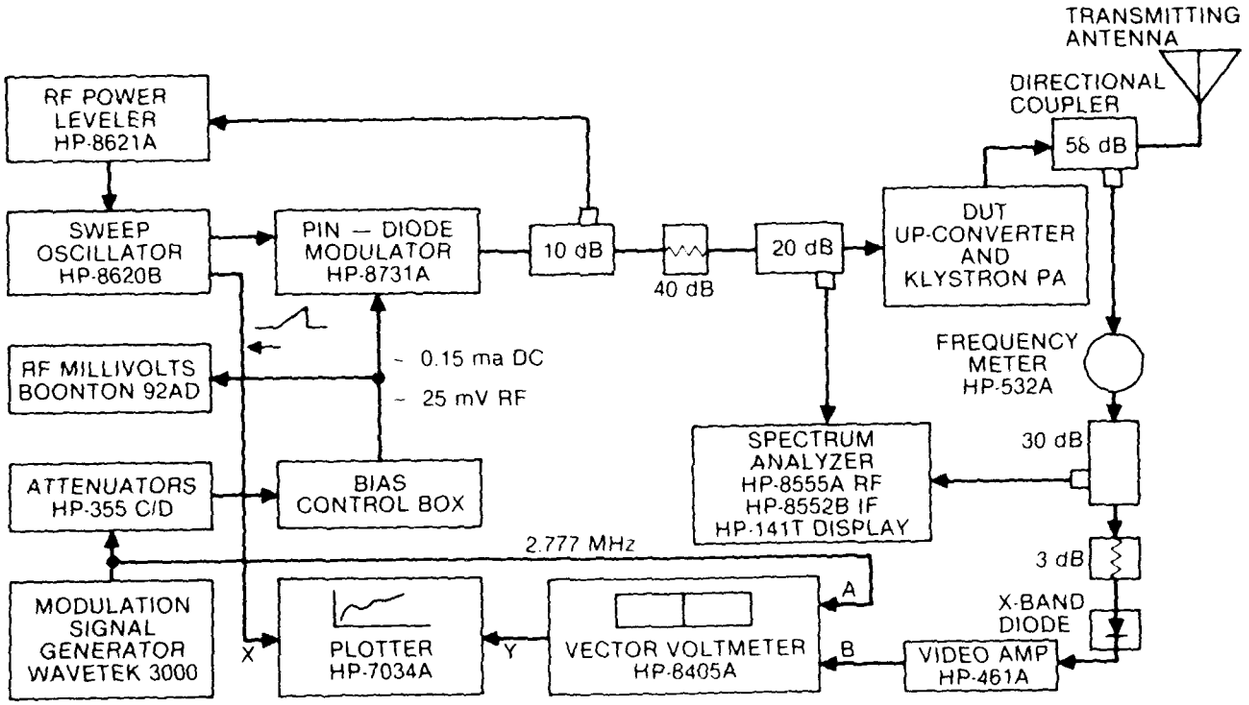

Fig. 3-2. Differential Group Delay Measurement Set-Up

reading is provided to the Y-axis of the X-Y plotter pen-recorder. When the VVM sensitivity in degrees per volt is multiplied by the plotter sensitivity in volts per inch, a wide variety of resolutions is available, yielding delay distortion in milliseconds, microseconds, or in nanoseconds per inch. Selection of proper modulation frequency enables direct scaling of the Y-axis outputs in degrees per inch of plotter paper (see Section 3.3).

Careful consideration must be given to the characteristics of the RF-modulating diode assembly, particularly in the microwave region. It should closely approach an ideal square-law detection characteristic over the range of signal levels to be used, or be used at a constant level during the test. It also needs a flat frequency characteristic over the range of passband widths to be swept. It may be necessary to use in-line attenuators to minimize reflections, which can be large enough to effect the distortion measurement of the DUT.

Before making distortion measurements, it is recommended that the diode-assembly itself be treated as a DUT, coupling it to the swept signal generator through enough attenuation to hold the diode at its proper signal level or operating range. The diode assembly's group delay plot then is taken and kept for later subtraction from the DUT characteristic.

It may be necessary to employ a video amplifier between the diode output and the VVM signal input to achieve a usable VVM input level. When a poor VVM output S/N is being experienced, it may be possible to include a suitable bandpass filter in the circuit between the diode and the VVM input (see Table III of Ref. 30). Stable, noise-free traces have been achieved successfully at VVM and plotter sensitivities of 12° deg per inch on the X-Y plotter curve. At high sensitivities, the importance of using in-line attentuators becomes apparent, since small mismatches do show up as DUT distortion. To determine the extent of mismatch distortion, it is wise to perform several test-set calibration runs similar to those recommended above for the diode assembly. The delay distortion and amplitude distortion characteristics found in the test set <u>can</u> be subtracted directly from the final DUT distortion curves.

When preparing a test setup it is desirable to have available an oscilloscope adequate to observe the modulating waveform purity at the output of the demodulator diode, as well as at the post-detection amplifier output. It is also very desirable to employ a suitable spectrum analyzer and to have on hand an assortment of attenuators to assure a properly modulated signal at the correct input level to the DUT. Although it has been found that a highly distorted amplitude modulated DUT waveform contributes no apparent degradation to the resulting phase characteristic, a certain amount of PIN-diode bias may still be desirable (see Ref. 17) to assure a clean input signal.

Small vertical offset shifts in the plotted delay curve have been observed on the VVM phasemeter output to the Y axis of the plotter as the modulator output level and percentage modulation was varied over ranges from below 100% to well over 400%.

AM-to-PM conversion effects can be measured using the subject test setup. The DUT input signal level is stepped through its dynamic signal range and a differential group-delay (DGD) plot is made at each level on the same sheet of plotter paper. Time delay variation or phase shift of the modulation can be read directly from the calibrated plot.

When the distance or inaccessibility of the device under test is a problem, requiring use of long signal lines, it may be necessary to set up a means to enable remote control of test equipment and recorders, and to use line-drivers at the input end of long coaxial-cable runs, particularly from the diode-demodulator video-amplifier output to the VVM input. Great care is worthy of expenditure in order to prevent ground-loops, even in simple laboratory bench setups, to avoid erroneous and/or misleading group delay information and worthless phase distortion plots. The swept generator and its modulator should be located physically close to the DUT input in terms of carrier wavelengths, to avoid generation of parabolic distortion components created by any long waveguide runs. Attenuators can often be used to minimize mismatch ripple if adequate initial signal power is available.

It is difficult to overemphasize the fact that accurate frequency markers on the DGD plots will greatly ease generation of departure functions.

For example, a swept generator may be calibrated to 1 percent of indicated frequency, but when operating at 8000 MHz, the error is 80 MHz, which is enough to create intolerable inaccuracy in identifying the relationship between a DUT passband and its throughout spectrum. Frequency markers injected into the DUT passband appear as little "twiches" on the X-Y plot as the input signal is swept over the marker frequency. Absorption-type frequency meters have been used successfully (HP-532-A) when enough synthesizers were not available to produce marker frequencies. It is possible to use an HP-532-A to identify the center of the passband on the X-Y plot, and to use the frequency sweep on a spectrum analyzer as indicative of sweeper frequency limits for calibration of the X-Y plotter frequency-axis, using the equipment shown in Fig. 3-2.

3.2 PIN-DIODE AMPLITUDE MODULATORS

When using a PIN-diode modulator, it is suggested that some form of carrier-frequency power leveling be employed and that its individual group delay performance be verified while the leveling device is in place and operating properly. This may be done by connecting a spectrum analyzer at the input to the DUT and setting the anayzer amplitude display to LINEAR. It will be possible to observe individually the modulated carrier and its sideband components, watching their amplitudes vary separately as the signal generator is swept through the DUT passband frequencies. Ideally the carrier and its two side-bands would remain at a constant amplitude at the input to the DUT, varying in amplitude and phase only at the DUT output. Input variation is due to the presence of PIN-diode modulator transfer-function distortion, to the imperfection of the carrier-power leveler, as well as to the extent to which the cable and input impedance mismatches contribute to the output delay distortion reading. Their total effect should be determined, and may be investigated by this method.

It will prove useful to have conveniently at hand an easy means for varying the PIN-diode DC bias, as well as the AC modulating signal magnitude. By use of the above-described technique, the best operating point of the modulator may be ascertained by observing the sideband distribution on the

spectrum analyzer, and verified when the oscilloscope is attached to read demodulator-diode output and VVM "B" input. Best operating point may be determined by observation of high signal-to-noise ratio on the oscilloscope and a clear trace on the plotter. Purity of demodulated signal waveform is of less importance than the above considerations.

Figure 3-3 shows the schematic diagram of a PIN-diode bias box that has been used successfully with the HP-8731-A modulator. It shows the modulating signal coupled to the PIN-diode modulator through a ferrite-core transformer having an impedance ratio of 50-ohms primary to about 300-ohms secondary. A direct-current bias originates from a battery equipped with an on-off and reversing switch, a multi-turn potentiometer to make vernier bias adjustments, and a 1 - 0 - 1 milliameter to monitor and record actual bias current.

A radio-frequency voltmeter is useful to measure and document the modulating voltage at the input to the PIN-diode. For the setups typically used, the DC bias is about 0.15 ma, and the AC voltage is about 25 mv at 2.777 MHz. The test operator must make his own adjustments to determine the combination required to obtain the most useful group delay and amplitude distortion information.

3.3. RESOLUTION VERSUS PARAMETER SENSITIVITY

When making group delay measurements from which to derive departure functions, it is advisable to preselect test parameter limits which will provide adequate time-delay or phase resolution in the intervals over which performance evaluation is important.

For example, when sweeping a passband, the carrier-modulating frequency should be chosen low enough to yield a phase departure function compatible with producing adequate resolution over the smallest frequency cell required for the signalling speeds to be employed. The carrier modulation-frequency should be equal to one-half or less than the smallest element of bandwidth over which resolution visibility is required. A modulation frequency of five percent of the passband width usually will provide adequate X-axis data resolution. Use of lower modulation frequencies reduces the time-resolution so a tradeoff is required. The governing criterion must be

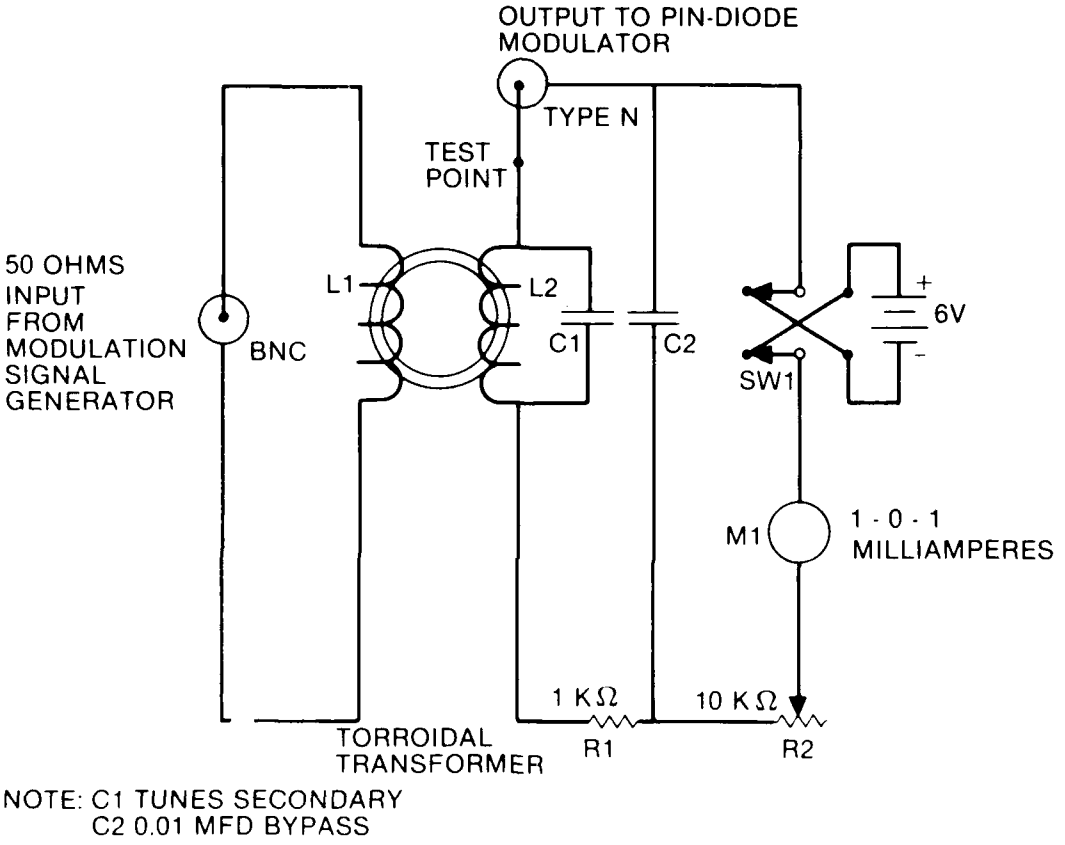

Fig. 3-3. PIN-Diode Modulator Bias Box

determined from the desired measurement accuracy, if not stated in performance specifications.

Test parameter sensitivity and data resolution are related through the Δf and the $\Delta\theta$ needed to produce a desired accuracy. Figure 2-7 clarifies that relationship via "envelope delay" as the value of a particular ordinate divided by its corresponding abscissa.

$$\text{Envelope delay} = \theta/\omega \text{ seconds} \tag{3.1}$$

but it is necessary to determine the differential delay between the two sidebands and the least-squares linear fit to formulate the departure function.

The following relationships permit examination of the tradeoffs between the test parameters.

$$\text{Differential delay} = \frac{\Delta\theta}{\Delta\omega} \text{ radians} \div \text{radians per sec} \tag{3.2}$$

$$= \text{sec}$$

or,
$$\Delta t = \frac{\frac{2\pi}{360} \times \Delta\theta \text{ radians}}{2\pi\Delta f \text{ radians/sec}} = \frac{1}{360} \frac{\Delta\theta}{\Delta f} \text{ sec} \tag{3.3}$$

for $\Delta\theta$ in deg and for Δf in Hertz.

The modulating frequency Δf required for a given resolution element Δt, is expressed by rewriting 3.3 as follows:

$$\Delta f = \frac{\Delta\theta}{360 \times \Delta t} \text{ Hz} \tag{3.4}$$

As an example, to obtain Δt resolution = 10^{-9} sec and a $\Delta\theta$ = 1 deg requires that

$$\Delta f = \frac{1}{360 \times 10^{-9}} = \frac{1000}{360} \times 10^{6} \tag{3.5}$$

$$= 2.777 \text{ MHz}$$

giving a phase slope averaged over an interval of 2 × 2.777 MHz, or 5.555 MHz.

Table 3-1 presents various relationships between modulating frequencies and the resolution available.

Table 3.1. Resolution Trade-Offs

Differential Delay Resolution Cell	Differential Phase Resolution Cell (deg)	Modulating Frequency
1 millisec	1	2.778 Hz
1 microsec	1	2.778 KHz
1 nanosec	1	2.778 MHz
1 millisec	10	27.778 Hz
1 microsec	10	27.778 KHz
1 nanosec	10	27.78 MHz
10 millisec	1	0.277 Hz
10 microsec	1	277.8 Hz
10 nanosec	1	277.8 kHz
10 nanosec	10	2.778 MHz

4. TYPICAL LOSS CALCULATION EXAMPLES

4.1 INTERPRETING A DIFFERENTIAL GROUP DELAY PLOT

In this section, two examples of differential group delay loss computation are studied. One case is further examined to test for phase-shift specification compliance.

Figure 4-1 presents a group delay plot measured in a 25 kHz channel of an in-service communications relay satellite (MARISAT). The plot was taken to enable determination of specification compliance. The design performance specification required ≤ 0.1 radian phase-shift over any 2500 Hz segment within the central 80% of the passband.

The signal generator in the test set-up was amplitude-modulated by a 282 Hz signal and the carrier was stepped across the passband in 666-2/3 Hz intervals. The phase resolution thus obtainable is averaged over an interval of 2×283, or 566 Hz, at each step, which is well within the specification measurement interval (2500 Hz) required to verify the delay resolution. Calculating the corresponding time delay resolution from Eq. 3.3

$$\Delta t = \frac{1}{360} \times \frac{\Delta\theta}{\Delta f} = \frac{0.1 \times 57.3}{360 \times 283} \text{ sec}$$

$$= 56.2 \text{ microsec} \qquad (4.1)$$

The specification was not stated in terms of time resolution, but if it had been, the instrumentation would have been required to yield

$$\Delta t \leq \frac{0.1 \times 57.3}{360 \times 2500} = 6.36 \text{ microsec} \qquad (4.1a)$$

Examination of Fig. 4-1 reveals a Y-axis scale factor of ten microseconds per inch, and an X-axis resolution of 4000 Hz per inch. For manual integration of the group delay curve, the apparent minimum phase resolution-cell size is, for $\Delta f = 4000$ Hz and $\Delta t = 10 \times 10^{-6}$ microsec,

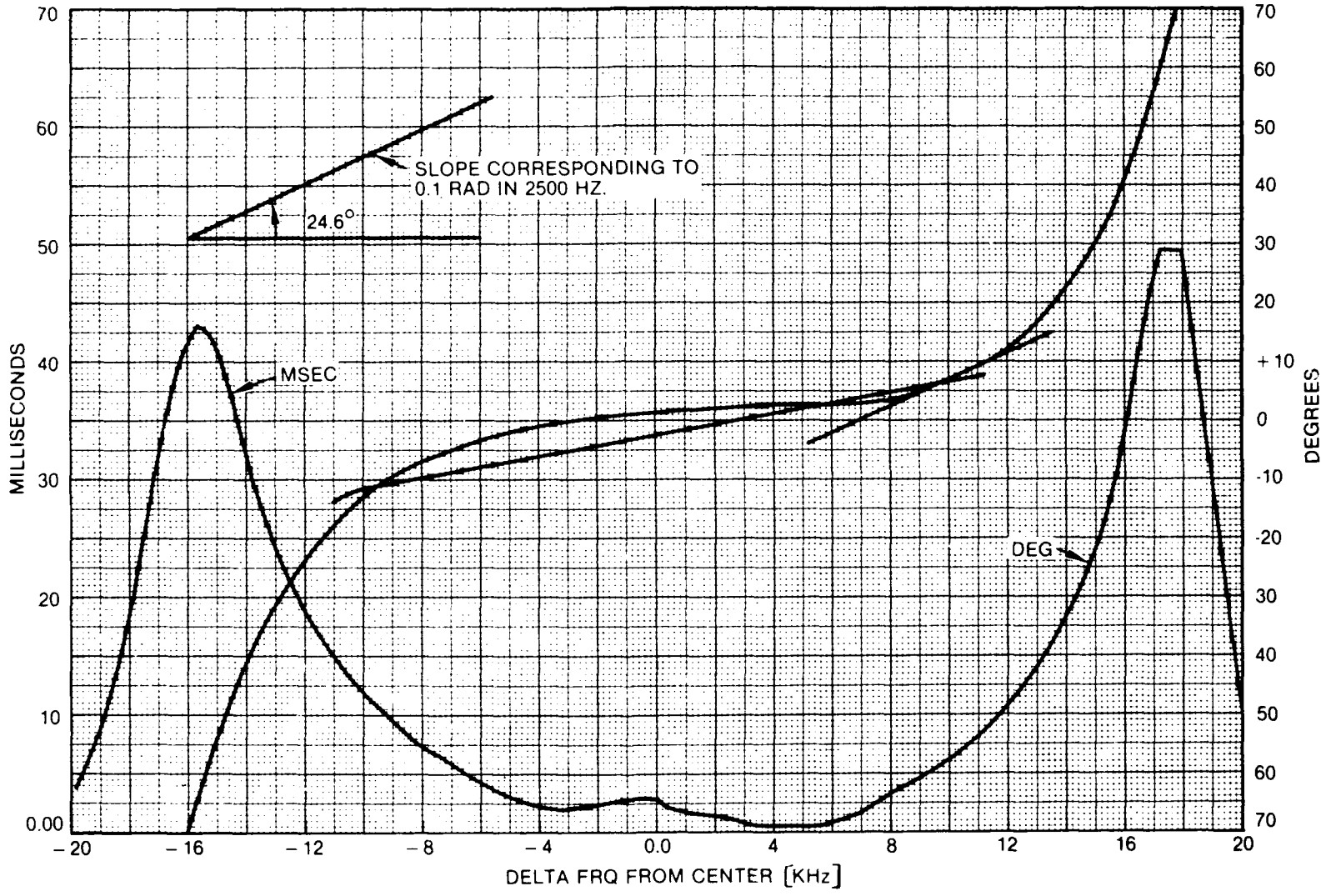

Fig. 4-1. Measured Group Delay and Integrated Phase Passband Characteristic

$$\Delta\theta = 360 \times \Delta f \Delta t$$
$$= 360 \times 4000 \times 10 \times 10^{-6}$$
$$= 14.4 \text{ deg per square inch} \qquad (4.2)$$

But since there are 400 small square cells per square inch on the graph paper used, the available or visible phase resolution actually is 14.4/400 = 0.036 deg per cell. The test setup therefore provides a phase resolution visibility more than two orders of magnitude better than required, and obtains phase slope resolution over an interval one-fourth (four times better than) that which would satisfy the specification.

At the low-frequency delay peak of Fig. 4-1, the differential group delay contribution of 42.5 microsec to the relay channel phase shift, over an interval of twice the modulating frequency of 283 Hz, is calculated from

$$\Delta\theta = 360 \times \Delta\omega\Delta t$$
$$= 360 \times 2 \times 283 \times 42.5 \times 10^{-6}$$
$$= 8.66 \text{ deg per 566 Hz interval} \qquad (4.2a)$$

At the high-frequency end of the passband, the 49 microsec peak delay indicates an averaged phase shift at that point of

$$\Delta\theta = 360 \times 2 \times 283 \times 49 \times 10^{-6}$$
$$= 9.98 \text{ deg per 566 Hz interval} \qquad (4.2b)$$

The 80% bandwidth points of a 25 kHz-wide passband occur at ±10 kHz from band center. The differential group delay at those points is found from Fig. 4-1 to be about 11.2 and 6.5 microsec, so the phase-shift slope over an interval equal to twice the modulating frequency, i.e., 566 Hz, is given by

$$\Delta\theta = 2.28 \text{ and } 1.32 \text{ deg, respectively}$$

Since the delay values inside the passband are less than the values at the 80% points, it is apparent that this communications relay channel performs better than specification.

Special significance attaches to the frequency at which the peaks of [illegible], as they correspond closely to the 3-dB or half-power points on [illegible] points. It can be inferred quickly that 3-dB points based upon [illegible] cannot be relied upon to provide high-quality binary PSK [illegible] because of the DGD distortion which is usually present in the vicinity of the 3-dB points. Use of 1-dB points will usually suffice for bandedge determination, but are not readily located from a DGD plot.

4.3 A COMPUTER CURVE-FITTED PHASE DEPARTURE FUNCTION

Equation (4.3) resulted from application of a computer curve-fitting program to the group delay data of Fig. 4.1. The equation given was integrated manually to obtain the corresponding phase function. The phase equation was converted to a departure function by removal of the first two terms and entering the remaining terms into the loss-computation equation (Eq. 2.15). The first term represents hardware throughput delay and is therefore part of radio propagation time. The second term is assumed to be tracked out and eliminated by FM synchronization circuitry.

Assuming hard-limiting, spectral truncation at the first nulls, and spectral center coincidence with passband center, the calculated loss to a digital BPSK signal was 0.0122 dB.

$$\theta(X) = 0.409703 + 0.31732X - 0.046614X^2 + 0.0036766X^3 - 0.000027719X^4 + 0.0000326721X^5 \quad (4.3)$$

It should be rather obvious, but sometimes is overlooked, that care must be taken to assure that the same units of measurement are used in determining the frequency coordinates for the loss equations as are used throughout the computer evaluation. Inadvertant use of dissimilar units can result in

losses that are magnificently low, or are outlandishly high. The latter tendency is sufficient to cause careful review, but unusually low losses might be overlooked.

The smooth cubic-shaped curve shown in Fig. 4-1 is the end result of the manual integration, and was used to verify phase specification compliance, rather than for loss determination.

For comparitive purposes, the group delay curve of Fig. 4-1 was subjected to the manual loss-calculation processed and summarized in Table 4-1 and in Fig. 4-2. A HP-97 computer, used with the twelve-interval integral Table F-14 for loss calculation in this manner, yielded a loss of approximately 0.01 dB, assuming a $(\sin x/x)^2$ spectral distribution with first nulls located at ±12 kHz. Direct comparison between manual and computer methods yielded 0.00856 dB and 0.0122 dB respectively, showing nearly identical results, or consistency to 0.01 ± .002 dB.

4.3 MEANING OF THE COEFFICIENTS IN THE PHASE DEPARTURE FUNCTION

At this time, it may prove instructive to examine more closely the previously introduced Taylor-Maclaurin series expansion on the phase function because of the opportunity it affords to relate each coefficient to the particular type of hardware phenomenon causing it. To do so, use will be made of the following expression for a generalized passband phase-shift characteristic (Eq. 4.4) which may be obtained by integration of a curve-fitted differential group delay plot, or by curve-fitting a manually integrated DGD phase plot

$$\theta(\omega) = \theta_o + \theta_1(\omega - \omega_o) + \theta_2(\omega - \omega_o)^2 + \theta_3(\omega - \omega_o) + \ldots \theta_n(\omega - \omega_o)^n \ldots \quad (4.4)$$

where ω represents frequency under consideration

ω_o represents passband center frequency and/or carrier frequency

θ_o represents accumulated circuit or link phase shift

θ_1 represents the linear network least-squares fit, or/and phase tracking error

Table 4.1. Phase Distortion Loss Calculations for Fig. 4.1

Δt_i	[illegible]	[illegible]	[illegible]	[illegible]	Cos $\Delta\phi$ [illegible]
[illegible]	[illegible]	[illegible]	-28.188	[illegible].323	[illegible]
[illegible]	[illegible]	[illegible]	[illegible]	[illegible]	[illegible]
[illegible]	[illegible]	[illegible]	[illegible]	[illegible]	[illegible]5966
[illegible]	[illegible]	[illegible]	[illegible]	[illegible]	[illegible]
[illegible]	[illegible]	[illegible]	[illegible]	[illegible]	[illegible]
[illegible]	[illegible]	[illegible]	[illegible]	[illegible]	[illegible]88911
[illegible]	[illegible]	[illegible]	[illegible]	[illegible]	[illegible]
[illegible]	[illegible]	[illegible]	[illegible]	[illegible]	[illegible]
[illegible]	[illegible]	[illegible]	[illegible]	[illegible]	[illegible]
[illegible]	[illegible]	[illegible]	[illegible]	[illegible]	[illegible]
[illegible]	[illegible]	[illegible]	[illegible]	[illegible]	[illegible]
[illegible]	[illegible]	[illegible]	[illegible]	[illegible]	[illegible]
[illegible]	[illegible]	[illegible]	[illegible]	[illegible]	--
[illegible]	[illegible]	[illegible]	[illegible]	[illegible]	[illegible]
[illegible]	[illegible]	[illegible]	[illegible]	[illegible]	[illegible]
[illegible]	[illegible]	[illegible]	[illegible]	[illegible]	[illegible]
[illegible]	[illegible]	[illegible]	[illegible]	[illegible]	[illegible]
[illegible]	[illegible]	[illegible]	[illegible]	[illegible]	[illegible]
[illegible]	[illegible]	[illegible]	[illegible]	[illegible]	[illegible]
[illegible]	[illegible]	[illegible]	[illegible]	[illegible]	[illegible]
[illegible]	[illegible]	[illegible]	[illegible]	[illegible]	[illegible]
[illegible]	[illegible]	[illegible]	[illegible]	[illegible]	[illegible]
[illegible]	[illegible]	[illegible]	[illegible]	[illegible]	[illegible]
[illegible]	[illegible]	[illegible]	[illegible]	[illegible]	[illegible]
					[illegible]

Scale Factors

Δt = [illegible]μs/cell

Δf = 200 Hz/cell

$\Delta\phi$ = 360 [illegible]

= [illegible]°/cell

= [illegible] sq inch

[illegible] cells/sq inch

$\sum$ [illegible] = 2.833567

$\left[\frac{2.833567}{[illegible]}\right]$ = [illegible]

[illegible] dB

[illegible]

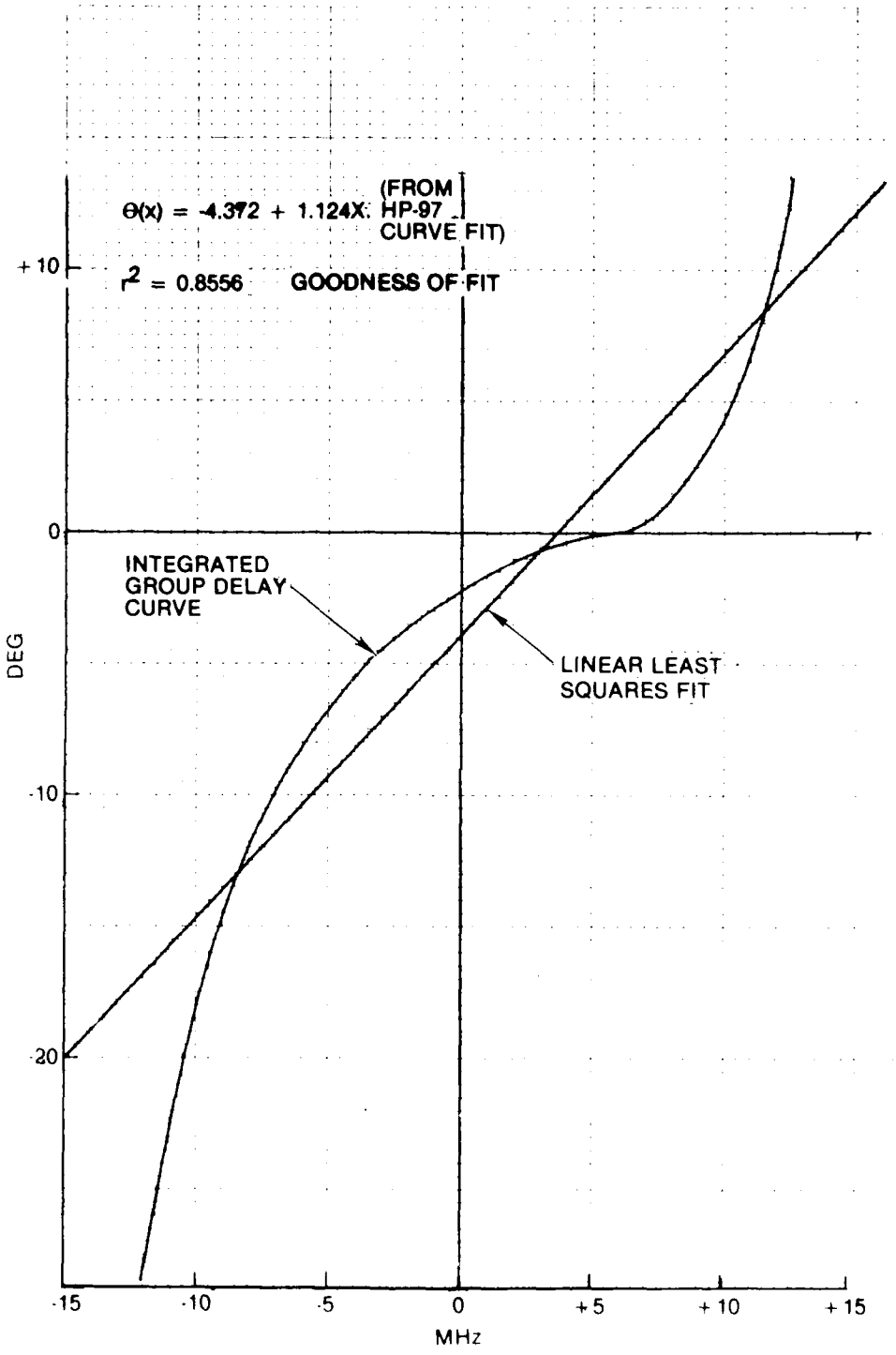

Fig. 4-2. Manually Integrated Group Delay Curve from Fig. 4-1

θ_2	represents parabolic waveguide run and passband filter parabolic phase characteristics lumped together
θ_3	represents cubic components from skewed passbands, perhaps arising in off-center-tuned klystron tanks
θ_4 to θ_n	represent higher-order terms related to passband ripple and/or mismatch reflection effect accumulations

The departure function will not have the θ_o term because absolute phase delay through a network usually is inconsequential. The θ_1 term may or may not be neglected, depending on the residual error in the clock-tracking synchronizing processes but is ideally very close to zero.

The remaining terms represent the departure function about the passband center, or the carrier-frequency/spectral center ω_o, therefore appearing in the typical form

$$\theta(\omega) = \theta_2(\omega - \omega_o)^2 + \theta_3(\omega - \omega_3)^3 + \ldots\theta_n(\omega - \omega_n)^n \qquad (4.5)$$

When expressed in terms of frequency displacement from band center, $\omega_o = 0$ and the expression (4.5) becomes simply the Maclaurin power series

$$\theta(\omega) = \sum_{-n}^{+n} \theta_n(\omega)^n + R_n \quad \text{for } n \geq 2 \qquad (4.6)$$

when the remainder term R_n becomes too small to effect results of the loss computation significantly, say less than 0.1 dB or so.

4.4 MANUAL CALCULATION OF DIFFERENTIAL GROUP DELAY DISTORTION LOSS

From Figure 4-3 differential group delay distortion loss is calculated manually. Measurements were taken with the test setup of Fig. 3-2. In normal use the sideband 700 MHz IF output of the specific DUT is translated in an up-converter to X band. A klystron amplifies the X band signal to about 2 KW. A sample of the signal is obtained via a nominally 60 dB directional coupler (58 dB measured) placed in the waveguide between the klystron and the antenna. The sampled signal is fed to a 3-dB coaxial in-line attentuator preceding the crystal-diode rectifier assembly, arriving at a level of zero dBm. In the test setup, the CW output of a swept signal generator is externally

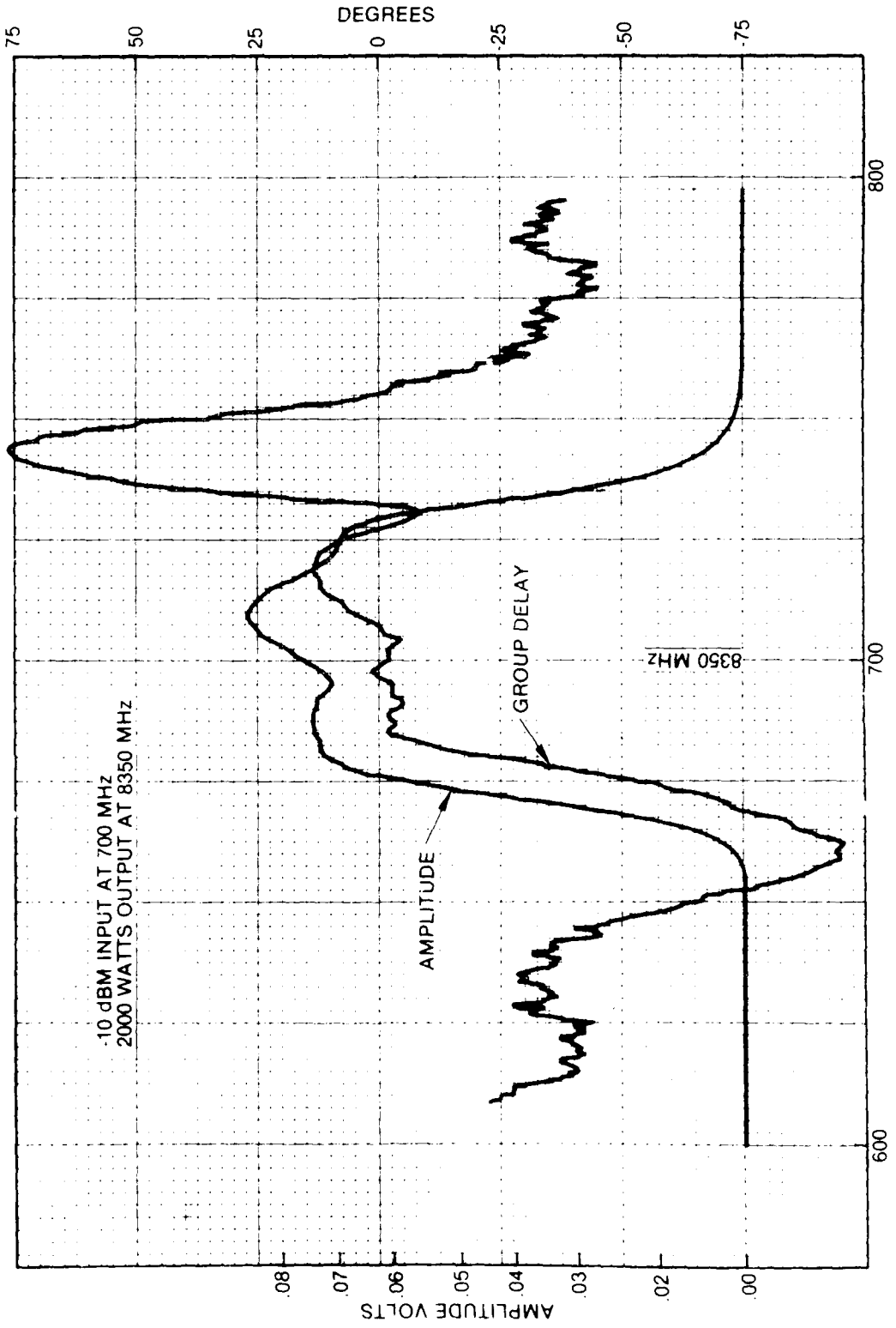

Fig. 4-3. Differential Group Delay Plot with Integrated Phase Curve

AD-A099 187 AEROSPACE CORP EL SEGUNDO CA SATELLITE SYSTEMS DIV F/G 17/2.1
SIGNAL PROCESSING DISTORTION LOSS IN SPREAD-SPECTRUM COMMUNICAT--ETC(U)
OCT 80 A C LYTLE
UNCLASSIFIED TR-0081(6724-01)-1 SD-TR-81-20 F04701-80-C-0081 NL

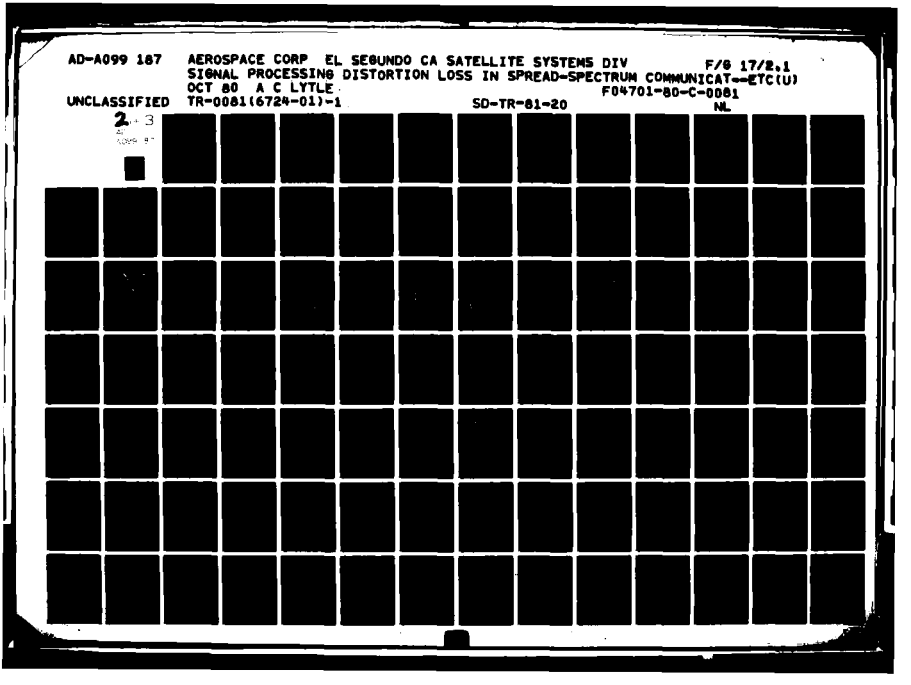

amplitude-modulated by a 2.777 MHz signal and leveled at -10 dBm at the input to the up-converter. The signal generator was carefully calibrated to sweep the 600 - 800 MHz band. Reference to Fig. 4-3 shows that the plot could have been expanded by readjusting the sweep range to ±50 MHz instead of ± 100 MHz, based upon the resulting group delay plot. The "negative" and the "positive" peaks indicate a slightly skewed passband approximately 55 MHz in width. However, the phase resolution available was more than adequate for the spectral energy loss calculation.

The scale factors of Fig. 4-4 are 7.2 nanosec per inch on the Y axis, and 25 MHz per inch on the X axis. For use in numerical integration, each small square contributes the value

$$\frac{7.2 \times 10^{-9}}{10} \times \frac{25 \times 10^{+6}}{10} \times 360 = 0.648 \text{ deg}$$

The 7.2 nanosec per inch value comes from a VVM sensitivity of 36 nanosec per volt, multiplied by a plotter Y-axis sensitivity of 0.2 volts per inch. The factors of 10 in each denominator come from ten subdivisions per inch on the graph paper. At a modulation frequency of 2.777 MHz, one deg per cycle corresponds exactly to one nanosecond per X-axis subdivision.

Table 4-2 summarizes all the data utilized in computation of the phase departure function and signal loss. Column 1 shows X-axis frequency intercepts at frequency intervals of 2.5 MHz. Column 2 shows the small-square y_i count between successive frequency intervals. Column 3 provides a running sum of the square count, starting from 705 MHz as the arbitrary band center, going both higher and lower in frequency from 705 MHz. The values are signed "positive" on the high frequency side of band center, and "negative" on the low-frequency side. This slope sign should be expected, as the passband distortion function is superimposed on the general system phase function, and accords therefore with the network reactance theorem, in which reactance is a positive-increasing function of frequency (Ref. 8, Vol 1). Numerical integration was done from the nearest spectral center zero-phase point (705 MHz) by taking the values in Column 3 and multiplying them by the scale factor 0.648 deg per cell. Each was then recorded in Column 4 as the phase

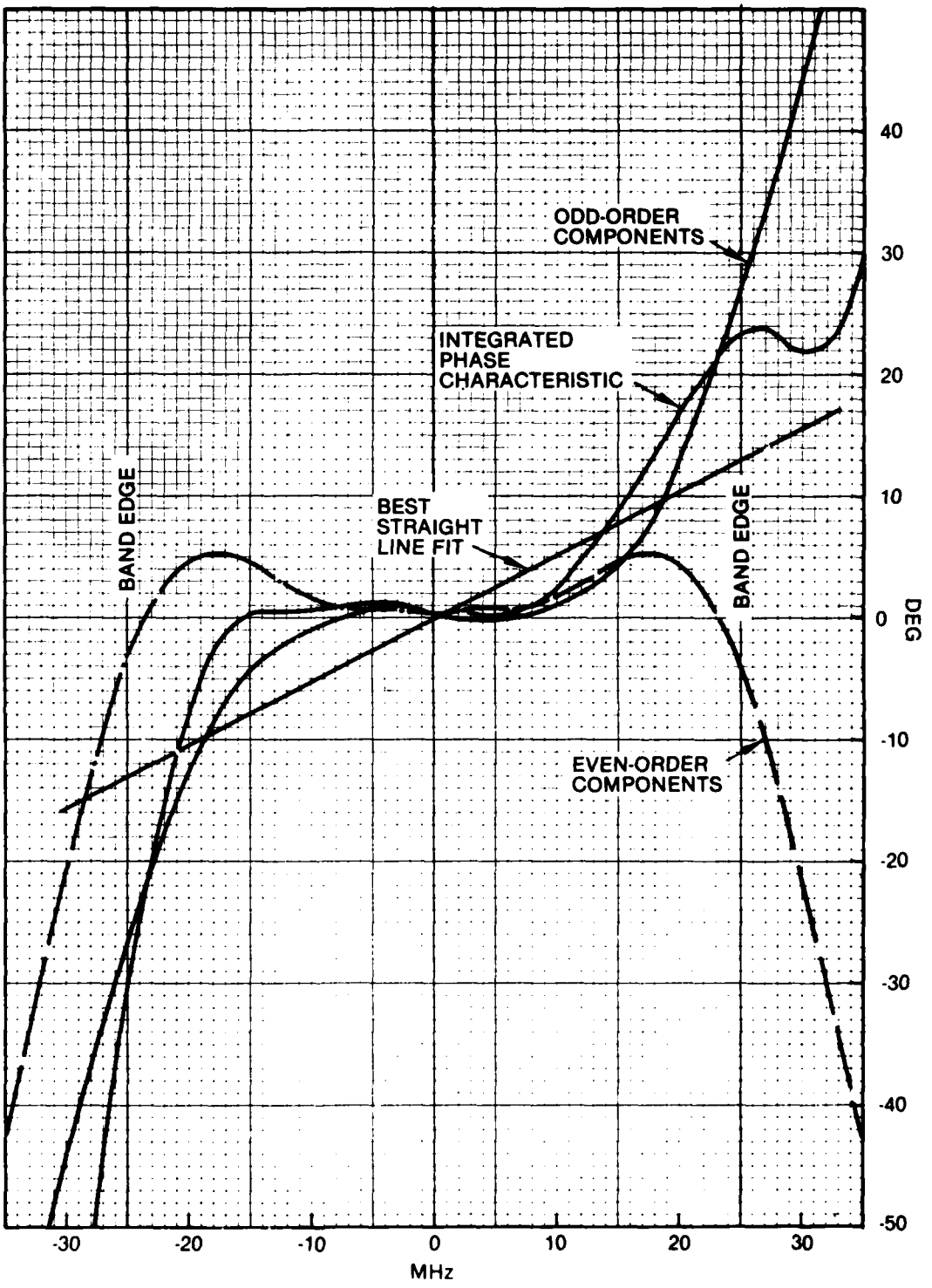

Fig. 4-4. Finding the Best Straight-Line Fit to the Integrated Differential Delay Plot

Table 4.2. Phase Distortion Loss and Phase Departure Tradeoff

(IHDRT Uplink Fig. 4-3)

@ 8350 Klystron Channel 6

Scale Factor = 0.648°/cell

1 f_i	2 v_i	3 Σv_i	4 deg	5 Odd	6 Even	7 $\Delta\theta$	8 $\int_a^b$	9 Register	10 $\cos \Delta\theta \int_a^b$	11 X axis
655	-33	-311.3	-201.7							
657.5	-36	-278.3	-180.3							
660	-36.7	-242.3	-157.							
662.5	-37.3	-205.6	-133.2	-71.00						
665	-34.5	-168.3	-109.1	-42.95	-71.00					
667.5	-32	-133.8	- 86.7	-32.4	-54.95					
670	-29	-101.8	- 66.	-22.05	-43.95					
672.5	-24.5	- 72.8	- 47.2	-11.85	-35.35	-32.9				
675	-20.5	- 48.3	- 31.3	- 4.00	-27.3	-18.3	0.001201	A	0.001140	-π
677.5	-14.8	- 27.8	- 18.	1.35	-19.35	- 6.3	0.009544	9	0.009486	2.827
680	- 9.	- 13.0	- 8.4	4.25	-12.65	+ 2.0	0.028814	8	0.028796	2.513
682.5	- 3.5	- 4.0	- 2.6	5.10	- 6.25	+ 6.5	0.060291	7	0.059903	2.199
685	0	0.5	+ 0.3	4.6	- 4.3	+ 8.1	0.102985	6	0.101958	1.885
687.5	- 0.2	0.5	+ 0.3	2.9	- 2.45	+ 6.8	0.153441	5	0.152362	1.571
690	- 0.3	0.7	+ 0.5	1.55	- 1.05	+ 5.7	0.206098	4	0.205079	1.257
692.5	- 0.6	1.0	0.6	0.60	0.0	+ 4.5	0.254168	3	0.253384	0.942
695	0	1.6	1.	0.50	- 0.50	+ 3.6	0.290869	2	0.290295	0.628
697.5	1.3	1.6	1.	0.65	+ 0.35	+ 2.3	0.310740	1	0.310490	0.314
700	0.3	0.3	0.2	-	-	0	-	-	0	0
702.5	0.2	0.5	0.3	0.65	- 0.35	- 1.0	0.310740	1	0.310693	+0.314
705	- 0.5	0	0	0.50	+ 0.50	- 2.6	0.290869	2	0.290570	0.628
707.5	1.	1.	0.6	0.60	0.0	- 3.3	0.254168	3	0.253746	0.942
710	3.	4.	2.6	1.55	1.05	- 2.6	0.206098	4	0.205886	1.257
712.5	4.	8.	5.2	2.9	2.45	- 1.3	0.153441	5	0.153402	1.571
715	5.8	13.8	8.9	4.6	4.3	1.1	0.102985	6	0.102966	1.885
717.5	6.	19.8	12.8	5.10	6.25	3.7	0.060291	7	0.060165	2.199
720	6.3	26.1	16.9	4.25	12.65	6.5	0.028814	8	0.029629	2.513
722.5	5.8	31.9	20.7	1.35	19.35	9.0	0.009544	9	0.009426	2.827
725	4.0	35.9	23.3	- 4.00	27.3	10.3	0.001201	A	0.001182	+π
727.5	0.4	36.3	23.5	-11.85	35.35	9.2				
730	- 2.5	33.8	21.9	-22.05	43.95	6.0				
732.5	+ 2.	35.8	23.2	-32.4	54.95	6.3				
735	+15	50.8	32.9	-42.95	71.00	14.7				
737.5	+23	73.8	47.8	-71.00		28.3				
740	+28	101.8	66.				Σ = 2.836301		Σ = 2.829558	
742.5	+31	142.8	92.5							
745	+31	173.8	112.6							

$$20 \log \frac{2.829558}{2.836301} = -0.0207 \text{ dB}$$

reading at that frequency. The points were then plotted on Fig. 4-3 as dots, and were plotted again with expanded scales on Fig. 4-4 to facilitate estimation of the "best-fit straight line" of phase. The best fit line should be the same straight line derived from the "line of equal areas" introduced and shown on Fig. 2-5.

Another method for determining the linear phase component consists of breaking down the data of Column 4 into its "even" and "odd" components, recording them in Columns 6 and 5, respectively, and plotting them per Fig. 4-4 (see Ref. 14, Section 42.8). Since the even components would average to a straight line of zero slope, they need be considered no further. A best straight-line was established by trial and error, using as a criterion estimated equal area above and below the odd plot with respect to the established spectral limits of ±25 MHz and with zero-departure at midband. Good agreement was obtained compared with the fit found above. A planimeter could be used to check the equal-area computation or estimation.

Another more sophisticated method for obtaining the linear phase term makes use of the availability of computers that have linear least squares curve-fitting routines. An excellent discussion on using computers for linear least squares curve fitting is contained in Ref. 47, page 10 and Appendix 2A. Some computers will calculate the best fit, plot the line, and then print out the equation. The equation found for this example using an HP-97 is

$$\theta(\omega) = 0.52\omega \tag{4.7}$$

which provides intercepts of ± 13 deg at ± 25 MHz (see Fig. 4-4).

Points constituting the departure function are now calculated as the difference between Eq. (4.7) and the values given in Column 4, and are recorded in Column 7. Column 7 is plotted on Fig. 4-5 for instructional purposes and shows a dip at about f_i = 31 MHz which is attributed to klystron cavity tuning. Since the dip lies outside the passband, it is ignored. In Fig. 4-5 a scale of ± π has been overlaid on the frequency axis to co-locate the $(\sin x/x)^2$ spectral distribution nulls with band edges.

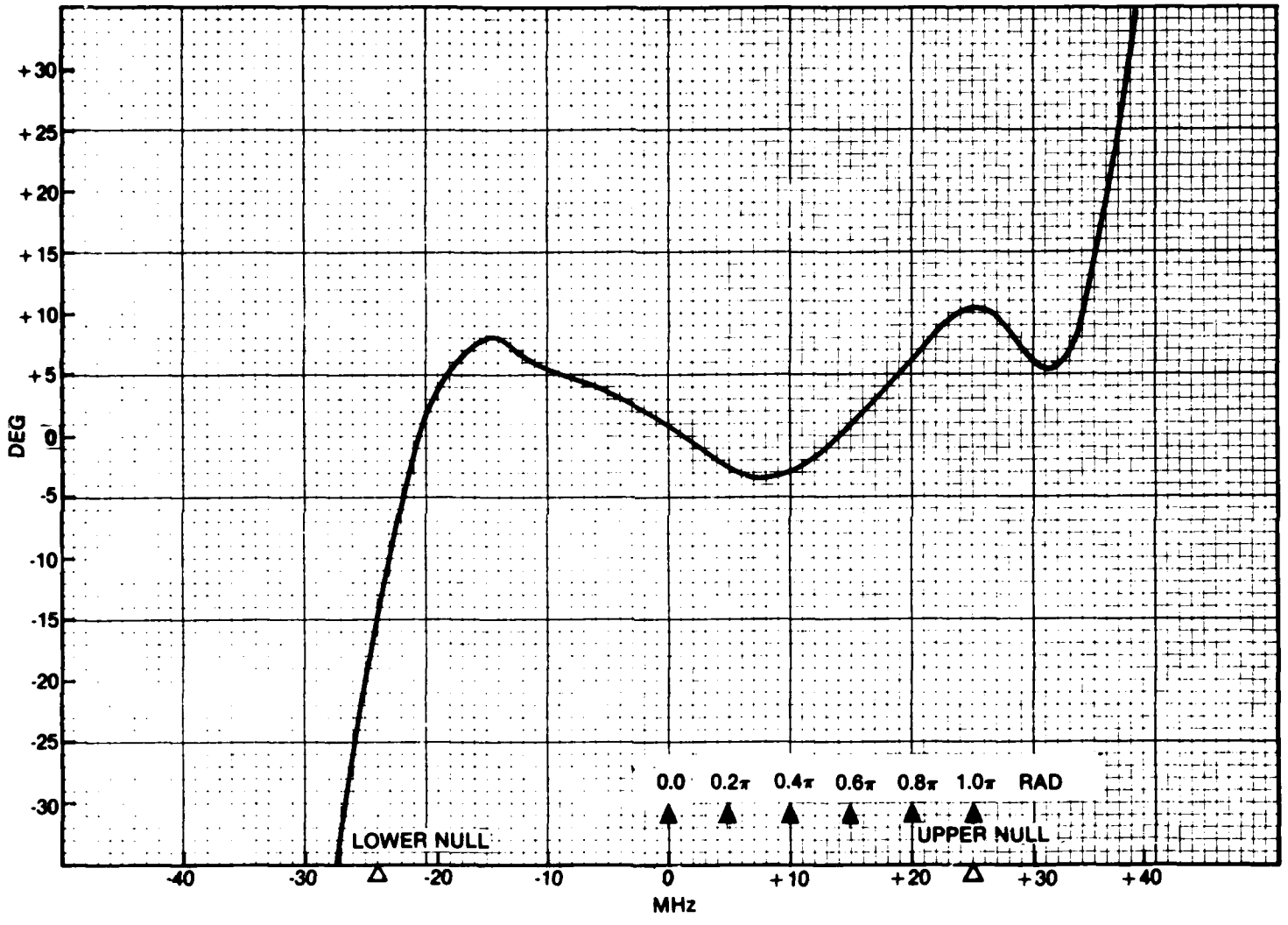

Fig. 4-5. Phase Departure Function for Figs. 4-2/4-3

Column 8 contains the values of the spectral weighting function obtained by dividing the spectrum from band center out to the first null into ten equal parts. Those values are found listed in Table F-12 for a theoretically perfect spectrum. As recorded in Column 8 of Table 4-2, the greatest weighting values are found closest to the band center. Column 10 contains the products of the phase departure function angle cosines with the value of the weighting-function integral at each corresponding interval across the passband. Then Column 8 is summed from top to bottom and the result is tallied, and the same thing done for Column 10. The Column 10 sum is divided by the Column 8 sum to get the ratio of power actually available to power theoretically available, as derived in Eq. (2.15). Applying Eqs. (1.12) and (2.15), the signal energy loss due to differential group delay distortion is found to be

$$\text{Loss} = 20 \log_{10} \left[\frac{2.829558}{2\text{x}1.418151}\right] = -0.0207 \text{ dB}$$

Column 9 merely lists the memory registers used in an HP-97, and Column 11 contains references to the stepped X-axis limits of integration from the Tables of Section F.12. The sum of Column 8 serves to crosscheck the double-sided integral value shown above and first calculated from Eq. (1.5), and represents zero energy loss from integrating between first nulls.

An actual application in the form of Eq. (2.15), utilizing summations for manual calculation instead of integrals as for analytical expressions, results in the following adaptation of Eqs. (2.16) and (1.12):

$$\text{dB Loss} = 20 \log_{10}\left[0.5K \sum_{-n}^{+n} \{\cos \Delta\theta_i\} \int_i^{i+1} \left[\frac{\sin \Delta x_i}{\Delta x_i}\right]^2 dx\right]$$

$$\text{for } i = \frac{2m}{m} \text{ and for integer } n \qquad (4.8)$$

in the interval $0 \leq n \leq m/2$ where m = the number of resolvable integration cells into which the passband frequency axis has been divided, and $K = 0.705143$ from Eq. (2.16). Tables have been provided in Appendix F for values of the $(\sin x/x)^2$ integral sectored in 2 through 12 frequency-axis cells.

4.5 LOSS CALCULATION BY AVERAGE PHASE DISTORTION DEPARTURE ANGLES

Since the loss function is a cosine and hence an even function, an unweighted average departure angle may be used in estimating DGD distortion loss. As an example, an arithmetic average will be obtained from the curve of Fig. 4-5 by summing phase angle magnitudes over 50 intervals of 1 MHz, each lying between spectral nulls

$$\sum_{i=-25}^{i=25} |\theta_i| = 218.30 \text{ deg} \tag{4.9}$$

Over 50 units of abscissa, this provides an average ordinate of

$$\frac{218.30}{50} = 4.37 \text{ deg} \tag{4.10}$$

According to Eq. (2.51) that angle would be correspond to a loss of

$$20 \log_{10} \cos(4.37) = -0.0252 \text{ dB} \tag{4.11}$$

Working backwards from the totals given in Columns 8 and 10 of Table 4-2, an equivalent departure function phase angle may be obtained using the inverse of Eq. (2.51):

$$\Psi = \cos^{-1}\left[\frac{2.829558}{2.836314}\right]$$

$$= 3.95 \text{ deg} \tag{4.12}$$

The small differences in losses (0.0207 dB vs 0.0252 dB) and in angles (4.37 vs 3.95 deg) may cause the reader to question the depth of analysis required in handling well-behaved passbands.

Before entering into a lengthy analytical departure-function derivation, the designer should consider the complexity of the DGD plot, the accuracy required of the loss calculation, as well as the time and facilities available for the analysis. Most plots can be analyzed in three hours, depending upon the number of data points, and familiarity with the procedures involved.

SECTION V. SPECIFYING PASSBAND CHARACTERISTICS

5. INTRODUCTION

This section introduces ideas for alternative ways to specify allowable passband delay distortion. The prospective user should select the method most suitable for his application. Probably the best is given in Section 5.5.

5.1 THE STEPPED-PASSBAND APPROACH

Figure 5-1 shows two stepped outlines whose corners correspond roughly to a parabolic shape about both the X axis and the Y axis. The shaded area above the upper and below the lower outlines represents areas of specification non-compliance, in the sense that phase distortion departure functions must lie between the shaded areas, and not in them. Departure functions meeting that requirement could take various forms from simple parabolas to complex higher-order functions. Distortion loss computed at the geometric limits defined in Fig. 5-1 is greater than the loss computed from any physically realizable monotonic function which could be made to lie within those limits. It may be intuitively obvious that high-order phase-distortion terms of high magnitude will seldom exist in most realizable designs. As shown in Appendix A, high-order ripple of arbitrary amplitude contributes less to loss than ripple distortion of lower order, however distributed.

The limits outlined in the example of Fig. 5-1 correspond to a digital PN $(\sin x/x)^2$ spectral distribution with the first nulls ± 30 MHz from the carrier. Passband phase is controlled within but not outside those limits. Evaluation of the loss produced by the passband distortion characterized in Fig. 5-1 proceeds from application of Eq. (4.8) as summarized in Table 5-1. Due to perfect passband symmetry, application of Eq. (4.8) to the right half of the passband is simplified by dividing it into six equal parts. Values of the $(\sin x/x)^2$ integral evaluated over six equal intervals are found in Table F-8. The integral Tables F-4 through F-13 may be used to accomodate other passband sub-partitioning up to and including twelve equal sections on each

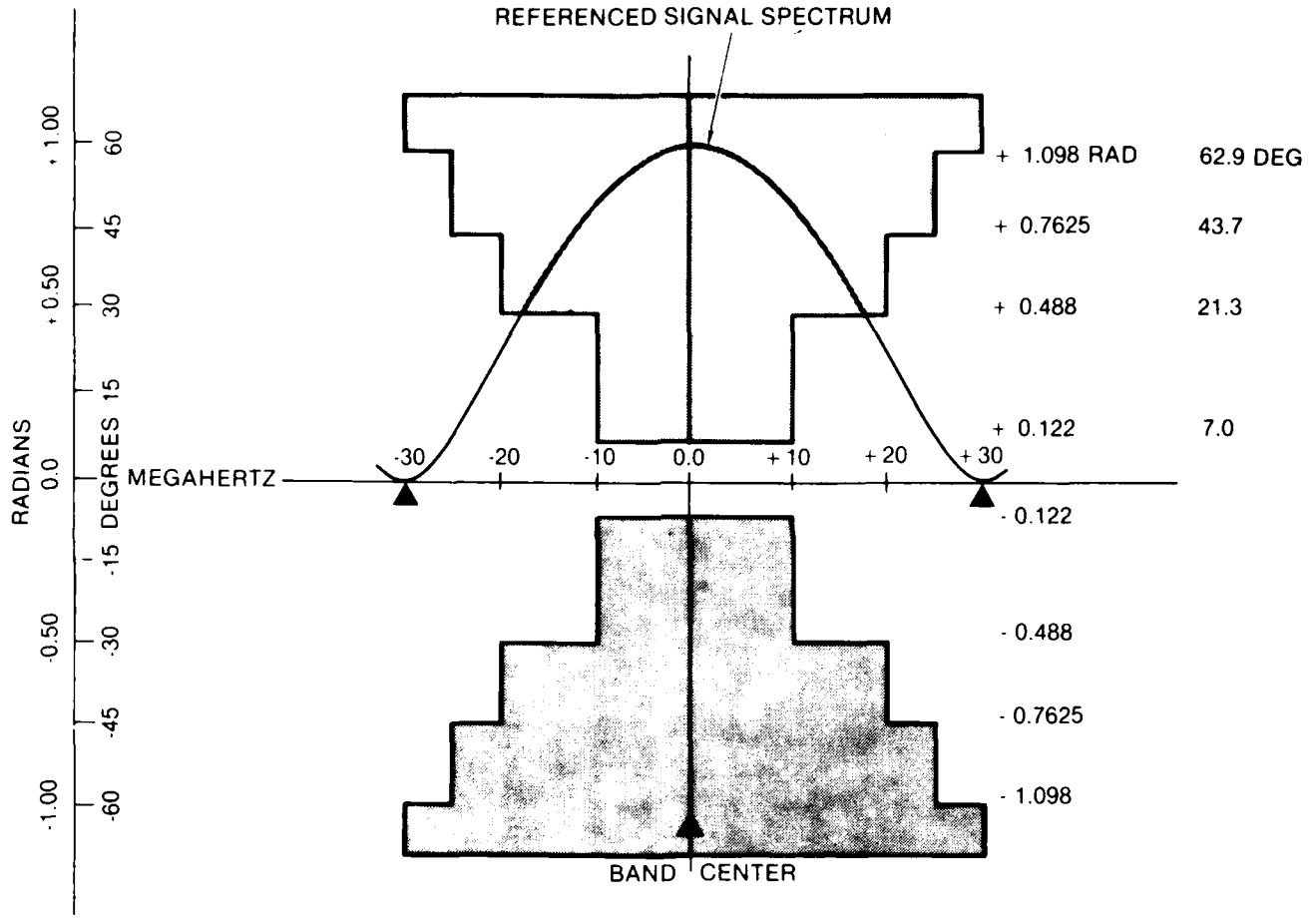

Fig. 5-1. A Typical Allocated Envelope of a Phase Distortion Departure Function

Table 5-1. Calculating Spectral Energy Loss in Step-Limited Departure Function Phase Envelope Having Perfect Passband Symmetry

$$\text{Loss} = 20 \log_{10} \sum_{n\Delta\theta=0}^{\pi} 0.7051 \cos \Delta\theta \int_a^b \left(\frac{\sin x}{x}\right)^2 dx \quad \text{dB} \qquad (5.1)$$

Evaluating the above produces the following table of values:

Step in MHz a – b	Step $\Delta\theta$ rad	Integral a to b	Cosine $\Delta\theta$ × Integral
0 – 5	0.122	0.5079930	0.5042172
5 – 10	0.122	0.4221966	0.4190585
10 – 15	0.488	0.2851267	0.2518445
15 – 20	0.488	0.1472746	0.1446795
20 – 25	0.7625	0.0495524	0.0358319
25 – 30	1.098	0.0060023	0.0027356
	Σ	1.4181506	1.3583673

$$\text{Loss} = 20 \log_{10} \left[\frac{1.3583673}{1.4181506}\right]$$

$$= -0.374 \text{ dB}$$

$$\text{Equivalent Average Phase Angle} = \cos^{-1} \left[\frac{1.3583673}{1.4181506}\right]$$

$$= 0.2914 \text{ rad} = 16.7 \text{ deg}$$

side of band center. Analysis demonstrates that the loss so obtained is indeed greater than the loss that would be experienced by any parabola or other smooth function laid within the stepped envelope. Reference to the Loss Tables of Appendix A may reduce time otherwise spent in analysis.

5.2 A TYPICAL PHASE LINEARITY ALLOCATION

Table 5-2 allocates phase distortion among several elements of a communications link terminal in a rather practical manner, and Fig. 5-2 summarizes the information in stepped quadrants. The loss calculation is accomplished in Table 5-3.

Careful study of the subsystem TOTAL lines of Table 5-2 will reveal that the phase allocations of the preselection filter, the parametric amplifier, and the line-driver are root-sum-squared (RSS'd) and then added arithmetically to the waveguide-run distortion, the RF-Distortion characteristic, and the down-converter phase allocations. This is an effective method for direct combination of bounds on existing equipment having known characteristics (items D, E, and F) with allocations for the new items A, B, and C. If the transmit chain and the receive chain phase characteristics for all items were to be RSS'd, the overall specification sums would be nearly halved, from 97.09 and 91.58 milliradians to 59.73 and 49.31 milliradians respectively. To meet such tight requirements probably would require equalization at several points. Perhaps the most cost-effective point at which to apply equalization, if required, may well be in a low level intermediate frequency amplifier, using strip-line or lumped-constant methods as appropriate to the wavelengths involved (see Refs. 21 through 24).

It is appropriate that transmitter and receiver phase distortion characteristics are specified independently, because hardware items will usually not be co-located nor supplied by the same vendor.

Reference to Table 5-3 will show how the delay-distortion loss through the relay terminal represented by Table 5-2 and Figure 5-2 was calculated, based upon use of Eq. 4.8. Values of the $(\sin x/x)^2$ integral over four equal intervals of frequency were obtained directly from Table F-6.

Table 5.2. A Phase Linearity Allocation for a Typical Communication Link Terminal

PHASE LINEARITY ALLOCATION			
Receive Chain	Linearity (mrad)		
	40 MHz	60 MHz	80 MHz
A. Preselect filter	± 35	±100	±200
B. Paramp	± 26.2	± 61.1	± 87
C. Line driver	± 17.5	± 26.2	± 35
D. W. G. run	± 5	± 10	± 15
E. RF distribution	± 10	± 15	± 20
F. Down converter	± 35	± 80	±120
Subsystem total = $D+E+F+\sqrt{A^2 + B^2 + C^2}$	± 97.09	±225.08	±375.89
Spec	±100	±250	±400

Transmit Chain	Linearity (mrad)		
	20 MHz	60 MHz	80 MHz
A. Up converter	± 35	±100	±120
B. IPA	± 17.5	± 35	± 44
C. Klystron	± 20	± 50	±100
D. Output Assembly	± 20	± 50	±100
E. W. G. run	± 10	± 35	± 60
Subsystem total = $A+D+E+\sqrt{B^2 + C^2}$	± 91.58	±246.03	±389.25
Spec	±100	±250	±400
Grand Total	±200	±500	±863

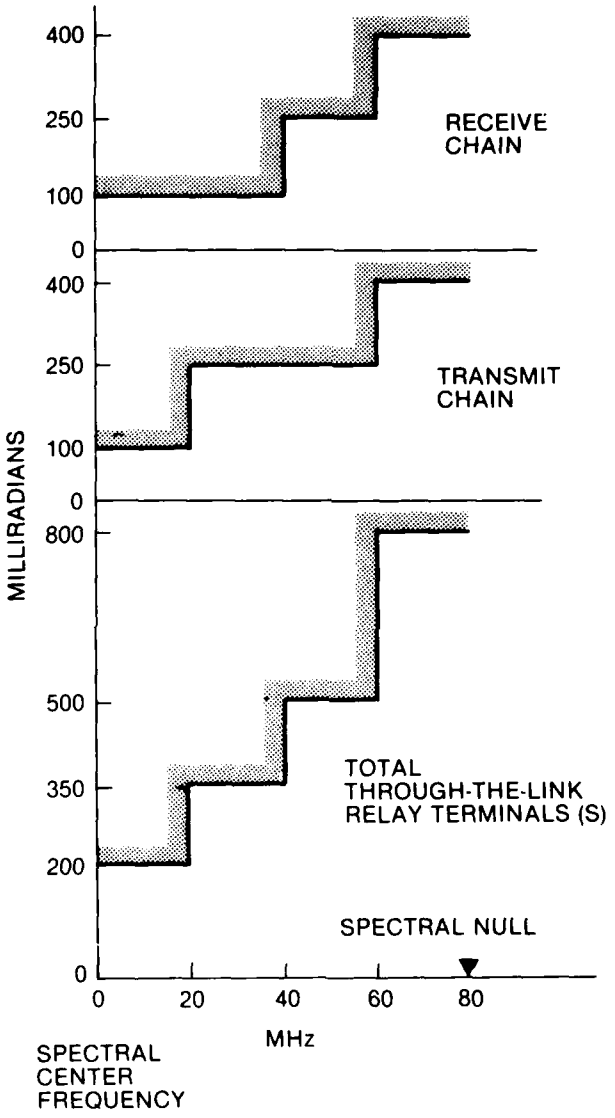

Fig. 5-2. System Specification Quadrant for Loss Analysis of Table 5-2

Table 5-3. Loss Calculation for the Link Specification Model Given in Table 5-2

Step in MHz a	b	Step Δθ rad	Integral a to b	Cosine Δθ × Integral
0	20	0.200	0.7341414	0.7195074
20	40	0.350	0.4811748	0.4520025
40	60	0.500	0.1808489	0.1587098
60	80	0.800	0.0219854	0.0153174
			$\sum$ 1.4181505	1.3455371

$$\text{Loss} = 20 \log_{10} \left[\frac{1.3455371}{1.4181505} \right]$$

$$= -0.456 \text{ dB}$$

Equivalent average phase angle = $\cos^{-1}$ [ ] = 0.3214 rad = 18.414 deg

5.3 DIRECT SPECIFICATION OF ALLOWABLE LOSS

From a specification-writing point of view, a convenient method for specifying allowable in-band phase distortion is to list the technical parameters involved and to identify their bounds. This must include at least the following points:

- Allowable differential group delay loss between upper and lower frequency limits is specified in dB. Amplitude distortion loss should be specified separately, if it will be a factor.
- The passband frequency limits between the 1-dB points shall be _____MHz centered about _____MHz. Options include specification of other points in the passband response, such as 3 dB, 20 dB, etc. However, the 1-dB points should always be specified. (See Fig. 1-3). Passband ripple limits should also be specified.
- Measurement techniques should be specified, but if left to the contractor's choice, sufficient test detail must be provided to insure desired compliance with the specifications.

It should be noted that when procuring hardware from several different sources, difficulties may arise from the necessity to allocate phase distortion to the separate assemblies in the attempt to obtain an overall allowable distortion figure. A method limiting distortion losses by equalization may be required, on an individual or distributed basis.

5.4 GROUP DELAY SPECIFICATION BY PHASE SLOPE

An interesting and effective method for controlling the specification of passband phase distortion characteristics is to identify an allowable limit of departure-function slope over a given increment of bandwidth, per Fig. 2-7. Phase slope is a measure of time delay, so this method of determining specification compliance is similar to that which has been reported upon earlier in Section 4.1. As usual, the differential group delay (DGD) characteristic is determined directly from measurements taken in the frequency domain. Moreover the X-Y plot of the DGD characteristic may be utilized directly in the time doman, since Fourier components, each with its direct measurement of time delay, may be read directly from the DGD plot, and

approximate keying waveforms reconstructed. If desired, the method derived in Section 2.2, and summarized by Eqs. (2.10) to (2.13) may be used to construct an exact time waveform.

Typical statements which must appear in the distortion control specification in some form include these:

- Departure function slope must be controlled to $\leq$ _____deg or radians over a frequency increment of _____(M)Hz at every point in the central (80%) of the passband, or, between the 1-dB points.
- The passband frequency limits between the 1-dB points shall be _____MHz centered about _____MHz. Options include specifying other points in the passband, such as the 3-dB or 20-dB points, etc. However, the 1-dB points should always be specified (see Fig. 1-3).
- Measurement techniques should be specified, or, if left to the contractor's choice, must provide sufficient detail to insure demonstration compliance with the desired specifications.

If it is not important to know the signal energy distortion loss, Eqs. (2.15) and (4.8) may be ignored. After the phase departure function has been plotted, it is necessary only to construct a reference slope, incorporating the specification values. The reference device may be a simple triangular transparency whose vertical dimension is scaled in the allowed radian or degree departures, and whose horizontal dimension is the stated frequency increment. The device is then slid over the departure.

It is also feasible to approach the evaluation processes in terms of time delay per unit frequency interval, by applying the scale directly to a suitably scaled DGD plot. Either of these methods will usually be superior to attempting compliance determination directly from DGD plots manually, permitting manual inspection for equivalent Δt wave-form distortion over specified frequency intervals. See Section 4.1 for test-parameter selection criteria.

5.5 DISTORTION ALLOCATION BY EQUIVALENT AVERAGE DEPARTURE FUNCTION ANGLE SPECIFICATION

In Section 2.8 the concept of an equivalent average departure function (ADF) angle was developed. Equation (2.51) is a result of that derivation. Section 4 gave comparisons of equivalent ADF distortion angles,

derived via the arc-cosine of the power-loss ratio L_d [see Eq. (2.15)]. When a calculated loss characteristic was compared to a hardware passband distortion plot in which an average departure function had been obtained, it was found that no significant difference existed. Therefore, this alternative method for apportioning equipment specifications may recommend itself.

Working backward from the allowable DGD distortion loss requirement, an average angle may be calculated. For example: assume an allowable loss of 0.45 dB. Then, working Eq. (2.51) inversely,

$$-0.45 = 20 \log_{10} L_d$$

where L_d is as defined in Eq. (2.15). Then, solving for

$$L_d = 10^{-\frac{0.45}{20}} = 0.9495$$

Solving for the ADF angle:

$$\cos^{-1} L_d = 18.28 \text{ degrees} = 0.319 \text{ radian}$$

This method of distortion allocation should include statements relative to the conditions of measurement, to wit.

- An equivalent departure function distortion angle shall be determined from dividing the passband departure function into _____ subintervals across the passband to provide requisite measurement accuracy.
- The passband frequency limits between the 1-dB points shall be _____MHz. Options include specifying other points in the passband, such as at 3 dB, 20 dB etc. However, the 1-dB response should always be specified (see Fig. 1-3).
- The average departure function angle shall not exceed _____deg (radians) referred to the carrier-frequency (passband center frequency) as the zero-phase reference point, over any _____MHz portion within specified 1-dB points.

SECTION VI. CONCLUSIONS AND RECOMMENDATIONS

6.1 CONCLUSIONS

Analytical consideration of phase and amplitude non-linearity losses in digital phase-shift-keyed communication systems typically has been incomplete or ignored, resulting in specifications more stringent than actually required to meet system performance objectives. Use of the departure function allows a rigorous analytical evaluation of system degradation loss with a minimal amount of data manipulation. Even that capability is now and herein reduced to a hand-calculator operation, in this instance tailored for the HP-97, HP-34, or equivalent.

Among the significant points revealed in the course of this study are the following:

1. Phase linearity is most important in the central two-thirds of the signal passband.
2. Amplitude linearity may, in some cases, be of minimal relative importance.
3. Passband amplitude response tuning may be used to compensate for some phase distortion loss.
4. A high passband ripple-rate is to be preferred to a low ripple rate.
5. Sine ripple causes less distortion loss than cosine ripple.
6. Amplitude and phase distortion losses usually can be determined separately and easily by use of departure functions.
7. In cascaded networks of passbands, non-complementary amplitude passband shapes should be considered due to the possibility of noise enhancement effects between receiver and transmitter terminals.

6.2 RECOMMENDATIONS

In the specification and design of communication systems, consideration is usually given to terminal cost versus idealized system performance. One area which historically has increased system cost with only a marginal improvement in system performance has been to over-control phase and amplitude linearity in the attempt to achieve the last few tenths of a dB in system

performance. The use of techniques presented in this study led the author to the conclusions stated in Section 6.1. From these conclusions it is clear that future digital PN-PSK systems designed as recommended below, while not providing the ultimate in possible performance, would provide cost-effective, near-optimum performance.

1. System performance should be considered in terms of an allowable combined end-to-end degradation loss - NOT in terms of independent black-box or subsystem phase and amplitude losses, even though separately determinable.
2. Consideration should be given to use of low-level passband predistortion to negate the need for high-level equalization.
3. Distortion losses should be specified at BOTH system and subsystem levels, rather than distortion alone, unless the transmitted spectral characteristics cannot be divulged until "air time."
4. Specification of passband characteristics by average distortion angle, derived from allowable loss specification, should prove more satisfactory all around than the present method of stepped passband response allocation.

See also pages C-2 and D-4 appended for additional design considerations.

REFERENCES

1. Transmission Systems for Communications, fourth edition; Bell Telephone Laboratories, Western Electric Co., Technical Publications, Winston-Salem, NC (1971).

2. Sunde, E.D., Communication Systems Engineering Theory, Wiley Series on Systems Engineering & Analysis (1969).

3. Graham, J.W., & Ehrman, L. (Signatron, Inc.), Nonlinear System Modeling and Analysis with Applications to Communications Receivers, RADC-TR-73-178, Rome Air Development Center, Air Force Systems Command, Griffiss Air Force Base, NY 13441.

4. Chan, Chan, & Chan, Analysis of Linear Networks and Systems, Addison & Wesley (1972).

5. Temex & Mitra, Modern Filter Theory and Design, Wiley-Interscience (1973).

6. Valkenburg, Van, Introduction to Modern Network Synthesis.

7. Bode, Network Analysis & Feedback Amplifier Design, D. Van Nostrand Co., Inc. (1945).

8. Guillemin, E.A., Communication Networks, Vols. I & II, Wiley & Sons.

9. Kudsia & O'Donovan, Microwave Filters for Communication Systems, Artech House/Horizon House - Microwave, Inc., 610 Washington St., Dedham, MA 02026.

10. Guillemin, E.A., Synthesis of Passive Networks, John Wiley & Sons.

11. Hamming, R.W., Digital Filters, Prentice Hall 1977.

12. "Analysis & Exact Synthesis of Cascaded Commensurate Transmission-Line C-Section All-Pass Networks," IEEE Transactions MTT-14, pp. 285-291 (Jun 1966), and Vol. MTT-14, pp. 498-499 (Oct 1966).

13. LaFara, R.L., Computer Methods for Science and Engineering, Hayden.

14. Sams, H.W., Reference Data for Radio Engineers, ITT (fifth edition).

15. Conte & de Boor, Elementary Numerical Analysis, an Algorithmic Approach, 2d ed., McGraw Hill.

16. Dixon, R.C., Spread Spectrum Communication Systems, Wiley & Sons.

17. Hewlett-Packard Application Note AN-77-4.

18. LeFande, R.A., "Spread Spectrum Communication Systems" - Dixon, IEEE Press, p. 319.

19. Bennett and Davey, Data Transmission, McGraw Hill, Ch 4, 7, 10.

20. Sunde, E.D., "Pulse Transmission in the Presence of Phase Distortion," Bell System Technical Journal Vol. 40, March 1961, pp. 353-422.

21. Rosenfield & Juels, "Group Delay Equalization in Communications Systems," COMSTRON-SEG Applications Bulletin 175, 120-30 Jamaica Avenue, Richmond Hill, N.Y. 11418

22, Hoffman, C. R., "Develop Your Own Effective Delay Distortion Equalizer," Engineering Design News, 5 April 1977.

23. Szentirmai, G., "The Problem of Phase Equalization," IRE Transactions in Circuit Theory, Sys & Ckt Theory 1959, p. 272.

24. Davies, M.W., "Phase - Adjusting All-Pass Networks," Proceedings of the IRE Australia, November 1962, p. 637.

25. Lathi, B.P., Signals, Systems, and Controls, INTEXT Educational Publishers, N. Y. & London.

26. Cristal, E.G., "Theory & Design of Transmission Line All-Pass Equalizers," IEEE Transactions, MTT-17, p. 28 (Jan 1969).

27. Papoulis, A., The Fourier Integral and Its Applications, McGraw-Hill, 1962.

28. Lange, F.H., Correlation Techniques, London Iliffe & Van Nostrand, Princeton.

29. Fano, R.M., Signal to Noise Ratio in Correlation Detectors," MIT Research Laboratory Technical Report 186, February 1951.

30. Hewlett-Packard Vector Volt Meter Manual HP-8405A.

31. Gardner & Barnes, Transients In Linear Systems, John Wiley & Sons, 1942.

32. Bracewell, R., The Fourier Transform and Its Applications, McGraw-Hill 1965.

33. Panter, P.F., Modulation, Noise, and Spectral Analysis, McGraw-Hill.

34. Papoulis, A., Systems and Transformations with Applications in Optics, McGraw-Hill, 1968.

35. "Differential Phase and Gain at Work," Hewlett-Packard Applications Note 175-1.

36. Gold, R., "Optimal Binary Sequences for Spread Spectrum Multiplexing," IEEE Press "Spread Spectrum Techniques" - Dixon, p. 119.

37. Wylie, C.R., Advanced Engineering Mathematics, 4th ed., McGraw-Hill.

38. Golomb, S.W. et al., Digital Communications with Space Applications, Prentice-Hall EE Series, 1964.

39. Spilker, J.J., Digital Communications by Satellite, Prentice-Hall Electrical Engineering Series, 1977.

40. Rabiner, L.R. and Gold, R., Theory and Application of Digital Signal Processing, Prentice-Hall, 1975.

41. Rabiner, L.R. and Rader, C.M., Eds., "Digital Signal Processing,"IEEE Press Reprint Series, 1972.

42. Dixon, R.C., Ed., "Spread Spectrum Techniques," IEEE Press Selected Reprint Series 1976.

43. Guillemin, E.A., The Mathematics of Circuit Analysis," John Wiley & Sons, Technology Press, 1949.

44. Frederick & Carlson, Linear Systems in Communication and Control, John Wiley & Sons, 1971.

45. Guillemin, E.A., Synthesis of Passive Networks, John Wiley & Sons, 1957.

46. Sokolnikoff, I.S. and E.S., Higher Mathematics for Engineers and Physicists, Sections 10, 11, 12, 13, McGraw-Hill.

47. Daniel and Wood, Fitting Equations to Data, Wiley International, 1971.

48. Burrington and May, Handbook of Probability and Statistics with Tables, 2nd Ed., Section 12, McGraw-Hill, 1970.

49. Papoulis, A., Probability, Random Variables, and Stochastic Processes, McGraw-Hill, New York, 1965.

50. Nyquist, H. and Brant, S. Measurement of Phase Distortion, pp. 522 - 549 BSTJ, 1930.

APPENDIX A. PHASE DISTORTION

A.1 REPRESENTATIVE PRE-COMPUTED PHASE DISTORTION LOSS FUNCTIONS

Phase distortion loss curves are presented providing visibility directly for a wide range of departure functions. Figures A-1 to A-3 display energy content versus percentage of bandwidth occupancy where band limits are pre-established as $\pm 1/\tau$. Figures A-4 through A-6 provide similar information but in dB form, permitting more visibility over a wider loss range versus band edge phase shift than is available using linear presentations.

In Fig. A-7, losses for phase distortion departure functions of the form $\theta(\omega) = \theta_n \omega^n$ are presented for values of $1 = n = 5$ vs stated band-edge distortion coefficient values.

Loss curves are presented for ripple functions for various ripple rates, ripple magnitudes, and passband utilization factors from Figs. A-8 through A-15. These have considered sine and cosine ripple independently.

Sine and cosine ripple, in combination with various types of power-series phase-shift terms are presented in Figs. A-16 through A-25. Only the first three powers of n are included, as they represent the majority of cases likely to be encountered. Computer programs are included in Appendix E to facilitate further investigation.

If a designer has the option to specify the type and magnitude of ripple terms (as in Butterworth and Tchebyshev filter design) he should control those which minimize band-center nonlinearity. Sine ripple is therefore preferred to cosine ripple. As may be observed from Fig. A-13, a high ripple rate is better than a low ripple rate, and allows use of higher-magnitude ripple terms in filter design.

Strong interdependence is often observed between the power-series terms and the ripple terms in a departure function, controlling the extent to which processing losses must be considered when operating at or near band edges.

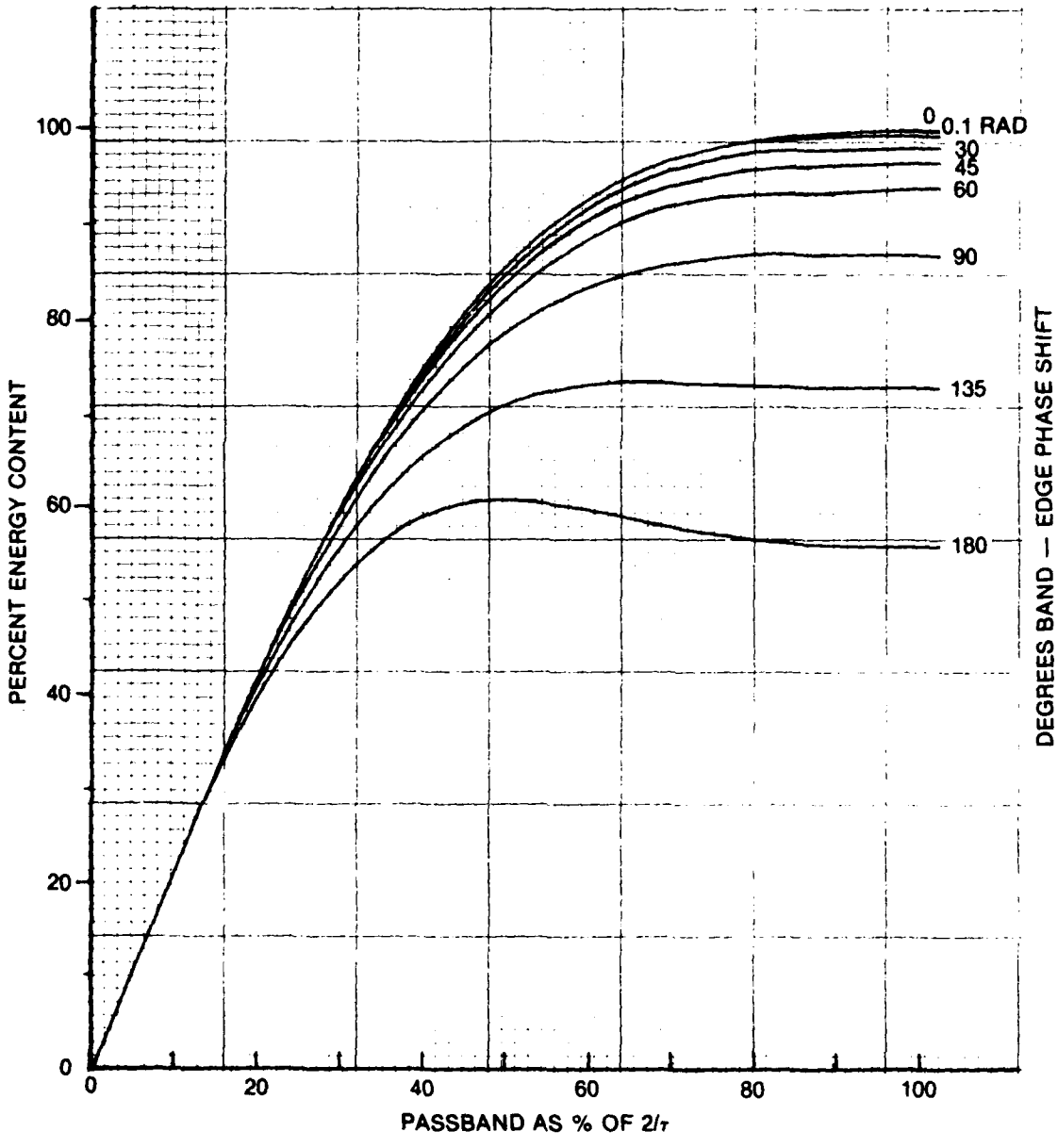

Fig. A-1. Spectral Energy Distribution for First-Order Phase Departure Function

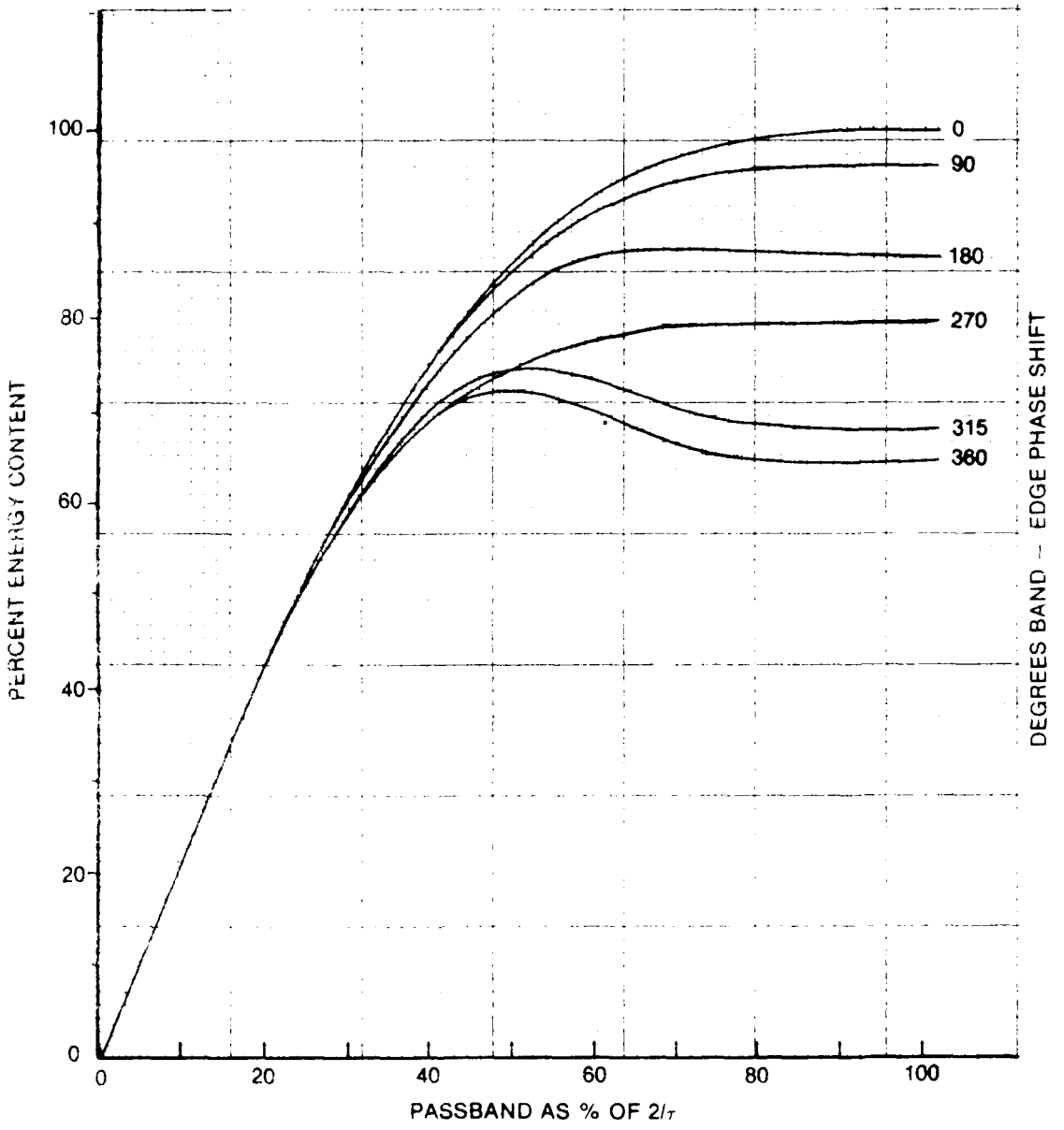

Fig. A-2. Spectral Energy Distribution for Second-Order Phase Departure Function

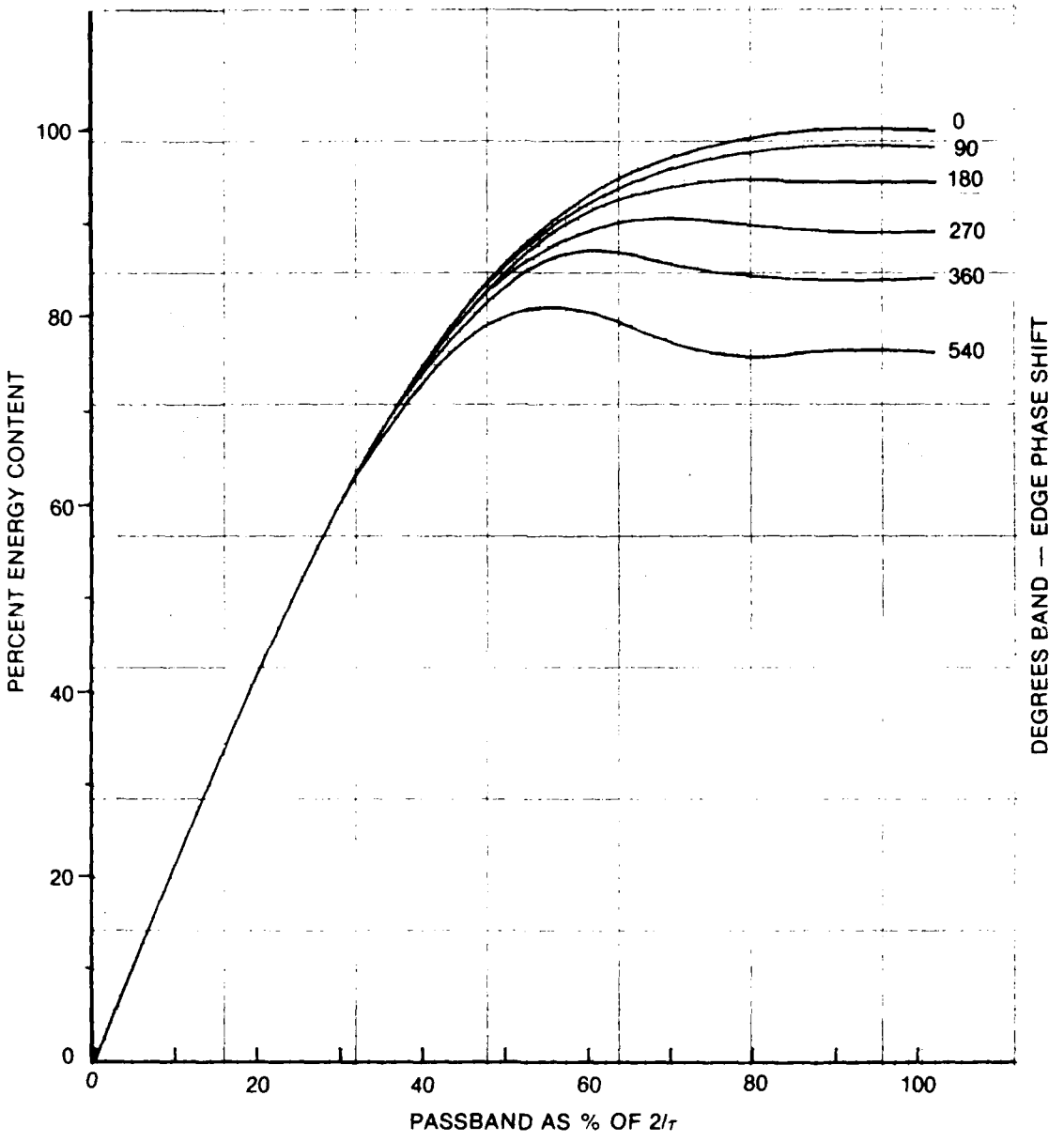

Fig. A-3. Spectral Energy Distribution for Third-Order Phase Departure Function

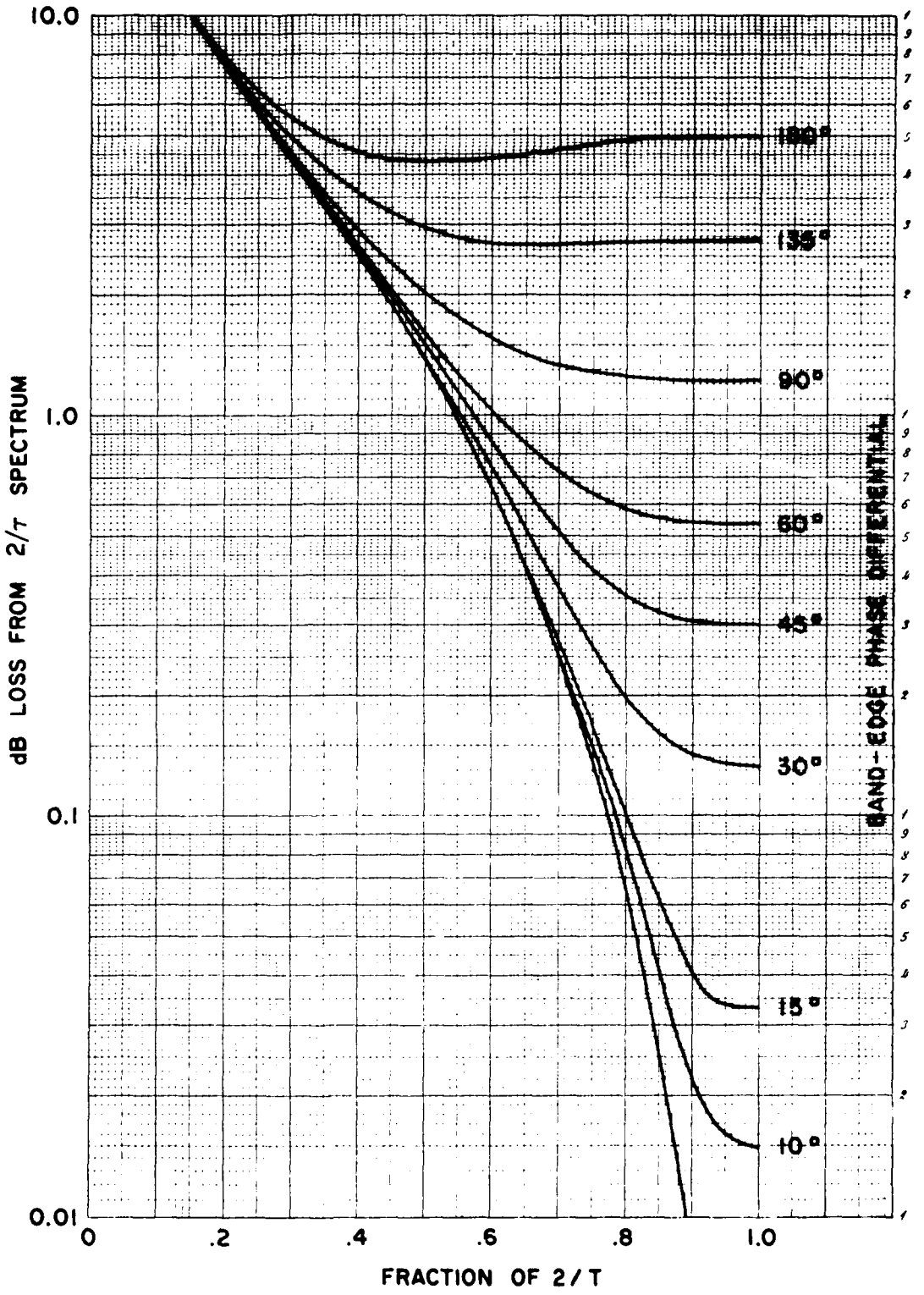

Fig. A-4. Spectral Energy Loss vs Passband Utilization First-Order Phase Departure

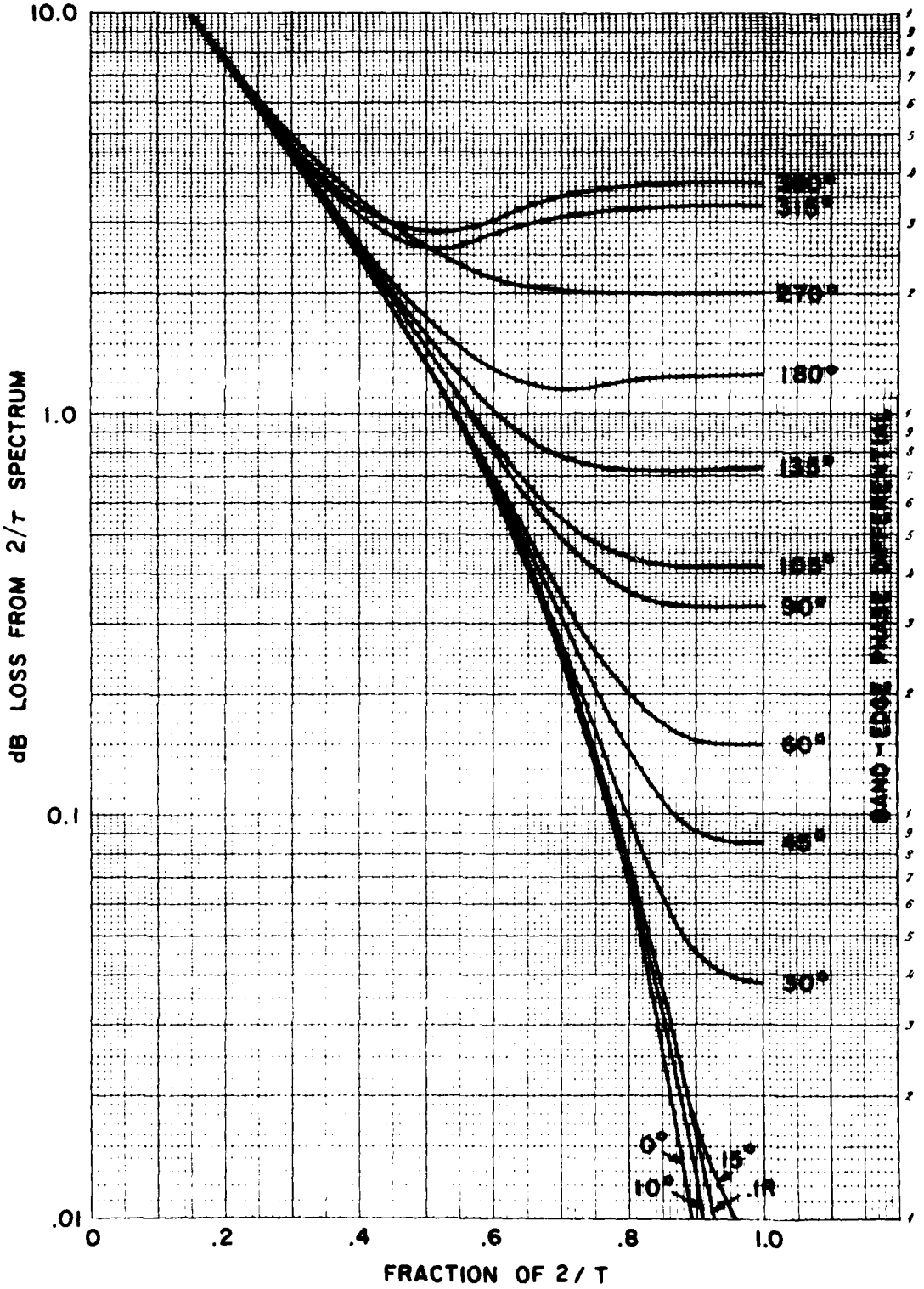

Fig. A-5. Spectral Energy Loss vs Passband Utilization, Parabolic Phase Departure

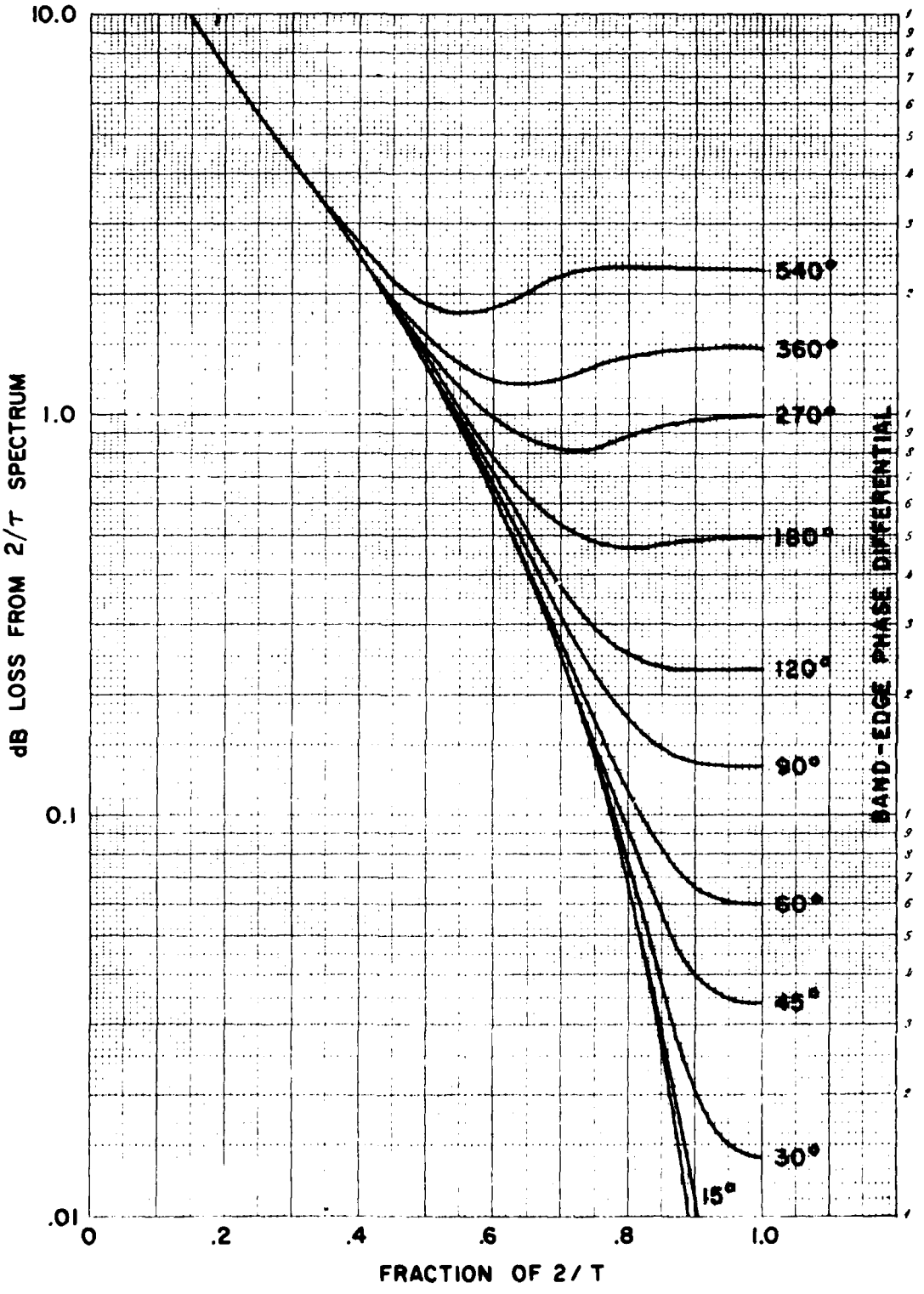

Fig. A-6. Spectral Energy Loss vs Passband Utilization, Cubic Phase Departure

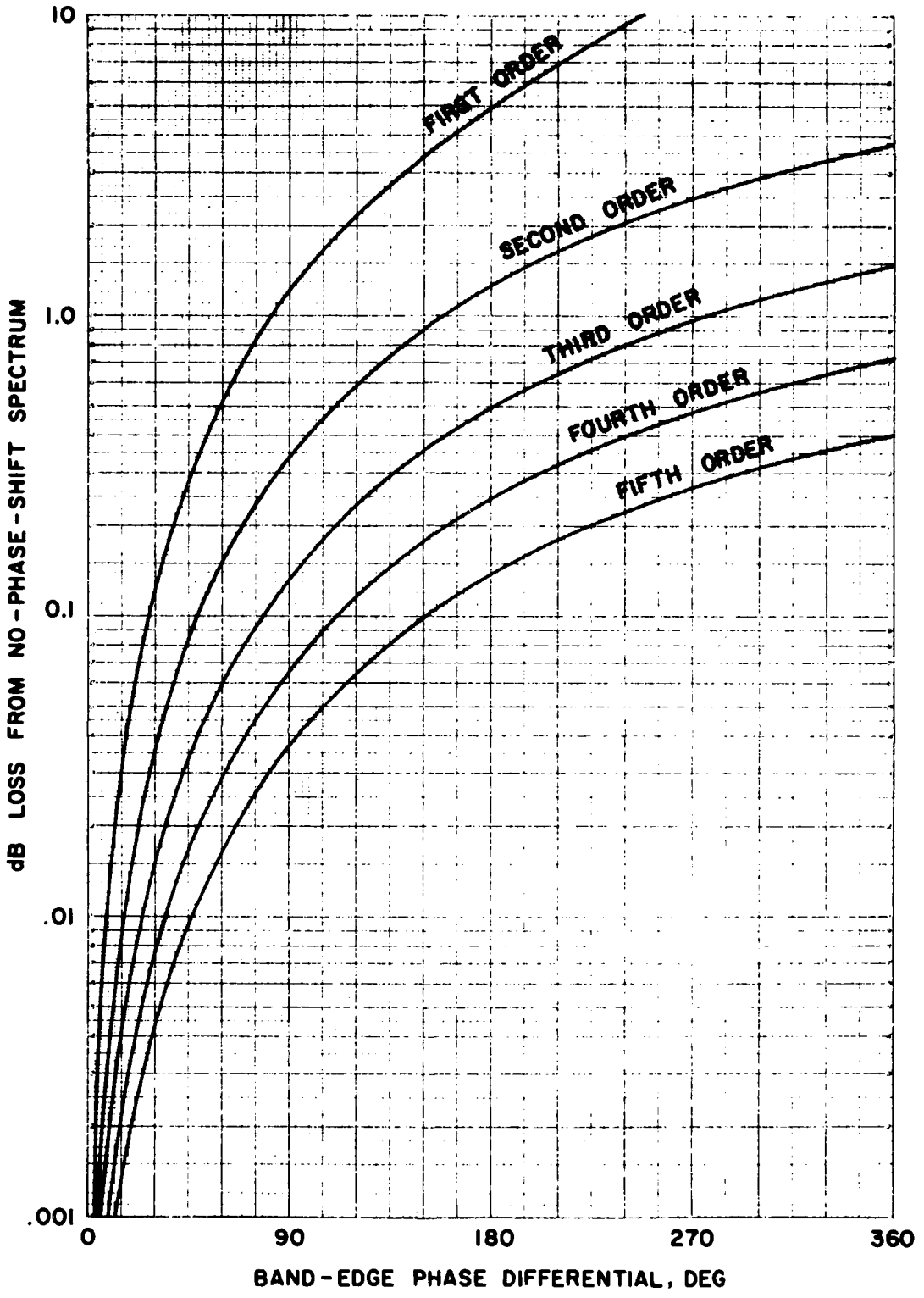

Fig. A-7. Spectral Energy Loss vs Power-Law Phase Departure Functions

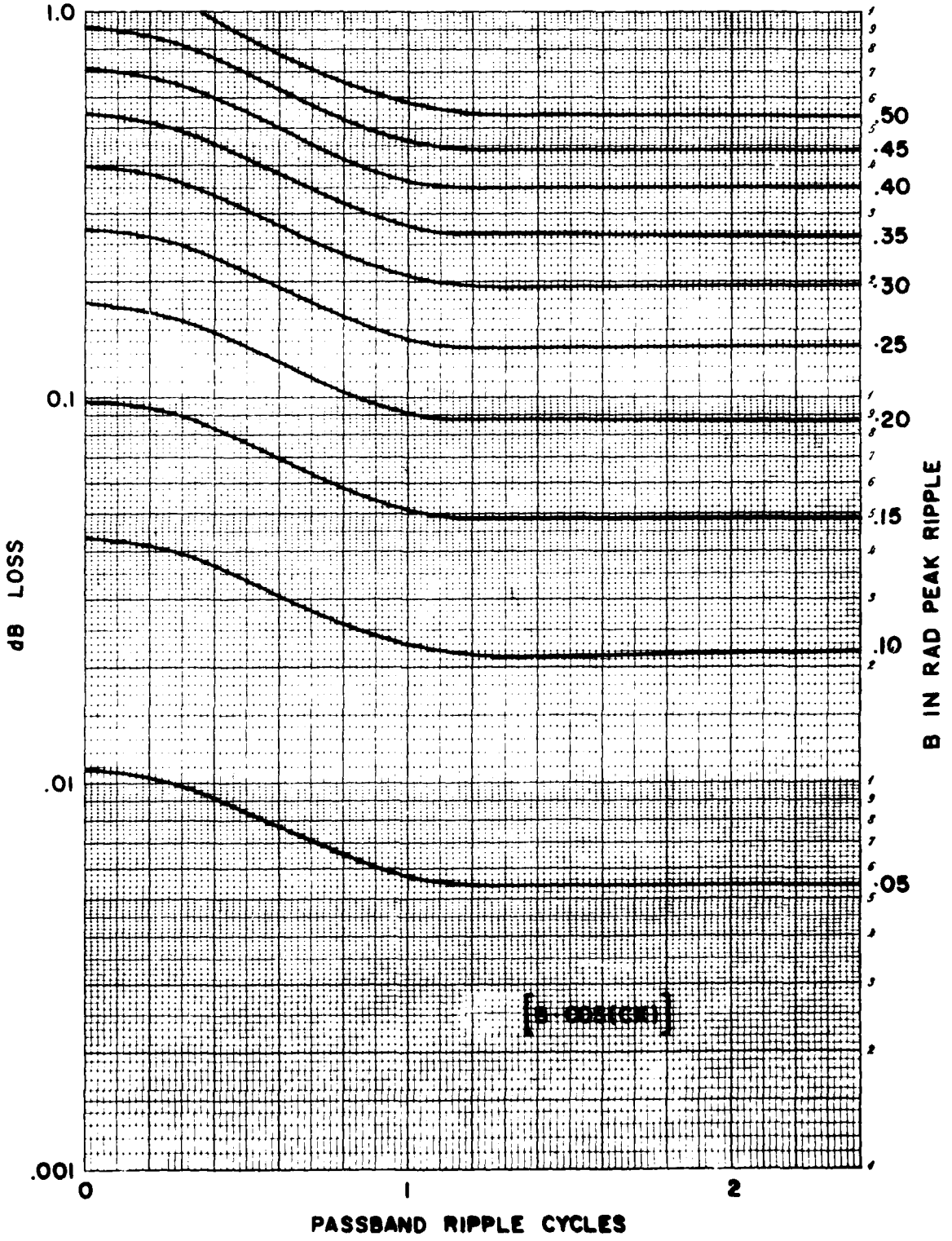

Fig. A-8. Spectral Energy Loss Due to Cosine Phase Ripple (Radian Argument)

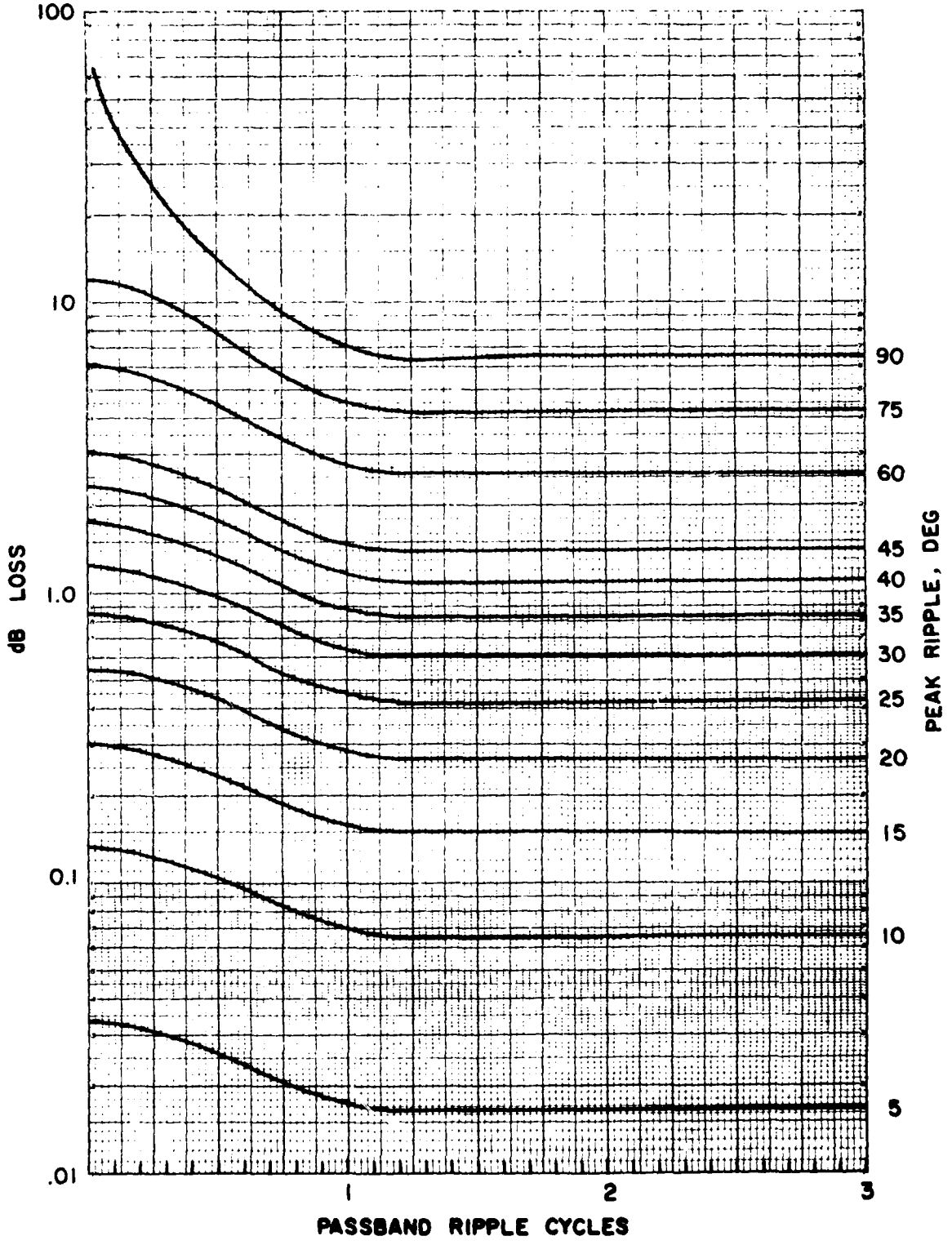

Fig. A-9. Spectral Energy Loss for Cosine Phase Ripple vs Magnitude and Ripple Rate

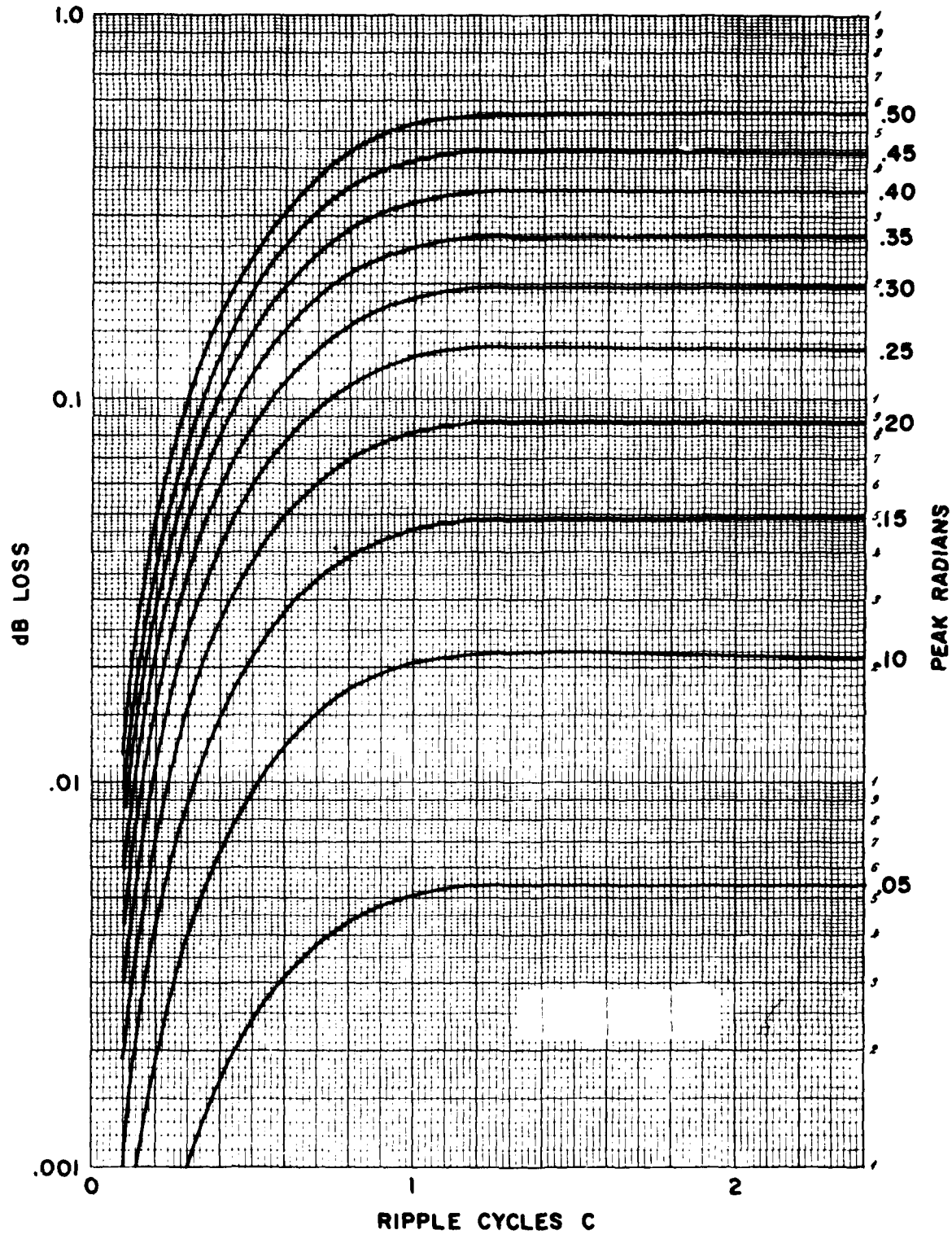

Fig. A-10. Spectral Energy Loss for Sine Phase Ripple vs Magnitude and Ripple Rate (radians)

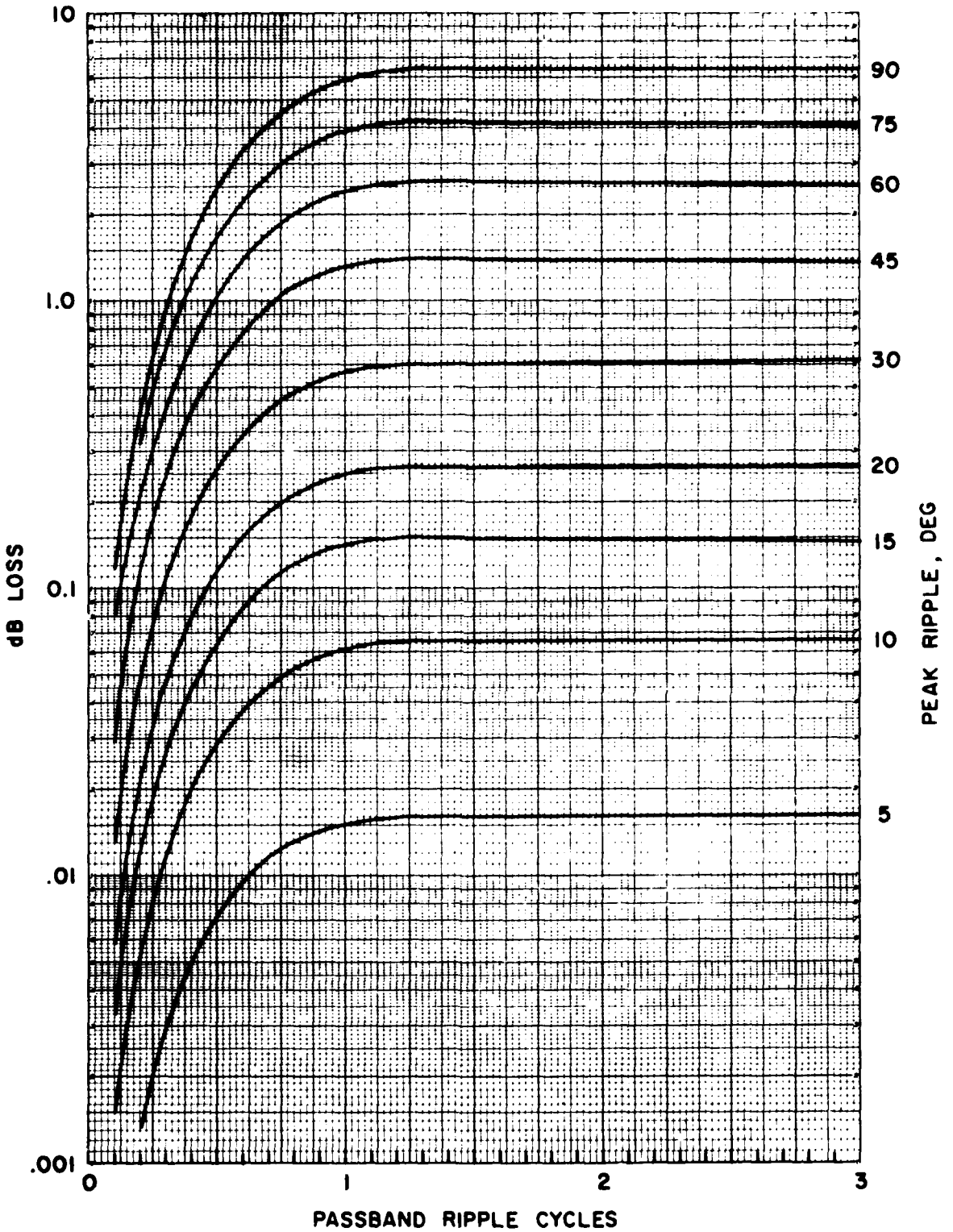

Fig. A-11. Spectral Energy Loss for Sine Phase Ripple vs Rate and Magnitude (degree arg)

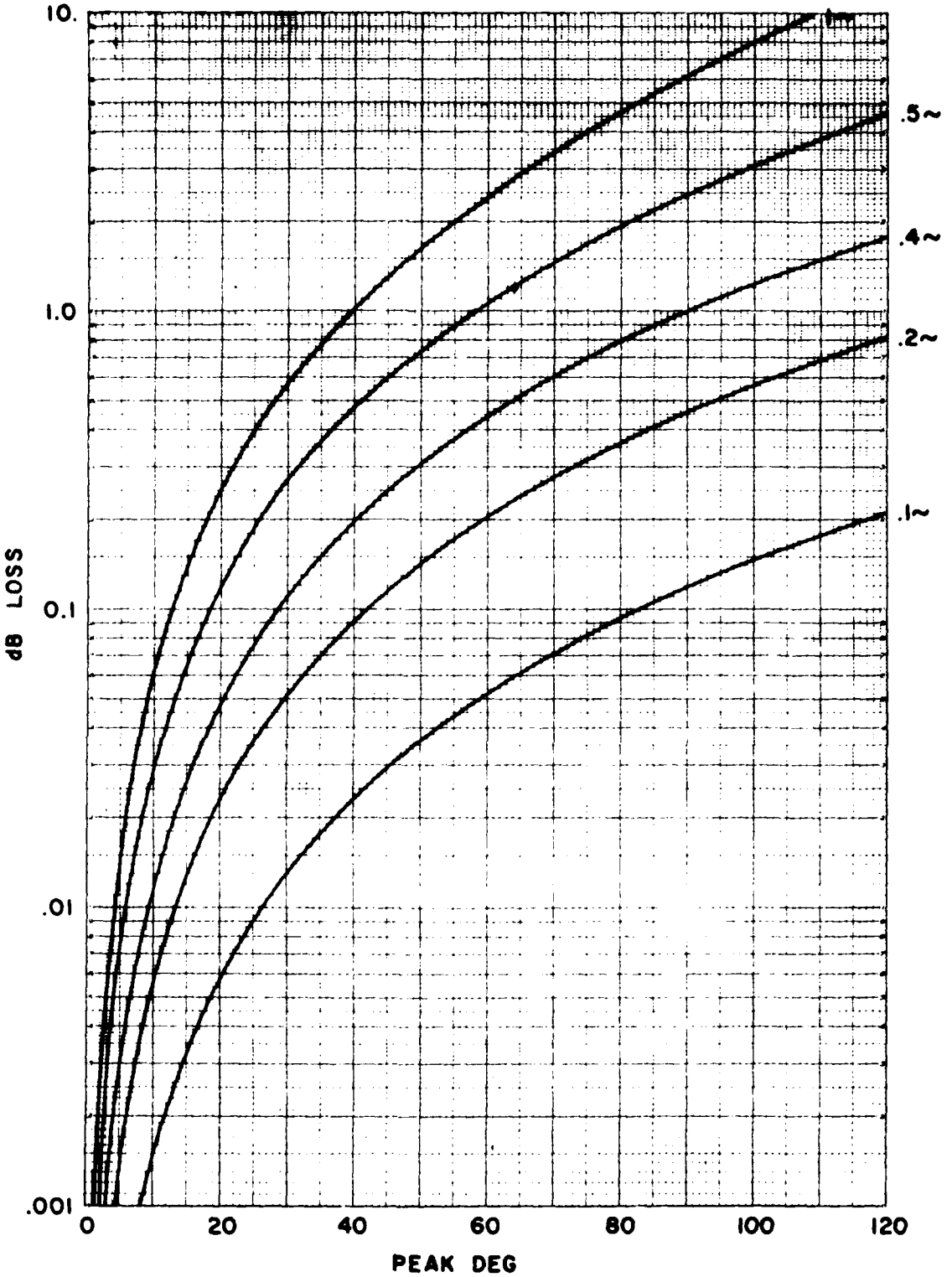

Fig. A-12. Spectral Energy Loss for Sine Phase Ripple for Various Rates and Magnitudes (deg)

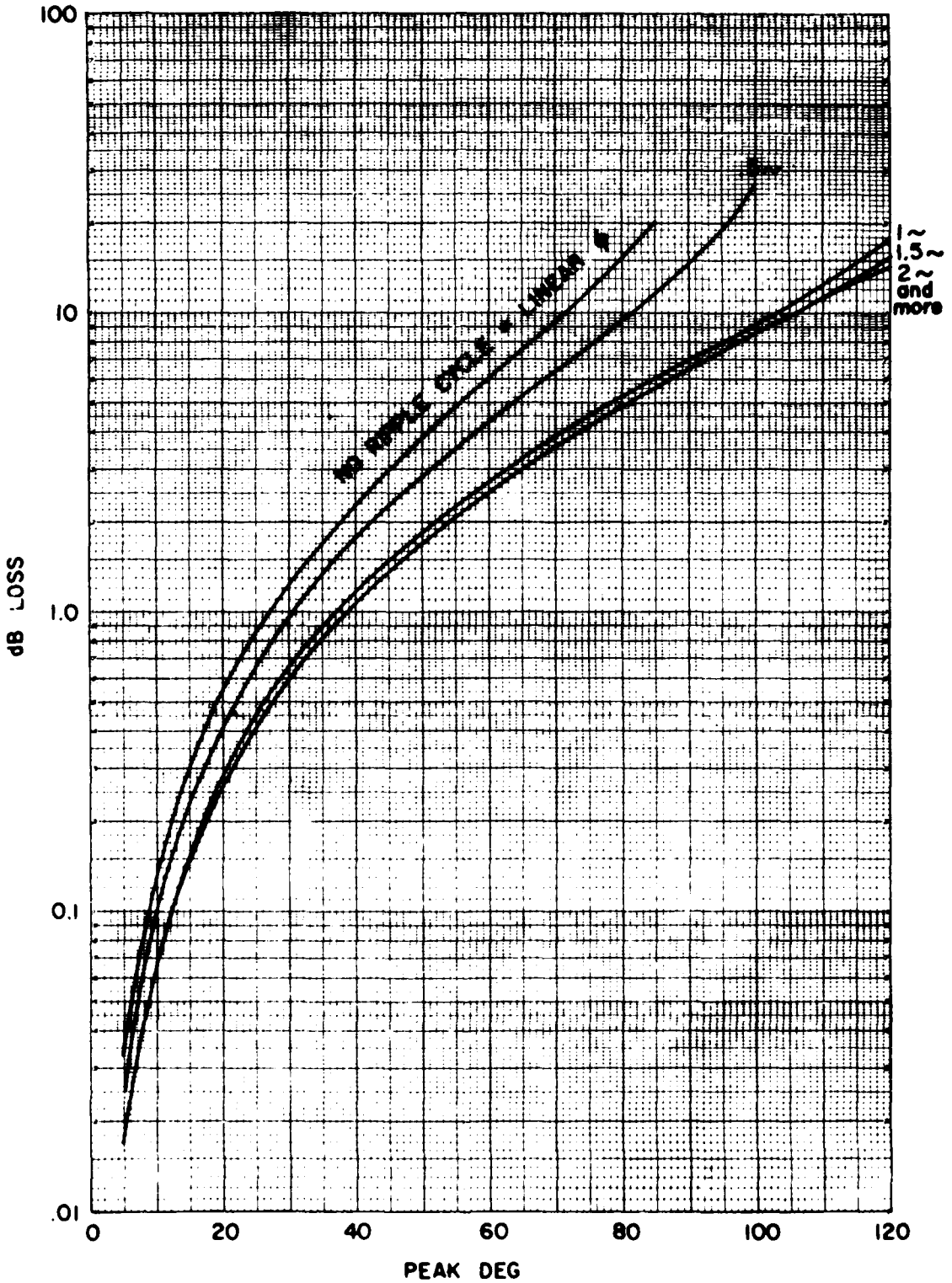

Fig. A-13. Signal Energy Losses as a Function of Ripple Rate vs Peak Ripple Magnitude (deg)

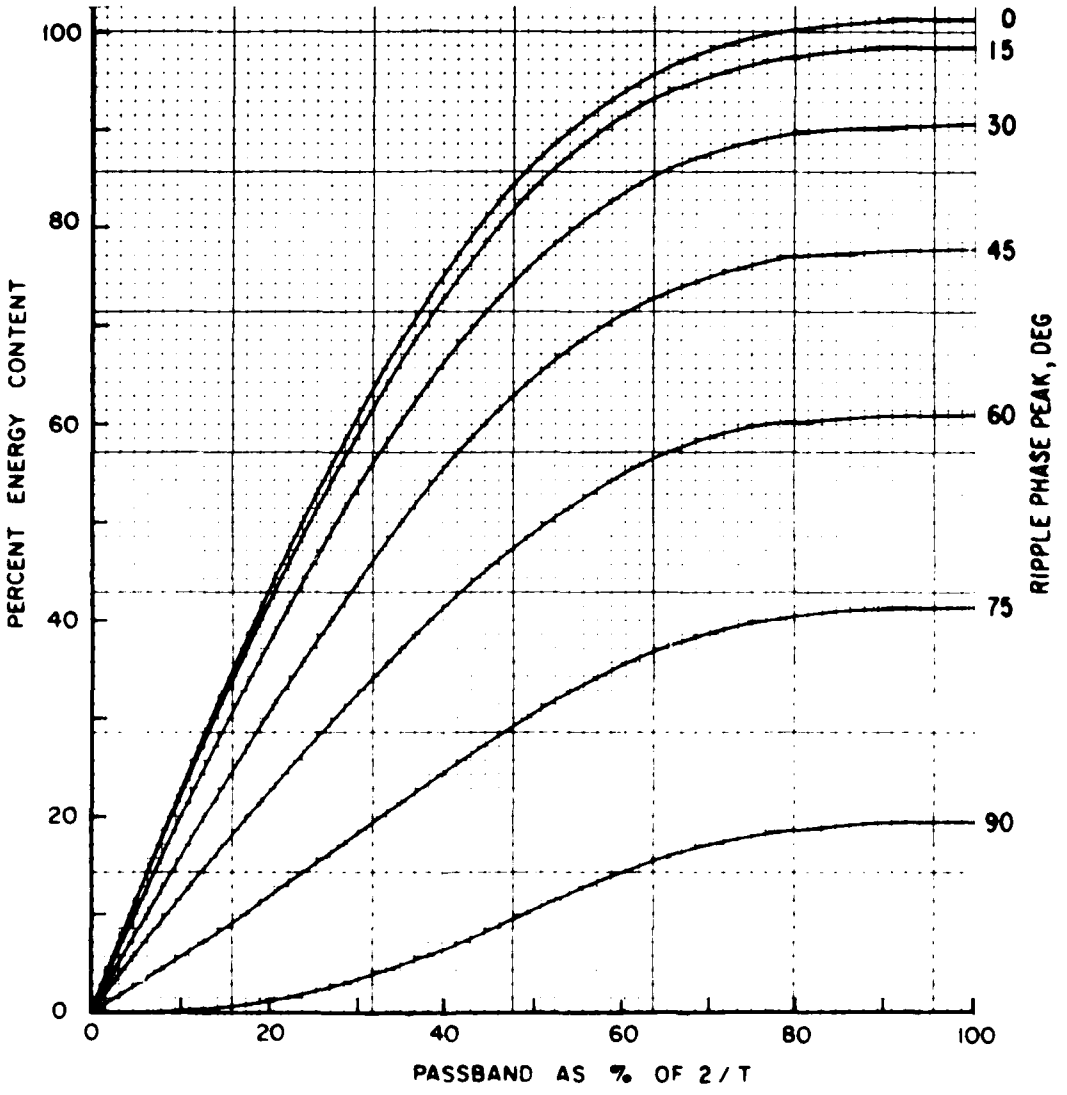

Fig. V 14. Spectral Energy Distribution for Half-Cycle Cosine Ripple in Half-Passband

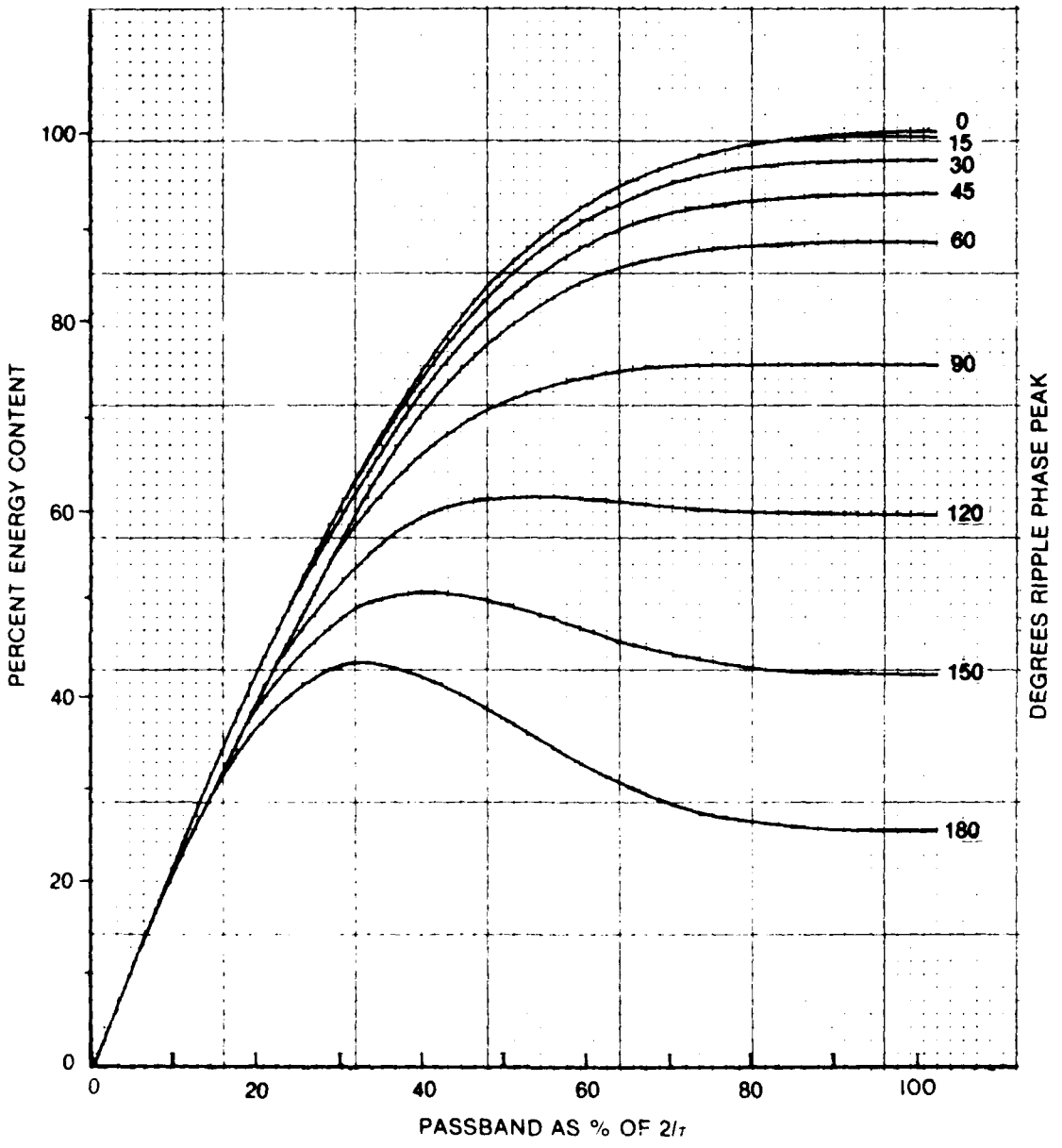

Fig. A-15. Spectral Energy Distribution for Half-Cycle Sine Ripple in Half-Passband

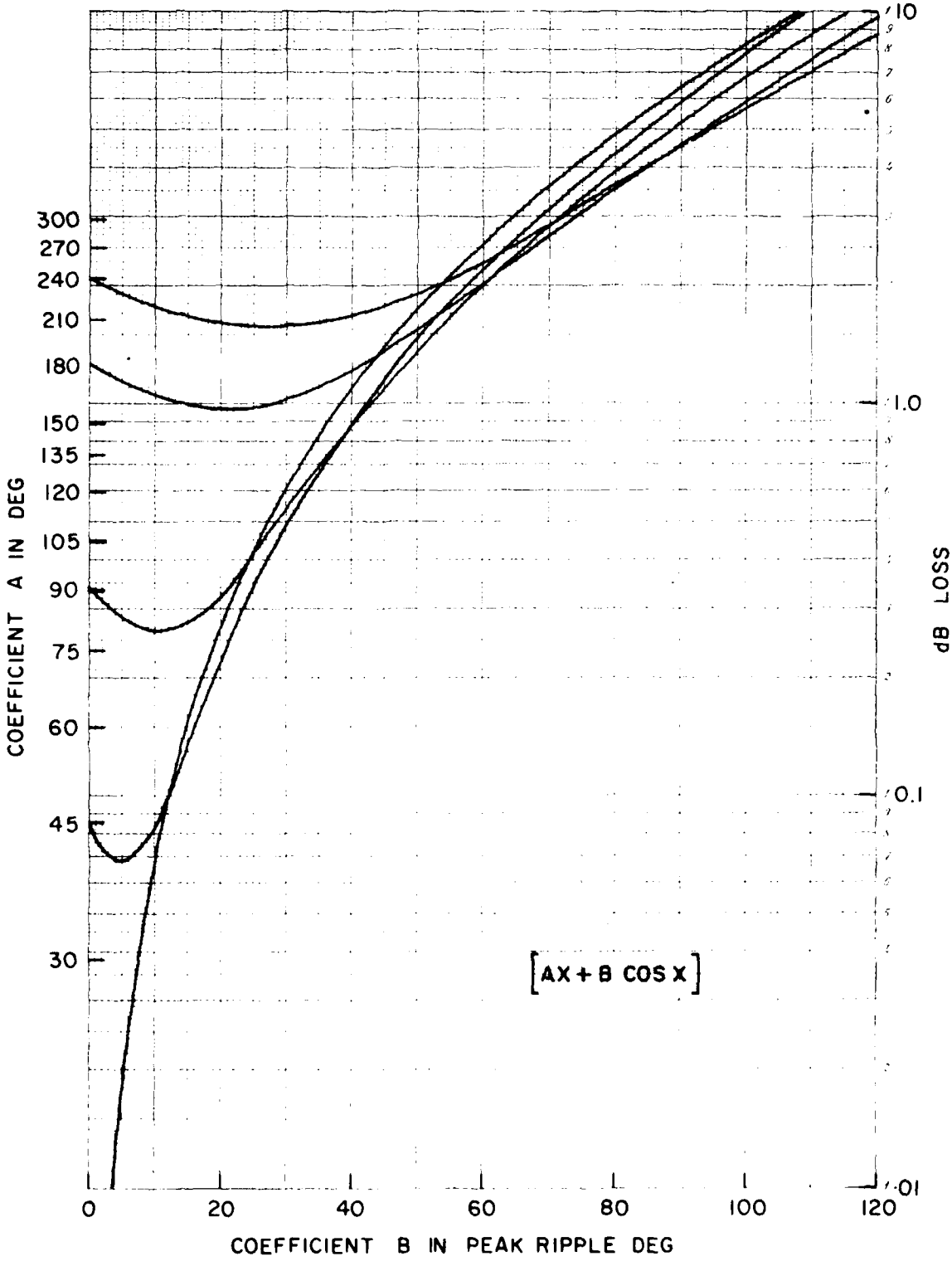

Fig. A-16. Signal Energy Losses Due to Combined Linear and Cosine Phase Ripple

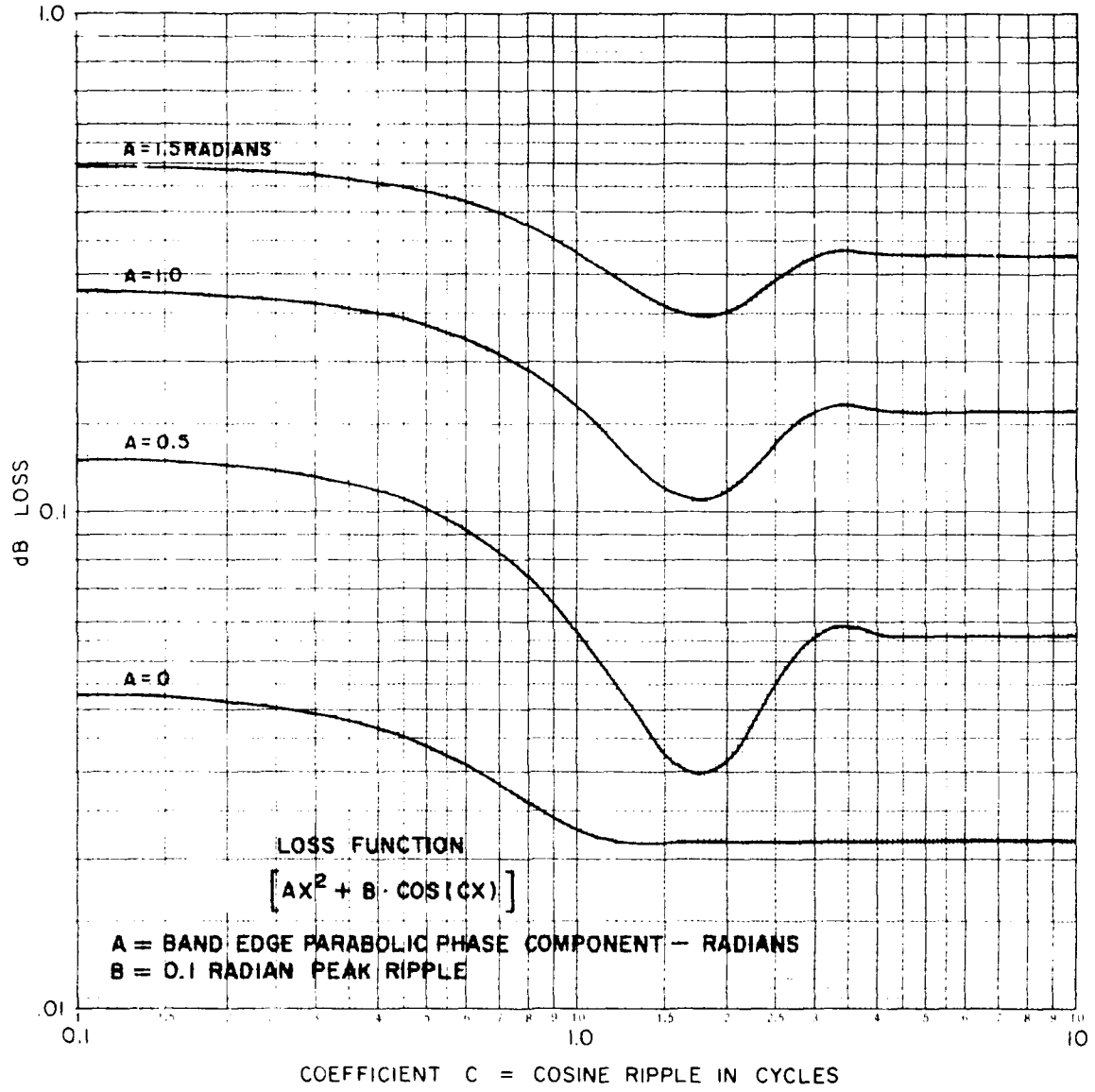

Fig. A-17. Signal Energy Losses Due to Combined Parabolic Term and Cosine Ripple Departure Function (0.1-radian peak)

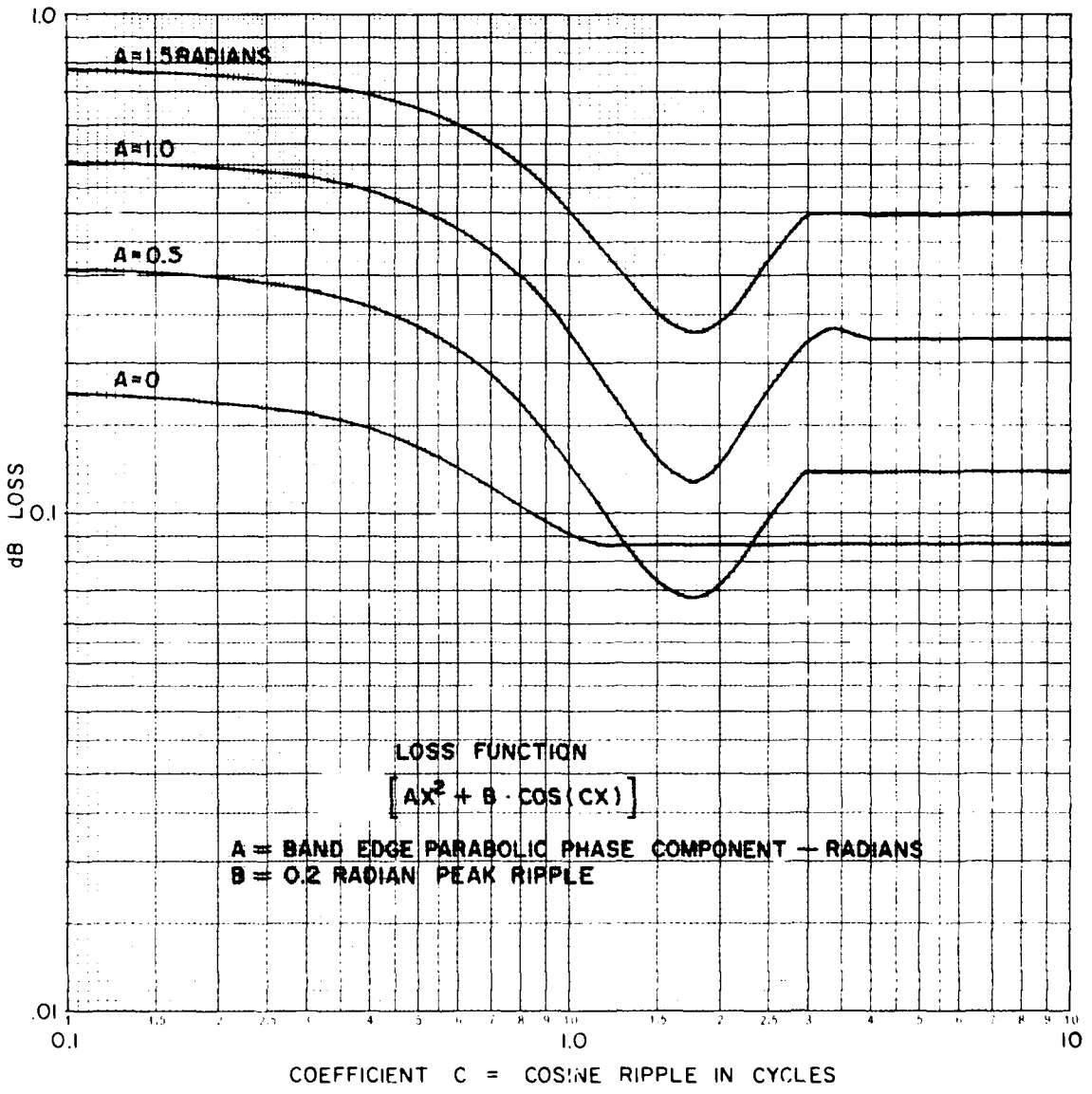

Fig. A-18. Signal Energy Losses Due to Combined Parabolic Term and Cosine Ripple Departure Function (0.2-radian peak)

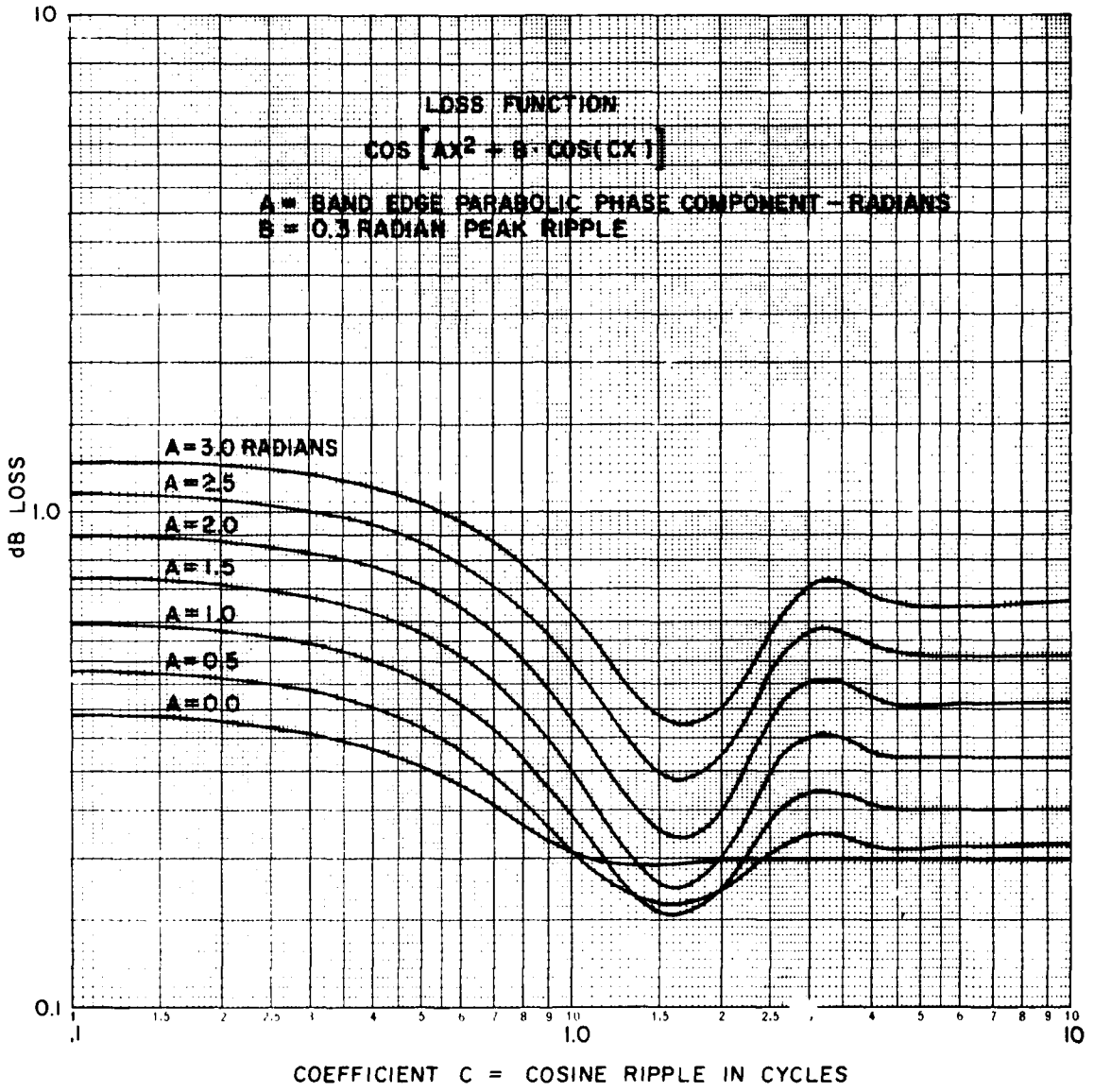

Fig. A-19. Signal Energy Losses Due to Combined Parabolic Term and Cosine Ripple Departure Function (0.3-radian peak)

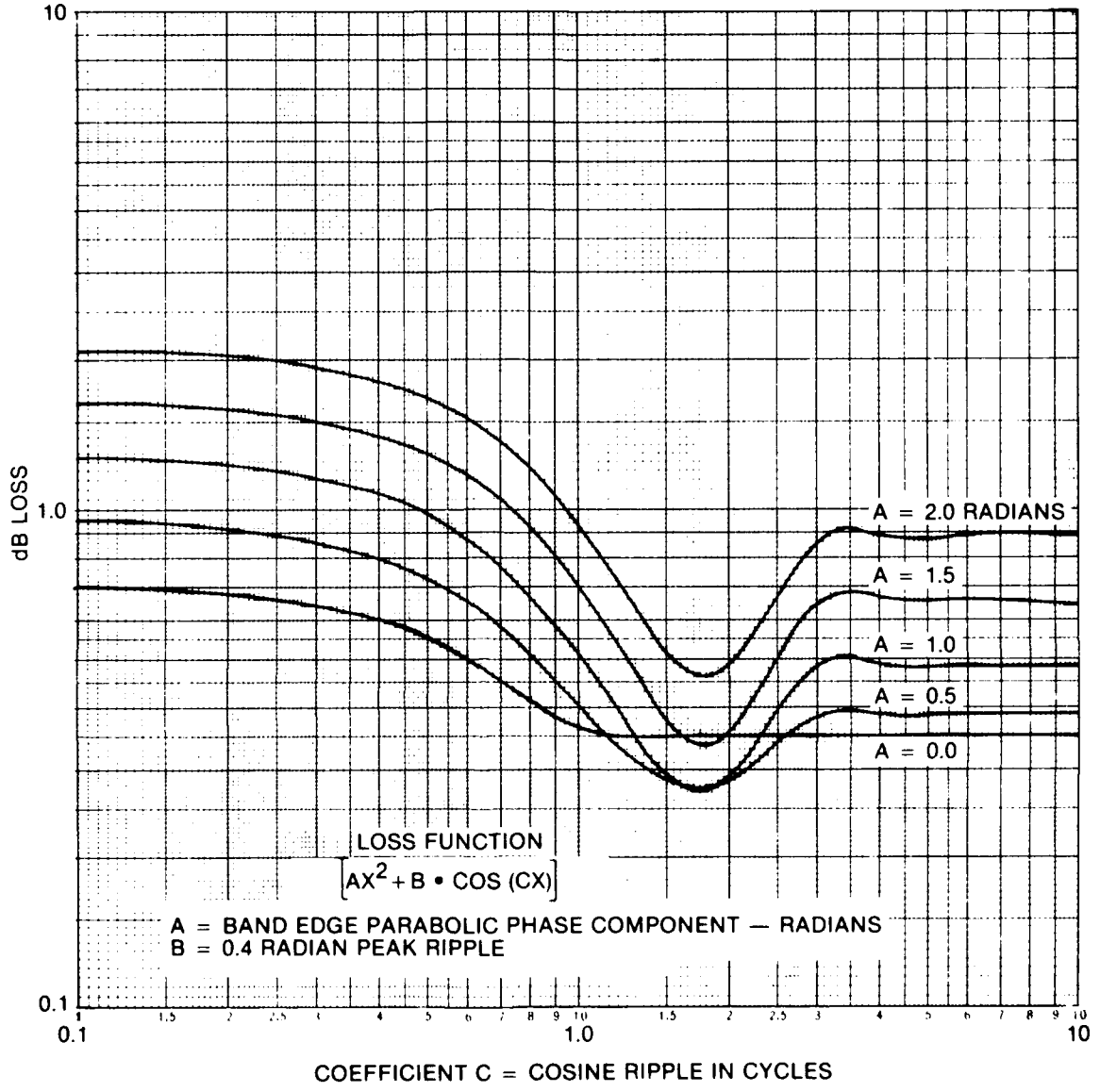

Fig. A-20. Signal Energy Losses Due to Combined Parabolic Term and Cosine Ripple Departure Function (0.4-radian peak)

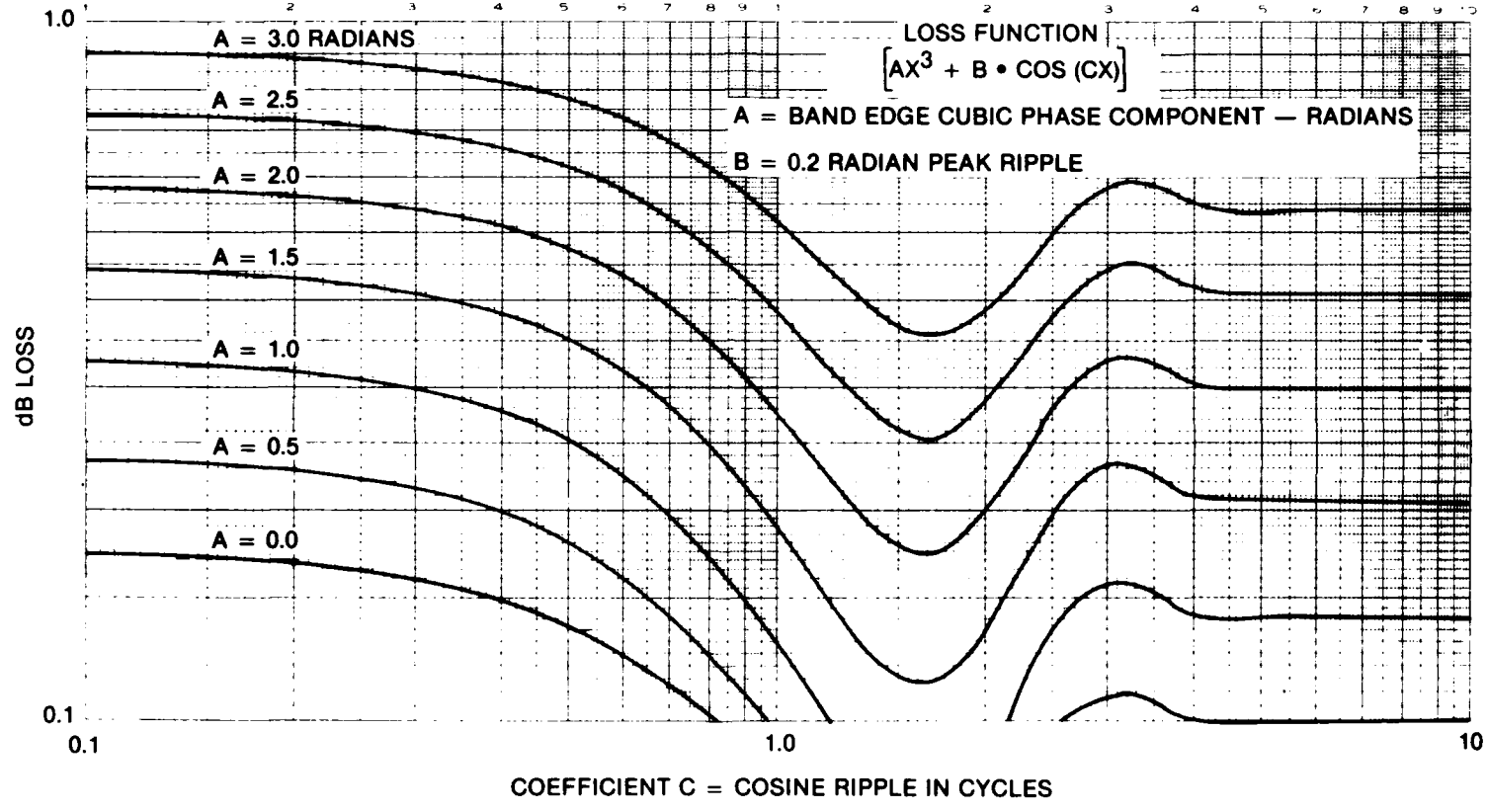

Fig. A-21. Signal Energy Losses Due to Combined Cubic Term with Cosine Ripple Departure Function (0.2-radian peak)

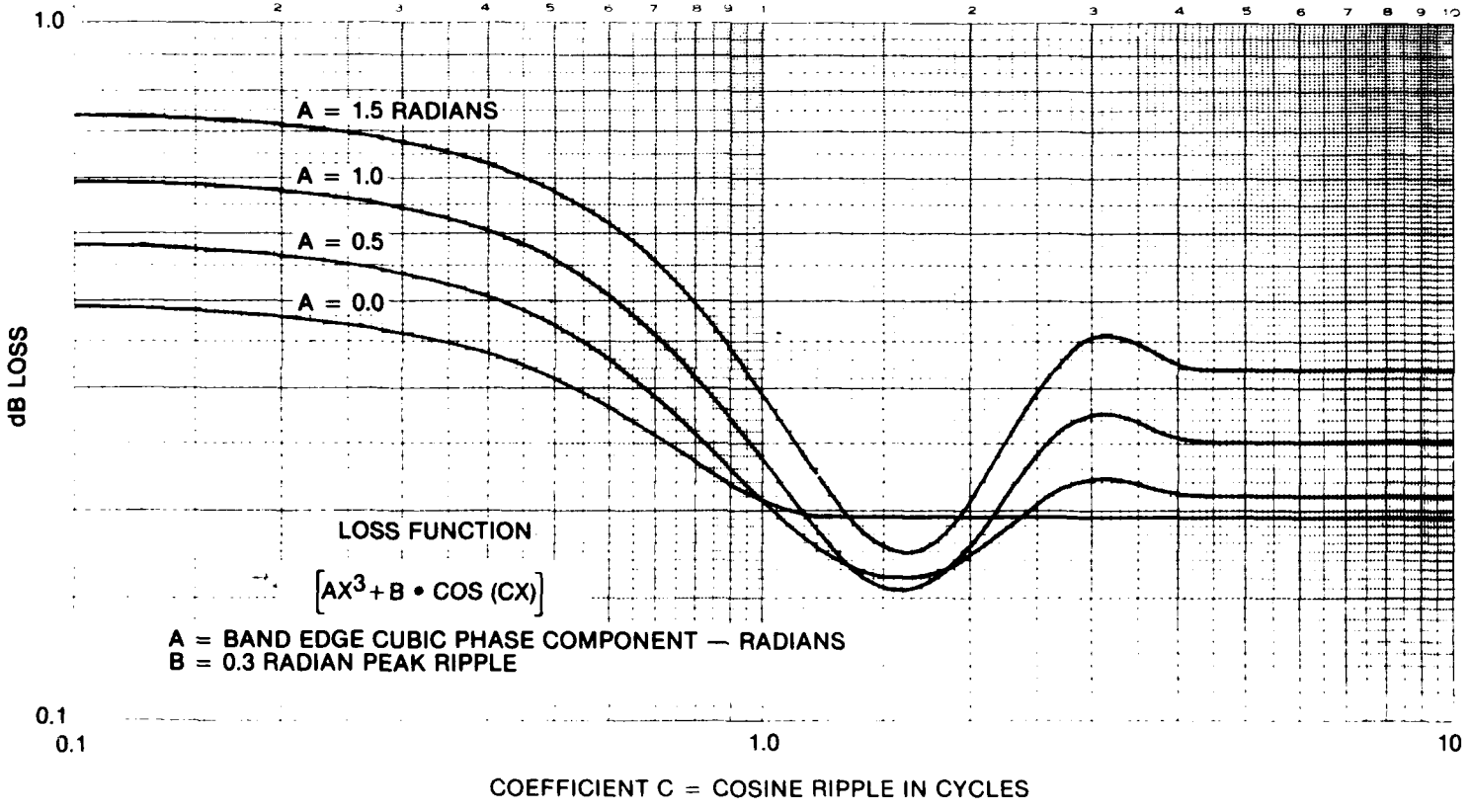

Fig. A-22. Signal Energy Losses Due to Combined Cubic Term with Cosi · Ripple Departure Function (0.3-radian peak)

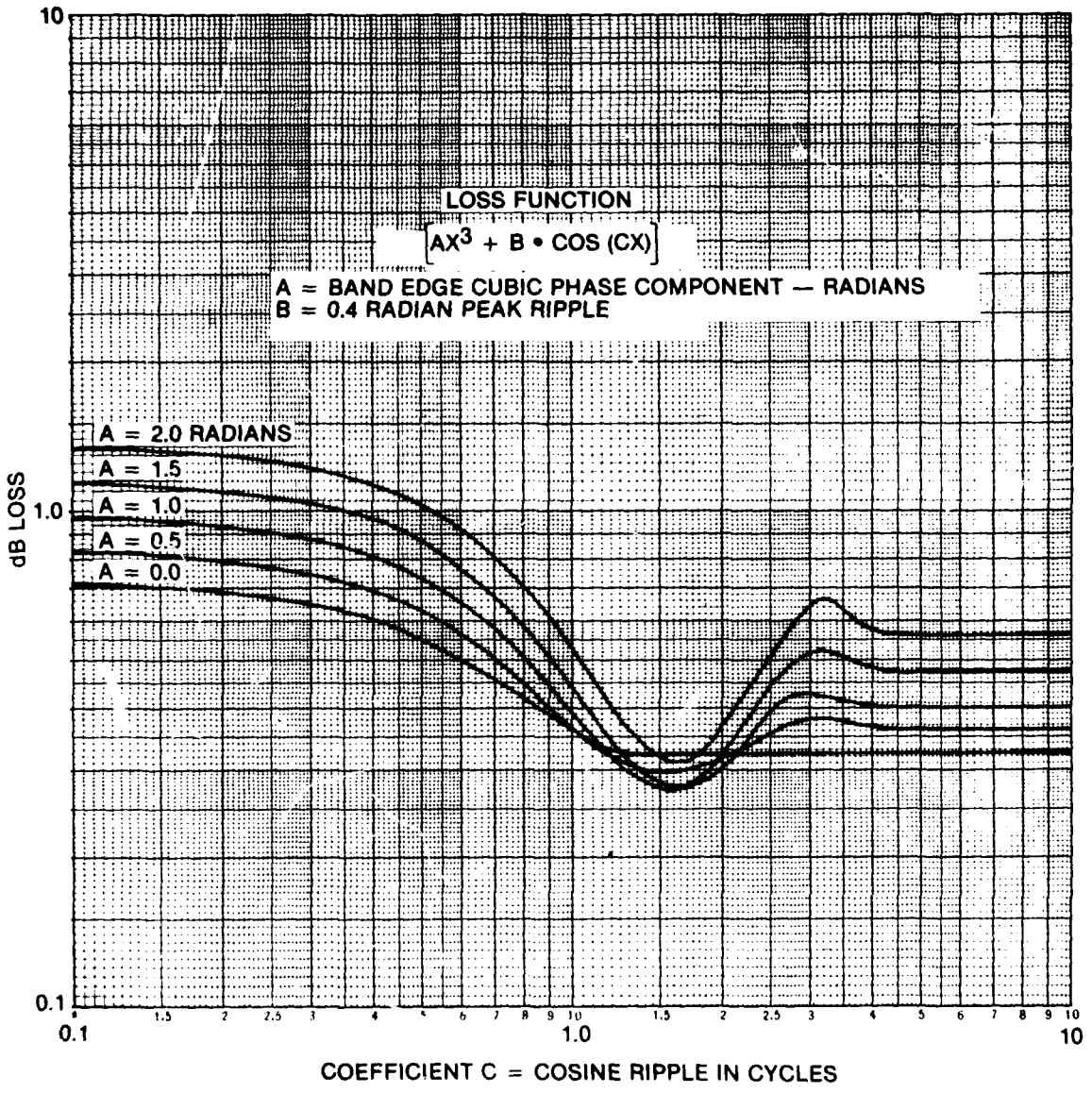

Fig. A-23. Signal Energy Losses Due to Combined Cubic Term with Cosine Ripple Departure Function (0.4-radian peak)

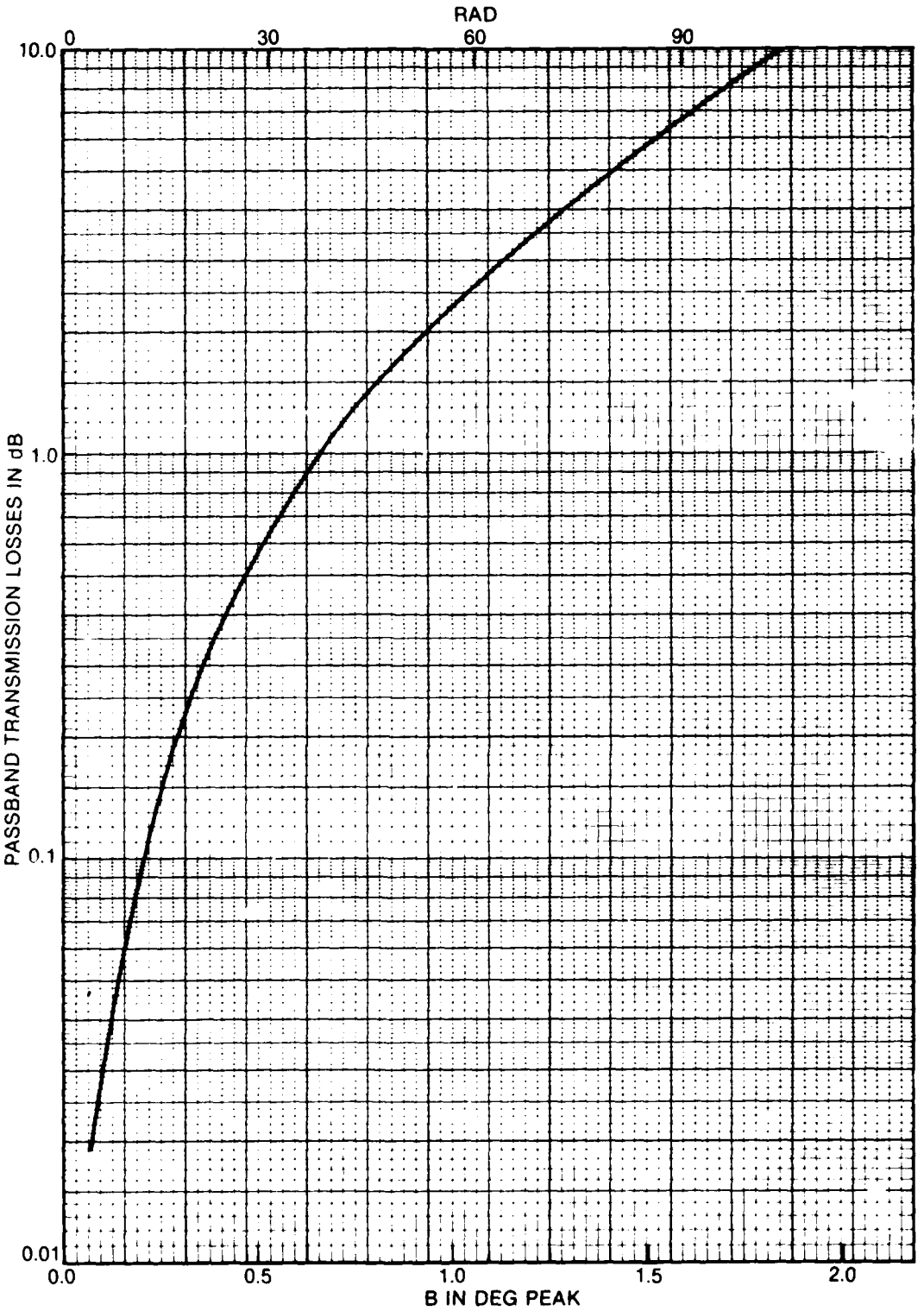

Fig. A-24. Losses for Phase Distortion Function of Sine or Cosine Ripple, Four or More Cycles

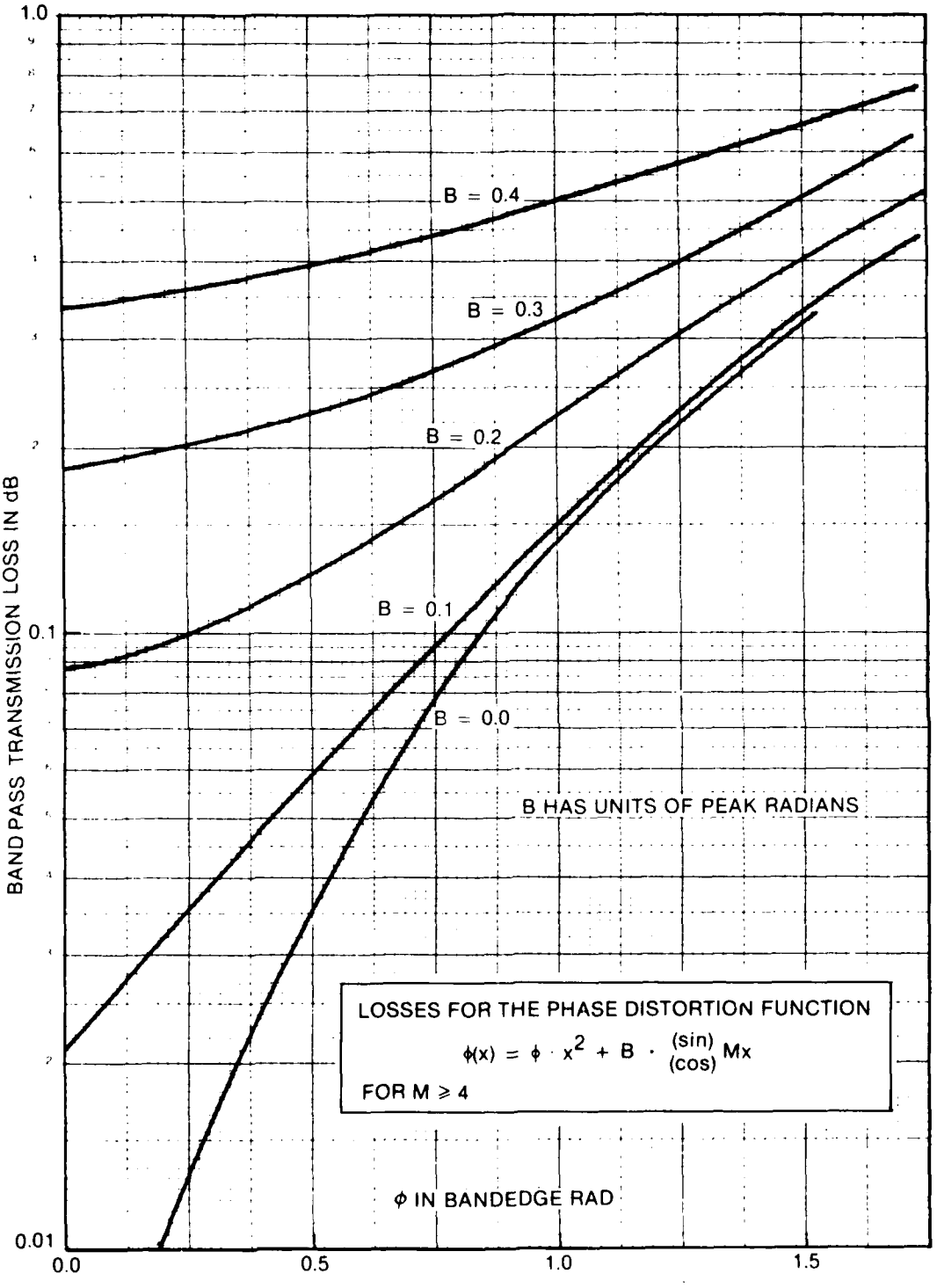

Fig. A-25. Losses for Phase Distortion Function, Sine or Cosine Ripple, Four or More Ripple Cycles, plus Parabolic Term of Varying Magnitude

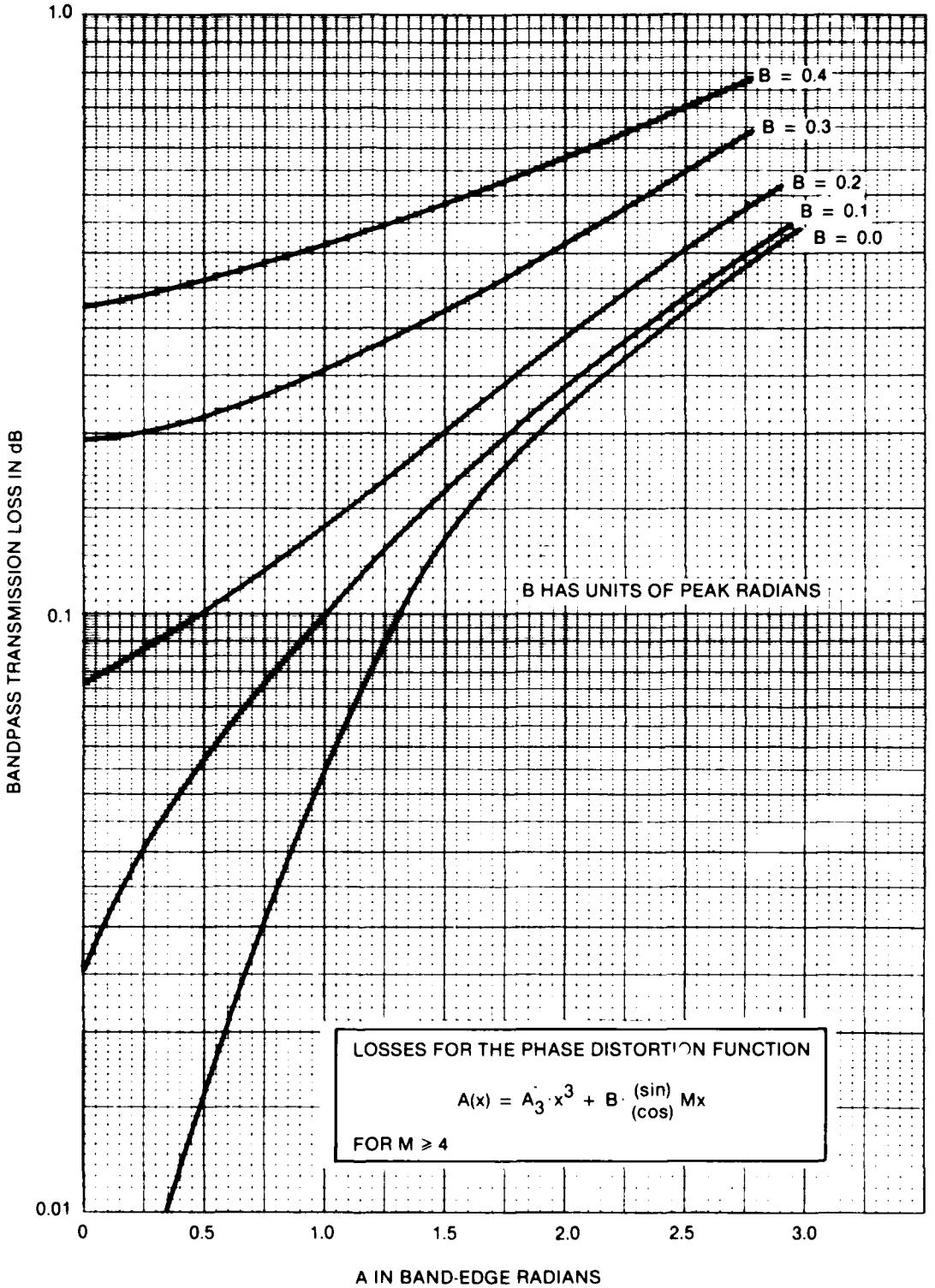

Fig. A-26. Losses for Phase Distortion Function, Sine or Cosine Ripple, Four or More Ripple Cycles, plus Cubic Term of Varying Magnitude

A.2 USING THE CURVES

Several typical problems are posed to illustrate how the precalculated curves of this appendix are utilized.

1. A linear least-squares fit has been subtracted from a certain passband phase characteristic, leaving a parabolic distortion phase departure function having a value of 105° at first spectral null frequencies. What distortion loss will that amount of distortion cause?

Answer: Consult Fig. A-7. Find 105° on the abscissa. Go vertically to the Second-Order (parabolic) curve and read off 0.46 dB.

2. A passband has a phase distortion characteristic consisting of one-half cycle of sine ripple between spectral null frequencies. The magnitude of the phase ripple is 60° peak-to-peak. What is the distortion loss?

Answer: Enter Fig. A-11 at 0.5 cycle and go up to the 30° peak line (half of 60° peak-to-peak). Read off 0.26 dB.

3. A certain communication system has a phase distortion characteristic consisting of an equivalent synchronizing clock-timing error of 45° and a single passband cycle of cosine ripple of 50° peak magnitude. What is the corresponding distortion loss?

Answer: Consult Fig. A-16 and enter the abscissa at 50°. Determine where the 45° curve of the left ordinate intersects the 50° line. On the right-side ordinate scale read off the value 1.46 dB.

4. After subtracting out the linear-least-squares straight line from a passband phase function, the remaining distortion characteristic has a third-order (cubic) term of 60° and 3-1/4 cycles of cosine ripple of 25° peak magnitude. What is the associated loss?

Answer: Consult Fig. A-23 since 25° ripple corresponds closely to 0.4 radians. Enter the abscissa at 3.25 and go up to the 1 radian curve (1.0 radians is equivalent to 57.3 degrees, which is the closest tabulated value to 60°. Read 0.5 dB.

APPENDIX B. AMPLITUDE DEPARTURE FUNCTIONS

B.1 REPRESENTATIVE PRE-COMPUTED AMPLITUDE DISTORTION DEPARTURE FUNCTIONS

Amplitude distortion by definition is present when the device under test (DUT) transfer function departs from the ideal of rectangular shape. Such distortion is present to some extent in most systems, and is noted, even in the presence of hard limiting, since the signal in question has been passed through many circuit elements. The digital waveform is inevitably modified to some discernible degree by the device and system amplitude passband functions.

A case of particular interest is presented for the system designer or analyst when a distorted passband characteristic has preceded the correlator-demodulator and the received signal is correlated with an undistorted local replica spectrum. The demodulator output bears the imprint of both amplitude characteristics [see Eq. (C.5.7)]. The analysis performed in this section considers several such cases, using as an amplitude reference the power level existing at band-center. With this definition, it is possible to realize "apparent gain" in a departure function, since some sideband components may be emphasized relative to their theoretical band-center reference-spectrum local counterparts.

When a channel utilizes ideal amplitude limiting, its output amplitude characteristic is flat. Amplitude distortion is not present, so the associated amplitude departure function is unity. Remaining sources of signal loss, if any, are due to the presence of a phase departure function, and are treated per preceding sections.

B.2 DERIVING THE AMPLITUDE DEPARTURE FUNCTION

When a quasi-linear case is to be considered, some analytical expression for passband humps, valleys, and ripple must be found. If a passband function looks like an inverted parabola, or some more complex function, the manner of using the computer curve-fitting process does not

change from the methods used in Section 4 (see Eqs. (2.4) and (2.52) and the subsection entitled "Developing the Departure Function"). Amplitude departure functions, as with phase departure functions, may contain power series terms augmented by terms from a Fourier series, representing a function offset from band center in radian-frequency units. A simple passband ripple case is discussed below.

Inside the $\pm 1/\tau$ limits of the rectangular outline of Fig. B-1, the amplitude function may be defined by the expression

$$A(\omega) = 1 - a \cos m(\omega - \omega_o) \qquad (B.1)$$

where m represents the number of ripple cycles. In Fig. B-1, m = 1.5 but could be any odd multiple of 1/2 consistent with physical realizability. Retaining the same frequency scale factors as developed for the phase departure functions simplifies computer evaluation by adaptation of previously derived programs (see Appendix E).

The relationship between linear amplitude ripple as shown in Fig. B-1 and its expression in terms of "decibels peak-to-peak" is given by the expression

$$R = 10 \log_{10} \left[\frac{1 + a}{1 - a} \right] \qquad (B.2)$$

Figures B-2, B-3, and B-4 show the relationship between a and R over a wide range of values. Using this information often eases the task of interrelating plotter data, test data, and analytical expression of specification wording.

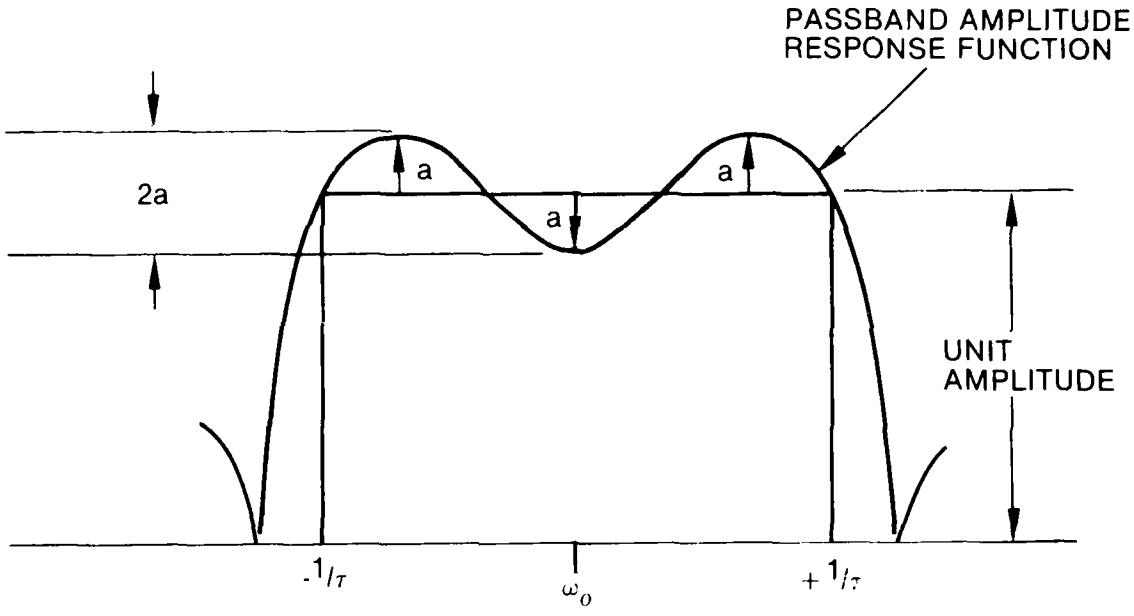

Fig. B-1. Passband Amplitude Ripple

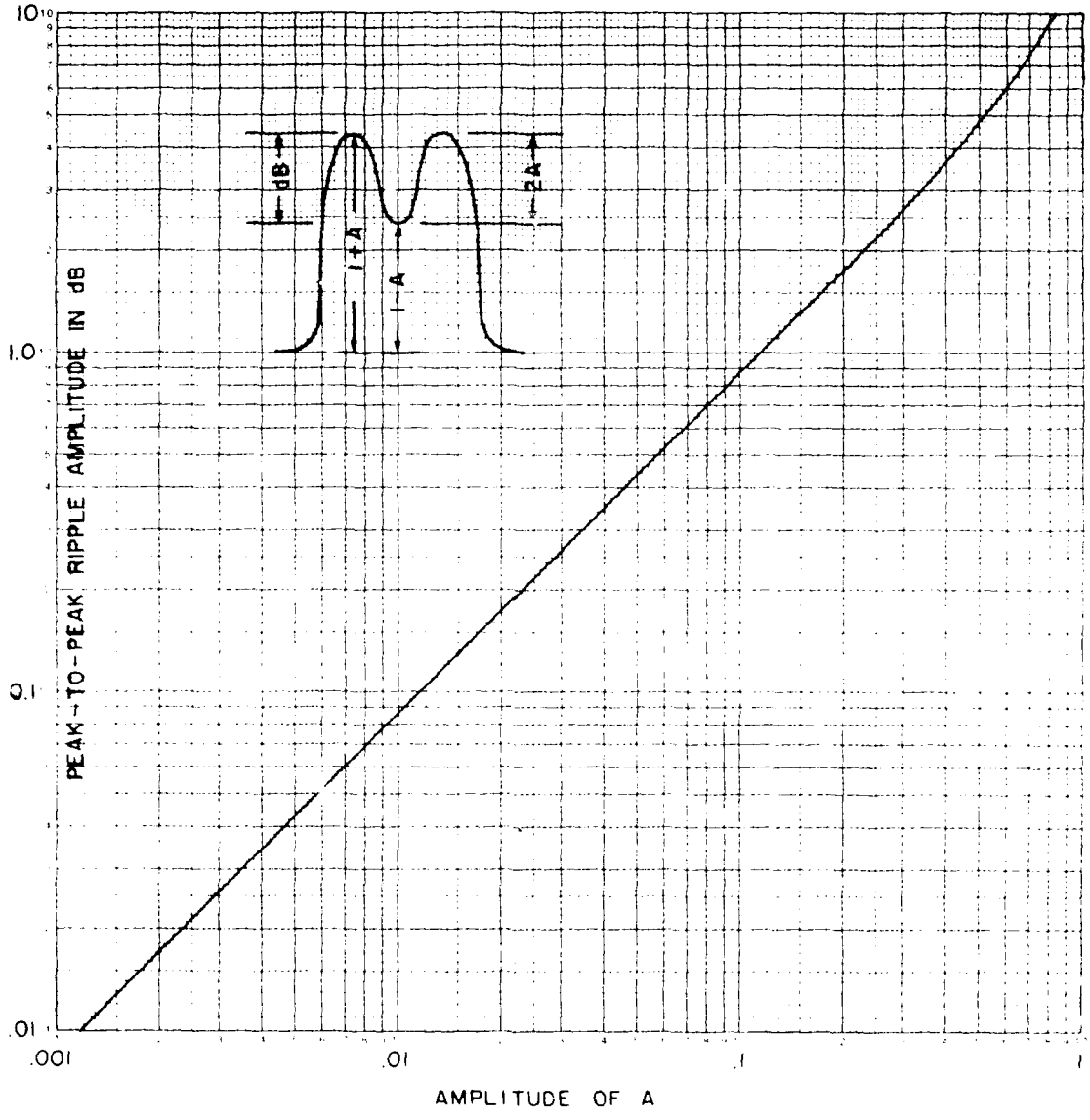

Fig. B-2. Relating Peak-to-Peak Ripple in dB to linear Peak Amplitude "A"

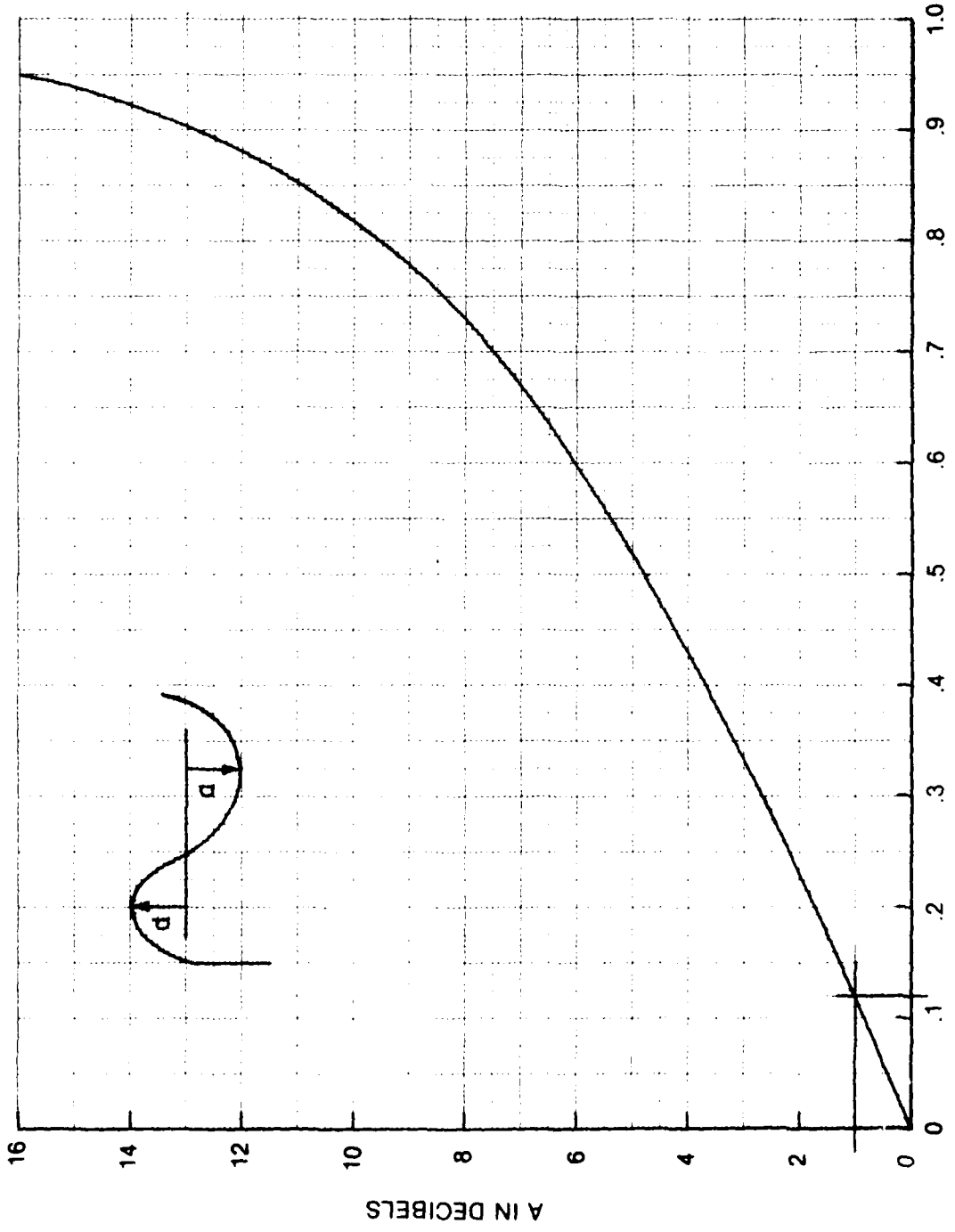

Fig. B-3. Relating Peak Linear Ripple to Ripple in dB

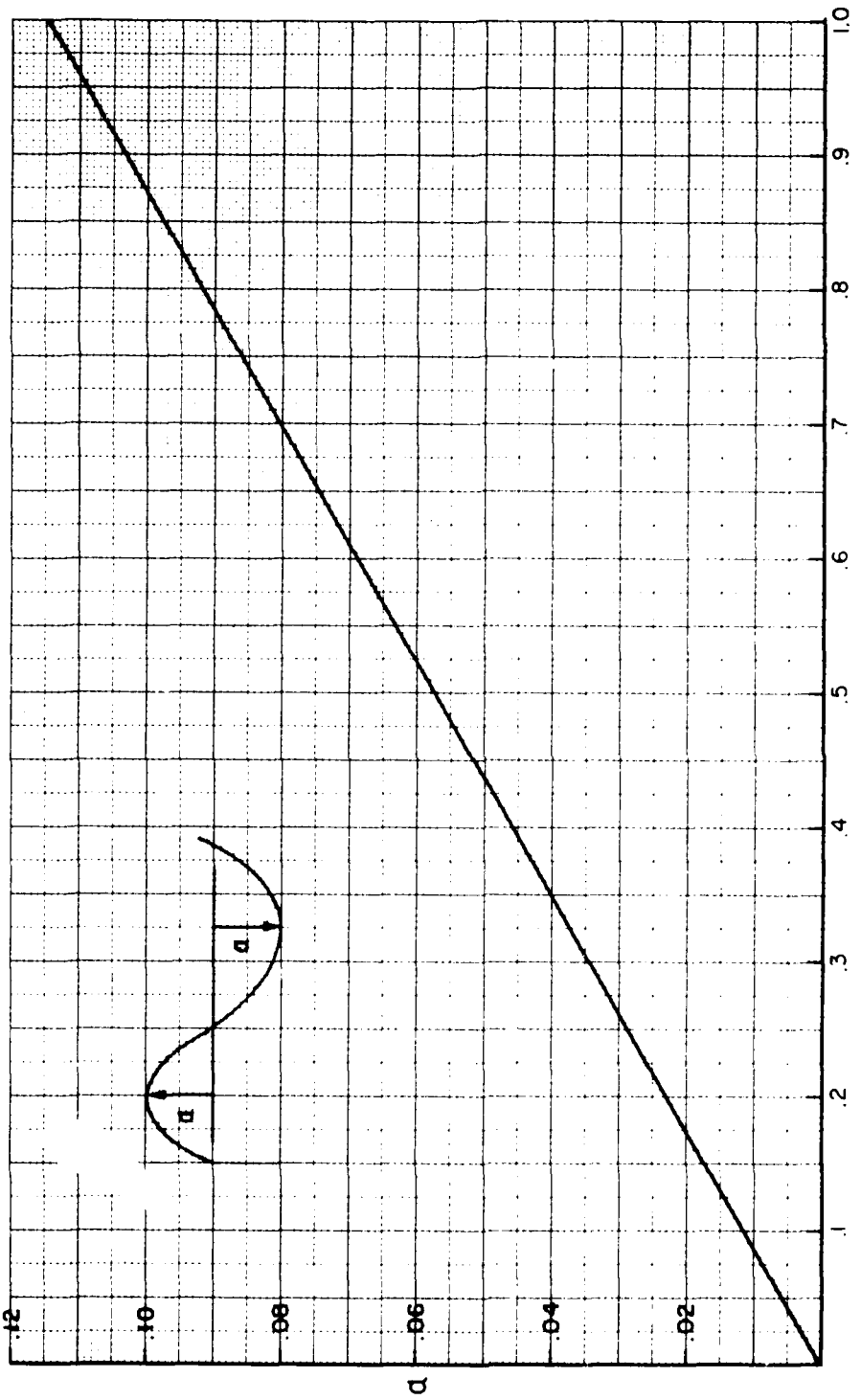

Fig. B-4. Expanded Scale of Fig. B-3, Peak Linear Ripple to dB

B.3 COMPUTING THE AMPLITUDE DEPARTURE FUNCTION

Signal power loss is determined from the ratio of the areas under the envelope received at the correlator to the area under the envelope of the locally generated reference spectral distribution. This is expressed as

$$\text{Loss} = 10 \log_{10} \left[\frac{\text{Power Received}}{\text{Power Generated}} \right] \tag{B.3}$$

where the spectral products yield power calculable from the following integral expression:

$$\text{Loss} = 20 \log_{10} \int_{n}^{+m} A(x) \left(\frac{\sin x}{x} \right)^2 dx \tag{B.4}$$

where

$$A(x) = 1 - a \cos (mx) \tag{B.5}$$

and coefficient "a" represents the peak of the ripple value as shown in Fig. B-1, and "m" is the ripple coefficient in cycles across the passband. As noted, "m" need not have integral values. Variable x represents the quantity $\omega - \omega_0$.

Dividing through the value of the above integral by the value of that integral when ripple term a = 0 normalizes the expression. The equation actually to be mechanized on the computer then takes the form

$$\text{dB Loss} = 20 \log_{10} \left[\frac{\int_0^{\pi} [1 - a \cos (mx)] \left(\frac{\sin x}{x} \right)^2 dx}{\int_0^{\pi} \left(\frac{\sin x}{x} \right)^2 dx} \right] \qquad \text{(B.6)}$$

where the numerical value of the denominator is 1.4181516. Passband non-symmetry may require integration from band edge to band edge instead of from band center to one band edge.

B.4 A CURVE-FITTED AMPLITUDE DEPARTURE FUNCTION

Figure B-5 represents the measured passband amplitude function of the same satellite channel whose differential group delay characteristic is shown in Fig. 4-1. An available seven-point curve-fitting program was used, after linearizing the dB plot of Fig. 4-1. The following linear amplitude passband approximation function was obtained.

$$\begin{aligned} A(x) = {} & 0.9697 + 0.001211x - 0.0008549x^2 \\ & - 0.0001879x^3 + 0.000015738x^4 \\ & + 0.0000022522x^5 - 0.0000000734x^6 \\ & - 0.0000000061x^7 \end{aligned} \qquad \text{(B.7)}$$

where $x = 0$ at band center. Inspection of Fig. B-5 and Eq. B.7 will reveal passband non-symmetry, so this equation requires integration over the entire region between the lower and the upper passband $1/\tau$ points. Units for x are kiloHertz, plus-or-minus from band center.

The departure function obtained per Eq. (2.4) is found by subtraction, and becomes

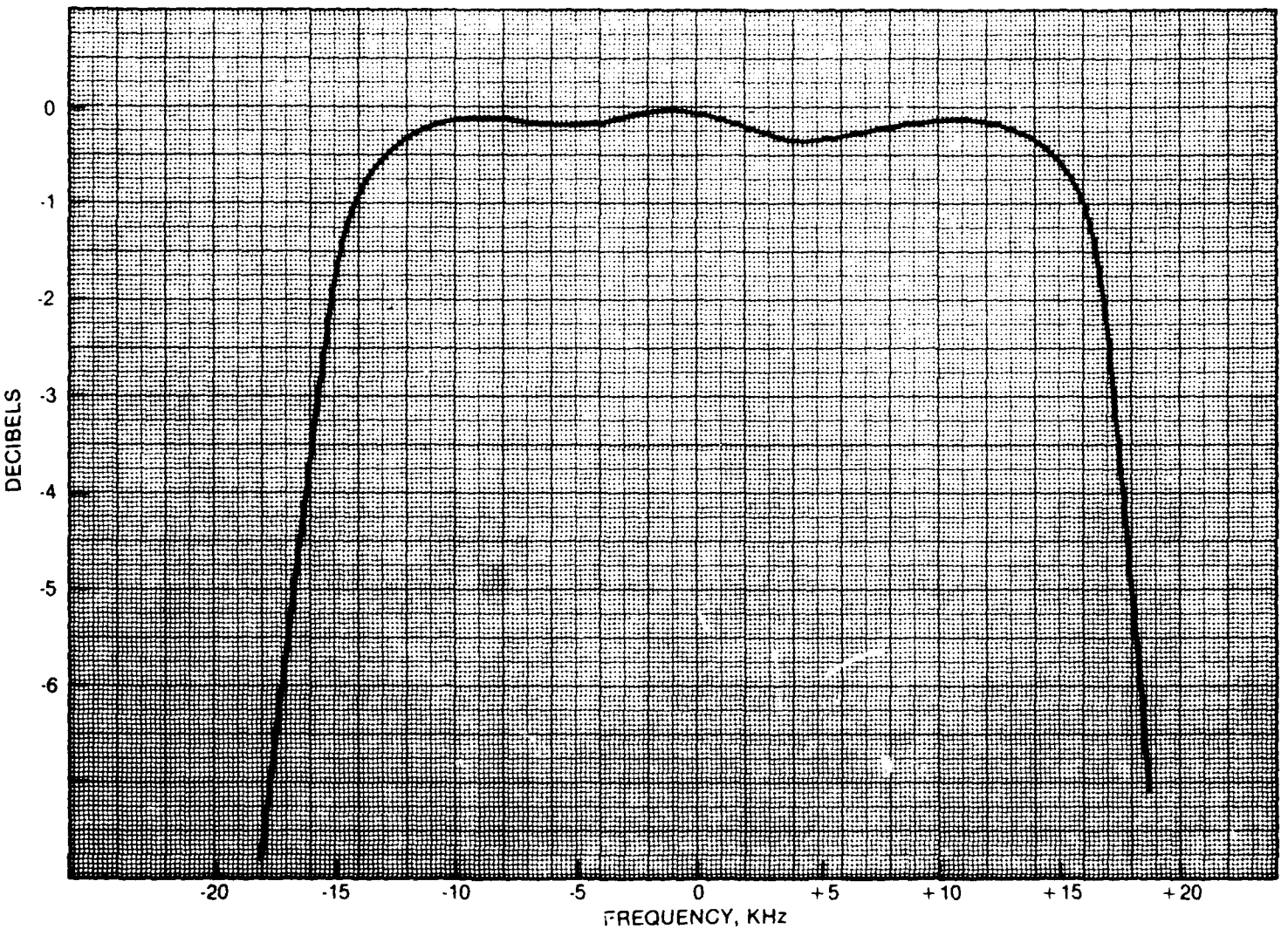

Fig. B-5. Passband Amplitude Characteristic

$$
\begin{aligned}
A(\omega) &= 1 - a\,(x) \\
&= -\,0.001211\omega + 0.0008549\omega^2 \\
&\quad + 0.0001879\omega^3 - 0.000015738\omega^4 \\
&\quad - 0.0000022522\omega^5 + 0.0000000734\omega^6 \\
&\quad + 0.0000000061\omega^7
\end{aligned}
\qquad \text{(B.8)}
$$

where x is replaced by normalization of the frequency variable $0 \leq \omega \leq \pm 16$ kHz in units of kiloHertz.

To obtain the total distortion loss resulting from passing a PN signal through this signalling channel, account must be taken of both the phase loss and the amplitude loss, respectively resulting in the total 0.1678 + 0.0122 = 0.18 dB for the subject channel. That loss would be at the edge of resolvability when performing most normal functional acceptance tests, indicating that this passband should perform with excellence for normal communications services.

B.5 SOME COMPUTATIONAL RESULTS

Figures B-6 and B-7 provide a family of loss curves for various rates and magnitudes of additive and subtractive cosine amplitude ripple, respectively. Figure B.8 provides similar information for subtractive sine ripple.

Figure B-6 shows that the effects of passband amplitude ripple can be characterized either by gains or by losses as indicated respectively in the legend. Whether gain or loss is experienced is determined by the extent to which the negative half-cycles of ripple reduce the spectral energy content more or less than the augmentation provided by the positive half-cycles [see Eq. (B.1)].

Some design guidance derived from the preceding information includes the following points.

1. Passband amplitude-response dips should be kept outside of the central portion of the signal spectrum.

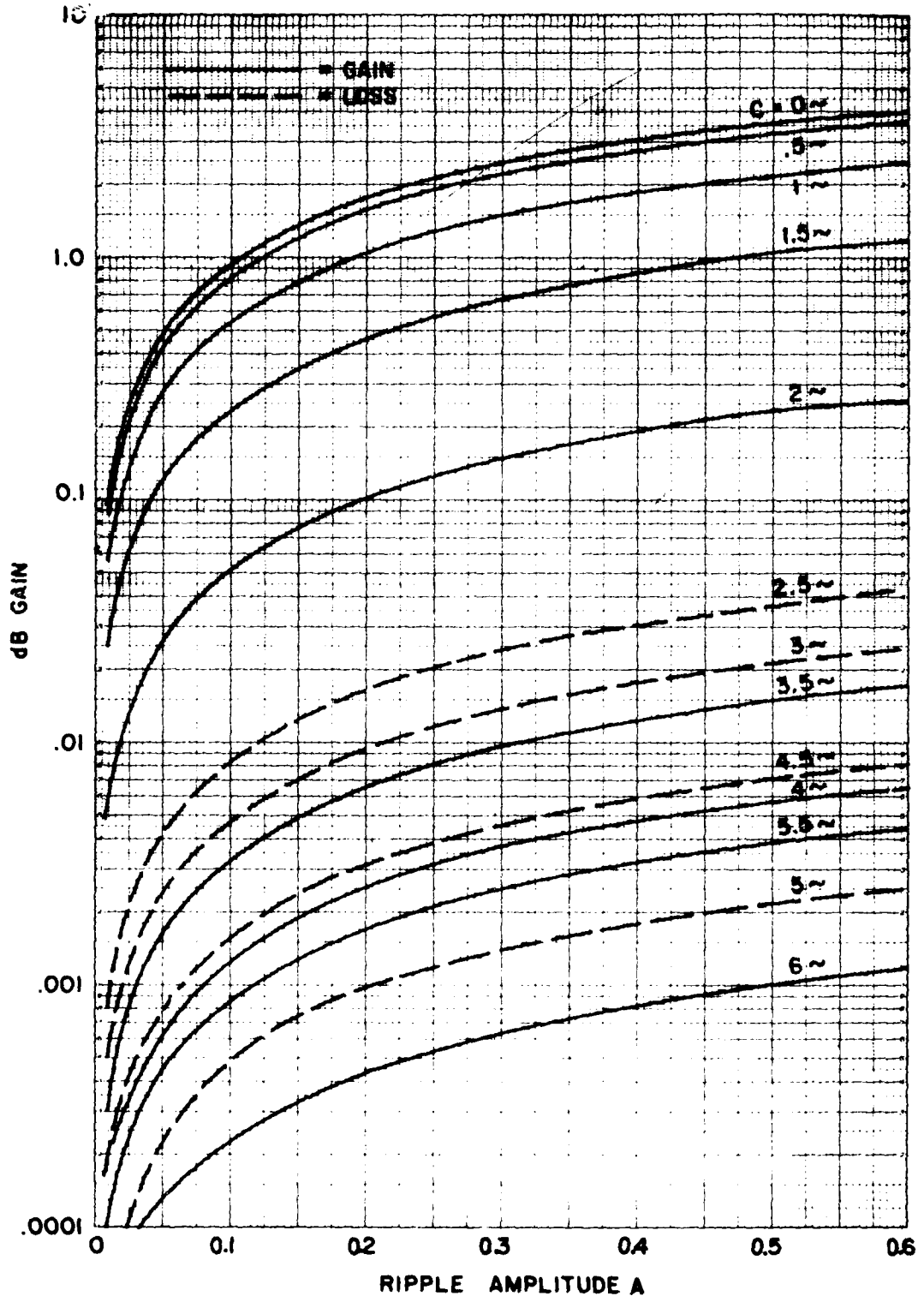

Fig. B-6. 1 + A • cos(C • x) Amplitude Ripple

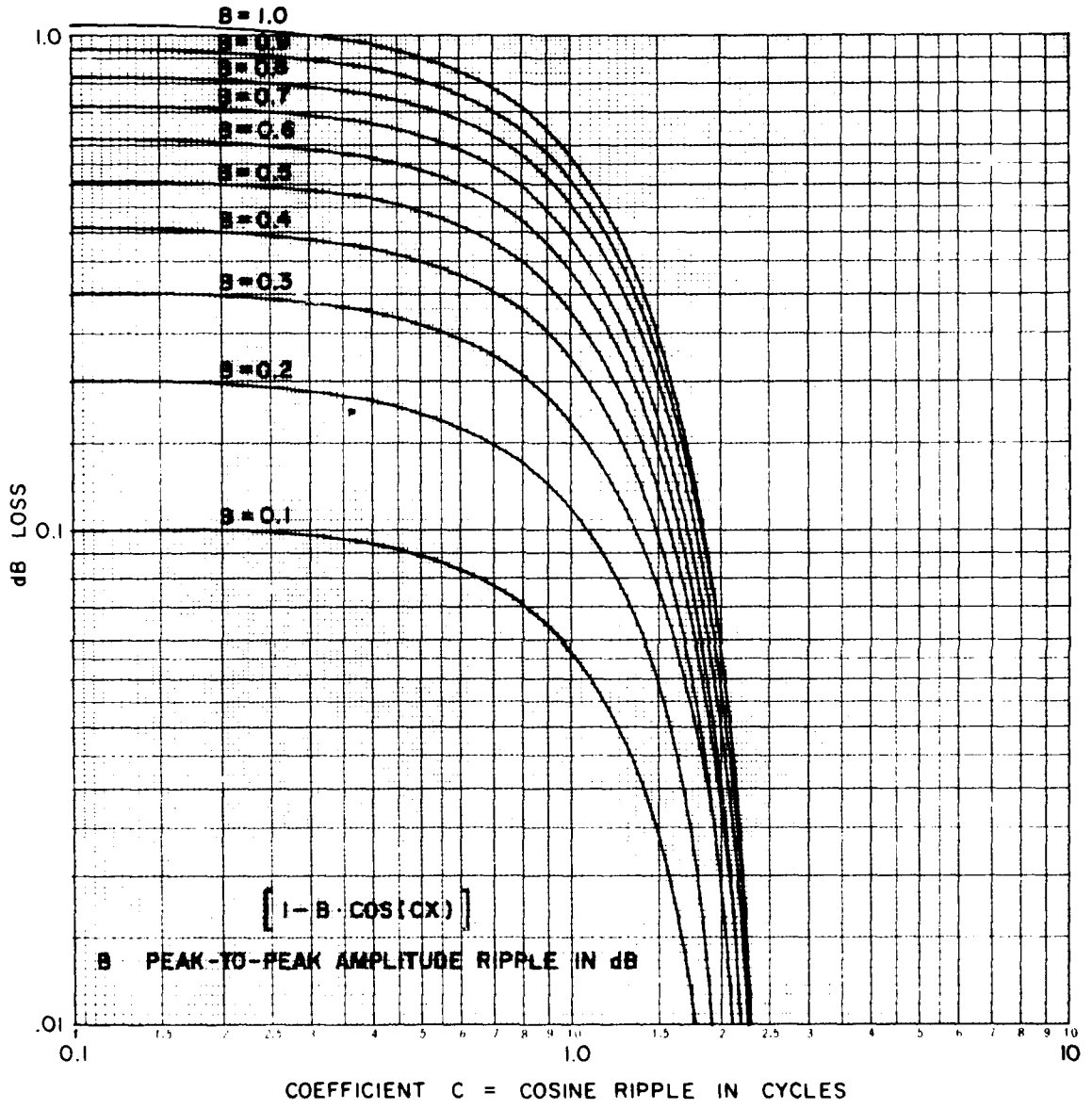

Fig. B-7. 1 - B • cos(C • x) Amplitude Ripple

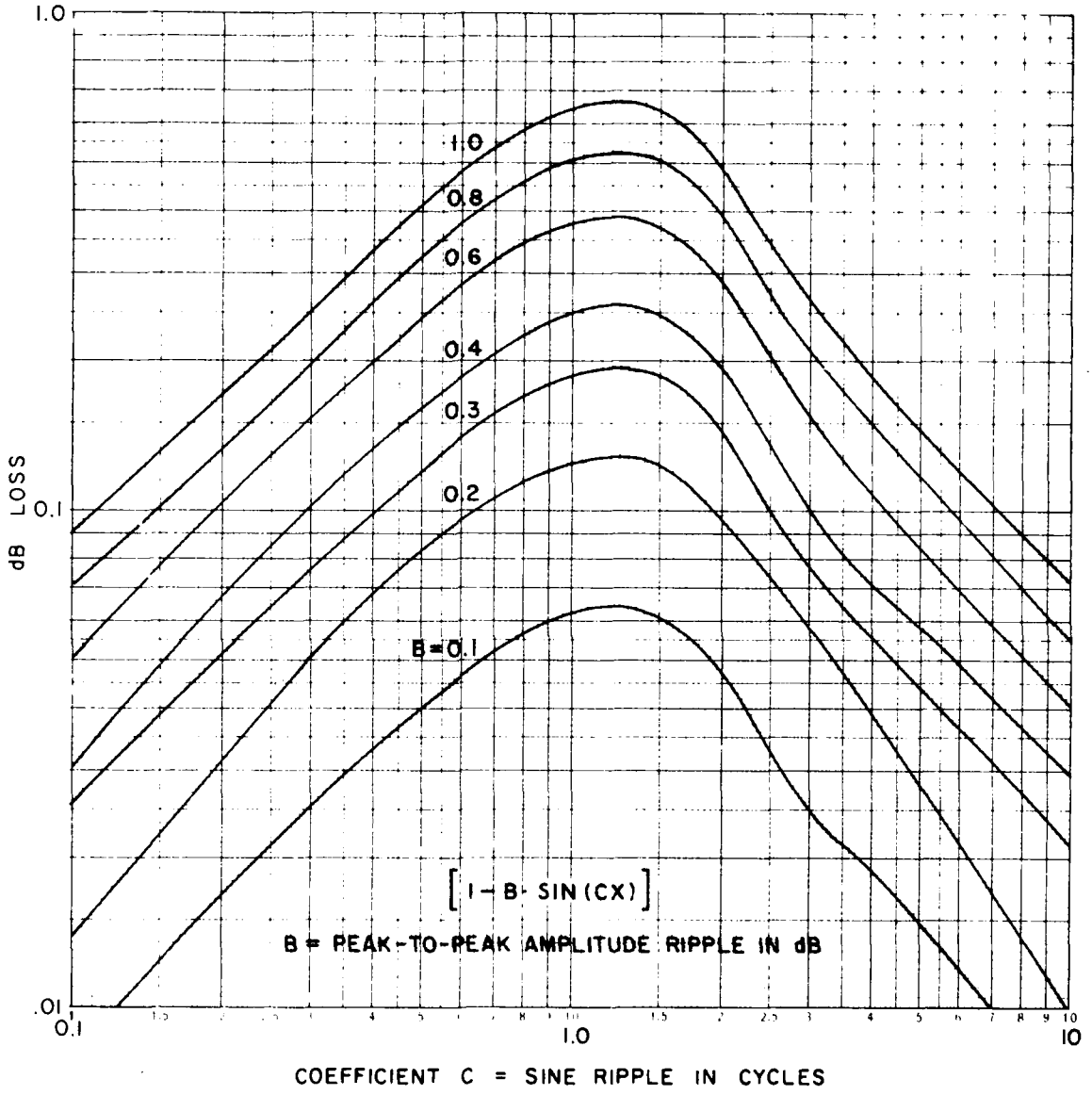

Fig. B-8. 1 - B • sin(C • x) Amplitude Ripple

2. Bandwidth probably can be reduced to two-thirds of the usual $2/\tau$ value with little loss, providing the phase characteristic is kept quasi-linear.

3. Phase distortion losses usually are the more severe of the two types.

4. Phase equalization may be of greater value than amplitude equalization when considering cost effectiveness.

5. Amplitude distortion may be more easily reduced by limiting than phase distortion is reduced by phase equalization.

6. It will sometimes be feasible to compensate for phase distortion by judicious application or allocation via juggling pole and zero locations in appropriate portions of the circuitry.

APPENDIX C. COMBINED AMPLITUDE AND PHASE DISTORTION LOSS CALCULATION

Most band-limited systems exhibit some amount of non-linear distortion in both amplitude response and phase response characteristics. Departures from the ideal rectangular passband and from the linear-phase characteristic have been shown to exhibit calculable signal distortion losses, appearing as a reduction in utilizable spectral energy. An opportunity is provided via Tables C-1 through C-11 to examine passband energy distribution as a function of several combinations of additive and subtractive amplitude ripple distortion with and without phase distortion of either or both linear and parabolic types. The peak-to-peak cosine amplitude ripple in the examples is 1.0 dB at 1.5 cycles across the passband. The derivations of Section 2, in which it was shown that the amplitude and the phase distortion losses may be calculated separately, will be utilized here. Each distortion loss factor will be derived, converted to dB, and added. The filter characteristics upon which the examples are based were drawn from typical hardware characteristics, akin to Fig. B-1.

Table C-1 presents the cumulative energy distribution pattern at 0.01 radian intervals versus spectral utilization in the presence of 1-dB peak-to-peak additive cosine ripple and 45° of parabolic phase departure.

Table C-2 similarly presents the energy distribution in the presence of 1-dB additive cosine ripple without phase distortion. Note that the presence of additive amplitude ripple $(1 + A(\omega))$ enhances the received signal strength 0.24 dB over the theoretical value of 0 dB experienced with a flat passband (see Table C-4).

Table C-3 presents the energy distribution due to phase distortion without amplitude ripple distortion. The phase departure of 45° at band edge results in a net loss of 0.09 dB which is consistent with the combined net gain of 0.16 dB shown in Table C-1, i.e., $0.24 - 0.09 \simeq 0.16$ dB.

Table C-4 has been included for reference purposes, enabling direct comparison with the other printouts in this appendix. It represents spectral energy distribution in the total absence of any kind of distortion.

Table C-1. Loss Table 1 dB pk-pk Ripple of 1.5 Cycles plus 45° Parabolic Phase Distortion

```
          F(X) TIMES (SIN(X)/X) S[illegible] IN DECIBELS
            NORMALIZED TO [illegible]
FOR  F(X) = (1+A(X))(COS(L(X)+P(X)+C(X)+FCOS(X)(X)+ESIN(X)))((SIN(X)/X)
           A(X) = 1.0 DB PK-PK RIPPLE AMPLITUDE IN 1.5 CYCLES
           L(X) = 00 DEGREES LINEAR DISTORTION AT BAND EDGE
           P(X) = 45 DEGREES PARABOLIC DISTORTION
           C(X) = 0 DEGREES CUBIC DISTORTION
       FCOS(X) = 00 DEGREES PEAK AND 0.0 CYCLES RIPPLE
       ESIN(X) = 00 DEGREES PEAK AND 0.0 CYCLES RIPPLE
         INTEGRATED FROM ZERO TO X IN STEPS OF 0.01 RADIAN
```

X	0.00	0.01	0.02	0.03	0.04	0.05	0.06	0.07	0.08	0.09
0.0	-1[illegible]	-4[illegible]	-36.07	-32.56	-30.05	-28.12	-26.53	-25.20	-24.04	-23.0[illegible]
1	-[illegible].11	-21.[illegible]	-20.55	-19.84	-19.20	-18.60	-18.04	-17.52	-17.03	-16.56
2	-16.1[illegible]	-15.71	-15.31	-14.93	-14.56	-14.21	-13.88	-13.56	-13.25	-12.95
3	-12.67	-12.[illegible]	-12.12	-11.86	-11.61	-11.37	-11.13	-10.90	-10.68	-10.47
4	-10.2[illegible]	-10.06	-9.85	-9.66	-9.47	-9.29	-9.11	-8.93	-8.76	-8.60
5	-8.[illegible]	-8.27	-8.12	-7.97	-7.82	-7.67	-7.52	-7.39	-7.25	-7.12
6	-6.99	-6.86	-6.73	-6.61	-6.49	-6.37	-6.25	-6.14	-6.03	-5.92
7	-5.81	-5.70	-5.60	-5.50	-5.40	-5.30	-5.20	-5.11	-5.01	-4.92
8	-4.83	-[illegible].74	-4.66	-4.57	-4.49	-4.40	-4.32	-4.24	-4.16	-4.07
9	-4.01	-3.9[illegible]	-3.8[illegible]	-3.79	-3.72	-3.65	-3.58	-3.51	-3.45	-3.[illegible]
1.0	-3.[illegible]	-3.[illegible]	-3.1[illegible]	-3.13	-3.07	-3.01	-2.95	-2.89	-2.84	-2.78
1	-2.73	-2.67	-2.62	-2.57	-2.52	-2.47	-2.42	-2.37	-2.32	-2.27
2	-2.23	-2.1[illegible]	-2.14	-2.09	-2.05	-2.00	-1.96	-1.92	-1.88	-1.84
3	-1.80	-1.76	-1.72	-1.69	-1.65	-1.61	-1.58	-1.54	-1.50	-1.47
4	-1.44	-1.40	-1.37	-1.34	-1.31	-1.28	-1.25	-1.22	-1.19	-1.16
5	-1.13	-1.10	-1.07	-1.05	-1.02	-1.00	-.97	-.94	-.92	-.90
6	-.87	-.85	-.83	-.80	-.78	-.76	-.74	-.72	-.69	-.67
7	-.65	-.63	-.62	-.60	-.58	-.56	-.54	-.52	-.51	-.49
8	-.47	-.46	-.44	-.43	-.41	-.40	-.38	-.37	-.35	-.34
9	-.32	-.31	-.30	-.29	-.27	-.26	-.25	-.24	-.23	-.21
2.0	-.20	-.19	-.18	-.17	-.16	-.15	-.14	-.13	-.12	-.11
1	-.11	-.10	-.09	-.08	-.07	-.06	-.06	-.05	-.04	-.04
2	-.03	-.02	-.01	-.01	-.00	.00	.01	.02	.02	.03
3	.03	.04	.04	.05	.05	.06	.06	.06	.07	.07
4	.08	.08	.08	.09	.09	.09	.10	.10	.10	.11
5	.11	.11	.12	.12	.12	.12	.12	.13	.13	.13
6	.13	.13	.14	.14	.14	.14	.14	.14	.15	.15
7	.15	.15	.15	.15	.15	.15	.15	.15	.16	.16
8	.16	.16	.16	.16	.16	.16	.16	.16	.16	.16
9	.16	.16	.16	.16	.16	.16	.16	.16	.16	.16
3.0	.16	.16	.16	.16	.16	.16	.16	.16	.16	.16
1	.16	.16	.16	.16	.16	.16	.16	.16	.16	.16

Table C-2. Loss Table 1 dB pk-pk Ripple of 1.5 Cycles plus Zero Phase Distortion

F(X) STEPS (SIN(X)/X) SQUARED IN DECIBELS
NORMALIZED TO 0.0 FOR UNDISTORTED SPECTRUM

FOR F(X) = (1+A(X))(COS(L(X)+B(X)+C(X)+COS(2X)+ISIN(2X)))((SIN(X)/X)2)

A(X) = 1.0 IF PEAK-PEAK RIPPLE AMPLITUDE IN 1.5 CYCLES
L(X) = 90 IF LINEAR PHASE DISTORTION AT BAND EDGE
B(X) = 90 IF QUADRATIC PHASE DISTORTION
C(X) = 0 IF CUBIC DISTORTION
COS(2X) = 90 DEGREES PHASE AT 0.0 CYCLES RIPPLE
SIN(2X) = 90 DEGREES PHASE AND 0.0 CYCLES RIPPLE
INTERPOLATED FROM ZERO TO X IN STEPS OF 0.01 RADIAN

X	0.00	0.01	0.02	0.03	0.04	0.05	0.06	0.07	0.08	0.09
0.0	-142.18	-49.09	-36.07	-32.55	-30.05	-28.12	-26.53	-25.20	-24.04	-23.02
1	-22.11	-21.28	-20.53	-19.84	-19.20	-18.60	-18.04	-17.52	-17.03	-16.56
2	-16.12	-15.71	-15.31	-14.93	-14.56	-14.21	-13.88	-13.56	-13.25	-12.95
3	-12.67	-12.39	-12.12	-11.86	-11.61	-11.37	-11.13	-10.90	-10.68	-10.47
4	-10.26	-10.05	-9.85	-9.66	-9.47	-9.29	-9.11	-8.93	-8.76	-8.60
5	-8.43	-8.27	-8.12	-7.97	-7.82	-7.67	-7.53	-7.39	-7.25	-7.12
6	-6.99	-6.86	-6.73	-6.61	-6.49	-6.37	-6.25	-6.14	-6.03	-5.92
7	-5.81	-5.70	-5.60	-5.50	-5.39	-5.30	-5.20	-5.10	-5.01	-4.92
8	-4.83	-4.74	-4.65	-4.57	-4.48	-4.40	-4.32	-4.24	-4.16	-4.09
9	-4.01	-3.93	-3.86	-3.79	-3.72	-3.65	-3.58	-3.51	-3.44	-3.38
1.0	-3.31	-3.25	-3.19	-3.12	-3.06	-3.00	-2.95	-2.89	-2.83	-2.78
1	-2.72	-2.67	-2.61	-2.56	-2.51	-2.47	-2.41	-2.36	-2.31	-2.27
2	-2.22	-2.17	-2.13	-2.08	-2.04	-1.99	-1.95	-1.91	-1.87	-1.83
3	-1.79	-1.75	-1.71	-1.67	-1.63	-1.60	-1.56	-1.53	-1.49	-1.46
4	-1.42	-1.39	-1.36	-1.32	-1.29	-1.26	-1.23	-1.20	-1.17	-1.14
5	-1.11	-1.08	-1.06	-1.03	-1.00	-.97	-.95	-.92	-.90	-.87
6	-.85	-.82	-.80	-.78	-.76	-.73	-.71	-.69	-.67	-.65
7	-.63	-.61	-.59	-.57	-.55	-.53	-.51	-.49	-.48	-.46
8	-.44	-.42	-.41	-.39	-.38	-.36	-.35	-.33	-.32	-.30
9	-.29	-.27	-.26	-.25	-.23	-.22	-.21	-.20	-.18	-.17
2.0	-.16	-.15	-.14	-.13	-.12	-.11	-.10	-.09	-.08	-.07
1	-.06	-.05	-.04	-.03	-.02	-.01	-.01	.00	.01	.02
2	.02	.03	.04	.05	.05	.06	.07	.07	.08	.09
3	.09	.09	.10	.11	.11	.12	.12	.13	.13	.13
4	.14	.14	.15	.15	.16	.16	.16	.17	.17	.17
5	.18	.18	.18	.18	.19	.19	.19	.20	.20	.20
6	.20	.20	.21	.21	.21	.21	.21	.22	.22	.22
7	.22	.22	.22	.22	.22	.23	.23	.23	.23	.23
8	.23	.23	.23	.23	.23	.23	.23	.23	.24	.24
9	.24	.24	.24	.24	.24	.24	.24	.24	.24	.24
3.0	.24	.24	.24	.24	.24	.24	.24	.24	.24	.24
.1	.24	.24	.24	.24	.24	.24	.24	.24	.24	.24

Table C-3. Loss Table No Amplitude Ripple with 45° Parabolic Phase Distortion

F(X) TIMES (SIN(X)/X) SQUARED IN DECIBELS
NORMALIZED TO 0.0 DB PASSBAND REFERENCE

DB F(X) = (1-A(X))(COS(L(X)+P(X)+C(X)+ICOS(WX)+ISIN(WX)))((SIN(X)/X)2)

A(X) = 0.0 DB PEAK-TO-PEAK RIPPLE AMPLITUDE IN 0.0 CYCLES
L(X) = 00 DEGREES LINEAR DISTORTION AT BAND EDGE
P(X) = 45 DEGREES PARABOLIC DISTORTION
C(X) = 0 DEGREES CUBIC DISTORTION
ICOS(WX) = 00 DEGREES PEAK AND 0.0 CYCLES RIPPLE
ISIN(WX) = 00 DEGREES PEAK AND 0.0 CYCLES RIPPLE
INTEGRATED FROM ZERO TO X IN STEPS OF 0.01 RADIAN

X	0.00	0.01	0.02	0.03	0.04	0.05	0.06	0.07	0.08	0.09
0.0	-143.12	-43.04	-37.01	-33.49	-31.00	-29.06	-27.44	-26.14	-24.98	-23.96
1	-23.06	-22.22	-21.47	-20.77	-20.13	-19.53	-18.98	-18.45	-17.96	-17.49
2	-17.05	-16.63	-16.23	-15.85	-15.49	-15.14	-14.80	-14.48	-14.17	-13.87
3	-13.58	-13.30	-13.03	-12.77	-12.52	-12.27	-12.03	-11.80	-11.58	-11.36
4	-11.15	-10.94	-10.74	-10.54	-10.35	-10.17	-9.98	-9.81	-9.63	-9.46
5	-9.30	-9.13	-8.97	-8.82	-8.67	-8.52	-8.37	-8.23	-8.09	-7.95
6	-7.82	-7.69	-7.56	-7.43	-7.30	-7.18	-7.06	-6.94	-6.83	-6.71
7	-6.60	-6.49	-6.38	-6.28	-6.17	-6.07	-5.97	-5.87	-5.77	-5.68
8	-5.58	-5.49	-5.40	-5.31	-5.22	-5.13	-5.05	-4.96	-4.88	-4.80
9	-4.72	-4.64	-4.56	-4.49	-4.41	-4.34	-4.27	-4.19	-4.12	-4.05
1.0	-3.98	-3.91	-3.85	-3.78	-3.72	-3.65	-3.59	-3.53	-3.47	-3.41
1	-3.35	-3.29	-3.23	-3.17	-3.12	-3.06	-3.01	-2.96	-2.90	-2.85
2	-2.80	-2.75	-2.70	-2.65	-2.60	-2.56	-2.51	-2.46	-2.42	-2.37
3	-2.33	-2.29	-2.24	-2.20	-2.16	-2.12	-2.08	-2.04	-2.00	-1.96
4	-1.92	-1.89	-1.85	-1.81	-1.78	-1.74	-1.71	-1.67	-1.64	-1.61
5	-1.58	-1.55	-1.52	-1.49	-1.46	-1.43	-1.40	-1.37	-1.34	-1.31
6	-1.28	-1.26	-1.23	-1.20	-1.18	-1.15	-1.13	-1.10	-1.08	-1.06
7	-1.03	-1.01	-.99	-.97	-.95	-.93	-.91	-.89	-.86	-.84
8	-.82	-.81	-.79	-.77	-.75	-.73	-.72	-.70	-.68	-.67
9	-.65	-.64	-.62	-.61	-.59	-.58	-.56	-.55	-.53	-.52
2.0	-.51	-.50	-.48	-.47	-.46	-.45	-.44	-.43	-.42	-.41
1	-.40	-.39	-.38	-.37	-.36	-.35	-.34	-.33	-.32	-.31
2	-.30	-.30	-.29	-.28	-.27	-.27	-.26	-.25	-.25	-.24
3	-.24	-.23	-.22	-.22	-.21	-.21	-.20	-.20	-.19	-.19
4	-.18	-.18	-.17	-.17	-.17	-.16	-.16	-.16	-.15	-.15
5	-.15	-.14	-.14	-.14	-.13	-.13	-.13	-.13	-.12	-.12
6	-.12	-.12	-.12	-.11	-.11	-.11	-.11	-.11	-.11	-.10
7	-.10	-.10	-.10	-.10	-.10	-.10	-.10	-.10	-.09	-.09
8	-.09	-.09	-.09	-.09	-.09	-.09	-.09	-.09	-.09	-.09
9	-.09	-.09	-.09	-.09	-.09	-.09	-.09	-.09	-.09	-.09
3.0	-.09	-.09	-.09	-.09	-.09	-.09	-.09	-.09	-.09	-.09
1	-.09	-.09	-.09	-.09	-.09	-.09	-.09	-.09	-.09	-.09

Table C-4. Loss Table for Spectral Energy Distribution in a Distortion-Free Passband

THE INTEGRAL OF F(X) IN DECIBELS
WHERE F(X) = SIN(X)/X SQUARED NORMALIZED
INTEGRATED FROM ZERO TO X IN STEPS OF 0.01 RADIAN

X	0.00	0.01	0.02	0.03	0.04	0.05	0.06	0.07	0.08	0.09
0.0	-61.52	-21.52	-18.51	-16.75	-15.50	-14.53	-13.74	-13.07	-12.49	-11.98
1	-11.52	-11.11	-10.73	-10.39	-10.07	-9.77	-9.49	-9.23	-8.98	-8.75
2	-8.53	-8.32	-8.12	-7.93	-7.74	-7.57	-7.40	-7.24	-7.08	-6.93
3	-6.79	-6.65	-6.52	-6.38	-6.26	-6.14	-6.02	-5.90	-5.79	-5.68
4	-5.57	-5.47	-5.37	-5.27	-5.18	-5.08	-4.99	-4.90	-4.82	-4.73
5	-4.65	-4.57	-4.49	-4.41	-4.33	-4.26	-4.19	-4.11	-4.04	-3.98
6	-3.91	-3.84	-3.78	-3.71	-3.65	-3.59	-3.53	-3.47	-3.41	-3.36
7	-3.30	-3.25	-3.19	-3.14	-3.09	-3.03	-2.98	-2.93	-2.89	-2.84
8	-2.79	-2.74	-2.70	-2.65	-2.61	-2.57	-2.52	-2.48	-2.44	-2.40
9	-2.36	-2.32	-2.28	-2.24	-2.20	-2.17	-2.13	-2.09	-2.06	-2.02
1.0	-1.99	-1.95	-1.92	-1.89	-1.85	-1.82	-1.79	-1.76	-1.73	-1.70
1	-1.67	-1.64	-1.61	-1.58	-1.55	-1.53	-1.50	-1.47	-1.45	-1.42
2	-1.40	-1.37	-1.34	-1.32	-1.30	-1.27	-1.25	-1.23	-1.20	-1.18
3	-1.16	-1.14	-1.11	-1.09	-1.07	-1.05	-1.03	-1.01	-.99	-.97
4	-.95	-.94	-.92	-.90	-.88	-.86	-.85	-.83	-.81	-.80
5	-.78	-.76	-.75	-.73	-.72	-.70	-.69	-.67	-.66	-.64
	-.63	-.62	-.60	-.59	-.58	-.56	-.55	-.54	-.53	-.51
	-.50	-.49	-.48	-.47	-.46	-.45	-.44	-.42	-.41	-.40
8	-.39	-.38	-.38	-.37	-.36	-.35	-.34	-.33	-.32	-.31
9	-.30	-.30	-.29	-.28	-.27	-.27	-.26	-.25	-.24	-.24
2.0	-.23	-.22	-.22	-.21	-.21	-.20	-.19	-.19	-.18	-.18
1	-.17	-.17	-.16	-.16	-.15	-.15	-.14	-.14	-.13	-.13
2	-.12	-.12	-.11	-.11	-.11	-.10	-.10	-.10	-.09	-.09
3	-.09	-.08	-.08	-.08	-.07	-.07	-.07	-.06	-.06	-.06
4	-.06	-.05	-.05	-.05	-.05	-.05	-.04	-.04	-.04	-.04
5	-.04	-.03	-.03	-.03	-.03	-.03	-.03	-.02	-.02	-.02
6	-.02	-.02	-.02	-.02	-.02	-.02	-.01	-.01	-.01	-.01
7	-.01	-.01	-.01	-.01	-.01	-.01	-.01	-.01	-.01	-.01
8	-.00	-.00	-.00	-.00	-.00	-.00	-.00	-.00	-.00	-.00
9	-.00	-.00	-.00	-.00	-.00	-.01	-.01	-.01	-.01	-.01
3.0	-.00	-.00	-.00	-.00	-.00	-.00	-.00	-.00	-.00	-.00
1	-.00	-.00	-.00	-.00	-.00	-.00	-.00	-.00	-.00	-.00

END.

Table C-5 shows the effects of spectral energy loss in midband due to subtractive sine amplitude ripple $(1 - B(\omega))$, i.e., caused by midband "response droop" and band edge enhancement. The integrated spectral loss is found to be 0.25 dB.

Table C-6 takes the case of Table C-5 and adds to it the loss due to a 45° parabolic phase characteristic. The net loss is seen to increase by 0.09 dB to 0.34 dB.

Table C-7 presents the combined spectral energy distribution and distortion loss resulting from 30° linear and 45° parabolic phase departures, yielding a loss of 2.03 dB, without amplitude distortion.

Table C-8 shows the spectral energy distribution and distortion loss resulting from 30° linear phase departure only, yielding a loss of 1.34 dB, which is consistant with Fig. A-4 (no amplitude distortion).

Table C-9 demonstrates that a 30° linear loss summed with a 45° parabolic loss, in the presence of a 1-dB additive cosine amplitude ripple does not equal the loss resulting when <u>both</u> phase terms are present simultaneously. This should come as no surprise, considering the derivation required to produce Eq. (2.36), i.e., $\cos (A + B) \neq \cos A + \cos B$ (Ref. 14 Trig tables).

Table C-10 shows the large loss caused by the presence of midband droop, resulting in subtractive cosine ripple in the crucial central-spectrum zone. From Table C-10, a loss of 2.48 dB is compared to a loss 1.60 dB from Table C-9.

Table C-11 shows loss conditions as they would result from absence of the 1 dB peak-to-peak amplitude ripple component of Table C-10, resulting in approximately 0.5 dB less loss than given in that table.

From a study of the finding of these tables comes a set of useful guidelines capable of influencing the design and applications processes. These include:

1. The energy lying in the outer one-third of the signal spectrum contributes little to the useful energy of the received signal.

Table C-5. Loss Table for 1 dB Subtractive Ripple of 1.5 Cycles, No Phase Distortion

P(X) TIMES (SIN(X)/X) SQUARED IN DECIBELS
NORMALIZED TO AN UNDISTORTED SPECTRUM
FOR P(X) = (1-A(X))(COS(L(X)+P(X)+C(X)+DCOS(MX))+ESIN(NX)))((SIN(X)/X)2)
A(X) = 1.0 DB PK-PK RIPPLE AMPLITUDE IN 1.5 CYCLES
L(X) = 00 DEGREES LINEAR DISTORTION AT BAND EDGE
P(X) = 00 DEGREES PARABOLIC DISTORTION
C(X) = 0 DEGREES CUBIC DISTORTION
DCOS(MX) = 00 DEGREES PEAK AND 0.0 CYCLES RIPPLE
ESIN(NX) = 00 DEGREES PEAK AND 0.0 CYCLES RIPPLE
INTEGRATED FROM ZERO TO X IN STEPS OF 0.01 RADIAN

X	0.00	0.01	0.02	0.03	0.04	0.05	0.06	0.07	0.08	0.09
0.0	-144.18	-44.01	-38.07	-34.55	-32.05	-30.11	-28.53	-27.19	-26.03	-25.01
1	-24.10	-23.27	-22.52	-21.82	-21.15	-20.53	-20.02	-19.50	-19.00	-18.54
2	-18.09	-17.67	-17.27	-16.89	-16.52	-16.17	-15.83	-15.51	-15.19	-14.89
3	-14.60	-14.32	-14.05	-13.79	-13.53	-13.30	-13.04	-12.80	-12.58	-12.36
4	-12.14	-11.93	-11.73	-11.53	-11.33	-11.14	-10.96	-10.77	-10.60	-10.42
5	-10.25	-10.07	-9.89	-9.76	-9.61	-9.46	-9.31	-9.16	-9.01	-8.87
6	-8.73	-8.60	-8.46	-8.33	-8.20	-8.08	-7.95	-7.83	-7.71	-7.59
7	-7.47	-7.36	-7.24	-7.13	-7.02	-6.92	-6.81	-6.71	-6.60	-6.50
8	-6.40	-6.31	-6.21	-6.11	-6.02	-5.93	-5.84	-5.75	-5.66	-5.57
9	-5.49	-5.40	-5.32	-5.24	-5.16	-5.08	-5.00	-4.92	-4.84	-4.77
1.0	-4.69	-4.62	-4.55	-4.48	-4.41	-4.34	-4.27	-4.20	-4.14	-4.07
1	-4.01	-3.94	-3.88	-3.82	-3.75	-3.69	-3.63	-3.56	-3.52	-3.46
2	-3.40	-3.35	-3.29	-3.24	-3.19	-3.13	-3.08	-3.03	-2.98	-2.93
3	-2.88	-2.83	-2.78	-2.74	-2.69	-2.64	-2.60	-2.55	-2.51	-2.47
4	-2.42	-2.38	-2.34	-2.30	-2.26	-2.22	-2.18	-2.14	-2.10	-2.07
5	-2.03	-1.99	-1.96	-1.92	-1.89	-1.85	-1.82	-1.79	-1.75	-1.72
6	-1.69	-1.66	-1.63	-1.60	-1.57	-1.54	-1.51	-1.48	-1.45	-1.42
7	-1.40	-1.37	-1.34	-1.32	-1.29	-1.27	-1.24	-1.22	-1.20	-1.17
8	-1.15	-1.13	-1.11	-1.09	-1.06	-1.04	-1.02	-1.00	-.98	-.96
9	-.94	-.93	-.91	-.89	-.87	-.85	-.84	-.82	-.81	-.79
2.0	-.77	-.76	-.74	-.73	-.71	-.70	-.69	-.67	-.66	-.65
1	-.63	-.62	-.61	-.60	-.59	-.58	-.57	-.55	-.54	-.53
2	-.52	-.51	-.51	-.50	-.49	-.48	-.47	-.46	-.45	-.45
3	-.44	-.43	-.42	-.42	-.41	-.40	-.40	-.39	-.38	-.38
4	-.37	-.37	-.36	-.36	-.35	-.35	-.34	-.34	-.33	-.33
5	-.33	-.32	-.32	-.31	-.31	-.31	-.30	-.30	-.30	-.29
6	-.29	-.29	-.29	-.28	-.28	-.28	-.28	-.28	-.27	-.27
7	-.27	-.27	-.27	-.27	-.26	-.26	-.26	-.26	-.26	-.26
8	-.26	-.26	-.26	-.25	-.25	-.25	-.25	-.25	-.25	-.25
9	-.25	-.25	-.25	-.25	-.25	-.25	-.25	-.25	-.25	-.25
3.0	-.25	-.25	-.25	-.25	-.25	-.25	-.25	-.25	-.25	-.25
1	-.25	-.25	-.25	-.25	-.25	-.25	-.25	-.25	-.25	-.25

Table C-6. Loss Table for 1 dB Subtractive Ripple of 1.5 Cycles, plus 45° Parabolic Phase Distortion

```
                F(X) TIMES (SIN(X)/X) SQUARED IN DECIBELS
                  NORMALIZED TO AN UNDISTORTED SPECTRUM
FOR F(X) = (1-A(X))(COS(L(X)+P(X)+C(X)+ICOS(MX)+ESIN(NX)))((SIN(X)/X)2)
                   A(X) =  1.0 DB PK-PK RIPPLE AMPLITUDE IN 1.5 CYCLES
                   L(X) =  00 DEGREES LINEAR DISTORTION AT PAPE EDGE
                   P(X) =  45 DEGREES PARABOLIC DISTORTION
                   C(X) =   0 DEGREES CUBIC DISTORTION
                ICOS(MX) =  00 DEGREES PEAK AND 0.0 CYCLES RIPPLE
                ESIN(NX) =  00 DEGREES PEAK AND 0.0 CYCLES RIPPLE
                   INTEGRATED FLOM ZERO TO X IN STEPS OF 0.01 RADIAN
```

X	0.00	0.01	0.02	0.03	0.04	0.05	0.06	0.07	0.08	0.09
00	-144.18	-44.09	-39.07	-34.55	-32.05	-30.11	-28.53	-27.19	-26.03	-25.01
1	-24.19	-23.27	-22.52	-21.82	-21.18	-20.58	-20.02	-19.50	-19.00	-18.54
2	-18.09	-17.67	-17.27	-16.89	-16.52	-16.17	-15.83	-15.51	-15.19	-14.89
3	-14.60	-14.32	-14.05	-13.78	-13.53	-13.28	-13.04	-12.80	-12.58	-12.36
4	-12.14	-11.93	-11.73	-11.53	-11.33	-11.14	-10.96	-10.77	-10.60	-10.42
5	-10.25	-10.09	-9.92	-9.77	-9.61	-9.46	-9.31	-9.16	-9.01	-8.87
6	-8.73	-8.60	-8.46	-8.33	-8.20	-8.08	-7.95	-7.83	-7.71	-7.59
7	-7.47	-7.36	-7.25	-7.14	-7.03	-6.92	-6.81	-6.71	-6.61	-6.51
8	-6.41	-6.31	-6.21	-6.12	-6.02	-5.93	-5.84	-5.75	-5.66	-5.58
9	-5.49	-5.41	-5.32	-5.24	-5.16	-5.08	-5.00	-4.93	-4.85	-4.77
10	-4.70	-4.63	-4.56	-4.48	-4.41	-4.34	-4.28	-4.21	-4.14	-4.08
1	-4.01	-3.95	-3.89	-3.82	-3.76	-3.70	-3.64	-3.58	-3.53	-3.47
2	-3.41	-3.36	-3.30	-3.25	-3.20	-3.14	-3.09	-3.04	-2.99	-2.94
3	-2.89	-2.85	-2.80	-2.75	-2.70	-2.66	-2.61	-2.57	-2.53	-2.48
4	-2.44	-2.40	-2.36	-2.32	-2.28	-2.24	-2.20	-2.16	-2.12	-2.09
5	-2.05	-2.02	-1.98	-1.94	-1.91	-1.88	-1.84	-1.81	-1.78	-1.75
6	-1.72	-1.69	-1.66	-1.63	-1.60	-1.57	-1.54	-1.51	-1.48	-1.46
7	-1.43	-1.40	-1.38	-1.35	-1.33	-1.31	-1.28	-1.26	-1.24	-1.21
8	-1.19	-1.17	-1.15	-1.13	-1.11	-1.09	-1.07	-1.05	-1.03	-1.01
9	-.99	-.97	-.95	-.94	-.92	-.90	-.89	-.87	-.86	-.84
20	-.83	-.81	-.80	-.78	-.77	-.76	-.74	-.73	-.72	-.71
1	-.69	-.68	-.67	-.66	-.65	-.64	-.63	-.62	-.61	-.60
2	-.59	-.58	-.57	-.56	-.56	-.55	-.54	-.53	-.52	-.52
3	-.51	-.50	-.50	-.49	-.48	-.48	-.47	-.47	-.46	-.46
4	-.45	-.45	-.44	-.44	-.43	-.43	-.42	-.42	-.42	-.41
5	-.41	-.40	-.40	-.40	-.40	-.39	-.39	-.39	-.38	-.38
6	-.38	-.38	-.37	-.37	-.37	-.37	-.37	-.37	-.36	-.36
7	-.36	-.36	-.36	-.36	-.36	-.35	-.35	-.35	-.35	-.35
8	-.35	-.35	-.35	-.35	-.35	-.35	-.35	-.35	-.35	-.34
9	-.34	-.34	-.34	-.34	-.34	-.34	-.34	-.34	-.34	-.34
30	-.34	-.34	-.34	-.34	-.34	-.34	-.34	-.34	-.34	-.34
1	-.34	-.34	-.34	-.34	-.34	-.34	-.34	-.34	-.34	-.34

```
END.

00020*/,12X/* A(X) = 1.0 DB PK-PK RIPPLE AMPLITUDE IN 1.5 CYCLES*/
00030 XCPSPE=(1-0.11662*COS(1.5*X))*(COS((0.2821*X)**2))
RPP
```

Table C-7. Loss Table for Zero Amplitude Distortion, plus 30° Linear and 45° Parabolic Phase Distortion

F(X) TIMES (SIN(X)/X) SQUARED IN DECIBELS
NORMALIZED TO AN UNDISTORTED SPECTRUM
FOR F(X) = (1-A(X))(COS(L(X)+P(X)+C(X)+ECOS(NX)+ESIN(NX)))((SIN(X)/X)2)
A(X) = 0.0 TO PK-PK RIPPLE AMPLITUDE IN 0.0 CYCLES
L(X) = 30 DEGREES LINEAR DISTORTION AT BAND EDGES
P(X) = 45 DEGREES PARABOLIC DISTORTION AT BAND EDGES
C(X) = 0 DEGREES CUBIC DISTORTION
ECOS(NX) = 00 DEGREES PEAK AND 0.0 CYCLES RIPPLE
ESIN(NX) = 00 DEGREES PEAK AND 0.0 CYCLES RIPPLE
INTEGRATED FROM ZERO TO X IN STEPS OF 0.01 RADIAN

X	0.00	0.01	0.02	0.03	0.04	0.05	0.06	0.07	0.08	0.09
0.0	-143.12	-43.04	-37.01	-33.49	-31.00	-29.06	-27.48	-26.14	-24.98	-23.96
1	-23.05	-22.22	-21.47	-20.78	-20.14	-19.54	-18.99	-18.47	-17.97	-17.51
2	-17.07	-16.65	-16.25	-15.87	-15.51	-15.17	-14.83	-14.51	-14.20	-13.90
3	-13.62	-13.34	-13.07	-12.82	-12.57	-12.32	-12.09	-11.86	-11.64	-11.42
4	-11.22	-11.01	-10.82	-10.62	-10.44	-10.25	-10.07	-9.90	-9.73	-9.57
5	-9.40	-9.25	-9.09	-8.94	-8.79	-8.65	-8.51	-8.37	-8.24	-8.10
6	-7.97	-7.85	-7.72	-7.60	-7.48	-7.37	-7.25	-7.14	-7.03	-6.92
7	-6.82	-6.71	-6.61	-6.51	-6.42	-6.32	-6.23	-6.13	-6.04	-5.95
8	-5.87	-5.78	-5.70	-5.62	-5.53	-5.46	-5.38	-5.30	-5.23	-5.15
9	-5.08	-5.01	-4.94	-4.87	-4.80	-4.74	-4.67	-4.61	-4.55	-4.49
1.0	-4.43	-4.37	-4.31	-4.25	-4.20	-4.14	-4.09	-4.04	-3.99	-3.93
1	-3.89	-3.84	-3.79	-3.74	-3.70	-3.65	-3.61	-3.56	-3.52	-3.48
2	-3.44	-3.40	-3.36	-3.32	-3.28	-3.25	-3.21	-3.17	-3.14	-3.11
3	-3.07	-3.04	-3.01	-2.98	-2.95	-2.92	-2.89	-2.86	-2.83	-2.80
4	-2.78	-2.75	-2.73	-2.70	-2.68	-2.65	-2.63	-2.61	-2.59	-2.56
5	-2.54	-2.52	-2.50	-2.48	-2.46	-2.45	-2.43	-2.41	-2.39	-2.38
6	-2.36	-2.35	-2.33	-2.32	-2.30	-2.29	-2.27	-2.26	-2.25	-2.24
7	-2.22	-2.21	-2.20	-2.19	-2.18	-2.17	-2.16	-2.15	-2.14	-2.13
8	-2.12	-2.12	-2.11	-2.10	-2.09	-2.09	-2.08	-2.07	-2.07	-2.06
9	-2.06	-2.05	-2.05	-2.04	-2.04	-2.03	-2.03	-2.02	-2.02	-2.02
2.0	-2.01	-2.01	-2.01	-2.00	-2.00	-2.00	-2.00	-1.99	-1.99	-1.99
1	-1.99	-1.99	-1.99	-1.99	-1.98	-1.98	-1.98	-1.98	-1.98	-1.98
2	-1.98	-1.98	-1.98	-1.98	-1.98	-1.98	-1.98	-1.98	-1.98	-1.98
3	-1.98	-1.98	-1.98	-1.98	-1.98	-1.98	-1.98	-1.99	-1.99	-1.99
4	-1.99	-1.99	-1.99	-1.99	-1.99	-1.99	-1.99	-1.99	-2.00	-2.00
5	-2.00	-2.00	-2.00	-2.00	-2.00	-2.00	-2.00	-2.00	-2.01	-2.01
6	-2.01	-2.01	-2.01	-2.01	-2.01	-2.01	-2.01	-2.01	-2.01	-2.02
7	-2.02	-2.02	-2.02	-2.02	-2.02	-2.02	-2.02	-2.02	-2.02	-2.02
8	-2.02	-2.02	-2.02	-2.02	-2.03	-2.03	-2.03	-2.03	-2.03	-2.03
9	-2.03	-2.03	-2.03	-2.03	-2.03	-2.03	-2.03	-2.03	-2.03	-2.03
3.0	-2.03	-2.03	-2.03	-2.03	-2.03	-2.03	-2.03	-2.03	-2.03	-2.03
1	-2.03	-2.03	-2.03	-2.03	-2.03	-2.03	-2.03	-2.03	-2.03	-2.03

Table C-8. Loss Table for Zero Amplitude Ripple plus 30° Linear Phase Distortion

F(X) TIMES (SIN(X)/X) SQUARED IN DECIBELS
NORMALIZED TO AN UNDISTORTED SPECTRUM
FOR F(X) = (1-A(X))(COS(L(X)+P(X)+C(X)+LCOS(NX))+ESIN(NX)))((SIN(X)/X)2)
A(X) = 0.0 DB PEAK-PEAK RIPPLE AMPLITUDE IN 0.0 CYCLES
L(X) = 30 DEGREES LINEAR DISTORTION AT BAND EDGE
P(X) = 00 DEGREES PARABOLIC DISTORTION
C(X) = 0 DEGREES CUBIC DISTORTION
LCOS(NX) = 00 DEGREES PEAK AND 0.0 CYCLES RIPPLE
ESIN(NX) = 00 DEGREES PEAK AND 0.0 CYCLES RIPPLE
INTEGRATED FROM ZERO TO X IN STEPS OF 0.01 RADIAN

X	0.00	0.01	0.02	0.03	0.04	0.05	0.06	0.07	0.08	0.09
0.0	-143.12	-43.04	-37.01	-33.49	-31.00	-29.06	-27.49	-26.14	-24.94	-23.86
1	-23.05	-22.22	-21.47	-20.78	-20.14	-19.54	-18.99	-18.47	-17.97	-17.51
2	-17.07	-16.65	-16.25	-15.87	-15.51	-15.16	-14.83	-14.51	-14.20	-13.90
3	-13.61	-13.34	-13.07	-12.81	-12.56	-12.32	-12.08	-11.86	-11.63	-11.42
4	-11.21	-11.01	-10.81	-10.62	-10.43	-10.24	-10.07	-9.89	-9.72	-9.55
5	-9.39	-9.23	-9.08	-8.93	-8.78	-8.63	-8.49	-8.35	-8.22	-8.09
6	-7.96	-7.83	-7.70	-7.58	-7.46	-7.34	-7.23	-7.11	-7.00	-6.89
7	-6.79	-6.68	-6.58	-6.48	-6.38	-6.28	-6.19	-6.09	-6.00	-5.91
8	-5.82	-5.73	-5.65	-5.57	-5.48	-5.40	-5.32	-5.24	-5.17	-5.09
9	-5.02	-4.94	-4.87	-4.80	-4.73	-4.66	-4.60	-4.53	-4.47	-4.40
1.0	-4.34	-4.28	-4.22	-4.16	-4.10	-4.04	-3.99	-3.93	-3.88	-3.82
1	-3.77	-3.72	-3.67	-3.62	-3.57	-3.52	-3.48	-3.43	-3.38	-3.34
2	-3.29	-3.25	-3.21	-3.17	-3.13	-3.09	-3.05	-3.01	-2.97	-2.93
3	-2.89	-2.86	-2.82	-2.79	-2.75	-2.72	-2.69	-2.65	-2.62	-2.59
4	-2.56	-2.53	-2.50	-2.47	-2.44	-2.42	-2.39	-2.36	-2.34	-2.31
5	-2.29	-2.26	-2.24	-2.21	-2.19	-2.17	-2.15	-2.12	-2.10	-2.08
6	-2.06	-2.04	-2.02	-2.00	-1.98	-1.96	-1.95	-1.93	-1.91	-1.89
7	-1.88	-1.86	-1.85	-1.83	-1.82	-1.80	-1.79	-1.77	-1.76	-1.75
8	-1.73	-1.72	-1.71	-1.70	-1.68	-1.67	-1.66	-1.65	-1.64	-1.63
9	-1.62	-1.61	-1.60	-1.59	-1.58	-1.57	-1.56	-1.56	-1.55	-1.54
2.0	-1.53	-1.52	-1.52	-1.51	-1.50	-1.50	-1.49	-1.48	-1.48	-1.47
1	-1.47	-1.46	-1.46	-1.45	-1.45	-1.44	-1.44	-1.43	-1.43	-1.42
2	-1.42	-1.42	-1.41	-1.41	-1.40	-1.40	-1.40	-1.40	-1.39	-1.39
3	-1.39	-1.38	-1.38	-1.38	-1.38	-1.37	-1.37	-1.37	-1.37	-1.37
4	-1.36	-1.36	-1.36	-1.36	-1.36	-1.36	-1.36	-1.35	-1.35	-1.35
5	-1.35	-1.35	-1.35	-1.35	-1.35	-1.35	-1.35	-1.34	-1.34	-1.34
6	-1.34	-1.34	-1.34	-1.34	-1.34	-1.34	-1.34	-1.34	-1.34	-1.34
7	-1.34	-1.34	-1.34	-1.34	-1.34	-1.34	-1.34	-1.34	-1.34	-1.34
8	-1.34	-1.34	-1.34	-1.34	-1.34	-1.34	-1.34	-1.34	-1.34	-1.34
9	-1.34	-1.34	-1.34	-1.34	-1.34	-1.34	-1.34	-1.34	-1.34	-1.34
3.0	-1.34	-1.34	-1.34	-1.34	-1.34	-1.34	-1.34	-1.34	-1.34	-1.34
1	-1.34	-1.34	-1.34	-1.34	-1.34	-1.34	-1.34	-1.34	-1.34	-1.34

Table C-9. Loss Table for 1 dB Additive Amplitude Ripple at 1.5 Cycles plus 30° Linear and 45° Parabolic Phase Distortion Components

F(X) TIMES (SIN(X)/X) SQUARED IN DECIBELS
NORMALIZED TO AN UNDISTORTED SPECTRUM
F(X) = (1+A(X))(COS(L(X)+P(X)+C(X)+DCOS(MX)+ESIN(NX)))((SIN(X)/X)2)
A(X) = 1.0 DB PK-PK RIPPLE AMPLITUDE IN 1.5 CYCLES
L(X) = 30 DEGREES LINEAR DISTORTION AT BAND EDGES
P(X) = 45 DEGREES PARABOLIC DISTORTION AT BAND EDGES
C(X) = 0 DEGREES CUBIC DISTORTION
DCOS(MX) = 00 DEGREES PEAK AND 0.0 CYCLES RIPPLE
ESIN(NX) = 00 DEGREES PEAK AND 0.0 CYCLES RIPPLE
INTEGRATED FROM ZERO TO X IN STEPS OF 0.01 RADIAN

X	0.00	0.01	0.02	0.03	0.04	0.05	0.06	0.07	0.08	0.09
00	-142.18	-42.09	-36.07	-32.55	-30.05	-28.12	-26.54	-25.20	-24.04	-23.02
1	-22.11	-21.29	-20.53	-19.84	-19.20	-18.61	-18.05	-17.53	-17.04	-16.58
2	-16.14	-15.72	-15.33	-14.95	-14.59	-14.24	-13.91	-13.59	-13.28	-12.99
3	-12.70	-12.43	-12.16	-11.91	-11.66	-11.42	-11.19	-10.96	-10.74	-10.53
4	-10.33	-10.12	-9.93	-9.74	-9.55	-9.37	-9.20	-9.03	-8.86	-8.70
5	-8.54	-8.39	-8.23	-8.09	-7.94	-7.80	-7.66	-7.53	-7.40	-7.27
6	-7.14	-7.02	-6.90	-6.78	-6.67	-6.55	-6.44	-6.33	-6.23	-6.12
7	-6.02	-5.92	-5.82	-5.73	-5.63	-5.54	-5.45	-5.36	-5.28	-5.19
8	-5.11	-5.03	-4.95	-4.87	-4.79	-4.72	-4.64	-4.57	-4.50	-4.43
9	-4.36	-4.30	-4.23	-4.17	-4.10	-4.04	-3.98	-3.92	-3.86	-3.81
1.0	-3.75	-3.69	-3.64	-3.59	-3.54	-3.49	-3.44	-3.39	-3.34	-3.29
.1	-3.25	-3.20	-3.16	-3.12	-3.07	-3.03	-2.99	-2.95	-2.91	-2.88
.2	-2.84	-2.80	-2.77	-2.73	-2.70	-2.66	-2.63	-2.60	-2.57	-2.54
3	-2.51	-2.48	-2.45	-2.42	-2.40	-2.37	-2.34	-2.32	-2.29	-2.27
4	-2.24	-2.22	-2.20	-2.18	-2.16	-1	-2.09	-2.08	-2.06	-2.04
5	-2.04	-2.02	-2.00	-1.99	-1.97	-1.95	-1.94	-1.92	-1.91	-1.89
6	-1.88	-1.87	-1.85	-1.84	-1.83	-1.82	-1.80	-1.79	-1.78	-1.77
7	-1.76	-1.75	-1.74	-1.73	-1.72	-1.72	-1.71	-1.70	-1.69	-1.68
8	-1.68	-1.67	-1.66	-1.66	-1.65	-1.64	-1.64	-1.63	-1.63	-1.62
9	-1.62	-1.61	-1.61	-1.61	-1.60	-1.60	-1.59	-1.59	-1.59	-1.58
2.0	-1.58	-1.58	-1.58	-1.57	-1.57	-1.57	-1.57	-1.57	-1.56	-1.56
1	-1.56	-1.56	-1.56	-1.56	-1.56	-1.56	-1.56	-1.56	-1.56	-1.55
2	-1.55	-1.55	-1.55	-1.55	-1.55	-1.55	-1.55	-1.55	-1.55	-1.55
3	-1.55	-1.56	-1.56	-1.56	-1.56	-1.56	-1.56	-1.56	-1.56	-1.56
4	-1.56	-1.56	-1.56	-1.56	-1.56	-1.56	-1.57	-1.57	-1.57	-1.57
5	-1.57	-1.57	-1.57	-1.57	-1.57	-1.57	-1.57	-1.58	-1.58	-1.58
6	-1.58	-1.58	-1.58	-1.58	-1.58	-1.58	-1.58	-1.58	-1.58	-1.59
7	-1.59	-1.59	-1.59	-1.59	-1.59	-1.59	-1.59	-1.59	-1.59	-1.59
8	-1.59	-1.59	-1.59	-1.59	-1.59	-1.59	-1.59	-1.59	-1.60	-1.60
9	-1.60	-1.60	-1.60	-1.60	-1.60	-1.60	-1.60	-1.60	-1.60	-1.60
3.0	-1.60	-1.60	-1.60	-1.60	-1.60	-1.60	-1.60	-1.60	-1.60	-1.60
1	-1.60	-1.60	-1.60	-1.60	-1.60	-1.60	-1.60	-1.60	-1.60	-1.60

Table C-10. Loss Table for 1 dB Subtractive Ripple of 1.5 Cycles plus 30° Linear and 45° Parabolic Phase Distortion

```
F(X) = (1-A(X))(COS(L(X)+P(X)+C(X)+DCOS(MX)+ESIN(NX)))((SIN(X)/X)2)
       A(X) = 1.0 DB PK-PK RIPPLE AMPLITUDE IN 1.5 CYCLES
       L(X) = 30 DEGREES LINEAR DISTORTION AT BAND EDGES
       P(X) = 45 DEGREES PARABOLIC DISTORTION AT BAND EDGES
       C(X) =  0 DEGREES CUBIC DISTORTION
  DCOS(MX) = 00 DEGREES PEAK AND 0.0 CYCLES RIPPLE
  ESIN(NX) = 00 DEGREES PEAK AND 0.0 CYCLES RIPPLE
     INTEGRATED FROM ZERO TO X IN STEPS OF 0.01 RADIAN
```

X	0.00	0.01	0.02	0.03	0.04	0.05	0.06	0.07	0.08	0.09
0.0	-144.18	-44.09	-38.07	-34.55	-32.05	-30.12	-28.53	-27.20	-26.04	-25.02
1	-24.10	-23.28	-22.52	-21.83	-21.19	-20.59	-20.03	-19.51	-19.02	-18.55
2	-18.11	-17.69	-17.29	-16.91	-16.54	-16.19	-15.86	-15.54	-15.23	-14.93
3	-14.64	-14.36	-14.09	-13.83	-13.58	-13.33	-13.09	-12.86	-12.64	-12.42
4	-12.21	-12.00	-11.80	-11.61	-11.42	-11.23	-11.05	-10.87	-10.70	-10.53
5	-10.36	-10.20	-10.04	-9.89	-9.74	-9.59	-9.44	-9.30	-9.16	-9.03
6	-8.89	-8.76	-8.64	-8.51	-8.39	-8.27	-8.15	-8.03	-7.92	-7.80
7	-7.69	-7.59	-7.48	-7.38	-7.27	-7.17	-7.07	-6.98	-6.88	-6.79
8	-6.70	-6.61	-6.52	-6.43	-6.35	-6.26	-6.18	-6.10	-6.02	-5.94
9	-5.86	-5.79	-5.71	-5.64	-5.57	-5.50	-5.43	-5.36	-5.29	-5.23
1.0	-5.16	-5.10	-5.04	-4.97	-4.91	-4.85	-4.80	-4.74	-4.68	-4.63
1	-4.57	-4.52	-4.47	-4.42	-4.37	-4.32	-4.27	-4.22	-4.17	-4.13
2	-4.08	-4.04	-3.99	-3.95	-3.91	-3.87	-3.83	-3.79	-3.75	-3.71
3	-3.68	-3.64	-3.60	-3.57	-3.54	-3.50	-3.47	-3.44	-3.41	-3.37
4	-3.34	-3.32	-3.29	-3.26	-3.23	-3.20	-3.18	-3.15	-3.13	-3.10
5	-3.08	-3.06	-3.03	-3.01	-2.99	-2.97	-2.95	-2.93	-2.91	-2.89
6	-2.87	-2.85	-2.84	-2.82	-2.80	-2.79	-2.77	-2.75	-2.74	-2.73
7	-2.71	-2.70	-2.69	-2.67	-2.66	-2.65	-2.64	-2.63	-2.62	-2.61
8	-2.60	-2.59	-2.58	-2.57	-2.56	-2.55	-2.54	-2.54	-2.53	-2.52
9	-2.52	-2.51	-2.50	-2.50	-2.49	-2.49	-2.48	-2.48	-2.47	-2.47
0	-2.47	-2.46	-2.46	-2.46	-2.45	-2.45	-2.45	-2.44	-2.44	-2.44
2.1	-2.44	-2.44	-2.43	-2.43	-2.43	-2.43	-2.43	-2.43	-2.43	-2.43
2	-2.43	-2.43	-2.43	-2.43	-2.43	-2.43	-2.43	-2.43	-2.43	-2.43
3	-2.43	-2.43	-2.43	-2.43	-2.43	-2.43	-2.43	-2.43	-2.43	-2.44
4	-2.44	-2.44	-2.44	-2.44	-2.44	-2.44	-2.44	-2.44	-2.45	-2.45
5	-2.45	-2.45	-2.45	-2.45	-2.45	-2.45	-2.45	-2.46	-2.46	-2.46
6	-2.46	-2.46	-2.46	-2.46	-2.46	-2.46	-2.47	-2.47	-2.47	-2.47
7	-2.47	-2.47	-2.47	-2.47	-2.47	-2.47	-2.47	-2.48	-2.48	-2.48
8	-2.48	-2.48	-2.48	-2.48	-2.48	-2.48	-2.48	-2.48	-2.48	-2.48
9	-2.48	-2.48	-2.48	-2.48	-2.48	-2.48	-2.48	-2.48	-2.48	-2.48
3.0	-2.48	-2.48	-2.48	-2.48	-2.48	-2.48	-2.48	-2.48	-2.48	-2.48
1	-2.48	-2.48	-2.48	-2.48	-2.48	-2.48	-2.48	-2.48	-2.48	-2.48

```
00810 XCPSMP=(1-0.11468*COS(1.5*X))*(COS((0.5236*X)+(0.2821*X)**2
00820+ +(0.000*X)**3+0.00*SIN(0.0*X)+0.00*COS(0.0*X)))
00830+ *((SIN(X)/X)**2)*(0.7051)
```

Table C-11. Loss Table for Zero Amplitude Ripple plus 30° Linear and 45° Parabolic Phase Distortion

F(X) TIMES (SIN(X)/X) SQUARED IN DECIBELS
NORMALIZED TO AN UNDISTORTED SPECTRUM
F(X) = (1-A(X))(COS(L(X)+P(X)+C(X)+DCOS(MX)+ESIN(NX)))((SIN(X)/X)2)
A(X) = 0.0 DB PK-PK RIPPLE AMPLITUDE IN 1.5 CYCLES
L(X) = 30 DEGREES LINEAR DISTORTION AT BAND EDGES
P(X) = 45 DEGREES PARABOLIC DISTORTION AT BAND EDGES
C(X) = 0 DEGREES CUBIC DISTORTION
DCOS(MX) = 00 DEGREES PEAK AND 0.0 CYCLES RIPPLE
ESIN(NX) = 00 DEGREES PEAK AND 0.0 CYCLES RIPPLE
INTEGRATED FROM ZERO TO X IN STEPS OF 0.01 RADIAN

X	0.00	0.01	0.02	0.03	0.04	0.05	0.06	0.07	0.08	0.09
0.0	-143.12	-43.04	-37.01	-33.49	-31.00	-29.06	-27.48	-26.14	-24.98	-23.96
1	-23.05	-22.22	-21.47	-20.78	-20.14	-19.54	-18.99	-18.47	-17.97	-17.51
2	-17.07	-16.65	-16.25	-15.87	-15.51	-15.16	-14.83	-14.51	-14.20	-13.90
3	-13.62	-13.34	-13.07	-12.82	-12.57	-12.32	-12.09	-11.86	-11.64	-11.42
4	-11.22	-11.01	-10.82	-10.62	-10.44	-10.25	-10.07	-9.90	-9.73	-9.57
5	-9.40	-9.25	-9.09	-8.94	-8.79	-8.65	-8.51	-8.37	-8.24	-8.10
6	-7.97	-7.85	-7.72	-7.60	-7.48	-7.37	-7.25	-7.14	-7.03	-6.92
7	-6.82	-6.71	-6.61	-6.51	-6.42	-6.32	-6.23	-6.13	-6.04	-5.95
8	-5.87	-5.78	-5.70	-5.62	-5.53	-5.46	-5.38	-5.30	-5.23	-5.15
9	-5.08	-5.01	-4.94	-4.87	-4.80	-4.74	-4.67	-4.61	-4.55	-4.49
1.0	-4.43	-4.37	-4.31	-4.25	-4.20	-4.14	-4.09	-4.04	-3.99	-3.93
1	-3.89	-3.84	-3.79	-3.74	-3.70	-3.65	-3.61	-3.56	-3.52	-3.48
2	-3.44	-3.40	-3.36	-3.32	-3.28	-3.25	-3.21	-3.17	-3.14	-3.11
3	-3.07	-3.04	-3.01	-2.98	-2.95	-2.92	-2.89	-2.86	-2.83	-2.80
4	-2.78	-2.75	-2.73	-2.70	-2.68	-2.65	-2.63	-2.61	-2.59	-2.56
5	-2.54	-2.52	-2.50	-2.48	-2.46	-2.45	-2.43	-2.41	-2.39	-2.38
6	-2.36	-2.35	-2.33	-2.32	-2.30	-2.29	-2.27	-2.26	-2.25	-2.24
7	-2.22	-2.21	-2.20	-2.19	-2.18	-2.17	-2.16	-2.15	-2.14	-2.13
8	-2.12	-2.12	-2.11	-2.10	-2.09	-2.09	-2.08	-2.07	-2.07	-2.06
9	-2.06	-2.05	-2.05	-2.04	-2.04	-2.03	-2.03	-2.02	-2.02	-2.02
2.0	-2.01	-2.01	-2.01	-2.00	-2.00	-2.00	-2.00	-1.99	-1.99	-1.99
1	-1.99	-1.99	-1.99	-1.99	-1.98	-1.98	-1.98	-1.98	-1.98	-1.98
2	-1.98	-1.98	-1.98	-1.98	-1.98	-1.98	-1.98	-1.98	-1.98	-1.98
3	-1.98	-1.98	-1.98	-1.98	-1.98	-1.98	-1.98	-1.99	-1.99	-1.99
4	-1.99	-1.99	-1.99	-1.99	-1.99	-1.99	-1.99	-1.99	-2.00	-2.00
5	-2.00	-2.00	-2.00	-2.00	-2.00	-2.00	-2.00	-2.00	-2.01	-2.01
6	-2.01	-2.01	-2.01	-2.01	-2.01	-2.01	-2.01	-2.01	-2.01	-2.02
7	-2.02	-2.02	-2.02	-2.02	-2.02	-2.02	-2.02	-2.02	-2.02	-2.02
8	-2.02	-2.02	-2.02	-2.02	-2.03	-2.03	-2.03	-2.03	-2.03	-2.03
9	-2.03	-2.03	-2.03	-2.03	-2.03	-2.03	-2.03	-2.03	-2.03	-2.03
3.0	-2.03	-2.03	-2.03	-2.03	-2.03	-2.03	-2.03	-2.03	-2.03	-2.03
1	-2.03	-2.03	-2.03	-2.03	-2.03	-2.03	-2.03	-2.03	-2.03	-2.03

2. The distortion characteristics in the outer third of the passband may require less control than previously thought necessary.

3. Minimizing phase distortion seems to be more important than reduction of amplitude distortion, except at midband.

4. Phase losses in the outer half of the passband may be nearly neutralized by amplitude enhancement in that region, assuming negligible noise enhancement effects (see Appendix D).

5. Amplitude hard limiting is effective in reducing the effects of amplitude distortion, so in PN systems design should be employed whereever possible. Attention should also be directed to minimization of phase distortion.

6. Phase distortion ripple effects remaining after application of equalization may be evaluated by application of the charts and formulas presented herein. Repeated DGD plots and application of the curves can assist significantly in optimal reduction of phase distortion loss.

7. Obtaining system performance visibility via the method of Appendix C enables study of passband width, considering such variables as spectral utilization, distortion control, as well as hardware design and fabrication tradeoffs. Tables C-1 and C-2 show zero-loss after bandpass utilization of $x = 2.24/\pi$ and of $x = 2.17/\pi$, respectively, where $x = \pi$ at band edge, showing one needs control phase characteristics only within the central 70% of the first nulls.

APPENDIX D. NOISE ENHANCEMENT EFFECTS

D.1 S/N DEGRADATION DUE TO COMPLEMENTARY PASSBAND AMPLITUDE RIPPLE

In a linear system, the throughput passband amplitude characteristic of a receiver and a transmitter operating in tandem, under the condition of identical or complimentary envelope-ripple characteristics, may compensate into passband flatness, or may combine to produce degradation in the throughput signal-to-noise ratio (S/N) (Ref. 18).

When the center of the passband has a dip in midband gain, perhaps as typified by the passband of Fig. B-1, white Gaussian noise energy at the input may be emphasized to the extent that the correlator demodulator input S/N is degraded significantly. The following analysis is based upon the two special cases of identical and of complementary passband amplitude ripple. Tables D-1 through D-4 permit reader evaluation of the extent to which noise energy will be enhanced at the expense of signal energy under those two conditions. The findings are consistant with those of Appendix A in showing that the loss effects may be neglected if the ripple rate exceeds about 4 cycles across the passband for phase-shift-keyed applications.

D.2 CALCULATION OF THE DEGRADATION

Terms are defined for simple models of amplitude passband ripple similar to Eq. (D.1) and for the passband model of Fig. B-1. A receiving passband and a transmitting passband are defined inband by the following equations:

$$\text{Transmitter} \quad A_t(\omega) = 1 + a_t \cos(m\omega/4B) \tag{D.1}$$

$$\text{Receiver} \quad A_r(\omega) = 1 + a_r \cos(m\omega/4B) \tag{D.2}$$

Table D-1. S/N Loss Table for Amplitude Ripple Function (1 - a cos(Mx))

SIGNAL-TO-NOISE LOSS TABLE FOR AMPLITUDE FUNCTION (1-a(COS(mX)))

DEGRADATION IN DECIBELS VERSUS RIPPLE CYCLES 'm' IN PERIODS

PEAK-TO-PEAK RIPPLE IN DECIBELS

"m"	.10	.20	.30	.40	.50	.60	.70	.80	.90	1.00
0.	.101	.202	.305	.409	.514	.621	.728	.837	.947	1.057
.100	.100	.201	.303	.407	.511	.617	.724	.832	.941	1.051
.200	.098	.198	.298	.400	.503	.607	.712	.818	.925	1.033
.300	.096	.192	.290	.389	.489	.589	.691	.794	.898	1.003
.400	.092	.185	.279	.374	.469	.566	.664	.762	.862	.962
.500	.087	.176	.265	.355	.445	.537	.629	.723	.817	.912
.600	.082	.165	.248	.333	.413	.503	.590	.677	.765	.854
.800	.070	.140	.211	.282	.354	.426	.499	.572	.646	.720
1.000	.056	.113	.169	.226	.284	.342	.400	.458	.517	.575
1.200	.043	.085	.123	.171	.215	.258	.302	.345	.389	.433
1.400	.030	.060	.090	.121	.151	.182	.212	.243	.273	.304
1.600	.019	.039	.058	.078	.097	.117	.137	.156	.176	.195
1.800	.011	.022	.033	.045	.056	.067	.078	.089	.100	.111
2.000	.005	.010	.016	.021	.026	.031	.037	.042	.047	.052
2.200	.002	.003	.005	.006	.008	.009	.011	.012	.014	.015
2.400	-.000	-.001	-.001	-.002	-.002	-.002	-.003	-.003	-.003	-.004
2.800	-.001	-.002	-.003	-.004	-.005	-.005	-.006	-.007	-.008	-.009
3.200	-.000	-.000	-.000	-.000	-.000	-.000	-.000	-.000	-.000	-.000
3.600	.000	.001	.001	.001	.002	.002	.002	.003	.003	.004
4.000	.000	.000	.000	.001	.001	.001	.001	.001	.001	.001
5.000	-.000	-.000	-.000	-.000	-.000	-.000	-.000	-.000	-.000	-.000
6.000	.000	.000	.000	.000	.000	.000	.000	.000	.000	.000
7.000	-.000	-.000	-.000	-.000	-.000	-.000	-.000	-.000	-.000	-.000
8.000	.000	.000	.000	.000	.000	.000	.000	.000	.000	.000
9.000	-.000	-.000	-.000	-.000	-.000	-.000	-.000	-.000	-.000	-.000
*.000	.000	.000	.000	.000	.000	.000	.000	.000	.000	.000

Table D-2. S/N Loss Table for Amplitude Ripple Function (1 - a sin(Mx))

SIGNAL-TO-NOISE LOSS TABLE FOR AMPLITUDE FUNCTION (1 - a(SIN(mX)))

DEGRADATION IN DECIBELS VERSUS RIPPLE CYCLES "m" IN PERIODS

	PEAK-TO-PEAK RIPPLE IN DECIBELS									
"m"	.09	.17	.26	.35	.43	.52	.61	.70	.78	.87
0.	.000	.000	.000	.000	.000	.000	.000	.000	.000	.000
.100	.007	.015	.022	.030	.037	.045	.052	.060	.067	.075
.200	.015	.030	.044	.059	.074	.089	.104	.119	.134	.149
.300	.022	.044	.065	.087	.109	.131	.153	.176	.198	.220
.400	.029	.057	.085	.114	.143	.171	.200	.229	.258	.288
.500	.034	.069	.104	.138	.173	.208	.244	.279	.314	.350
.600	.040	.080	.120	.160	.201	.241	.282	.323	.365	.406
.300	.043	.087	.146	.195	.244	.294	.344	.394	.445	.495
1.000	.054	.107	.162	.216	.271	.326	.382	.438	.494	.551
1.200	.056	.111	.168	.224	.281	.339	.396	.454	.513	.572
1.400	.055	.110	.165	.221	.277	.333	.390	.447	.504	.562
1.600	.051	.103	.155	.208	.260	.314	.367	.421	.475	.529
1.300	.047	.094	.141	.189	.237	.285	.333	.382	.431	.480
2.000	.042	.083	.125	.167	.210	.252	.295	.338	.381	.425
2.200	.036	.073	.109	.146	.183	.220	.257	.294	.332	.369
2.400	.031	.063	.095	.126	.158	.190	.222	.254	.287	.319
2.600	.024	.048	.073	.097	.122	.146	.171	.195	.220	.245
3.200	.020	.040	.061	.081	.101	.122	.142	.163	.183	.204
3.600	.018	.036	.054	.072	.090	.108	.126	.145	.163	.181
4.000	.016	.033	.049	.065	.081	.098	.114	.131	.147	.164
5.000	.013	.025	.038	.050	.063	.075	.088	.101	.113	.126
6.000	.010	.021	.031	.042	.052	.063	.074	.084	.095	.105
7.000	.009	.018	.027	.035	.044	.053	.062	.071	.080	.089
8.000	.008	.016	.023	.031	.039	.047	.055	.062	.070	.078
9.000	.007	.014	.021	.027	.034	.041	.048	.055	.062	.069
*.000	.006	.012	.019	.025	.031	.037	.043	.050	.056	.062

for $|\omega| \leq 2\pi B$ where B is the band-edge frequency in Hertz and is defined outside the passband by

$$A_t(\omega) = A_r(\omega) = 0$$

where $\omega = 0$ at band center. The coefficients a_t and a_r are the peak departures from the ideal rectangular response and m is the amplitude ripple-rate coefficient as used previously in Eq. B.1.

The spectral bandwidth is taken as previously, from $-1/\tau$ to $+1/\tau$ where τ is the PN "chip" width. The power spectrum of the PN sequence is thus defined

$$P(\omega) = \left[\int_{-1/\tau}^{+1/\tau} \left(\frac{\sin \omega}{\omega} \right)^2 d\omega \right]^2 \qquad (D.4)$$

and is zero outside.

The equations used to derive the values of V_t and V_r appearing in Tables D-3 and D-4, and used in evaluation of Eq. (D.7) are similar to those previously used in deriving the amplitude departure functions [Eq. (B.2), etc.]. Tailored to the present application, they appear as follows:

$$V_t = 10 \log_{10} \left[\frac{1 + a_t}{1 - a_t} \right] \qquad (D.5)$$

and

$$V_r = 10 \log_{10} \left[\frac{1 + a_r}{1 - a_r} \right] \qquad (D.6)$$

Table D-3. Degradation in S/N for In-Phase Transmitter and Receiver Passband Ripples vs Ripple Rate

	S/N DEGRADATION L (dB)						
V_T → / m	0.0	0.25	0.5	1.0	1.5	3.0	V_R
1	0.000	0.000	0.001	0.004	0.008	0.026	↓
2	0.000	0.002	0.007	0.026	0.056	0.197	
4	0.000	0.002	0.007	0.028	0.063	0.236	0.0
8	0.000	0.002	0.007	0.028	0.063	0.234	
16	0.000	0.002	0.007	0.028	0.063	0.234	
1	0.000	0.000	0.000	0.002	0.006	0.021	
2	0.002	0.000	0.002	0.014	0.038	0.163	
4	0.002	0.000	0.002	0.016	0.044	0.196	0.25
8	0.002	0.000	0.002	0.016	0.044	0.194	
16	0.002	0.000	0.002	0.016	0.044	0.194	
1	0.001	0.000	0.000	0.000	0.003	0.016	
2	0.007	0.002	0.000	0.006	0.024	0.132	
4	0.007	0.002	0.000	0.007	0.028	0.160	0.5
8	0.007	0.002	0.000	0.007	0.028	0.159	
16	0.007	0.002	0.000	0.007	0.028	0.158	
1	0.004	0.002	0.000	0.000	0.000	0.009	
2	0.026	0.014	0.006	0.000	0.006	0.080	
4	0.028	0.016	0.007	0.000	0.007	0.100	1.0
8	0.028	0.016	0.007	0.000	0.007	0.098	
16	0.028	0.016	0.007	0.000	0.007	0.098	
1	0.008	0.006	0.003	0.000	0.000	0.005	
2	0.056	0.038	0.024	0.006	0.000	0.043	
4	0.063	0.044	0.028	0.007	0.000	0.054	1.5
8	0.063	0.044	0.028	0.007	0.000	0.053	
16	0.063	0.044	0.028	0.007	0.000	0.053	
1	0.026	0.021	0.016	0.009	0.005	0.000	
2	0.197	0.163	0.132	0.080	0.043	0.000	
4	0.236	0.196	0.160	0.100	0.054	0.000	3.0
8	0.234	0.194	0.159	0.098	0.053	0.000	
16	0.234	0.194	0.158	0.098	0.053	0.000	

In-Phase

Table D-4. S/N Degradation for Out-of-Phase Transmitter and Receiver Passband Ripple vs Ripple Rate

	S/N DEGRADATION L (dB)						
m \ V_T →	0.0	0.25	0.5	1.0	1.5	3.0	V_R
1	0.000	0.000	0.001	0.004	0.008	0.026	↓
2	0.000	0.002	0.007	0.026	0.056	0.197	
4	0.000	0.002	0.007	0.028	0.063	0.236	0.0
8	0.000	0.002	0.007	0.028	0.063	0.234	
16	0.000	0.002	0.007	0.028	0.063	0.234	
1	0.000	0.001	0.003	0.007	0.012	0.032	
2	0.002	0.007	0.015	0.040	0.077	0.236	
4	0.002	0.007	0.016	0.044	0.086	0.279	0.25
8	0.002	0.007	0.016	0.045	0.086	0.278	
16	0.002	0.007	0.016	0.045	0.086	0.277	
1	0.001	0.003	0.005	0.010	0.016	0.039	
2	0.007	0.015	0.027	0.059	0.102	0.279	
4	0.007	0.016	0.029	0.064	0.113	0.327	0.5
8	0.007	0.016	0.029	0.064	0.113	0.325	
16	0.007	0.016	0.029	0.064	0.113	0.324	
1	0.006	0.008	0.012	0.019	0.027	0.055	
2	0.027	0.042	0.061	0.106	0.162	0.375	
4	0.028	0.044	0.064	0.113	0.176	0.431	1.0
8	0.028	0.045	0.064	0.114	0.177	0.430	
16	0.028	0.045	0.064	0.114	0.177	0.429	
1	0.013	0.018	0.022	0.032	0.043	0.077	
2	0.062	0.084	0.109	0.167	0.236	0.486	
4	0.062	0.085	0.112	0.175	0.252	0.548	1.5
8	0.063	0.086	0.113	0.177	0.254	0.547	
16	0.063	0.086	0.113	0.177	0.254	0.547	
1	0.066	0.076	0.085	0.103	0.122	0.176	
2	0.240	0.282	0.327	0.425	0.533	0.895	
4	0.228	0.270	0.317	0.421	0.538	0.953	3.0
8	0.232	0.276	0.323	0.428	0.546	0.960	
16	0.233	0.277	0.324	0.429	0.547	0.960	

Out-Of-Phase

The signal-to-noise ratio degradation loss is then calculated from the following relationship:

$$\text{Loss} = 10 \log_{10} \left[\frac{\int (\sin \omega/\omega)^2 A_t(\omega) d\omega}{\int (\sin \omega/\omega)^2 A_r(\omega) d\omega} \right]^2 \qquad (D.7)$$

Table D-1 shows S/N loss for subtractive cosine ripple versus the number of ripple cycles m.

Table D-2 shows S/N loss for subtractive sine ripple versus number of ripple cycles m.

Table D-3 displays the value of the degradation for the case where the transmitter and the receiver ripples are in phase, as a function of their relative magnitudes via V_t and V_r. As suspected, the largest loss in S/N occurs for the case in which peak-to-peak ripples are most disparate, as when

$$V_t = 0.0 \text{ dB}$$

and

$$V_r = 3.0 \text{ dB}$$

for which the reduction or loss in S/N becomes 0.234 dB. Note the symmetry in exchanging the roles of V_t and V_r and that the loss ceases to increase for $m \geq 4$.

Table D-4 gives the loss for the worst-case ripple model, which occurs when $A_t(\omega)$ and $A_r(\omega)$ are "out of phase." Note that the worst case is reached for $V_t = V_r = 3$ dB at which point the S/N degradation is 0.96 dB.

The above derivation assumes maintenance of constant system noise temperature and transmitter power output.

The loss can, in theory, be made minimal by the expedient of adjusting the receiver amplitude ripple response to mirror that of the transmitter, all other parameters being held constant.

D.3 OBSERVATIONS AND CONCLUSIONS

Tables D-1 and D-2 show rather clearly that the greatest loss occurs when noise is allowed to over-emphasize the signal by removal of the central signal spectrum in the transmitter, and to exclude signal central components relative to the noise level in the receiver. Therefore, certain design rules emerge in clear priority. When designing system passband shapes, assuming control of same is possible:

1. Utilize ideal flat-top passbands, or
2. Make the passbands complementarily flat, or
3. Cause the spectral center to favor the center portion of both the transmitting and the receiving passbands.

It becomes evident that BOTH the differential group delay losses *AND* the S/N losses must be considered in evaluating system performance.

APPENDIX E. COMPUTER PROGRAMS

The FORTRAN IV computer programs in Tables E-1 through E-6 of this appendix were among those used in generating the data underlying the analyses of this report. Formats were designed for tabular printout on a timesharing teletype terminal, and are presented as references for working personnel who wish to verify the findings of this report, or to expand and extend those findings. The HP-34C programs in Tables E-7 through E-12 enable easy verification of the curves in Appendix A, and show how other examples may be treated.

Six timesharing and six HP-34C programs are provided, as described below:

1. Evaluation of the $(\sin x/x)^2$ integral (Table E-1) or any other suitable function.

2. Computing parabolic departure function loss in terms of specific band-edge characteristics (Table E-2).

3. Table E-3 computes loss due to cubic departure-function band-edge phase characteristics in radians.

4. Table E-4 computes loss due to a cosine phase ripple of various magnitudes and ripple rates.

5. Table E-5 computes loss due only to a passband amplitude characteristic as a function of ripple rate and magnitude.

6. Table E-6 shows a program used to evaluate the loss effects due to combined phase and amplitude departure functions, reading the output in tabular form to permit graphing.

7. Table E-7 enables a hand-held HP-34C to calculate signal energy loss due to residual or uncompensated linear phase departure, corresponding to Figure A-7.

8. Table E-8 enables an HP-34C to calculate signal energy loss due to residual parabolic phase departure, per the second-order curve in Figure A-7.

Table E-1. A FORTRAN Program for Computing the Integrals of Functions and the Reciprocals over the Interval A,B

```
PROGRAM   LSXSI

00100 PROGRAM LSXS (INPUT,OUTPUT)
00110 EXTERNAL XCFSMP
00120 A=1.0E-8
00130 B=3.14159265358979 3
00140 RELCON=1.0E-7
00150 CALL XCASMP(A,B,RELCON,RINT,IERR,XCFSMP)
00153 C=RINT
00155 D=1/C
00160 PRINT 70,RINT,D
00170 70 FORMAT(6X,F20.14,8X,F14.12)
00175 END
00180 FUNCTION XCFSMP(X)
00190 XCFSMP=((SIN(X)/X)**2)
00200 RETURN
00210 END
READY.
```

Table E-2. A FORTRAN Program for Computing Loss Due to Parabolic Phase Departure Function

```
00100 PROGRAM PADB (OUTPUT)
00110C ART LYTLE, NRL 5436, 5 SEPT 1974
00120C THIS PROGRAM COMPUTES AND TABULATES THE LOSSES IN DB DUE TO
00130C PARABOLIC PASSBAND PHASE CHARACTERISTICS FOR PNPSK SYSTEMS
00140C IN INTERVALS OF TEN DEGREES OF BAND-EDGEPHASE SHIFT. RANGE
00150C OF INTEGRATION IS FROM BAND CENTER TO FIRST SPECTRAL NULL.
00160C SPECTRAL AND PASSBAND SYMMETRY ARE ASSUMED.
00170 COMMON B
00180 EXTERNAL XCFSMP
00190 PRINT 20
00200 20 FORMAT(14X,*PARABOLIC PHASE DISTORTION LOSSES IN DB*,
00210+/,14X*BAND-EDGE DEGREES*,10X,*LOSSES IN DB*,//)
00220 A=1.0E-8
00230 DO 10 I=1,36
00240 RELCON=1.0E-8
00250 B=I*0.0175433
00260 C=B*57.29578
00270 PI=3.14159265
00280 CALL XCASMP(A,PI,RELCON,RINT,IERR,XCFSMP)
00290 SINT=20.*ALOG10(RINT*0.70512)
00300 PRINT 30,C,SINT
00310 30 FORMAT(18X,F3,14X,F10.4)
00320 10 CONTINUE
00330 END
00340 FUNCTION XCFSMP(X)
00350 COMMON B
00360 XCFSMP=((SIN(X)/X)**2)*(COS((0.10134)*B*X**2))
00370 RETURN
00380 END
READY.
```

Table E-3. A FORTRAN Program for Computing Cubic Departure Function Losses

```
00100 PROGRAM ACL31 (OUTPUT)
00110C
00120C ARTHUR C. LYTLE,JR., NRL CODE 5436 4 MARCH 1974
00130C
00140C SUBJECT PROGRAM CALCULATES THE POWER SPECTRAL DENSITY OF
00150C PSEUDONOISE (PN) QUADRAPHASE SHIFT KEYED (QPSK)
00160C MODULATION IN THE PRESENCE OF A SPECIFIC FORM OF CUBIC
00165C PHASE DISTORTION. SEE XCFSMP BELOW.
00170C
00180C INTEGRATION IS PERFORMED FROM ZERO FREQUENCY TO THE FIRST
00190C NULL OF THE SINE-SQUARED-X OVER X FUNCTION IN 0.01 RADIAN STEPS
00200C
00210 DIMENSION SINT(32,10),C(32,10)
00211 DIMENSION N(32)
00220 EXTERNAL XCFSMP
00230 A=1.0E-9
00240 DO 10 J=1,32
00250 DO 20 K=1,10
00260 IF(J.NE.1.OR.K.NE.1)GO TO 100
00270 C(1,1)=1.0E-9
00280 B=C(1,1)
00290 GO TO 200
00300 100 CONTINUE
00310 C(J,K)=(10*(J-1)+K-1)*0.01
00320 B=C(J,K)
00330 200 CONTINUE
00340 RELCON=1.0E-5
00350 CALL XCASMP(A,B,RELCON,RINT,IERR,XCFSMP)
00360 SINT(J,K)=RINT
00370 20 CONTINUE
00380 10 CONTINUE
00390 PRINT 70
00400 70 FORMAT(17X,*F(X) TIMES (SIN(X)/X) SQUARED*,
00403+2/,15X,*CUBIC DISTORTION 0.1 RADIAN AT BAND EDGE.*,
00405+2/,11X,*INTEGRATED FROM*,
00410+* ZERO TO X IN STEPS OF 0.01 RADIAN*,2/,*X*,2X,*0.00*,3X,
00420+*0.01*,3X,*0.02*,3X,*0.03*,3X,*0.04*,3X,*0.05*,3X,*0.06*,
00430+3X,*0.07*,3X,*0.08*,3X,*0.09*,/)
00440 DO 83 L=1,32
00450 IF(L.GT.10)GO TO 81
00460 N(L)=L-1
00470 GO TO 83
00480 81 CONTINUE
00490 IF(L.GT.20)GO TO 82
00500 N(L)=L-11
00510 GO TO 83
00520 82 CONTINUE
00530 IF(L.GT.30)GO TO 84
00540 N(L)=L-21
00542 GO TO 83
00544 84 CONTINUE
00546 N(L)=L-31
00550 83 CONTINUE
00600 DO 90 MROW=1,32
00605 PRINT 91, N(MROW)
00610 91 FORMAT(I1*)
00615 PRINT 40,(SINT(MROW,KOLM),KOLM=1,10)
00620 40 FORMAT(X,10F7.4)
00621 90 CONTINUE
00630 END
00640 FUNCTION XCFSMP(X)
00650 XCFSMP = (COS((0.14774*X)**3))*((SIN(X)/X)**8)
00660 RETURN
00670 END
READY.
```

Table E-4. A FORTRAN Program for Calculating Cosine Phase Ripple Loss

```
00100C LYTLE 13 SEPT 1974
00110 PROGRAM LCPR (OUTPUT)
00120 COMMON B,C
00130 EXTERNAL XCPSMP
00140 40 FORMAT(5/,19X,*COSINE RIPPLE PHASE DISTORTION LOSS*,
00150+/,21X,*RIPPLE FUNCTION = C*,5H*COS(,F3.1,3H*X),
00160+/,19X,*PEAK DEGREES*,9X,*DB LOSSES*,//)
00170C
00180 Z=1.E-8
00190 RELCON=1.0E-7
00200 PI=3.1415926535
00210C
00220 DO 10 J=1,9
00222 B=J-1
00230 PRINT 40,B
00232 NI=1
00234 IF(I.GE.8)NI=2
00240 DO 20 I=1,10,NI
00250 C=0.2618*(I-1)
00260 DO 20 I=1,13,NI
00270 IF(I.EQ.7)NI=2
00280 CALL XCPSMP(Z,PI,RELCON,RINT,IERR,XCPSMP)
00290 SINT=20 *ALOG10(RINT*0.705143249)
00300 PRINT 50,RINT
00310 CALL XCASMP(Z,PI,RELCON,RINT,IERR,XCPSMP)
00320 30 FORMAT(20X,F7.2,13X,F10.4)
00330 20 CONTINUE
00340 10 CONTINUE
00350 END
00360 FUNCTION XCPSMP (X)
00370 COMMON B,C
00380 XCPSMP=((SIN(X)/X)**2)*COS(COS(B*X))
00390 RETURN
00400 END
00410 XCPSMP=((SIN(X)/X)**2)*COS(C*COS(B*X))
READY.
```

Table E-5. A FORTRAN Program for Calculating Signal Energy Loss Due Only to Additive Passband Amplitude Cosine Ripple Distortion

```
00100 PROGRAM LCOMAR (OUTPUT)
00110 COMMON A,B
00120 EXTERNAL XCFSMP
00130 40 FORMAT(5/,19X,*AMPLITUDE RIPPLE DISTORTION LOSSES*,
00140+/,19X,*RIPPLE FUNCTION  =  (1+A*.5H*COS(,F3.1,4H*X)),
00150+/,19X,*PK-TO-PK RIPPLE IN DB*,4X,*DB LOSSES*,//)
00160C
00170 Z=1.E-8
00180 RELCON=1.0E-7
00190 PI=3.14159265358
00200C
00210 DO 10 J=1,9
00220 B=0.5*(J-1)
00240C
00250 PRINT 40,B
00260 DO 20 I=1,61
00270 R=0.1*(I-1)
00280 P=10.**(R/10.)
00290 A=(P-1.)/(P+1.)
00300 CALL XCASMP(Z,PI,RELCON,RINT,IERR,XCFSMP)
00310 SINT=20.*ALOG10(RINT*0.70514324197)
00320 PRINT 30,R,SINT
00330 30 FORMAT(20X,F7.2,13X,F10.4)
00340 20 CONTINUE
00350 10 CONTINUE
00360 END
00370 FUNCTION XCFSMP(X)
00380 COMMON A,B
00410 XCFSMP = (SIN(X)/X)**2*(1.+A*COS(B*X))
00420 RETURN
00430 END
READY.
```

Table E-6. A FORTRAN Program for Computing Loss Due to Simultaneous Subtractive Cosine Amplitude and Phase Distortion Using a Departure Function

```
00100      PROGRAM ACLAPC (OUTPUT)
00110C CALCULATES BOTH AMPLITUDE AND PHASE DISTORTION EFFECTS
00120C ARTHUR C. LYTLE, JR., NRL 5436
00130C UPDATED 14 AUGUST 1974 (NORMALIZED)
00140C THIS PROGRAM CALCULATES THE MODIFIED POWER SPECTRAL DISTRIBUTION
00145C AND NORMALIZES IT RELATIVE TO A PERFECT UNDISTORTED SPECTRUM,
00150C RESULTING FROM THE PRESENCE OF AMPLITUDE RIPPLE DISTORTION
00160C PLUS PHASE RIPPLE DISTORTION OF VARIOUS ORDERS AND MAGNITUDES
00170C TO EVALUATE SYSTEM PERFORMANCE WHEN APPLIED TO DIGITAL QPSK DATA
00180C TRANSMISSION USING PSEUDONOISE CODING AND CORRELATION DETECTION.
00190C INTEGRATION IS FROM PASSBAND CENTER TO FIRST SINX/X NULL.
00200C ENTER SPECIFIC VALUES IN XCHSMP AND IN THE HEADER BELOW. PHASE
00210C MAGNITUDES ARE REQUIRED IN RADIANS. OTHER VALUES ARE LINEAR.
00220C SPECTRAL AND PASSBAND SYMMETRY IS ASSUMED. NON-SYMMETRICAL
00230C SITUATIONS REQUIRE EXPRESSION AND INTEGRATION BETWEEN THE LOWER
00240C AND THE UPPER FIRST SIN(X)/X NULLS.
00250 DIMENSION SINT(32,10),C(32,10)
00260 DIMENSION W(32)
00270 EXTERNAL XCHSMP
00280 A=1.0E-9
00290 DO 10 J=1,32
00300 DO 20 K=1,10
00310 IF(J.NE.1.OR.K.NE.1)GO TO 100
00320 C(1,1)=1.0E-9
00330 P=C(1,1)
00340 GO TO 200
00350 100 CONTINUE
00360 C(J,K)=(10**(J-1)+K-1)*0.01
00370 P=C(J,K)
00380 200 CONTINUE
00390 RELCON=1.0E-5
00400 CALL XCASMP(A,P,RELCON,RINT,IERR,XCHSMP)
00410 SINT(J,K)=RINT
00420 20 CONTINUE
00430 10 CONTINUE
00440 PRINT 70
```

Table E-6. A FORTRAN Program for Computing Loss Due to Simultaneous Subtractive Cosine Amplitude and Phase Distortion Using a Departure Function (concluded)

```
00450 70 FORMAT(1HX,*F(X) TIMES (SIN(X)/X) SQUARED*,
00455+/,14X,*NORMALIZED TO AN INTENSITY SPECTRUM*,
00460+/,*FOR F(X) = (1-A(X))(COS(L(X)+P(X)+C(X)+ICOS(MX)+ISIN(NX)))*,
00470+*((SIN(X)/X)**2)*,
00480+/,12X,* A(X) = 2.0 DB PK-PK RIPPLE AMPLITUDE IN 1.5 CYCLES*,
00490+/,12X,* L(X) = 45 DEGREES LINEAR DISTORTION AT BAND EDGE*,
00500+/,12X,* P(X) = 90 DEGREES PARABOLIC DISTORTION AT BAND EDGES*,
00510+/,12X,* C(X) =180 DEGREES CUBIC DISTORTION AT BAND EDGE*,
00520+/,9X,*ICOS(MX) = 15 DEGREES PEAK AND 2.5 CYCLES RIPPLE*,
00530+/,9X,*ISIN(NX) = 30 DEGREES PEAK AND 1.5 CYCLES RIPPLE*,
00540+/,12X,*INTEGRATED FROM*,
00550+* ZERO TO X IN STEPS OF 0.01 RADIAN*,2/,*X*,2X,*0.00*,3X,
00560+*0.01*,3X,*0.02*,3X,*0.03*,3X,*0.04*,3X,*0.05*,3X,*0.06*,
00570+3X,*0.07*,3X,*0.08*,3X,*0.09*,2/)
00580 DO 83 L=1,32
00590 IF(L.GT.10)GO TO 81
00600 N(L)=L-1
00610 GO TO 83
00620 81 CONTINUE
00630 IF(L.GT.20)GO TO 82
00640 N(L)=L-11
00650 GO TO 83
00660 82 CONTINUE
00670 IF(L.GT.30)GO TO 84
00680 N(L)=L-21
00690 GO TO 83
00700 84 CONTINUE
00710 N(L)=L-31
00720 83 CONTINUE
00730 DO 90 M=1,32
00740 PRINT 91, N(M)
00750 91 FORMAT(I11)
00760 PRINT 40,(SINT(M,N),N=1,10)
00770 40 FORMAT(4,10F7.4)
00780 90 CONTINUE
00790 END
00800 FUNCTION XCOSSP(X)
00810 XCOSSP=(1-0.226*COS(1.5*X))*(COS((0.25*X)+(0.4*X)**2
00820+ +(0.466*X)**3+0.52*SIN(1.5*X)+0.26*(OS(2.5*X)))
00830+ *((SIN(X)/X)**2)*(0.7051)
00840 RETURN
00850 END
READY.
```

Table E-7. An HP-34C Program for Residual or Linear Phase Departure

$$\text{loss} = 20 \log \left[\frac{1}{K} \int_0^{\pi} \left(\frac{\sin x}{x} \right)^2 \cos A \left[\frac{x}{\pi} \right] dx \right]$$

Step	Activity	Variable
001	h Label A	
002	Store 0	x
003	Recall 0	x
004	f sin x	
005	Recall 0	x
006	:	(sin x/x)
007	gx^2	$(\quad)^2$
008	Store 1	
009	Recall 0	x
010	hπ	π
011	:	x/π
012	Recall 8	A
013	×	Ax/π
014	f cos	cos (Ax/π)
015	Recall 1	$(\sin x/x)^2$
016	×	$(\sin x/x)^2 \cos (Ax/\pi)$
017	Return	
018	h Label B	1
019	Enter	
020	Recall 9	1.41815157
021	:	[ ]
022	f log	
023	2	
024	0	
025	×	20 log [ ]

Notes:

Registers: 8 band-edge phase error in radians
9 x = 1.41815157

Typical running time: 1.5 sec for 4 places
.65 sec for 3 places
.60 sec for 2 places

Table E-8. An HP-34C Program for Figure A-7 (Parabolic or Second Order)

$$\text{Loss} = 20 \log \left[\frac{1}{K} \int_0^{\pi} \left(\frac{\sin x}{x} \right)^2 \cos C \left[\frac{x}{\pi} \right]^2 dx \right]$$

Step	Activity	Variable
001	h Label A	
002	Store R.0	x
003	Recall R.0	x
004	f sin	sin x
005	Recall R.0	x
006	÷	(sin x/x)
007	gx^2	$\left(\frac{\sin x}{x}\right)^2$
008	Store R.1	
009	Recall R.0	x
010	hπ	π
011	÷	x/π
012	gx^2	$(x/\pi)^2$
013	Recall 7	C
014	x	$C(x/\pi)^2$
015	f cos	$\cos C(x/\pi)^2$
016	Recall R.1	
017	×	$\left(\frac{\sin x}{x}\right)^2 \cos C\ (x/\pi)^2$
018	Return	
019	Enter	$\int f(x)\, dx$
020	h Label B	
021	Recall 9	K
022	÷	
023	f log	$\log_{10} [\int f(x)\, dx/K]$
024	Recall 6	20
025	×	$\text{Loss} = 20 \log \left[\frac{1}{K} \int \right]$ in dB

Notes:

Registers:

6	Store 20
7	Store C in radians
9	Store K = 1.418151157

AD-A099 187 AEROSPACE CORP EL SEGUNDO CA SATELLITE SYSTEMS DIV F/G 17/2.1
SIGNAL PROCESSING DISTORTION LOSS IN SPREAD-SPECTRUM COMMUNICAT--ETC(U)
OCT 80 A C LYTLE
UNCLASSIFIED TR-0081(6724-01)-1 F04701-80-C-0081
SD-TR-81-20 NL

END
DATE FILMED
6 81
DTIC

9. Table E-9 enables an HP-34C to calculate signal energy loss due to residual fourth-order phase departure, per the fourth-order curve of Figure A-7.

10. Table E-10 enables an HP-34C to calculate signal loss due to residual sine or cosine phase ripple of specific cycles of ripple across the passband, and of any given peak radian ripple. This program accompanies Figures A-8 through A-13 and A-24.

11. Table E-11 enables an HP-34C to calculate signal loss due to residual sine or cosine ripple plus a parabolic phase distortion component. This program accompanies Figures A-17 through A-20.

12. Table E-12 enables an HP-34C to calculate signal loss due to residual sine or cosine ripple plus a cubic phase distortion component. This program accompanies Figures A-21 through A-23.

Table E-9. An HP-34C Program for Figure A-7

$$\text{Loss} = 20 \log \left[\frac{1}{K} \int_0^{\pi} \left(\frac{\sin x}{x} \right)^2 \cos D \left[\frac{x}{\pi} \right]^4 dx \right]$$

Step	Activity	Variable
001	h Label A	
	Store 0	x
	Recall 0	x
	f sin x	
005	Recall 0	x
	÷	sin x/x
	gx^2	$(\sin x/x)^2$
	Store 1	
	Recall 0	x
010	hπ	π
	÷	x/π
	gx^2	$(x/\pi)^2$
	gx^2	$(x/\pi)^4$
	Recall 8	D
015	×	$D\ (x/\pi)^4$
	f cos	$\cos D\ (x/\pi)^4$
	Recall 1	$(\quad)^2$
	×	$(\sin x/x)^2 \cos (x/\pi)^4$
	h Return	
020	h Label B	
	Enter	[ ]
	Recall 9	1.41815157
	÷	
	f log	
025	2	
	0	
	×	20 log [ ]

Notes:

Registers 8 D in radians
9 K 1.41815157

Typical running time 60-90 sec for 3 places

Table E-10. An HP-43C Program for Figures A-8 through A-13, and A-24

$$\text{Loss} = 20 \log \left[\frac{1}{K} \int_0^{\pi} \left(\frac{\sin x}{x} \right)^2 \cos \left\{ B \begin{matrix} \cos \\ \sin \end{matrix} Cx \right\} dx \right]$$

Step	Activity	Variable
001	h Label A	
002	Store R.0	x
003	Recall R.0	x
004	f sin	sin x
005	Recall R.0	x
006	÷	sin x/x
007	gx^2	$(\sin x/x)^2$
008	Store R.1	
009	Recall R.0	x
010	Recall 7	C
011	×	Cx
012	f cos or f sin	cos Cx or sin Cx
013	Recall 8	B
014	×	$B \begin{matrix} \cos Cx \\ \sin Cx \end{matrix}$
015	f cos	$\cos \left\{ B \begin{matrix} \cos Cx \\ \sin Cx \end{matrix} \right\}$
016	Recall R.1	$\left(\frac{\sin x}{x} \right)^2$
017	×	$\left(\frac{\sin x}{x} \right)^2 \cos \left\{ B \begin{matrix} \cos Cx \\ \sin Cx \end{matrix} \right\}$
018	Return	
019	Enter	
020	h Label B	
021	Recall 9	
022	÷	K = 1.41815157
023	f log	
024	Recall 6	20
025	×	Loss in dB

Notes:

Registers
- 6 Store 20
- 7 Store ripple cycles
- 8 Store peak ripple B in radians
- 9 K

Typical running time 75 sec for three places.

Table E-11. An HP-34C Program for Figures A-17 through A-20 and A-25

$$L = 20 \log \left[\frac{1}{K} \int_0^{\pi} \left(\frac{\sin x}{x} \right)^2 \cos \left\{ A \left[\frac{x}{\pi} \right]^2 + B \begin{matrix} \sin \\ \cos \end{matrix} Mx \right\} dx \right]$$

Step	Activity	Variable
001	h Label A	
	Store R.0	x
	Recall .0	x
	f sin	sin x
005	Recall .0	x
	÷	(sin x/x)
	gx^2	
	Store .1	$\left(\frac{\sin x}{x}\right)^2$
	Recall .0	x
010	Recall 7	M
	×	Mx
	f cos	cos Mx or sin Mx
	Recall 8	B
	×	B cos Mx
015	Store .2	(B cos Mx)
	Recall .0	x
	hπ	π
	÷	x/π
	gx^2	$(x/\pi)^2$
020	Recall 5	A
	×	$A(x/\pi)^2$
	Enter	$A(x/\pi)^2$
	Recall .2	(B cos Mx)
	+	$A(x/\pi)^2$ + B cos Mx
025	f cos	cos $[A(x/\pi)^2$ + B cos Mx]
	Recall .1	
	×	$\left(\frac{\sin x}{x}\right)^2$ cos $\{A(x/\pi)^2$ + B cos Mx}
	Return	
	h Label B	
030	Enter	
	Recall 9	K = 1.41815157
	÷	
	f. log	
	Recall 6	
035	×	

Notes: **Registers**

5	A	radians
6	20	
7	M	ripple cycles
8	B	ripple magnitude radians
9	K = 1.41815157	

Typical running time: 150 sec for 3 places
50 sec for 2 places

Table E-12. An HP-34C Program for Figures A-21 through A-23 and A-26

$$\text{Loss} = 20 \log\left[\frac{1}{K}\int_0^{\pi}\left(\frac{\sin x}{x}\right)^2 \cos\left\{A\left[\frac{x}{\pi}\right]^3 + B\begin{matrix}\cos\\ \sin\end{matrix} Cx\right\} dx\right]$$

Step	Activity	Variable
001	h Label A	
002	Store R.0	x
003	Recall R.0	x
004	f sin x	sin x
005	Recall R.0	x
006	÷	(sin x/x)
007	gx^2	$(\sin x/x)^2$
008	Store R.1	
009	Recall .0	x
010	Recall 7	C
011	×	Cx
012	f cos or f sin	cos Cx or sin Cx
013	Recall 8	B
014	×	B cos Cx or B sin Cx
015	Store R.2	
016	Recall R.0	x
017	hπ	π
018	÷	x/π
019	Store R.3	(x/π)
020	gx^2	$(x\pi)^2$
021	Recall .3	(x/π)
022	×	$(x/\pi)^3$
023	Recall 5	A
024	×	$A(x/\pi)^3$
025	Recall R.2	B cos Cx or B sin Cx
026	+	$\{AC\ x/\pi)^3$ + B cos Cx etc$\}$
027	f cos	cos{ }
028	Recall R.1	( )
029	×	f(x)
030	Return	
031	Enter	$\int f(x)\,dx$
032	h Label B	
033	Recall 9	K = 1.41815157
034	÷	
035	f log	log [ ]
036	Recall 6	20
037	×	20 log [ ] in dB

Notes:

Registers	5	A in radians
	6	20
	7	C in cycles
	8	B in radians
	9	K = 1.41815157
Typical running time		180 sec for 3 places
		45 sec for 2 places
(for high values of C)		600 sec for 3 places

APPENDIX F. TABLES OF USEFUL FUNCTIONS

This appendix provides pre-computed tables and graphs of functions useful to the designer and analyst. In particular, tables of values are provided for functions that are difficult to find or are not available in published form. Use of these tables will make it possible to expedite and simplify certain of the operations which must be performed in the process of performing distortion loss calculations.

The contents and descriptions of the tables and graphs are as follows:

1. Figure F-1 plots the integrals of the sin (x)/x function and of the $(\sin x/x)^2$ function evaluated out to the first null to enable quantitative inspection of spectral energy distribution.

2. Table F-1 is a computer printout of the values for the sin (x)/x integral in 0.01 radian intervals.

3. Table F-2 is a computer printout of the values for the $(\sin x/x)^2$ integral in 0.01 radian intervals. This information is not readily available elsewhere.

4. Table F-3 provides calculated values of both the sin (x)/x and the $(\sin x/x)^2$ functions to enable Fig. F-1 to be utilized out to four decimal place accuracy.

5. Tables F-4 through F-14 provide computational results not known to be available in the literature which are necessary to solution of differential group delay and departure-function analysis problems. The value of the $(\sin x/x)^2$ integral between zero and pi is partitioned in 2, 3, 4, 5, 6, 7, 8, 9, 10, 11, and 12 equal slices. With this partitioning, most stepped-interval passband specifications can be evaluated on a hand calculator of medium sophistication, such as the HP-97 or equivalent.

Table F-3 may be useful to extrapolate between data points, providing other spectral partitioning not already provided elsewhere.

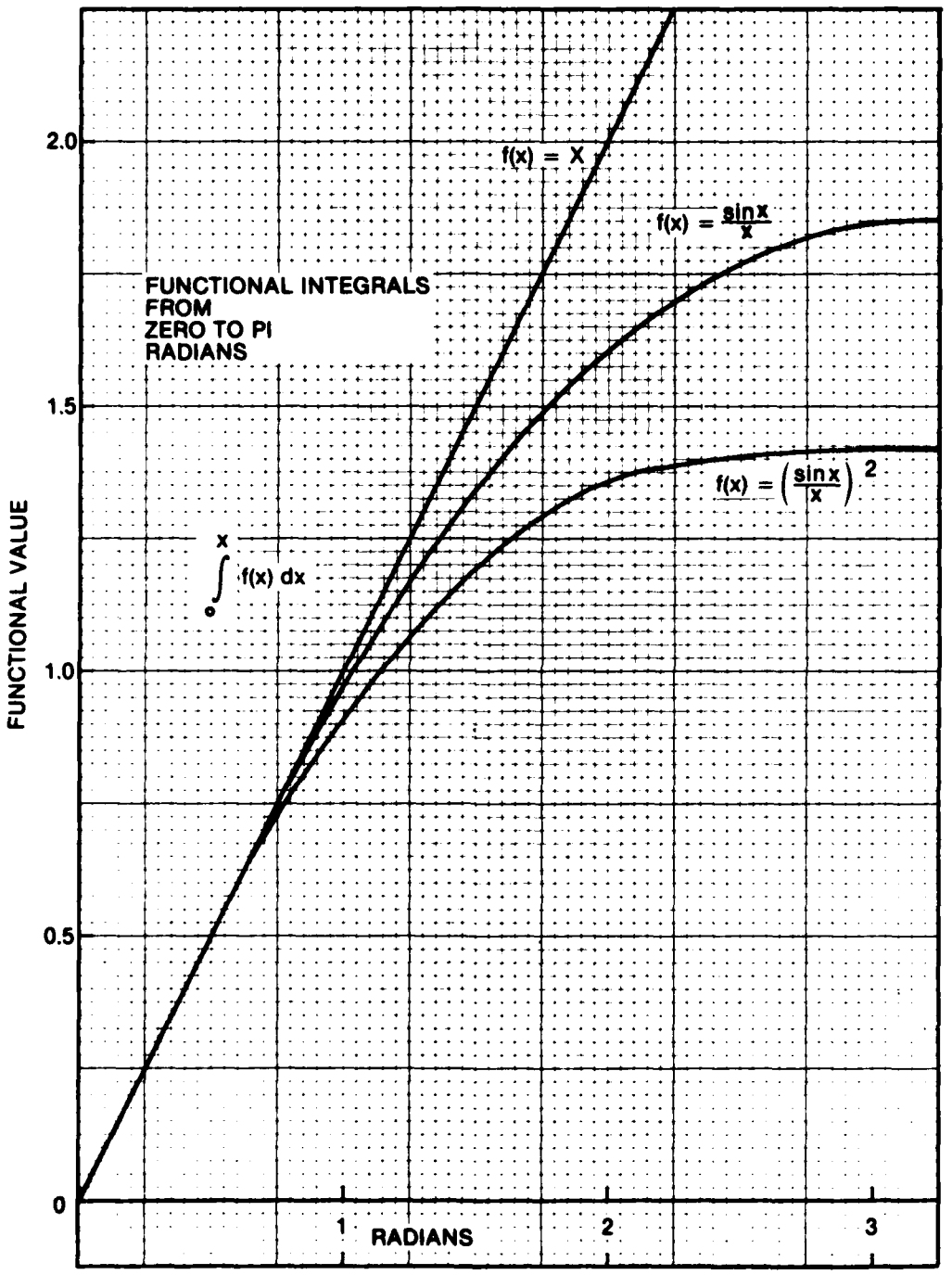

Fig. F-1. Curves of Functions

Table F-1. Table of Integral Values for the sin x/x Function

INTEGRAL OF SIN(X)/X

FROM ZERO TO PI IN 0.01 RADIAN INTERVALS

X	0.00	0.01	0.02	0.03	0.04	0.05	0.06	0.07	0.08	0.09
.0	0.	.0100	.0200	.0300	.0400	.0500	.0600	.0700	.0800	.0900
1	.0999	.1099	.1199	.1299	.1398	.1498	.1598	.1697	.1797	.1896
2	.1996	.2095	.2194	.2293	.2392	.2491	.2590	.2689	.2788	.2886
3	.2985	.3083	.3182	.3280	.3378	.3476	.3574	.3672	.3770	.3867
4	.3965	.4062	.4159	.4256	.4353	.4450	.4546	.4643	.4739	.4835
5	.4931	.5027	.5123	.5218	.5313	.5408	.5503	.5598	.5693	.5787
6	.5881	.5975	.6069	.6163	.6256	.6349	.6442	.6535	.6628	.6720
7	.6812	.6904	.6996	.7087	.7179	.7270	.7360	.7451	.7541	.7631
8	.7721	.7811	.7900	.7989	.8078	.8166	.8254	.8342	.8430	.8518
9	.8605	.8692	.8778	.8865	.8951	.9036	.9122	.9207	.9292	.9377
.0	.9461	.9545	.9629	.9712	.9795	.9878	.9960	1.0042	1.0124	1.0206
1	1.0287	1.0368	1.0448	1.0528	1.0608	1.0688	1.0767	1.0846	1.0924	1.1003
2	1.1080	1.1158	1.1235	1.1312	1.1388	1.1464	1.1540	1.1616	1.1691	1.1765
3	.1840	1.1914	1.1987	1.2060	1.2132	1.2206	1.2278	1.2349	1.2421	1.2492
4	1.2562	1.2632	1.2702	1.2772	1.2841	1.2909	1.2978	1.3046	1.3113	1.3180
5	1.3247	1.3313	1.3379	1.3445	1.3510	1.3574	1.3639	1.3703	1.3766	1.3829
6	1.3892	1.3954	1.4016	1.4077	1.4138	1.4199	1.4259	1.4319	1.4378	1.4437
7	1.4496	1.4554	1.4612	1.4669	1.4726	1.4782	1.4838	1.4894	1.4949	1.5004
8	1.5059	1.5112	1.5166	1.5219	1.5271	1.5323	1.5375	1.5426	1.5477	1.5528
9	1.5578	1.5627	1.5677	1.5725	1.5774	1.5821	1.5869	1.5916	1.5962	1.6008
0	1.6054	1.6099	1.6144	1.6189	1.6233	1.6276	1.6319	1.6362	1.6404	1.6445
1	1.6487	1.6528	1.6568	1.6608	1.6648	1.6687	1.6725	1.6764	1.6802	1.6839
2	1.6876	1.6913	1.6949	1.6985	1.7020	1.7055	1.7089	1.7123	1.7156	1.7189
3	1.7222	1.7254	1.7286	1.7317	1.7348	1.7379	1.7409	1.7439	1.7468	1.7496
4	1.7525	1.7553	1.7580	1.7607	1.7634	1.7660	1.7686	1.7712	1.7736	1.7761
5	1.7785	1.7809	1.7832	1.7855	1.7878	1.7900	1.7921	1.7943	1.7963	1.7984
6	1.8004	1.8024	1.8043	1.8062	1.8080	1.8098	1.8116	1.8133	1.8150	1.8166
7	1.8182	1.8198	1.8213	1.8228	1.8242	1.8256	1.8270	1.8283	1.8296	1.8309
8	1.8321	1.8333	1.8344	1.8355	1.8366	1.8376	1.8386	1.8396	1.8405	1.8413
9	1.8422	1.8430	1.8438	1.8445	1.8452	1.8459	1.8465	1.8471	1.8476	1.8482
0	1.8487	1.8491	1.8495	1.8499	1.8503	1.8506	1.8509	1.8511	1.8513	1.8515
1	1.8517	1.8518	1.8519	1.8519	1.8519	1.8519	1.8519	1...8518	1.8517	1.8516

Table F-2. Table of Integral Values of $(\sin x/x)^2$

(SINX/X) SQUARED

INTEGRATED FROM ZERO TO X IN STEPS OF 0.01 RADIANS

X	0.00	0.01	0.02	0.03	0.04	0.05	0.06	0.07	0.08	0.09
0.0	0.	.0100	.0200	.0300	.0400	.0500	.0600	.0700	.0799	.0899
.1	.0999	.1099	.1198	.1298	.1397	.1496	.1595	.1695	.1794	.1892
.2	.1991	.2090	.2188	.2287	.2385	.2483	.2581	.2678	.2776	.2873
.3	.2970	.3067	.3164	.3260	.3357	.3453	.3549	.3644	.3740	.3835
.4	.3930	.4024	.4119	.4213	.4307	.4400	.4494	.4587	.4679	.4772
.5	.4864	.4956	.5047	.5138	.5229	.5320	.5410	.5499	.5589	.5678
.6	.5767	.5855	.5943	.6031	.6118	.6205	.6291	.6378	.6463	.6549
.7	.6633	.6718	.6802	.6886	.6969	.7052	.7134	.7216	.7298	.7379
.8	.7459	.7539	.7619	.7698	.7777	.7856	.7934	.8011	.8088	.8164
.9	.8240	.8316	.8391	.8465	.8540	.8613	.8686	.8759	.8831	.8902
1.0	.8973	.9044	.9114	.9184	.9253	.9321	.9389	.9457	.9523	.9590
.1	.9656	.9721	.9786	.9850	.9914	.9977	1.0040	1.0102	1.0164	1.0225
.2	1.0286	1.0346	1.0405	1.0464	1.0523	1.0581	1.0638	1.0695	1.0751	1.0807
.3	1.0862	1.0917	1.0971	1.1024	1.1077	1.1130	1.1182	1.1233	1.1284	1.1335
.4	1.1384	1.1434	1.1482	1.1531	1.1578	1.1625	1.1672	1.1718	1.1764	1.1809
.5	1.1853	1.1897	1.1941	1.1984	1.2026	1.2068	1.2109	1.2150	1.2190	1.2230
.6	1.2269	1.2308	1.2346	1.2384	1.2421	1.2458	1.2494	1.2530	1.2565	1.2609
.7	1.2634	1.2668	1.2702	1.2734	1.2767	1.2799	1.2830	1.2861	1.2891	1.2921
	1.2951	1.2980	1.3008	1.3036	1.3064	1.3091	1.3118	1.3144	1.3170	1.3196
	1.3221	1.3245	1.3270	1.3293	1.3317	1.3340	1.3362	1.3384	1.3406	1.3427
2.0	1.3448	1.3468	1.3488	1.3508	1.3527	1.3546	1.3565	1.3583	1.3601	1.3618
.1	1.3635	1.3652	1.3669	1.3685	1.3700	1.3716	1.3731	1.3745	1.3759	1.3773
.2	1.3787	1.3800	1.3814	1.3826	1.3839	1.3851	1.3863	1.3874	1.3885	1.3896
.3	1.3907	1.3917	1.3927	1.3937	1.3947	1.3956	1.3965	1.3974	1.3982	1.3991
.4	1.3999	1.4007	1.4014	1.4021	1.4029	1.4035	1.4042	1.4049	1.4055	1.4061
.5	1.4067	1.4072	1.4078	1.4083	1.4088	1.4093	1.4098	1.4102	1.4106	1.4111
.6	1.4115	1.4118	1.4122	1.4126	1.4129	1.4132	1.4135	1.4138	1.4141	1.4144
.7	1.4147	1.4149	1.4151	1.4153	1.4156	1.4158	1.4159	1.4161	1.4163	1.4164
.8	1.4166	1.4167	1.4169	1.4170	1.4171	1.4172	1.4173	1.4174	1.4175	1.4176
.9	1.4176	1.4177	1.4177	1.4178	1.4178	1.4179	1.4179	1.4180	1.4180	1.4180
3.0	1.4180	1.4181	1.4181	1.4181	1.4181	1.4181	1.4181	1.4181	1.4181	1.4181
.1	1.4181	1.4182	1.4182	1.4182	1.4182	1.4182	1.4182	1.4182	1.4182	1.4182

Table F-3. Table of Numerical Values Computed for the Functions sin x/x and $(\sin x/x)^2$ in 0.01 Radian Intervals

x	$\frac{\sin x}{x}$	$\left(\frac{\sin x}{x}\right)^2$	x	$\frac{\sin x}{x}$	$\left(\frac{\sin x}{x}\right)^2$	x	$\frac{\sin x}{x}$	$\left(\frac{\sin x}{x}\right)^2$
0.00	1.000	1.000	0.40	0.9735	0.9478	0.80	0.8967	0.8041
0.01	1.000	1.000	0.41	0.9722	0.9452	0.81	0.8942	0.7996
0.02	1.000	1.000	0.42	0.9709	0.9426	0.82	0.8916	0.7950
0.03	1.000	1.000	0.43	0.9695	0.9399	0.83	0.8891	0.7905
0.04	1.000	1.000	0.44	0.9680	0.9371	0.84	0.8865	0.7858
0.05	1.000	0.999	0.45	0.9666	0.9343	0.85	0.8839	0.7812
0.06	0.999	0.999	0.46	0.9651	0.9314	0.86	0.8812	0.7765
0.07	0.999	0.998	0.47	0.9636	0.9285	0.87	0.8785	0.7718
0.08	0.999	0.998	0.48	0.9620	0.9255	0.88	0.8758	0.7671
0.09	0.999	0.997	0.49	0.9605	0.9225	0.89	0.8731	0.7623
0.10	0.998	0.997	0.50	0.9589	0.9194	0.90	0.8704	0.7575
0.11	0.998	0.996	0.51	0.9572	0.9163	0.91	0.8676	0.7523
0.12	0.998	0.995	0.52	0.9555	0.9131	0.92	0.8648	0.7479
0.13	0.997	0.994	0.53	0.9538	0.9098	0.93	0.8620	0.7430
0.14	0.997	0.993	0.54	0.9521	0.9065	0.94	0.8591	0.7381
0.15	0.996	0.993	0.55	0.9503	0.9031	0.95	0.8562	0.7331
0.16	0.996	0.991	0.56	0.9485	0.8997	0.96	0.8533	0.7282
0.17	0.995	0.990	0.57	0.9467	0.8963	0.97	0.8504	0.7232
0.18	0.995	0.989	0.58	0.9449	0.8928	0.98	0.8474	0.7182
0.19	0.994	0.988	0.59	0.9430	0.8892	0.99	0.8445	0.7131
0.20	0.993	0.987	0.60	0.9411	0.8856	1.00	0.8415	0.7081
0.21	0.993	0.985	0.61	0.9391	0.8820	1.01	0.8384	0.7030
0.22	0.992	0.984	0.62	0.9372	0.8783	1.02	0.8354	0.6979
0.23	0.991	0.982	0.63	0.9352	0.8745	1.03	0.8323	0.6928
0.24	0.990	0.981	0.64	0.9331	0.8707	1.04	0.8292	0.6876
0.25	0.990	0.979	0.65	0.9311	0.8669	1.05	0.8261	0.6825
0.26	0.989	0.978	0.66	0.9290	0.8630	1.06	0.8230	0.6773
0.27	0.988	0.976	0.67	0.9268	0.8950	1.07	0.8198	0.6721
0.28	0.987	0.9741	0.68	0.9247	0.8551	1.08	0.8166	0.6669
0.29	0.9860	0.9723	0.69	0.9225	0.8510	1.09	0.8134	0.6617
0.30	0.9851	0.9704	0.70	0.9203	0.8470	1.10	0.8102	0.6564
0.31	0.9841	0.9684	0.71	0.9181	0.8429	1.11	0.8069	0.6511
0.32	0.9830	0.9663	0.72	0.9158	0.8387	1.12	0.8037	0.6459
0.33	0.9819	0.9642	0.73	0.9135	0.8345	1.13	0.8004	0.6406
0.34	0.9808	0.9621	0.74	0.9112	0.8303	1.14	0.7970	0.6353
0.35	0.9797	0.9598	0.75	0.9089	0.8260	1.15	0.7937	0.6300
0.36	0.9785	0.9575	0.76	0.9065	0.8217	1.16	0.7903	0.6246
0.37	0.9773	0.9552	0.77	0.9041	0.8173	1.17	0.7870	0.6193
0.38	0.9761	0.9528	0.78	0.9016	0.8130	1.18	0.7836	0.6140
0.39	0.9748	0.9503	0.79	0.8992	0.8025	1.19	0.7801	0.6886

Table F-3. Table of Numerical Values Computed for the Functions sin x/x and $(\sin x/x)^2$ in 0.01 Radial Intervals (cont'd)

x	$\frac{\sin x}{x}$	$\left(\frac{\sin x}{x}\right)^2$	x	$\frac{\sin x}{x}$	$\left(\frac{\sin x}{x}\right)^2$	x	$\frac{\sin x}{x}$	$\left(\frac{\sin x}{x}\right)^2$
1.20	0.7767	0.6033	1.60	0.6247	0.3903	2.00	0.4546	0.2067
1.21	0.7732	0.5979	1.61	0.6206	0.3852	2.01	0.4503	0.2028
1.22	0.7698	0.5925	1.62	0.6165	0.3801	2.02	0.4459	0.1989
1.23	0.7663	0.5871	1.63	0.6124	0.3751	2.03	0.4416	0.1950
1.24	0.7627	0.5818	1.64	0.6083	0.3700	2.04	0.4372	0.1912
1.25	0.7592	0.5764	1.65	0.6042	0.3650	2.05	0.4329	0.1874
1.26	0.7556	0.5710	1.66	0.6000	0.3600	2.06	0.4285	0.1836
1.27	0.7520	0.5656	1.67	0.5959	0.3550	2.07	0.4241	0.1799
1.28	0.7484	0.5602	1.68	0.5917	0.3501	2.08	0.4198	0.1762
1.29	0.7448	0.5548	1.69	0.5875	0.3452	2.09	0.4154	0.1726
1.30	0.7412	0.5494	1.70	0.5833	0.3403	2.10	0.4111	0.1690
1.31	0.7375	0.5440	1.71	0.5791	0.3354	2.11	0.4067	0.1654
1.32	0.7339	0.5386	1.72	0.5749	0.3306	2.12	0.4023	0.1619
1.33	0.7302	0.5332	1.73	0.5707	0.3257	2.13	0.3980	0.1584
1.34	0.7265	0.5278	1.74	0.5665	0.3209	2.14	0.3936	0.1549
1.35	0.7228	0.5224	1.75	0.5623	0.3162	2.15	0.3893	0.1515
1.36	0.7190	0.5170	1.76	0.5580	0.3114	2.16	0.3848	0.1481
1.37	0.7153	0.5116	1.77	0.5538	0.3067	2.17	0.3805	0.1448
1.38	0.7115	0.5062	1.78	0.5495	0.3020	2.18	0.3762	0.1415
1.39	0.7077	0.5008	1.79	0.5453	0.2973	2.19	0.3718	0.1383
1.40	0.7039	0.4955	1.80	0.5410	0.2927	2.20	0.3675	0.1351
1.41	0.7001	0.4901	1.81	0.5368	0.2881	2.21	0.3632	0.1319
1.42	0.6962	0.4847	1.82	0.5325	0.2835	2.22	0.3588	0.1287
1.43	0.6924	0.4794	1.83	0.5282	0.2790	2.23	0.3545	0.1257
1.44	0.6885	0.4740	1.84	0.5239	0.2745	2.24	0.3501	0.1226
1.45	0.6846	0.4687	1.85	0.5196	0.2700	2.25	0.3458	0.1196
1.46	0.6807	0.4634	1.86	0.5153	0.2655	2.26	0.3415	0.1166
1.47	0.6768	0.4581	1.87	0.5110	0.2611	2.27	0.3372	0.1137
1.48	0.6729	0.4528	1.88	0.5067	0.2567	2.28	0.3328	0.1108
1.49	0.6690	0.4475	1.89	0.5024	0.2524	2.29	0.3285	0.1079
1.50	0.6650	0.4422	1.90	0.4981	0.2481	2.30	0.3242	0.1051
1.51	0.6610	0.4370	1.91	0.4937	0.2438	2.31	0.3199	0.1023
1.52	0.6570	0.4317	1.92	0.4894	0.2395	2.32	0.3156	0.0996
1.53	0.6531	0.4265	1.93	0.4851	0.2353	2.33	0.3113	0.0969
1.54	0.6490	0.4213	1.94	0.4807	0.2311	2.34	0.3070	0.0943
1.55	0.6450	0.4161	1.95	0.4764	0.2269	2.35	0.3028	0.0917
1.56	0.6410	0.4109	1.96	0.4720	0.2228	2.36	0.2985	0.0891
1.57	0.6369	0.4057	1.97	0.4677	0.2187	2.37	0.2942	0.0866
1.58	0.6329	0.4005	1.98	0.4634	0.2147	2.38	0.2899	0.0841
1.59	0.6288	0.3954	1.99	0.4590	0.2107	2.39	0.2857	0.0816

Table F-3. Table of Numerical Values Computed for the Functions sin x/x and $(\sin x/x)^2$ in 0.01 Radial Intervals (concluded)

x	$\frac{\sin x}{x}$	$\left(\frac{\sin x}{x}\right)^2$	x	$\frac{\sin x}{x}$	$\left(\frac{\sin x}{x}\right)^2$	x	$\frac{\sin x}{x}$	$\left(\frac{\sin x}{x}\right)^2$
2.40	0.2814	0.0792	2.80	0.1196	0.0143	3.20	-0.0182	0.0003
2.41	0.2772	0.0768	2.81	0.1159	0.0134	3.21	-0.0213	0.0005
2.42	0.2730	0.0745	2.82	0.1121	0.0126	3.22	-0.0243	0.0006
2.43	0.2687	0.0722	2.83	0.1083	0.0117	3.23	-0.0273	0.0007
2.44	0.2645	0.0700	2.84	0.1046	0.0109	3.24	-0.0303	0.0009
2.45	0.2603	0.0678	2.85	0.1009	0.0102	3.25	-0.0333	0.0011
2.46	0.2561	0.0656	2.86	0.0972	0.0094	3.26	-0.0362	0.0013
2.47	0.2519	0.0635	2.87	0.0935	0.0087	3.27	-0.0392	0.0015
2.48	0.2477	0.0614	2.88	0.0898	0.0081	3.28	-0.0421	0.0018
2.49	0.2436	0.0593	2.89	0.0861	0.0074	3.29	-0.0449	0.0020
2.50	0.2394	0.0573	2.90	0.0825	0.0068	3.30	-0.0478	0.0023
2.51	0.2352	0.0553	2.91	0.0789	0.0062	3.31	-0.0506	0.0026
2.52	0.2311	0.0534	2.92	0.0753	0.0057	3.32	-0.0535	0.0029
2.53	0.2269	0.0515	2.93	0.0717	0.0051	3.33	-0.0562	0.0032
2.54	0.2228	0.0496	2.94	0.0681	0.0046	3.34	-0.0590	0.0035
2.55	0.2187	0.0478	2.95	0.0646	0.0042	3.35	-0.0618	0.0038
2.56	0.2146	0.0460	2.96	0.0610	0.0037	3.36	-0.0645	0.0042
2.57	0.2105	0.0443	2.97	0.0575	0.0033	3.37	-0.0672	0.0045
2.58	0.2064	0.0426	2.98	0.0540	0.0029	3.38	-0.0699	0.0049
2.59	0.2023	0.0409	2.99	0.0505	0.0026	3.39	-0.0725	0.0053
2.60	0.1983	0.0393	3.00	0.0470	0.0022	3.40	-0.0752	0.0056
2.61	0.1942	0.0377	3.01	0.0436	0.0019	3.41	-0.0778	0.0060
2.62	0.1902	0.0362	3.02	0.0402	0.0016	3.42	-0.0804	0.0065
2.63	0.1861	0.0347	3.03	0.0369	0.0014	3.43	-0.0829	0.0069
2.64	0.1821	0.0332	3.04	0.0334	0.0011	3.44	-0.0855	0.0073
2.65	0.1781	0.0317	3.05	0.0300	0.0009	3.45	-0.0880	0.0077
2.66	0.1741	0.0303	3.06	0.0266	0.0007	3.46	-0.0905	0.0082
2.67	0.1702	0.0290	3.07	0.0233	0.0005	3.47	-0.0929	0.0086
2.68	0.1662	0.0276	3.08	0.0200	0.0004	3.48	-0.0954	0.0091
2.69	0.1622	0.0263	3.09	0.0167	0.0003	3.49	-0.0978	0.0096
2.70	0.1583	0.0251	3.10	0.0134	0.0002	3.50	-0.1002	0.0100
2.71	0.1544	0.0238	3.11	0.0102	0.0001			
2.72	0.1504	0.0226	3.12	0.0069	0.47888×10^{-6}			
2.73	0.1465	0.0215	3.13	0.0037	0.137167×10^{-6}			
2.74	0.1427	0.0204	3.14	0.0005	0.02573×10^{-6}			
2.75	0.1388	0.0193	3.15	-0.0027	0.0000	3.55	-0.1119	0.0125
2.76	0.1349	0.0182	3.16	-0.0058	0.33928×10^{-6}			
2.77	0.1311	0.0172	3.17	-0.0090	0.0001			
2.78	0.1273	0.0162	3.18	-0.0121	0.0001			
2.79	0.1234	0.0152	3.19	-0.0152	0.0002			

Tables F-4 through F-14 tabulate the functions

$$\int_a^b \left(\frac{\sin x}{x}\right)^2 dx \quad \text{and} \quad \int_0^b \left(\frac{\sin x}{x}\right)^2 dx$$

in the intervals $a \geq 0$, $b \leq \pi$, in steps of π/n for $2 \leq n \leq 12$.

Table F-4. Two Steps to Band Edge

Step Size π/2		Value of Integrand Limits	
a = n to b = n + 1		a = n to b = n + 1	a = 0 to b = n + 1
0	1	1.2153162	1.2153612
1	2	0.2028343	1.4181506

Table F-5. Three Steps to Band Edge

π/3			
0	1	0.9301896	0.9301896
1	2	0.4324013	1.3625909
2	3	0.0555597	1.4181506

Table F-6. Four Steps to Band Edge

π/4			
0	1	0.7341414	0.7341414
1	2	0.4811748	1.2153163
2	3	0.1808489	1.3961652
3	4	0.0219854	1.4181506

Table F-7. Five Steps to Band Edge

Step Size π/5		Value of Integrand Limits	
a = n to b = n + 1		a = n to b = n + 1	a = 0 to b = n + 1
0	1	0.6016096	0.6016096
1	2	0.4602657	1.0618752
2	3	0.2564261	1.3183013
3	4	0.0891047	1.4074060
4	5	0.0107446	1.4181506

Table F-8. Six Steps to Band Edge

π/6			
0	1	0.5079330	0.5079930
1	2	0.4221966	0.9301896
2	3	0.2851267	1.2153163
3	4	0.1472746	1.3625909
4	5	0.0495524	1.4121433
5	6	0.0060073	1.4181506

Table F.9. Seven Steps to Bandedge

Step Size π/7		Value of Integrand Limits	
a = n to b = n + 1		a = n to b = n + 1	a = 0 to b = n + 1
0	1	0.4389140	0.4389140
1	2	0.3833018	0.8222158
2	3	0.2888977	1.1111135
3	4	0.1825447	1.2936582
4	5	0.0906919	1.3843501
5	6	0.0301157	1.4144658
6	7	0.0036848	1.4181506

Table F-10. Eight Steps to Band Edge

π/8			
0	1	0.3860517	0.3860517
1	2	0.3480897	0.7341414
2	3	0.2810874	1.0152288
3	4	0.2000874	1.2153163
4	5	0.1216626	1.3369788
5	6	0.0591863	1.3961652
6	7	0.0195674	1.4157326
7	8	0.0024180	1.4181506

Table F-11. Nine Steps to Band Edge

Step Size π/9		Value of Integrand Limits	
a = n to b = n + 1		a = n to b = n + 1	a = 0 to b = n + 1
0	1	0.3443848	0.3443848
1	2	0.3173772	0.6617620
2	3	0.2684276	0.9301896
3	4	0.2064000	1.1365897
4	5	0.1417795	1.2783692
5	6	0.0842217	1.3625909
6	7	0.0405014	1.4030923
7	8	0.0133881	1.4164803
8	9	0.0016702	1.4181506

Table F-12. Ten Steps to Band Edge

π/10			
0	1	0.3107402	0.3107402
1	2	0.2908694	0.6016096
2	3	0.2541679	0.8557774
3	4	0.2060978	1.0618752
4	5	0.1534411	1.2153163
5	6	0.1029850	1.3183013
6	7	0.0602909	1.3785922
7	8	0.0288138	1.4074060
8	9	0.0095435	1.4169495
9	10	0.0012011	1.4181506

Table F-13. Eleven Steps to Band Edge

Step Size π/11		Value of Integrand Limits	
a = n to b = n + 1		a = n to b = n + 1	a = 0 to b = n + 1
0	1	0.2830268	0.2830268
1	2	0.2679954	0.5510222
2	3	0.2398428	0.7908650
3	4	0.2020688	0.9929338
4	5	0.1591721	1.1521060
5	6	0.1159183	1.2680243
6	7	0.0766005	1.3446248
7	8	0.0444314	1.3890562
8	9	0.0211694	1.4102256
9	10	0.0070328	1.4172584
10	11	0.0008922	1.4181506

Table F-14. Twelve Steps to Band Edge

π/12			
0	1	0.2598156	0.2598156
1	2	0.2481774	0.5079930
2	3	0.2261484	0.7341414
3	4	0.1960482	0.9301896
4	5	0.1609367	1.0911263
5	6	0.1241900	1.2153163
6	7	0.0890509	1.3043672
7	8	0.0582237	1.3625909
8	9	0.0335743	1.3961652
9	10	0.0159781	1.4121433
10	11	0.0053267	1.4174700
11	12	0.0006806	1.4181506

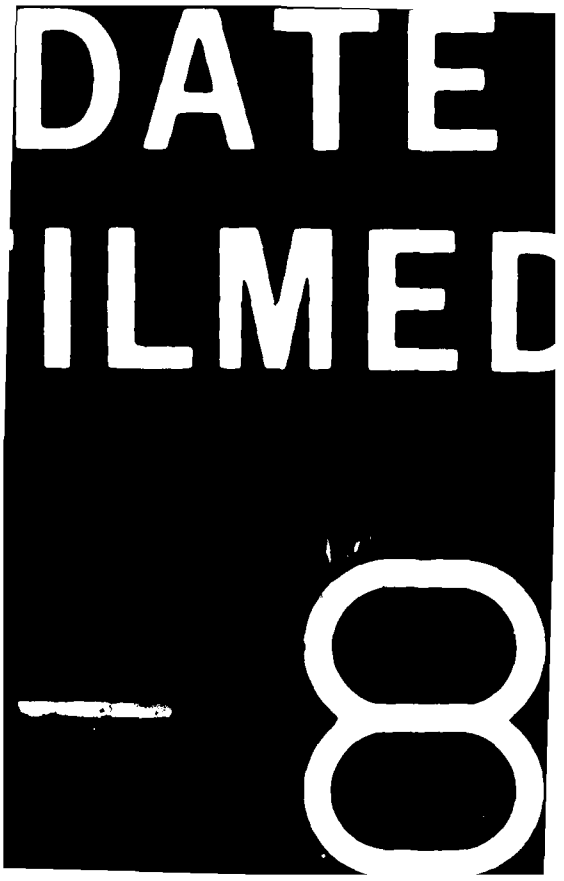
DATE
ILMED
8